

PULSED POWER SYSTEM

脈衝功率系統



Po-Yu Chang

Institute of Space and Plasma Sciences, National Cheng Kung University

2023 Fall Semester

Tuesday 9:10-12:00

Lecture 13

<http://capst.ncku.edu.tw/PGS/index.php/teaching/>

Online courses:

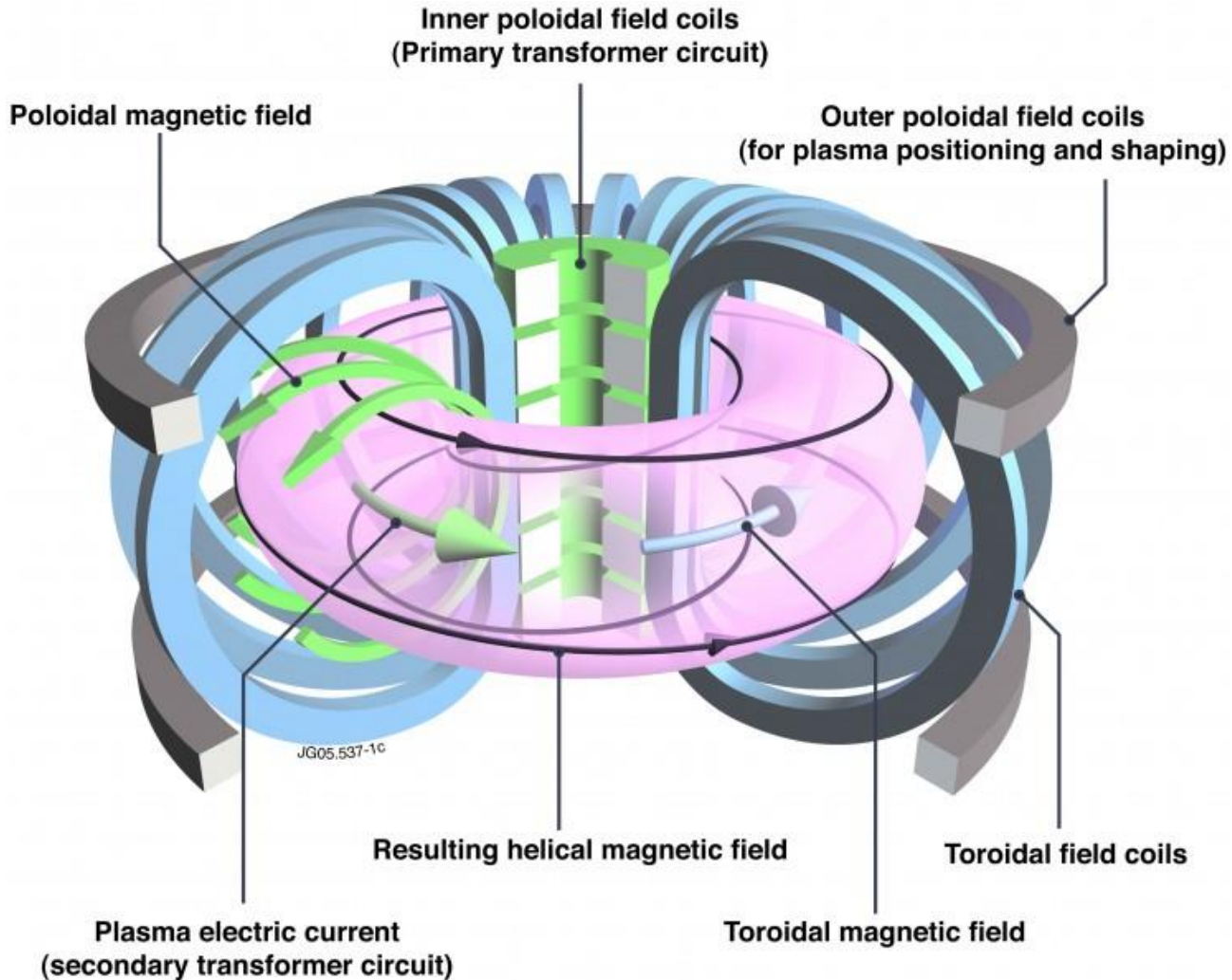
<https://nckucc.webex.com/nckucc/j.php?MTID=md577c3633c5970f80cbc9e821927e016>

Final project and final presentation

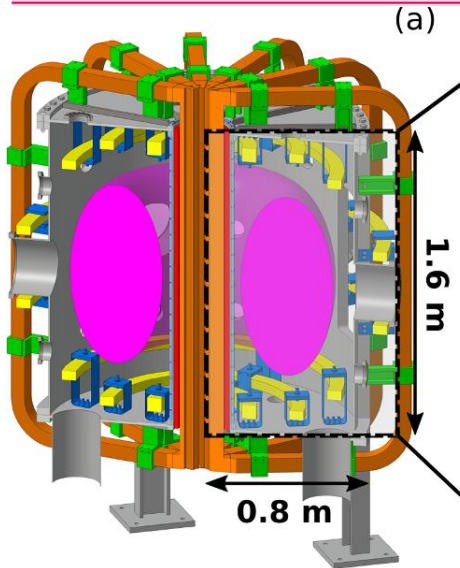


- **Final project:**
 - Due on 1/2.
- **Final presentation:**
 - 12/26 10:00.
 - 15 mins for each person
 - Applications of pulsed-power system

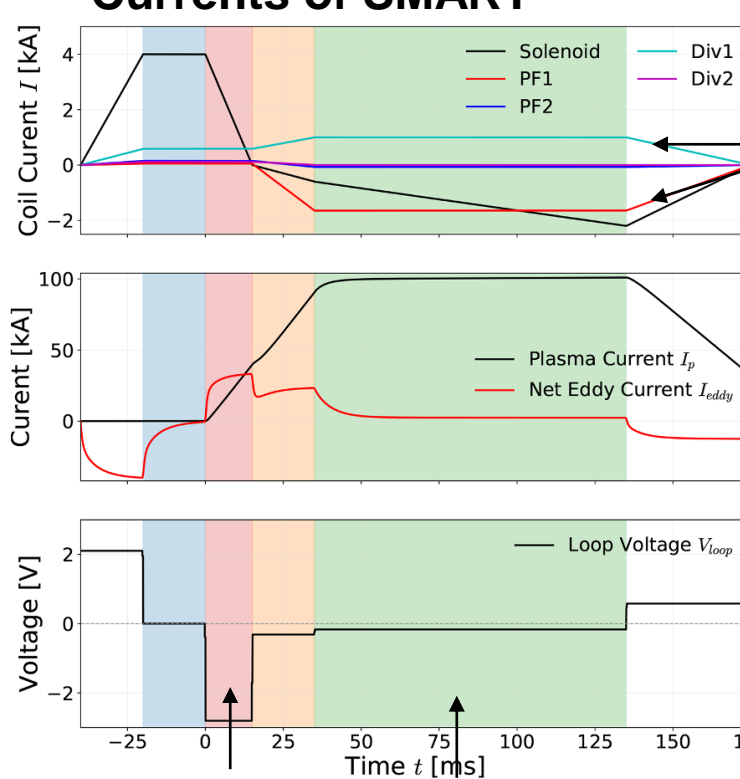
A tokamak is a device to achieve nuclear fusion via confinement plasma using magnetic field



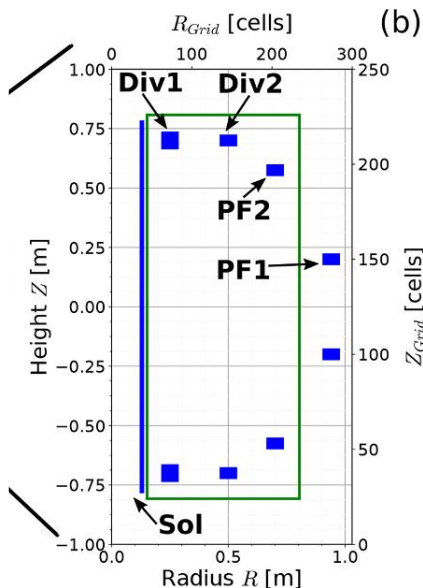
Currents with specific profiles needed to be provided to drive coils in Tokamaks to confine the plasma



• Currents of SMART



Equilibrium state can be achieved with poloidal field coils.



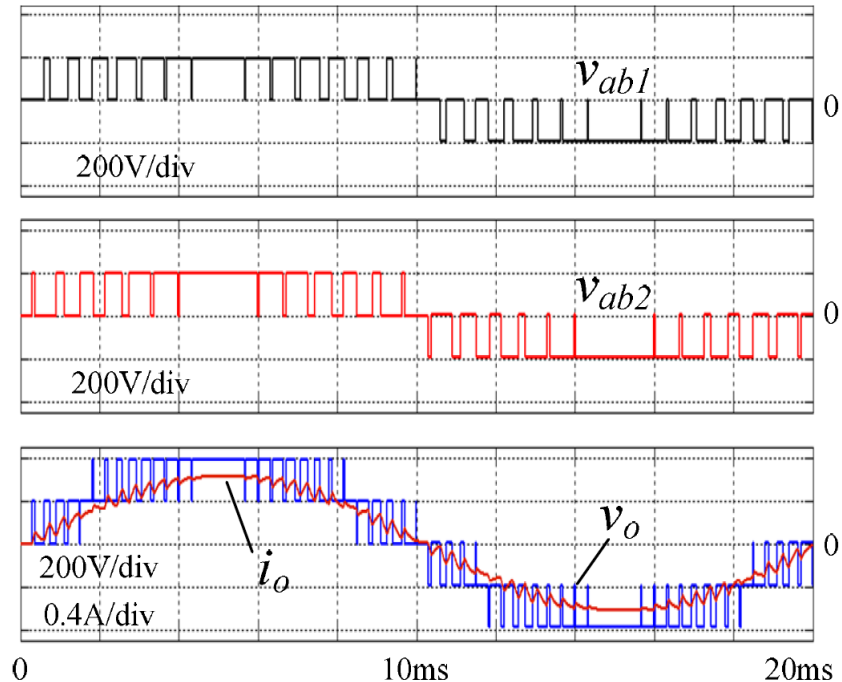
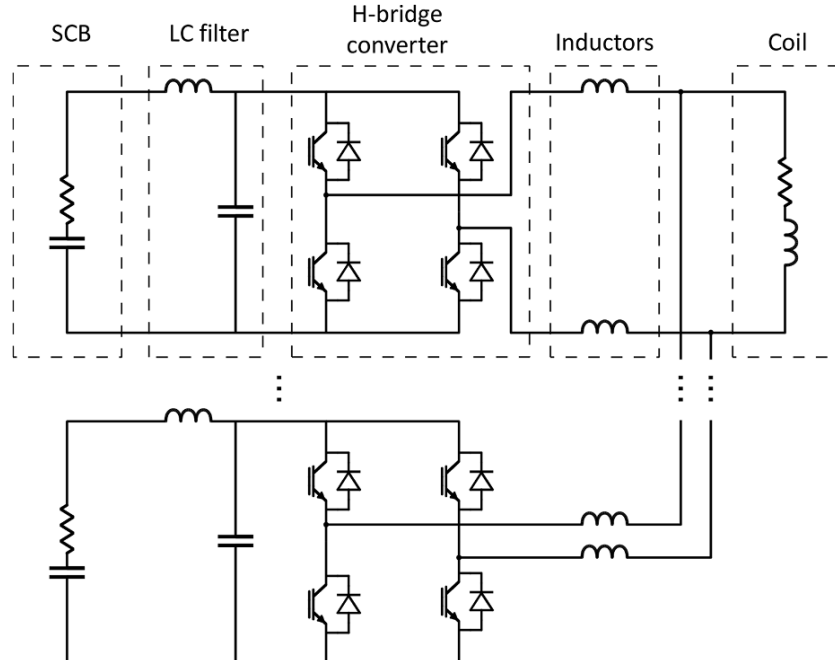
Breakdown Plasma current is driven.

- The current of the CS will be determined by the required breakdown voltage and plasma current.

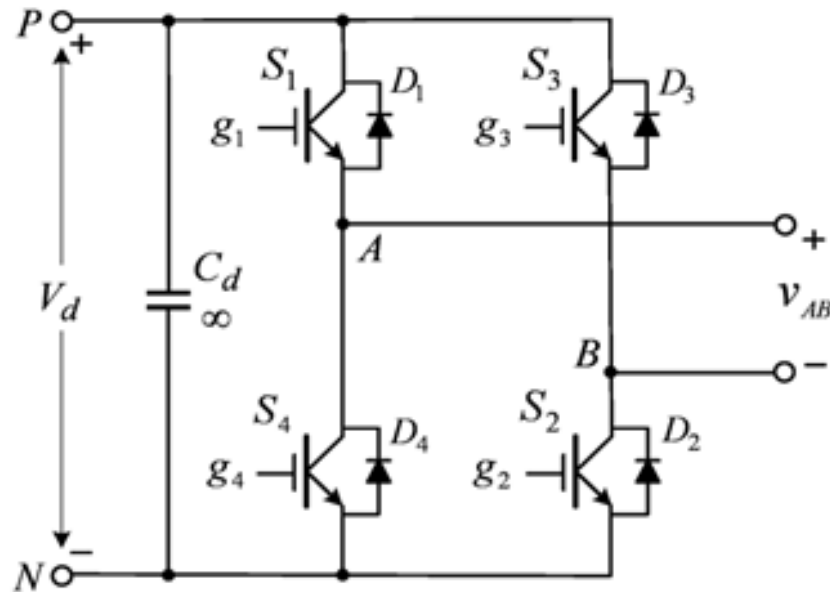
An H-bridge combining pulse width modulation technique will be used to provide the controllable currents



- H-bridge configuration provides the capability of reversing the current direction:
- Pulse width modulation provides the capability of controllable currents

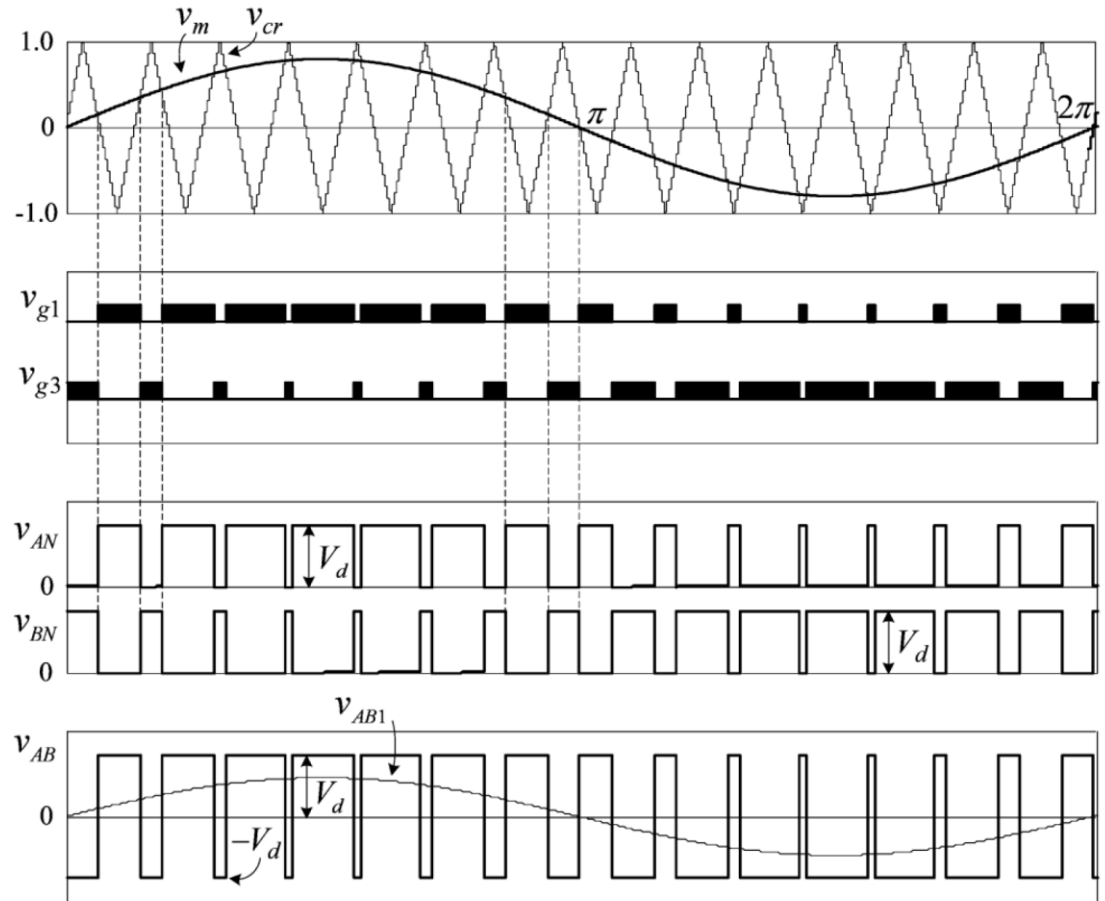
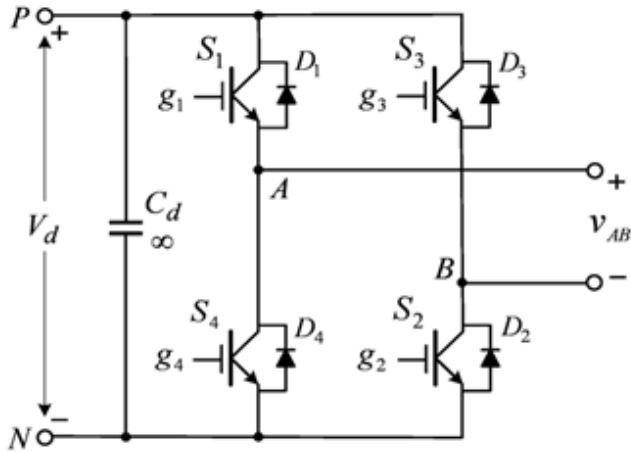


The output voltage is controlled by the status of switches S1~S4



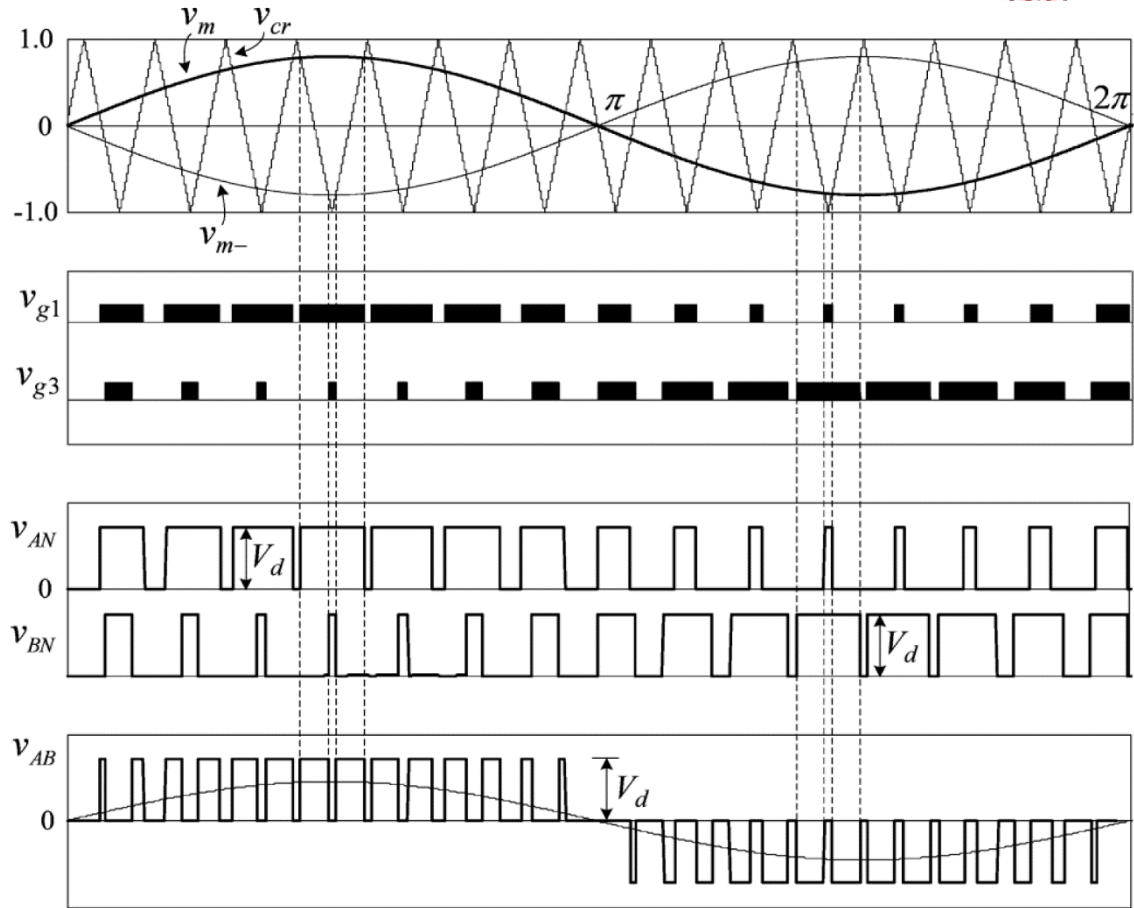
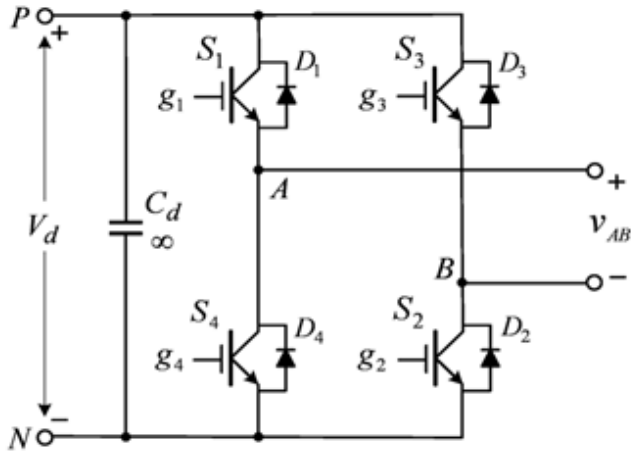
- **S₁/S₂ ON; S₃/S₄ Off: $V_{AB} = V_d$.**
- **S₁/S₂ Off; S₃/S₄ ON: $V_{AB} = -V_d$.**
- **S₁/S₂ ON; S₃/S₄ ON: $V_{AB} = 0$.**

Bipolar Modulation Scheme



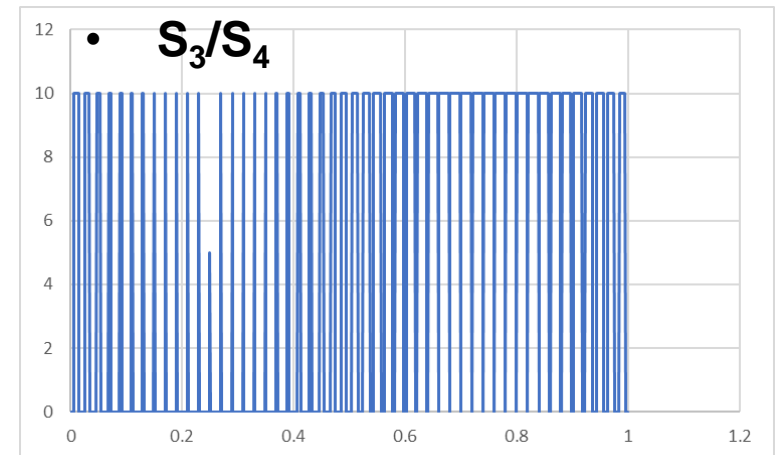
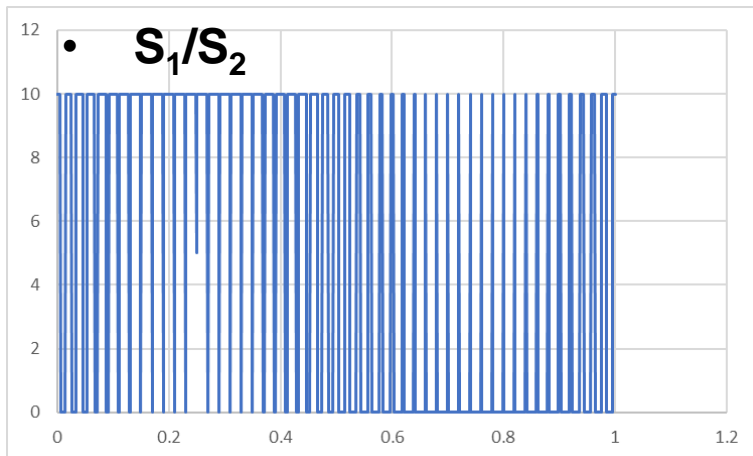
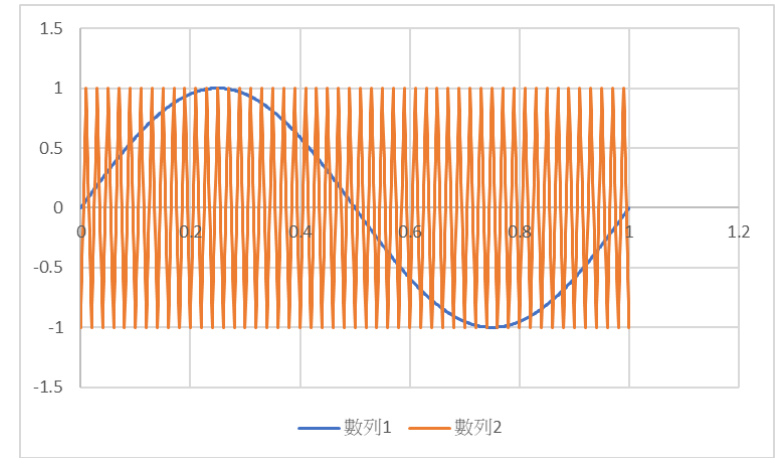
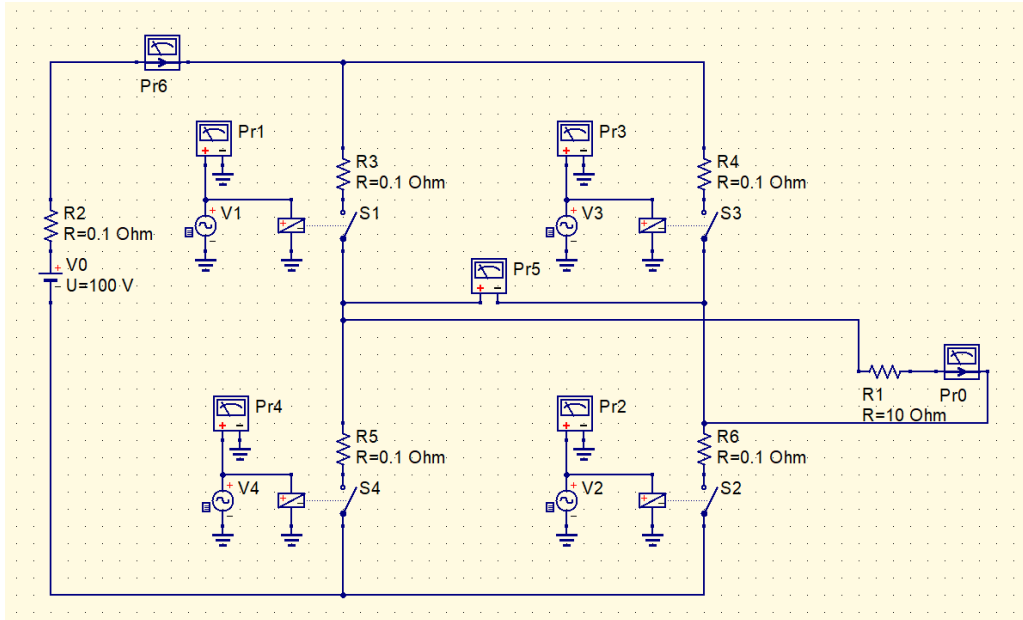
- **S_1/S_2 ON; S_3/S_4 Off: $V_{AB} = V_d$**
- **S_1/S_2 Off; S_3/S_4 ON: $V_{AB} = -V_d$**
- **S_1/S_2 ON; S_3/S_4 ON: $V_{AB} = 0$**

Unipolar Modulation Scheme

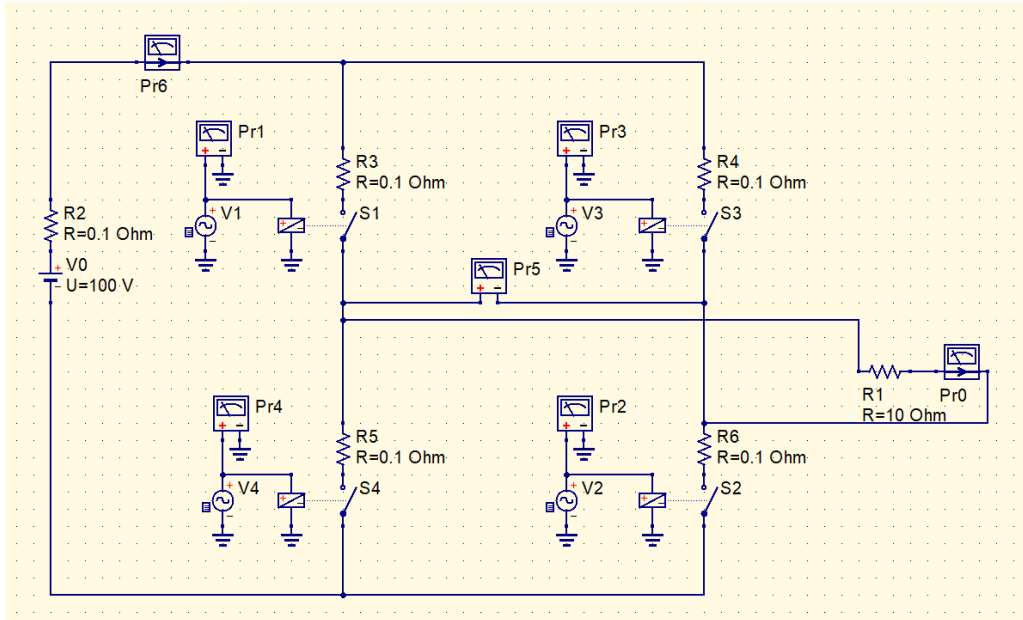


- S_1/S_2 ON; S_3/S_4 Off: $V_{AB} = V_d$
- S_1/S_2 Off; S_3/S_4 ON: $V_{AB} = -V_d$
- S_1/S_2 ON; S_3/S_4 ON: $V_{AB} = 0$.

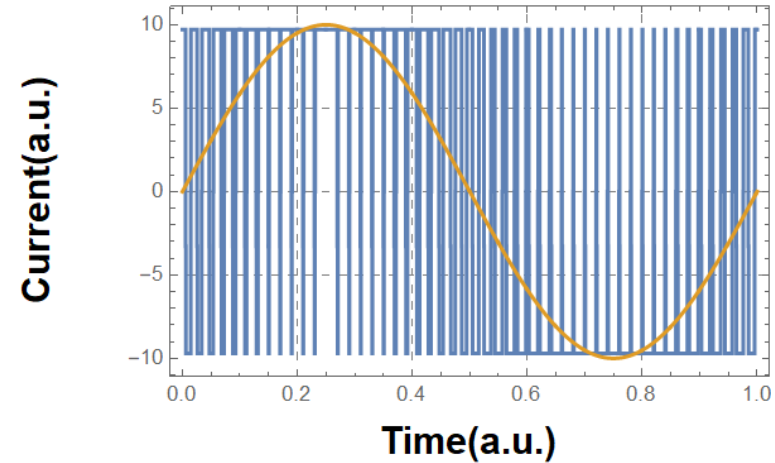
Simulation using bipolar modulation scheme



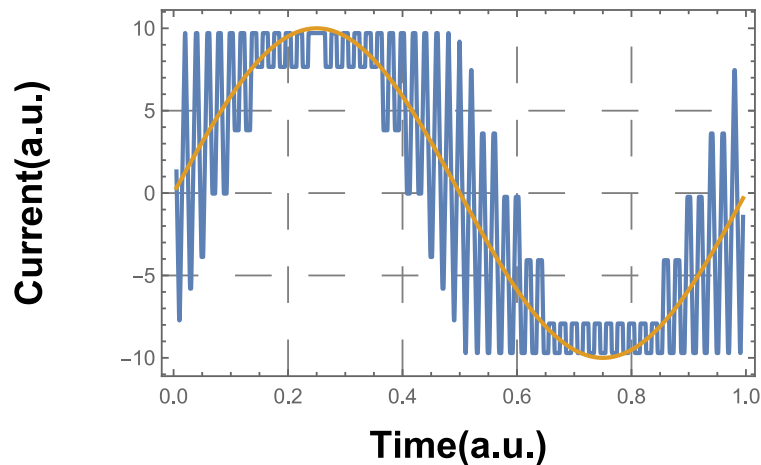
Simulation using bipolar modulation scheme



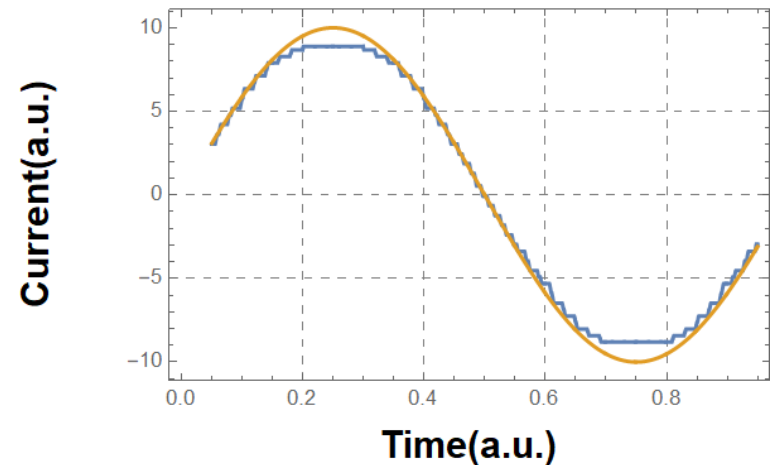
- Raw data



- Moving average = 100



- Moving average = 1000



Outlines



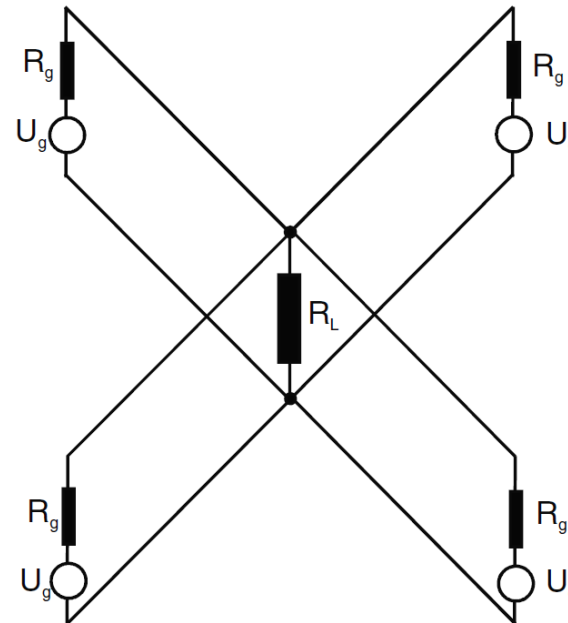
- **Power and voltage adding**
 - Marx generator
 - LC generator
 - Line pulse transformers
 - Induction voltage adder (IVA)
 - Linear induction accelerator (LIA)
 - Linear transformer driver (LTD)
- Diagnostics
 - Voltage measurement
 - Current measurement
- Applications of pulsed-power system

Power and voltage adding

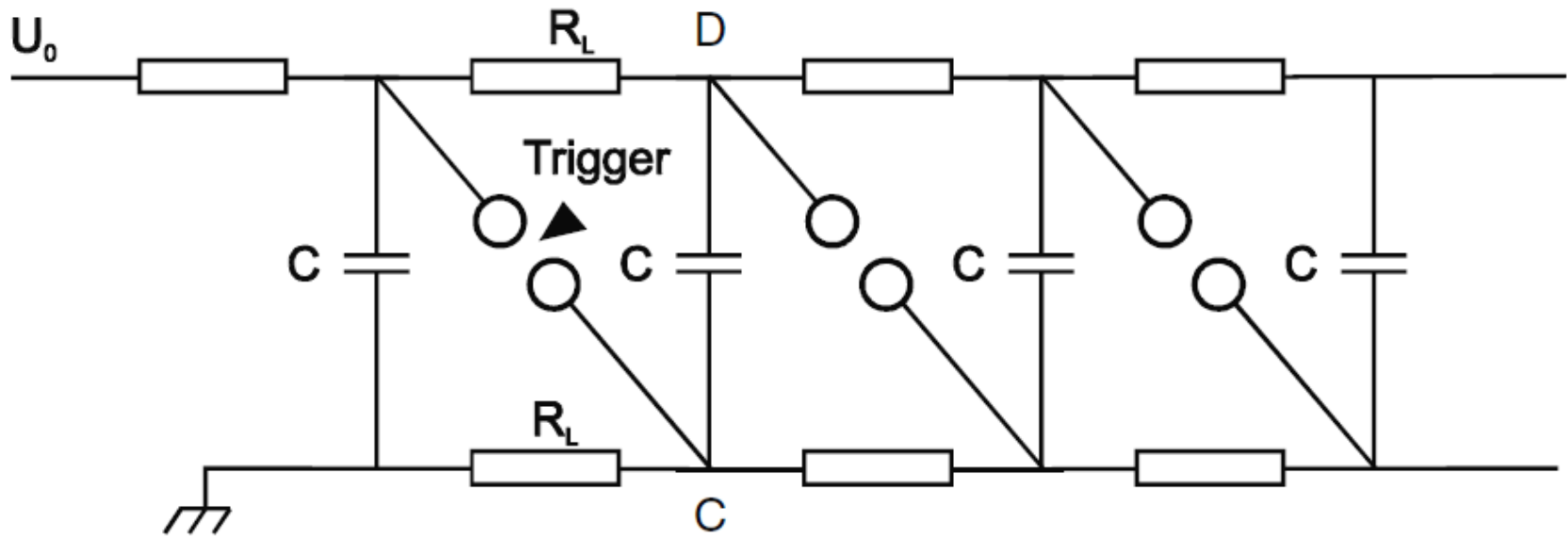


- For pulsed-power levels become very high (≥ 15 TW), the generator must be divided into separately units, which can be constructed much more compactly and thus use the available volume much more efficiently.
- Synchronizing independent lines requires special measures, e.g., laser-triggered switches with very low jitter.
- Match load needed:

$$R_L = \frac{R_g}{n}$$



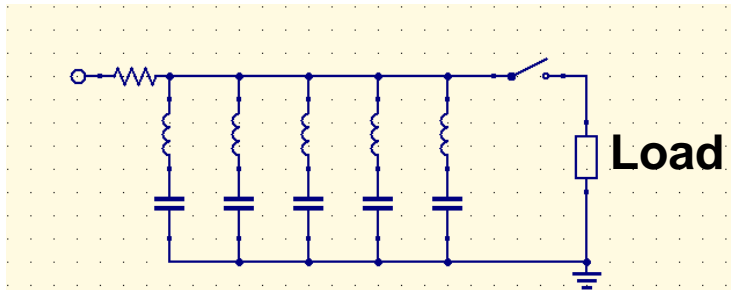
Marx generator



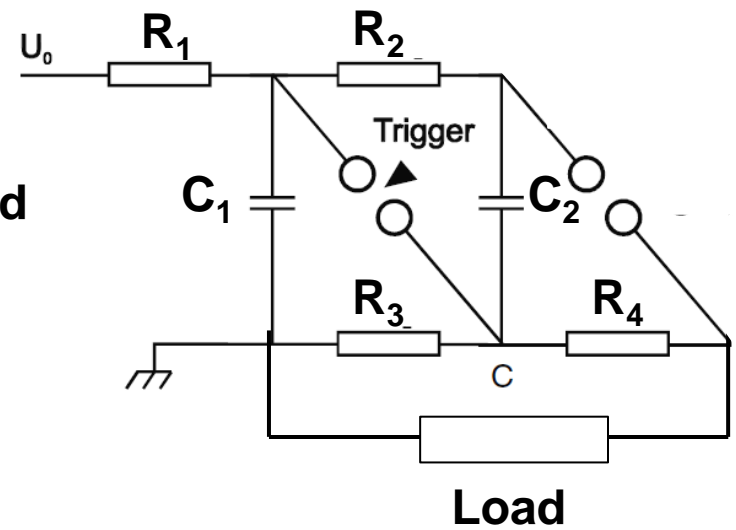
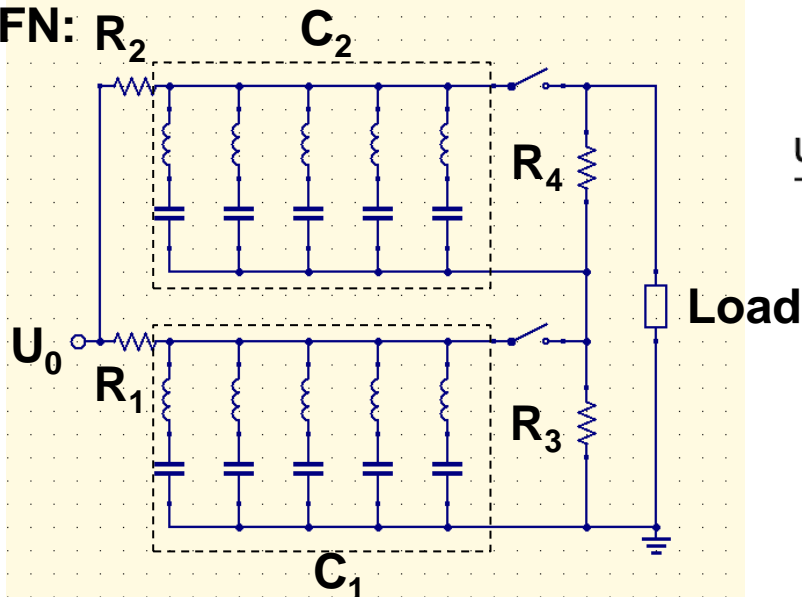
PFN-Marx



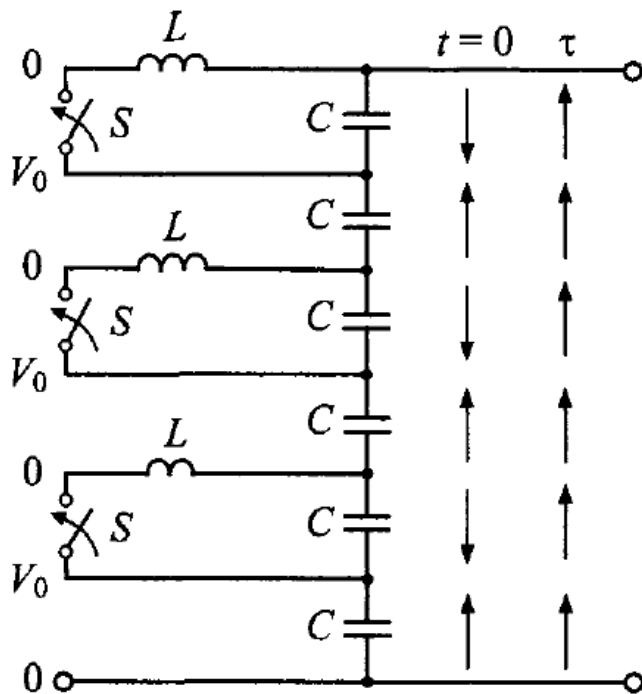
- PFN:



- 2-stage PFN:



LC generator

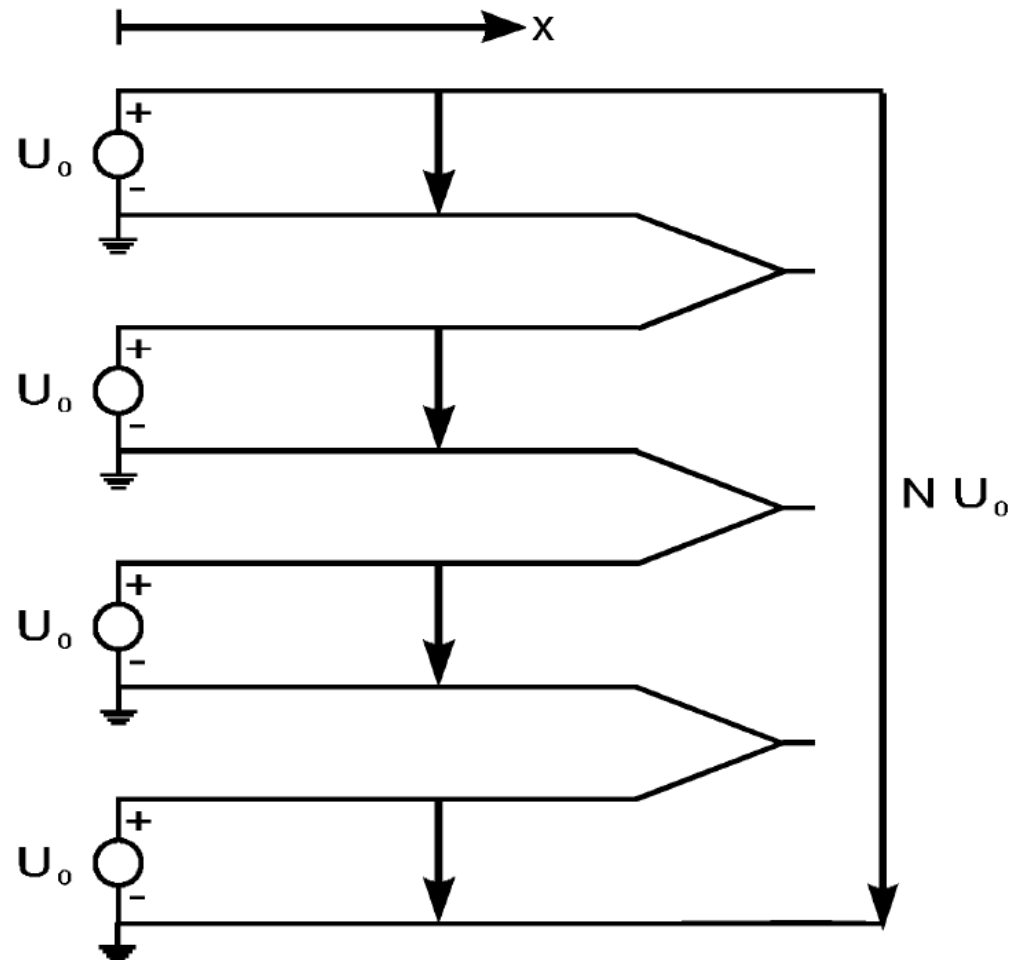


$$t = \tau = \pi\sqrt{LC} \quad V_{\text{out}} = NV_0$$

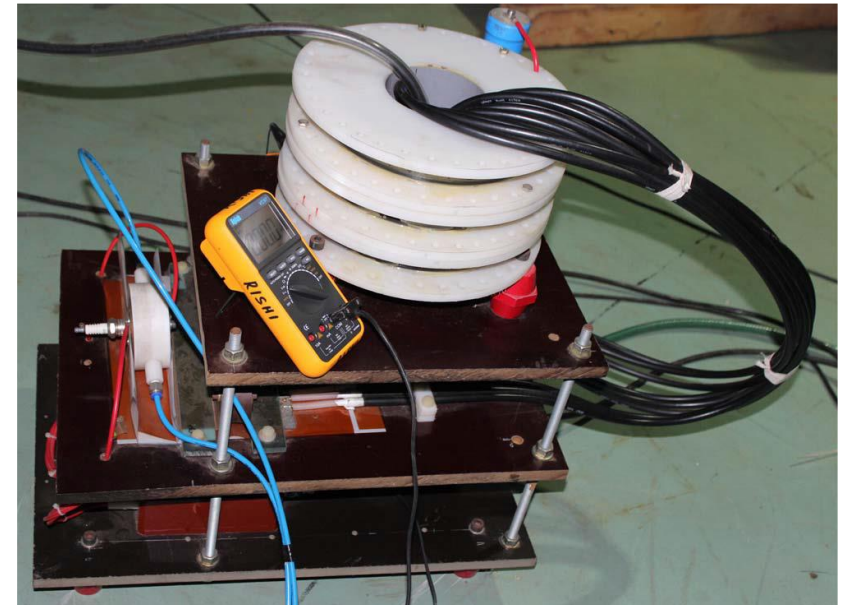
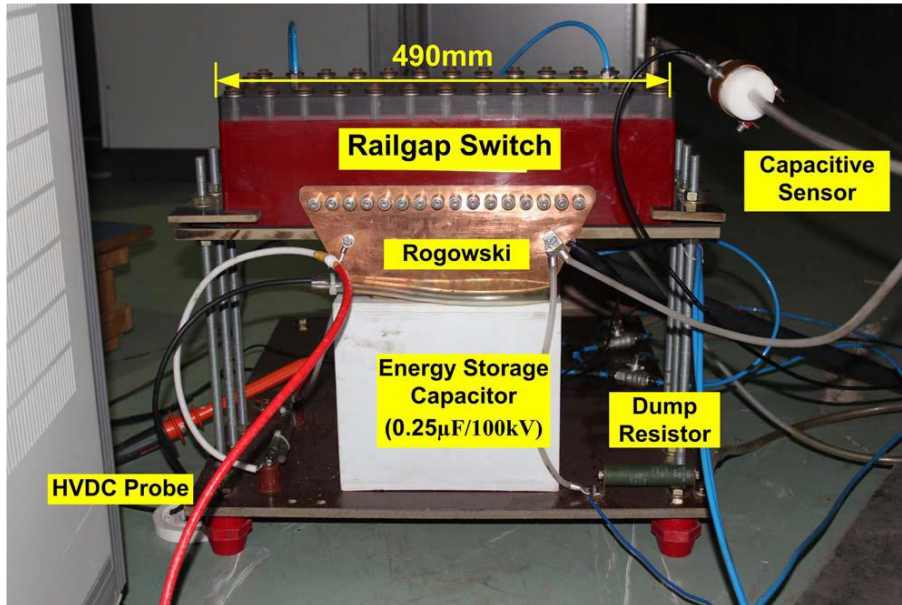
$$V_{\text{out}}(t) = NV_0[1 - e^{\alpha t} \cos(\omega t)]$$

- **Advantages:**
 - the number of switches is halved.
 - The resistances and inductances of the switches have no effect on the circuit output impedance if the LC generator picks up the load through an additional fast switch.
- **Disadvantage:** switches must be operated as simultaneously as possible.

Adding of voltage pulses by transit-time isolation

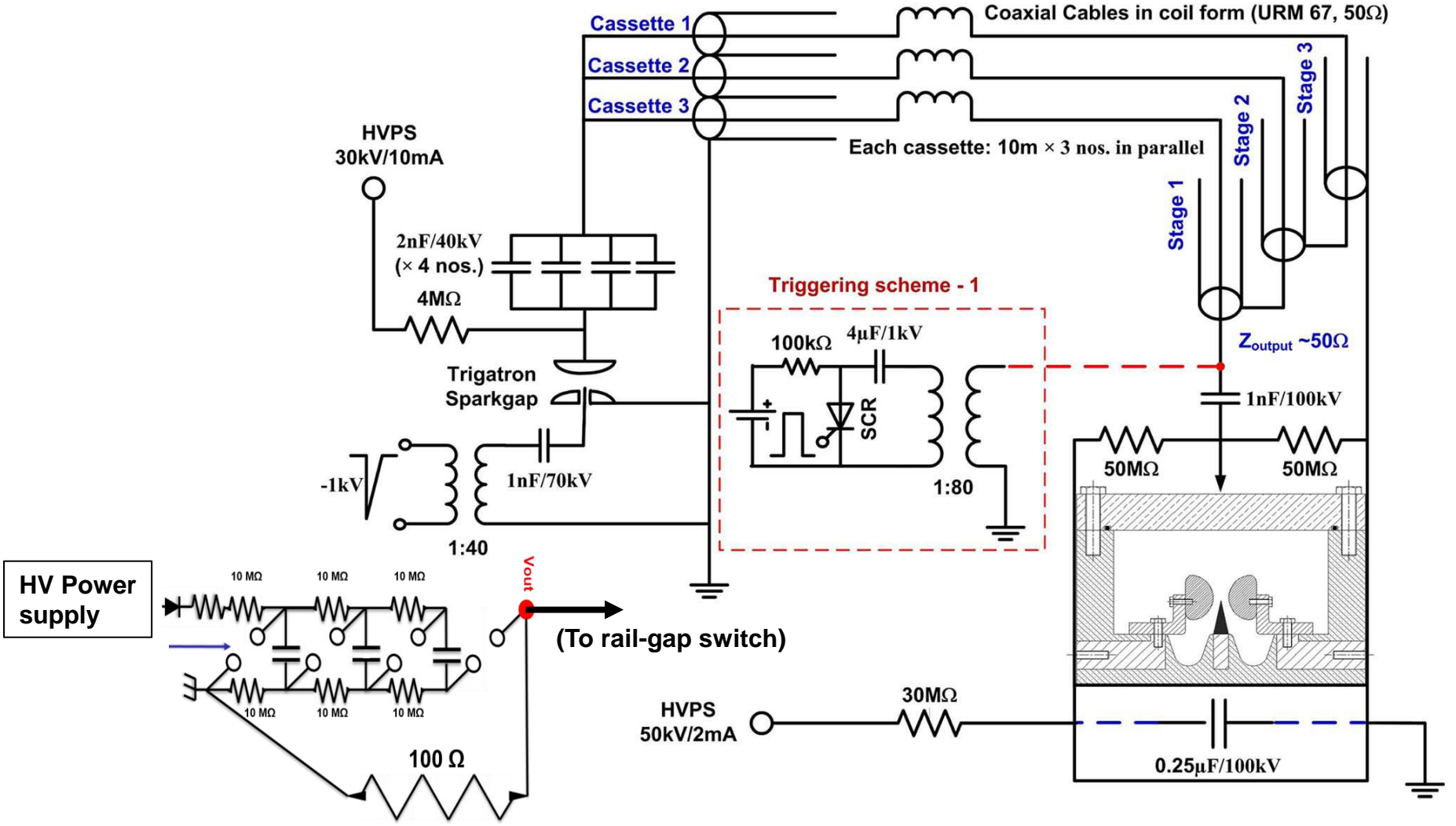


Transmission transformer



- **Multi-channel discharges between two rail-like electrodes will be triggered by a fast trigger pulse generator (rising speed > 5kV/ns).**

Transmission transformer



Line pulse transformers (LPT)

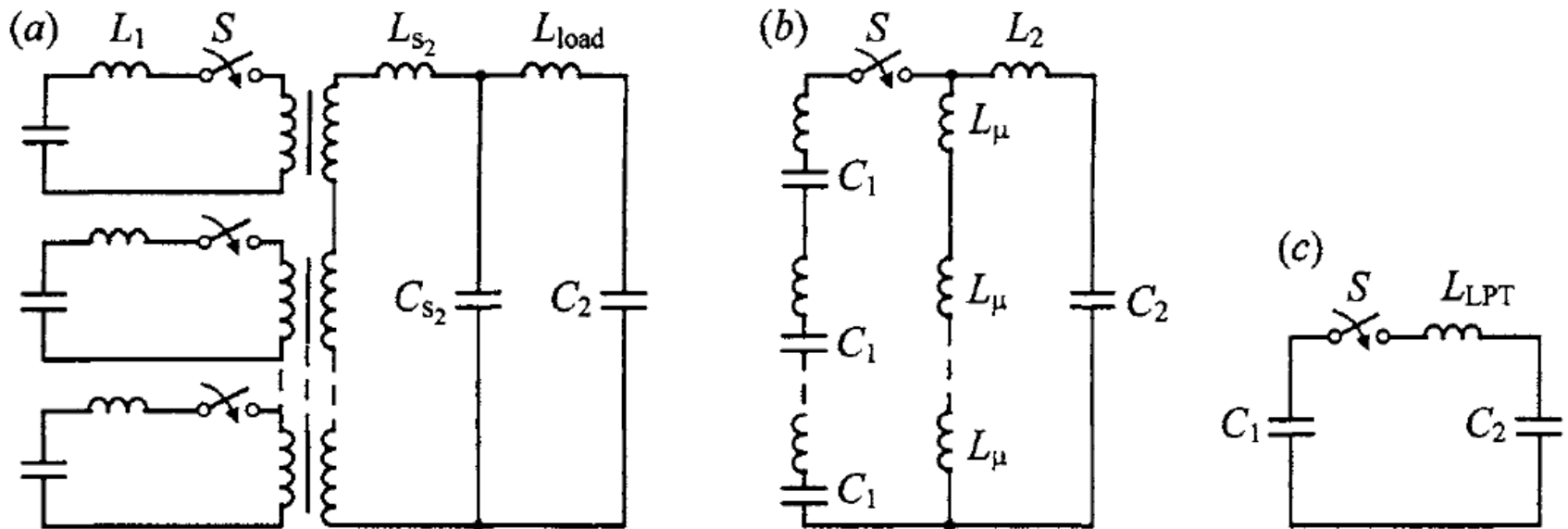
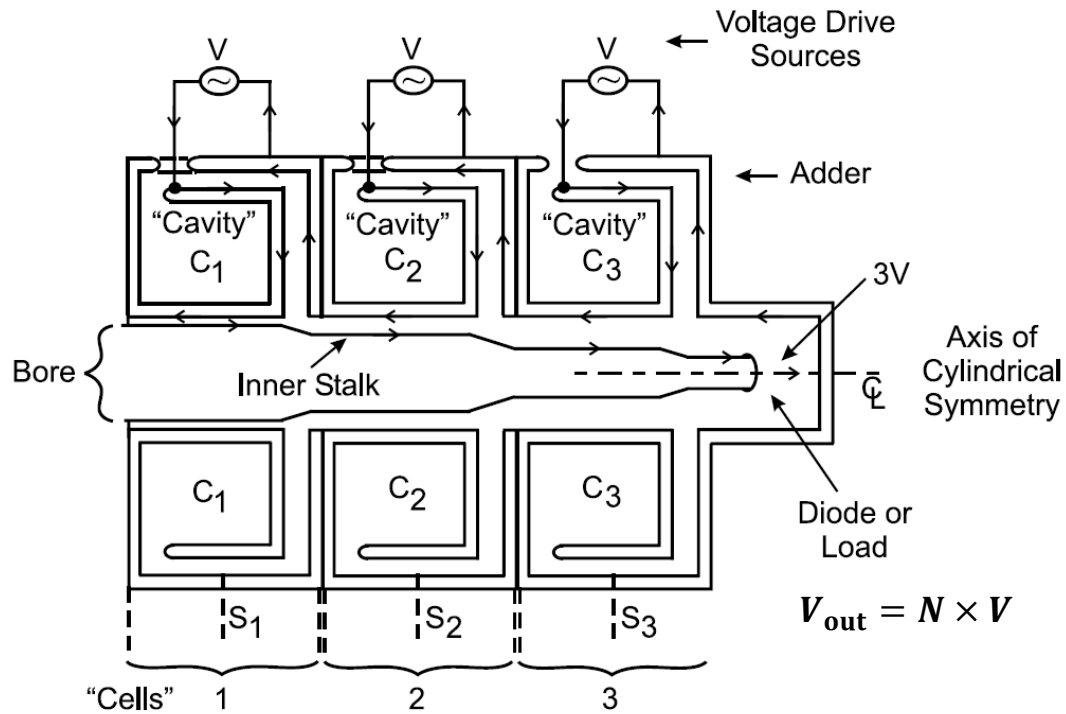
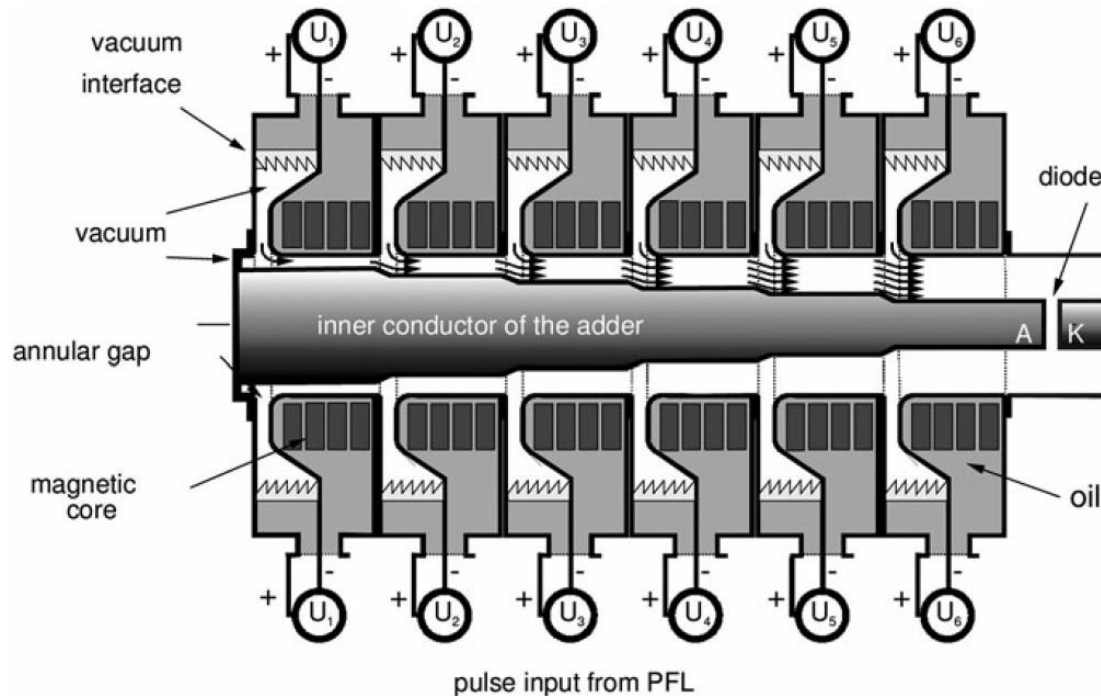


Figure 1.6. The equivalent (a), reduced (b), and simplified circuit (c) of a line transformer

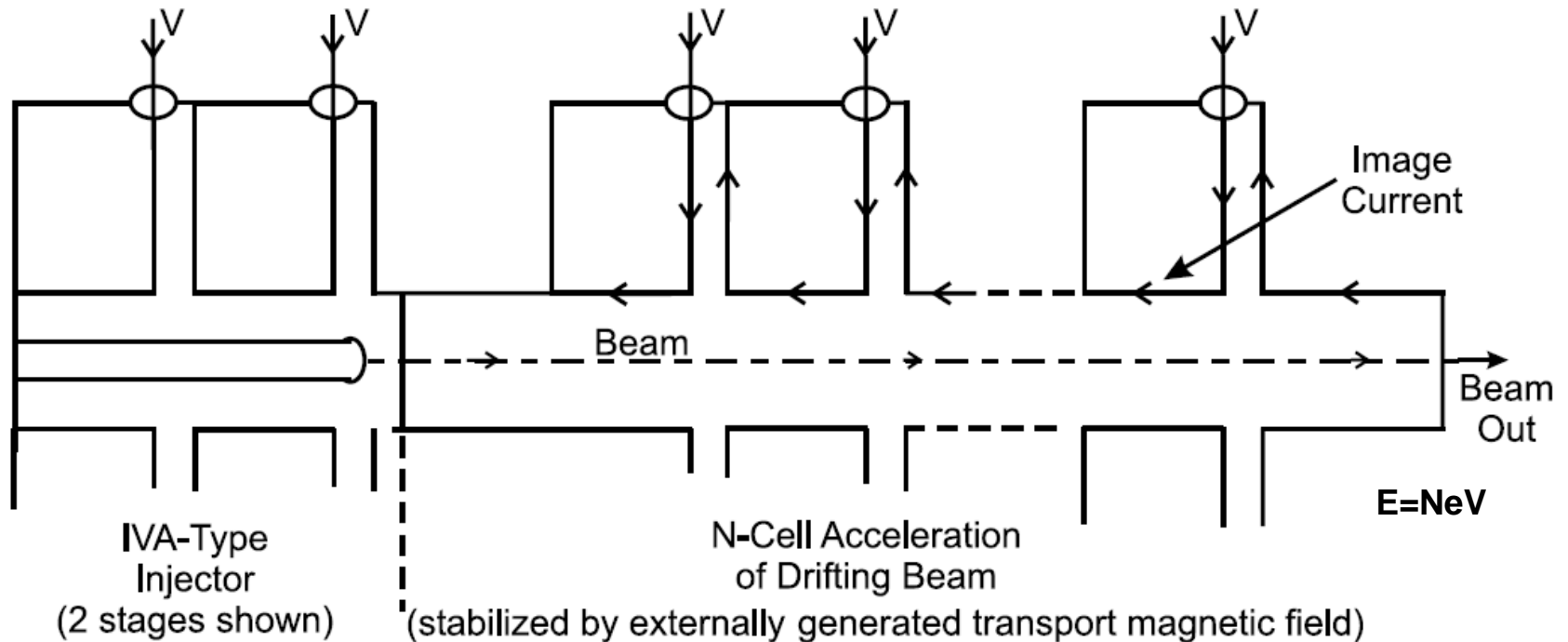
Induction voltage adder (IVA)



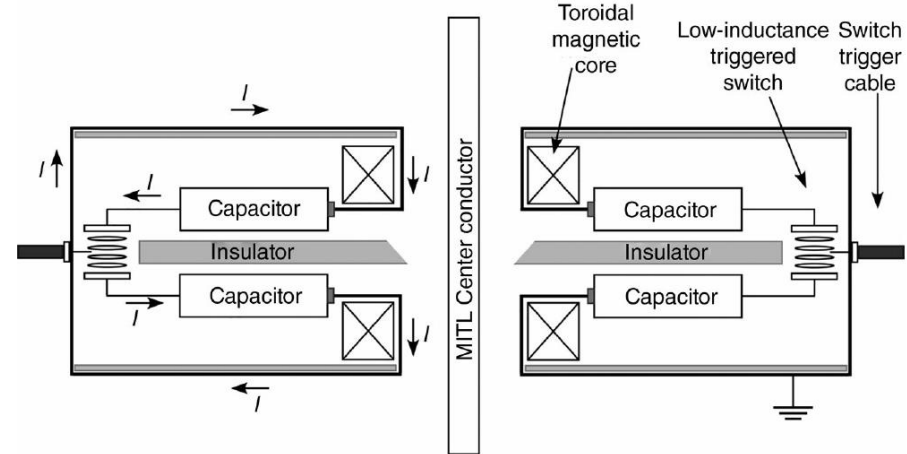
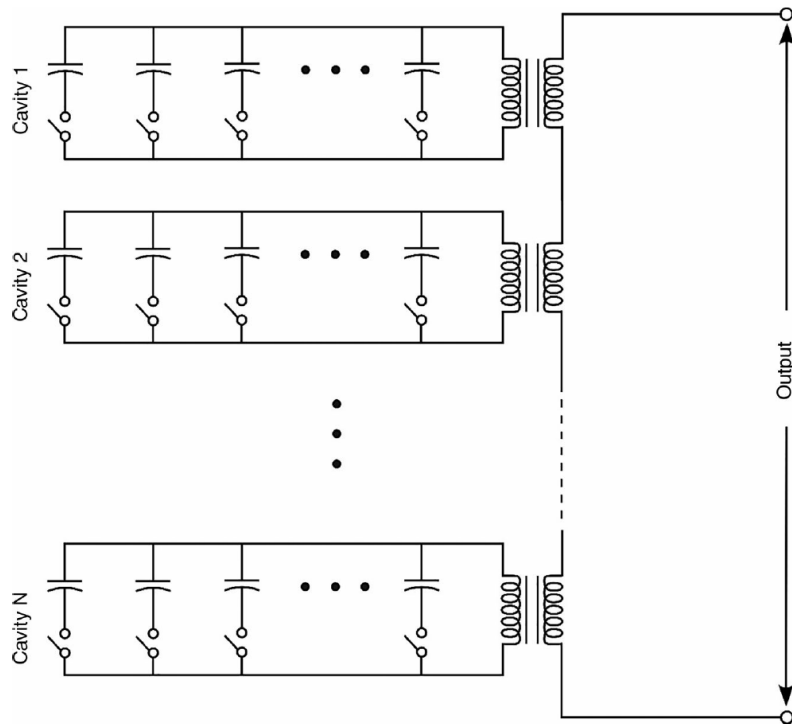
Example of IVA of KALIF-HELIA (High Energy Linear Induction Accelerator)



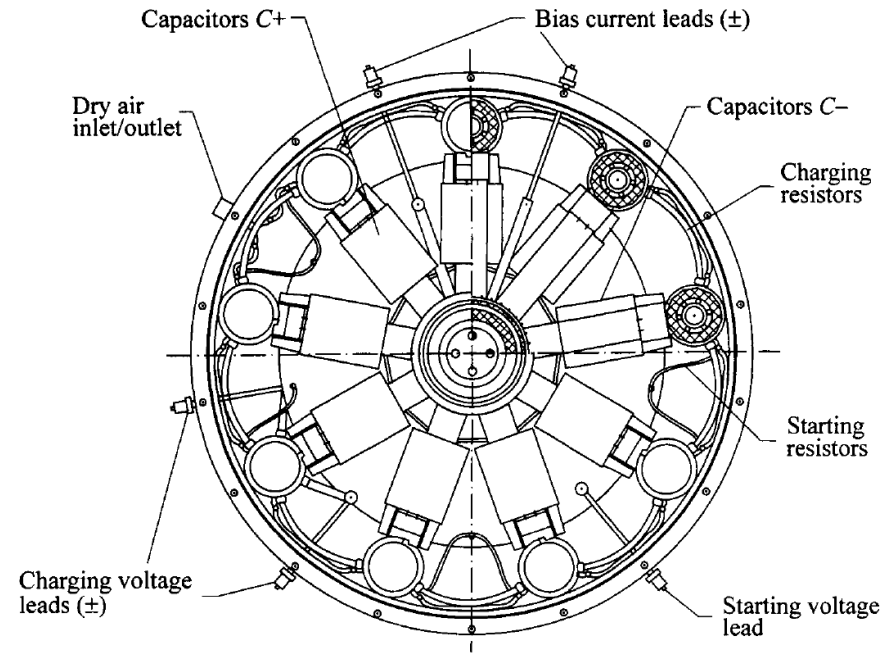
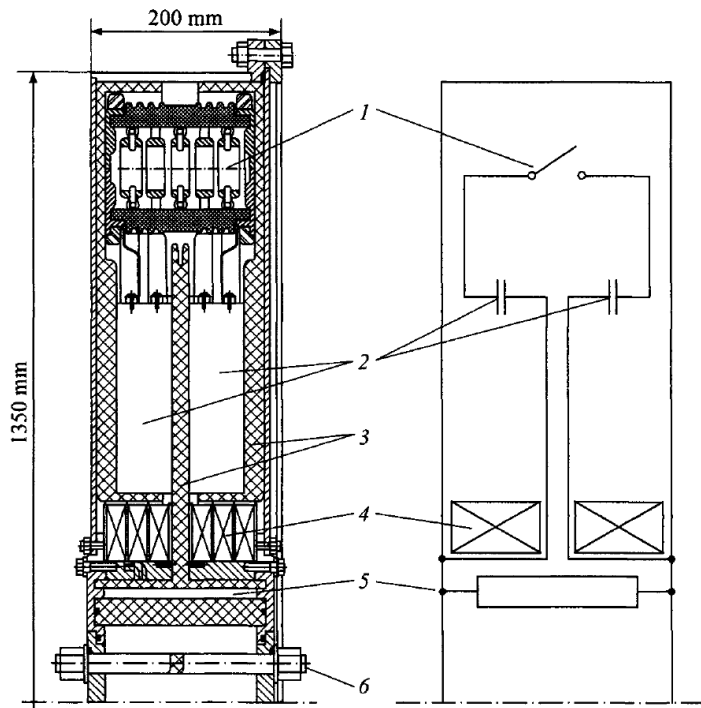
Linear Induction Accelerator (LIA)



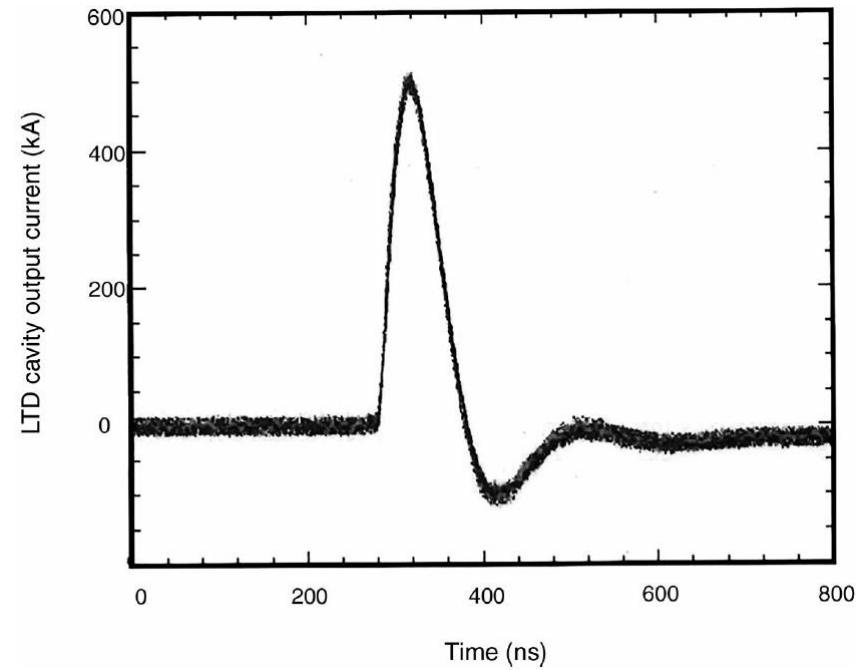
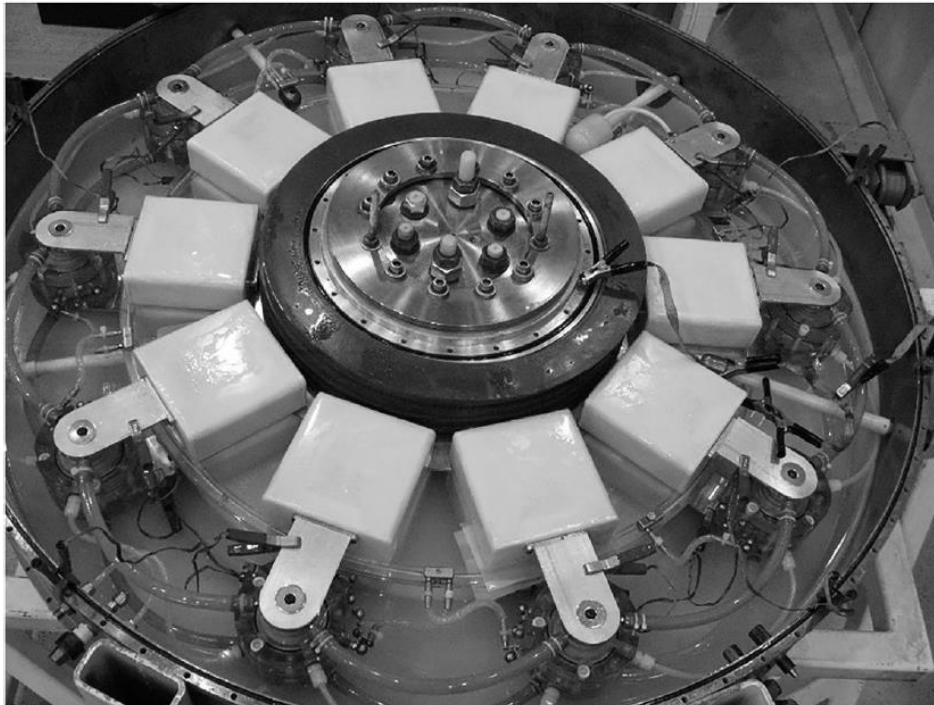
Linear Transformer Driver (LTD)



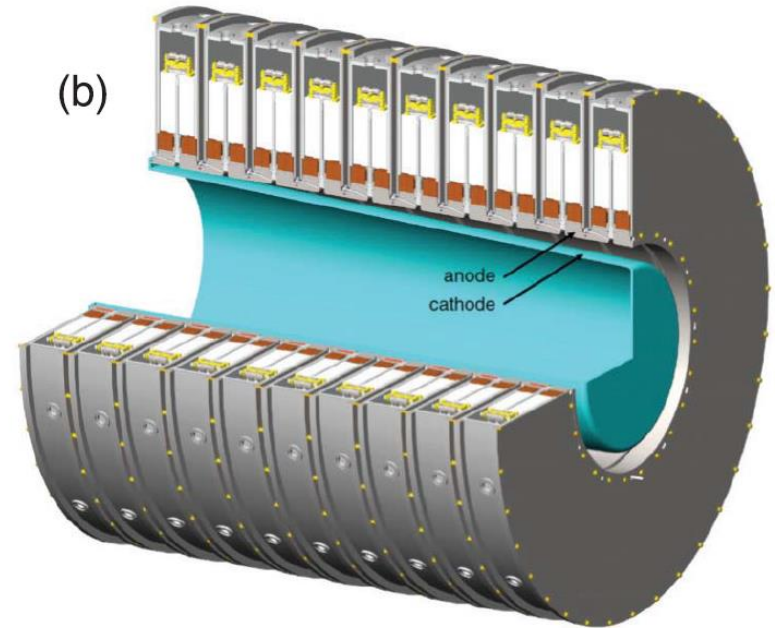
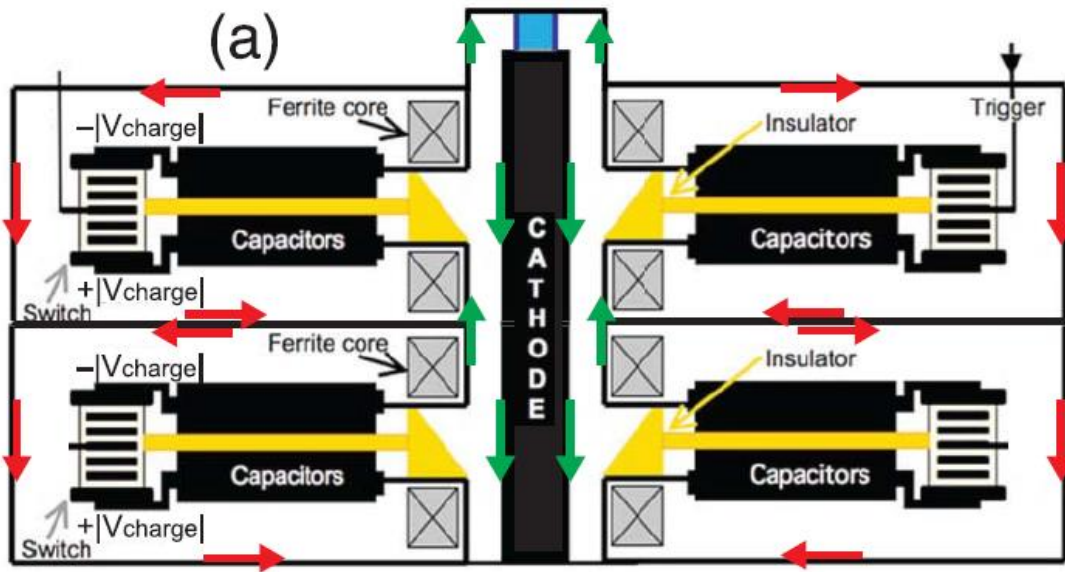
Linear Transformer Driver (LTD)



Linear transformer driver



Linear Transformer Driver (LTD)

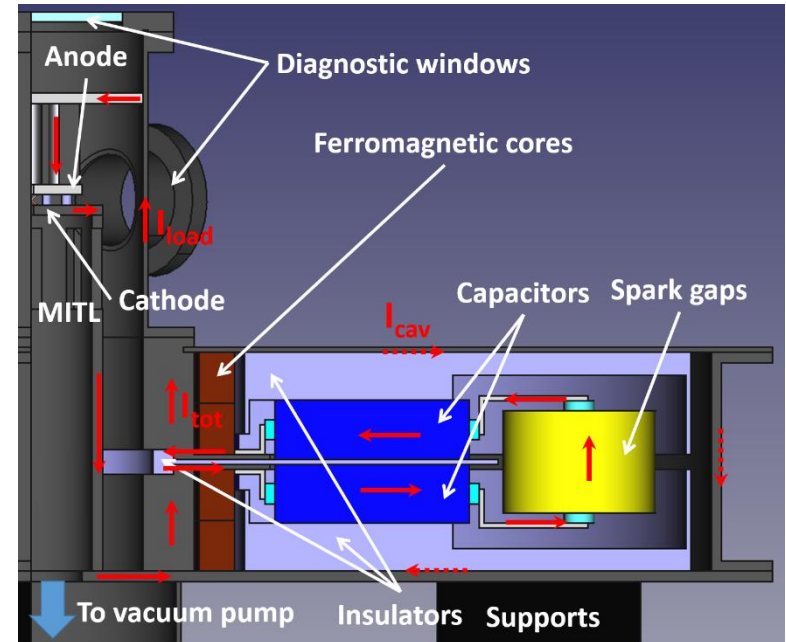
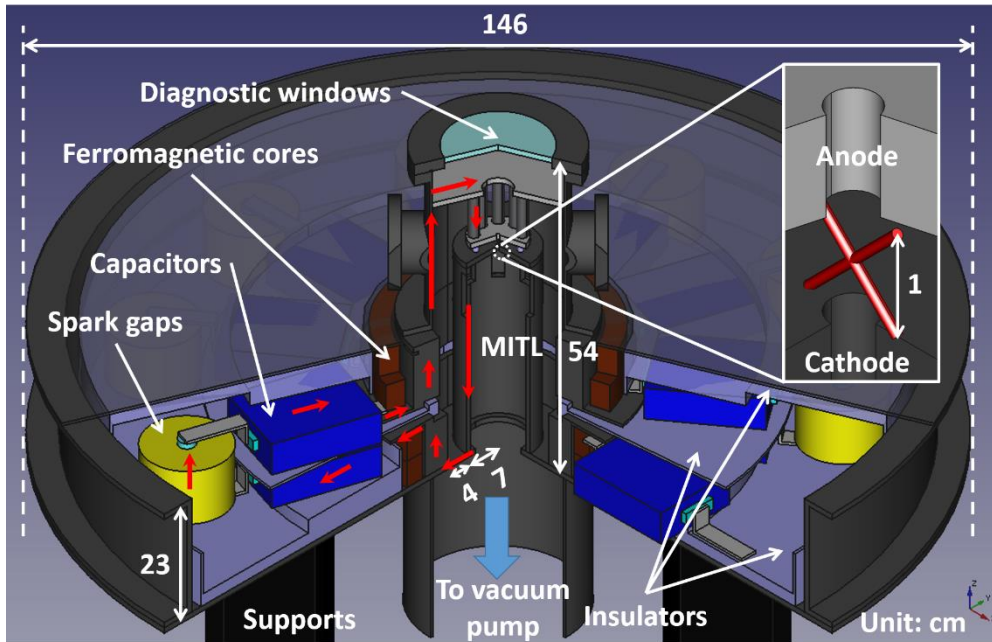


Characteristics of LTD



- **Advantages:**
 - LTD stages enclose the primary storage. The LTD driver is more compact compared to other generators having similar output parameters.
 - LTD driver is simple.
 - It is practical and convenient to be built with relatively small size capacitors, which necessarily have less capacitance C . => short pulse
 - It can be operated in both LPT and IVA modes.
- Small capacitor, and reduced inductance (because of connected in parallel) lead to short pulse width.
- To increase energy storage, high voltage is used.

Our design



Outlines



- Power and voltage adding
 - Marx generator
 - LC generator
 - Line pulse transformers
 - Induction voltage adder (IVA)
 - Linear induction accelerator (LIA)
 - Linear transformer driver (LTD)
- **Diagnostics**
 - **Voltage measurement**
 - **Current measurement**
- Applications of pulsed-power system

Diagnostics



- **The basic electrical quantities are always the electromagnetic fields E and B from which pulse current and voltage must be derived.**
- **A suitable sensor does not perturb the fields to be measured is achieved with**
 - **capacitive sensors;**
 - **inductive sensors;**
 - **electro-optical methods;**
 - **resistive voltage dividers. It may create weak points in the high-voltage insulation.**

Electromagnetic field sensors



- Rapidly changing electromagnetic fields, i.e., $\frac{d\vec{B}}{dt}$ or $\frac{d\vec{E}}{dt}$
 - induced currents / voltages in the conductors of a sensor.
 - only consider electrically short sensors:
 - size $< \lambda$ of the field where λ is the scale length or wavelength.
 - or $d \ll c\tau_r$, the distance of the wave that propagates where τ_r is the pulse rise time

→ conduction current density: $\vec{j}_c = \sigma \vec{E}$
displacement current density: $\vec{j}_d = \frac{\partial \vec{D}}{\partial t}$

Maxwell's eq:

$$\nabla \times \vec{E} = -\frac{\partial \vec{B}}{\partial t}$$
$$\nabla \times \vec{H} = \frac{\partial \vec{D}}{\partial t} + \vec{j}$$

Electromagnetic field sensors



- Ideal conducting sensor of area A :

$$i(t) = [j_c(t) + \dot{D}(t)]A = [\sigma E(t) + \epsilon \epsilon_0 \dot{E}(t)]A$$

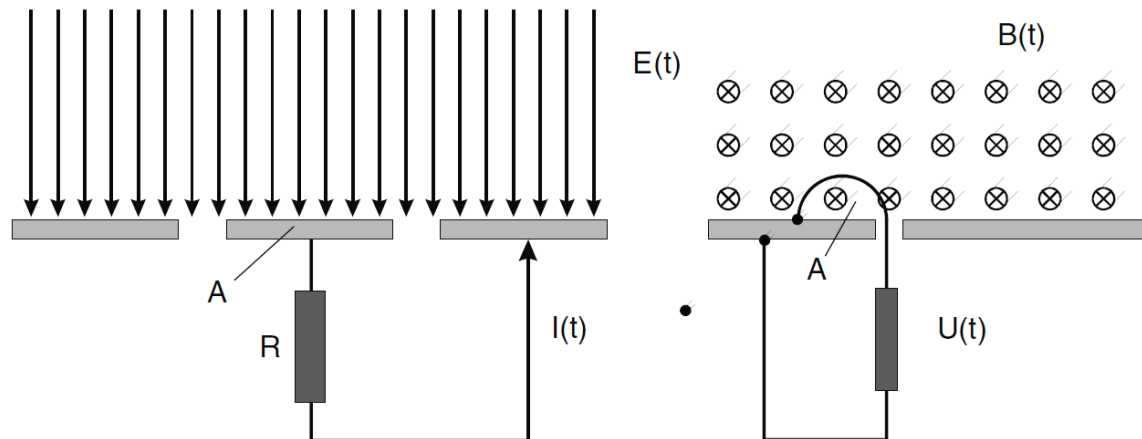
The sensitivity depends on σ , ϵ , A , $E(t)$, $\dot{E}(t)$, and ω .

- Alternating magnetic fields \Rightarrow induce currents in conducting loops.

$$u(t) = - \oint \dot{\vec{B}}(t) d\vec{A} \approx - \dot{\vec{B}}(t) \vec{A} \quad \Leftarrow \text{if field is homogeneous.}$$

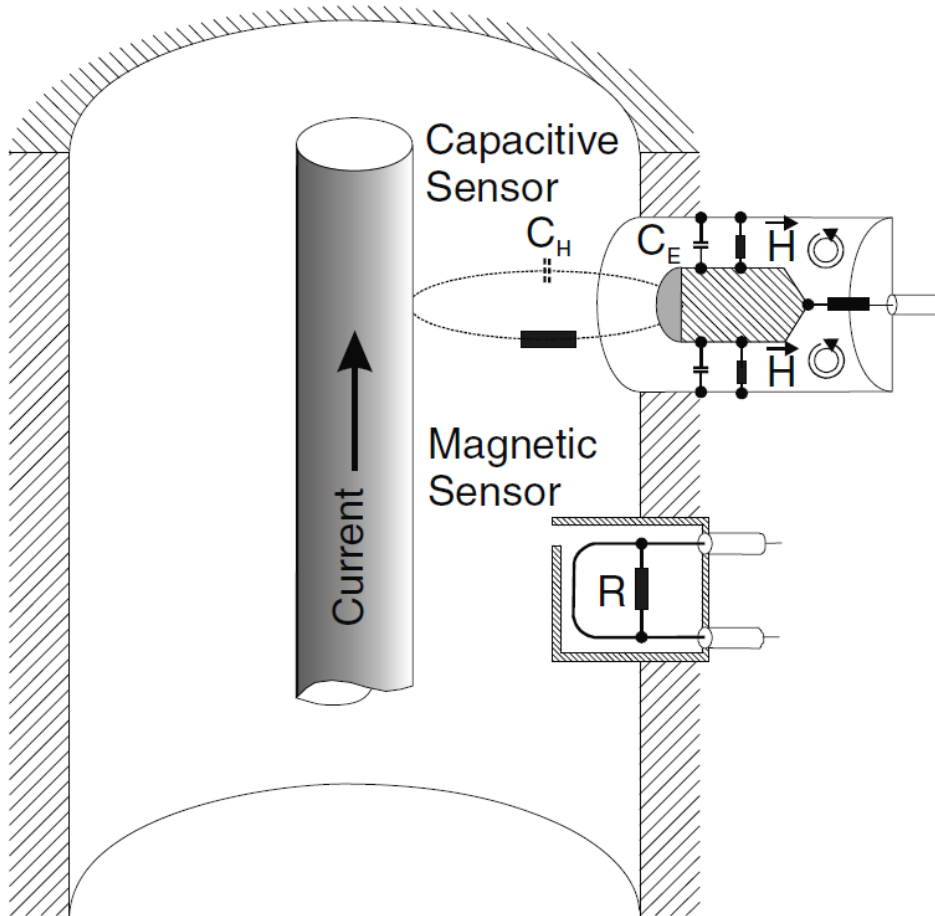
The sensitivity depends on A , $\dot{B}(t)$, and ω .

Quasistationary Fields



- The coupling may also couple the undesired noise.

Capacitive/Inductive sensors



$$u(t) = \frac{C_H}{C_H + C_E} U(t)$$

$$u(t) = - \oint \dot{\vec{B}}(t) d\vec{A} = - \frac{d\phi}{dt}$$

Capacitive sensor for voltage measurement



$$V_{in} = V_{C_1} + V_{out} \quad I_p = I_{C_2} + I_{R_S}$$

$$I_p = C_1 \frac{dV_{C_1}}{dt} \quad I_{C_2} = C_2 \frac{dV_{out}}{dt} \quad I_{R_S} = \frac{V_{out}}{R_S}$$

$$C_1 \frac{dV_{C_1}}{dt} = C_2 \frac{dV_{out}}{dt} + \frac{V_{out}}{R_S}$$

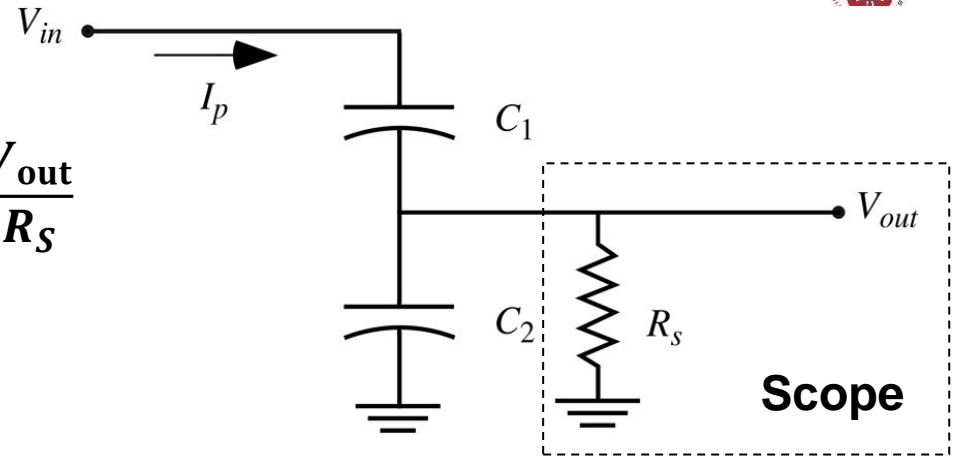
$$\frac{dV_{C_1}}{dt} = \frac{C_2}{C_1} \frac{dV_{out}}{dt} + \frac{V_{out}}{R_S C_1}$$

$$\frac{dV_{in}}{dt} = \frac{dV_{C_1}}{dt} + \frac{dV_{out}}{dt}$$

$$\frac{dV_{in}}{dt} = \left(\frac{C_1 + C_2}{C_1} \right) \frac{dV_{out}}{dt} + \frac{V_{out}}{R_S C_1}$$

$$\frac{V_{in}}{V_{out}} = \left(\frac{C_1 + C_2}{C_1} \right) + \frac{1}{sR_S C_1}$$

$$= \left(\frac{C_1 + C_2}{C_1} \right) \left[1 + \frac{1}{sR_S(C_1 + C_2)} \right]$$



$$\omega_{3dB} = \frac{1}{R_S(C_1 + C_2)}$$

- **Low frequency:**

$$V_{out} = \frac{C_1}{C_1 + C_2} V_{in}$$

- **High frequency:**

$$V_{out} = R_S C_1 \frac{dV_{in}}{dt}$$

Inductive sensor with RC integrator for current measurement



$$|u(t)| = \frac{d\phi}{dt} = L \frac{di}{dt} + Ri + \frac{1}{C} \int_0^t i dt'$$

$$|u(t)| = \frac{d\phi}{dt} = k \frac{di}{dt}$$

$$|u(t)| = \frac{d\phi}{dt} \approx Ri + \frac{1}{C} \int_0^t i dt'$$

$$u_s = \frac{1}{C} \int_0^t i dt' \Rightarrow C \dot{u}_s = i$$

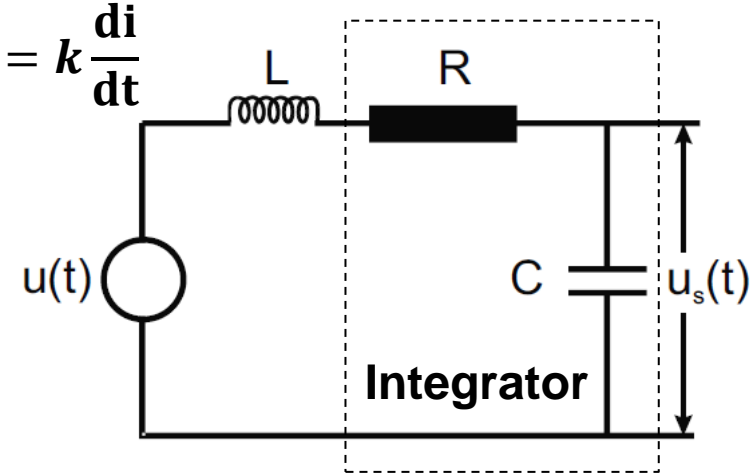
$$u = RC \dot{u}_s + u_s$$

$$\dot{u}_s + \frac{1}{RC} u_s = \frac{1}{RC} u$$

$$\dot{u}_s e^{\frac{1}{RC}t} + \frac{1}{RC} u_s e^{\frac{1}{RC}t} = \frac{1}{RC} u e^{\frac{1}{RC}t}$$

$$\frac{d}{dt} \left(u_s e^{\frac{1}{RC}t} \right) = \frac{1}{RC} u e^{\frac{1}{RC}t}$$

$$\int d \left(u_s e^{\frac{1}{RC}t'} \right) = \frac{1}{RC} \int_0^t u e^{\frac{1}{RC}t'} dt'$$



$$u_s e^{\frac{1}{RC}t} - u_s(0) = \frac{1}{RC} \int_0^t u e^{\frac{1}{RC}t'} dt'$$

$$u_s = \frac{e^{-\frac{1}{RC}t}}{RC} \int_0^t u e^{\frac{1}{RC}t'} dt' \approx \frac{1}{RC} \int_0^t u dt'$$

$$= \frac{k}{RC} i(t)$$

- Working regime:

$$RC \gg t \approx \frac{1}{\omega} \quad \omega \gg \frac{1}{RC}$$

Rogowski coil

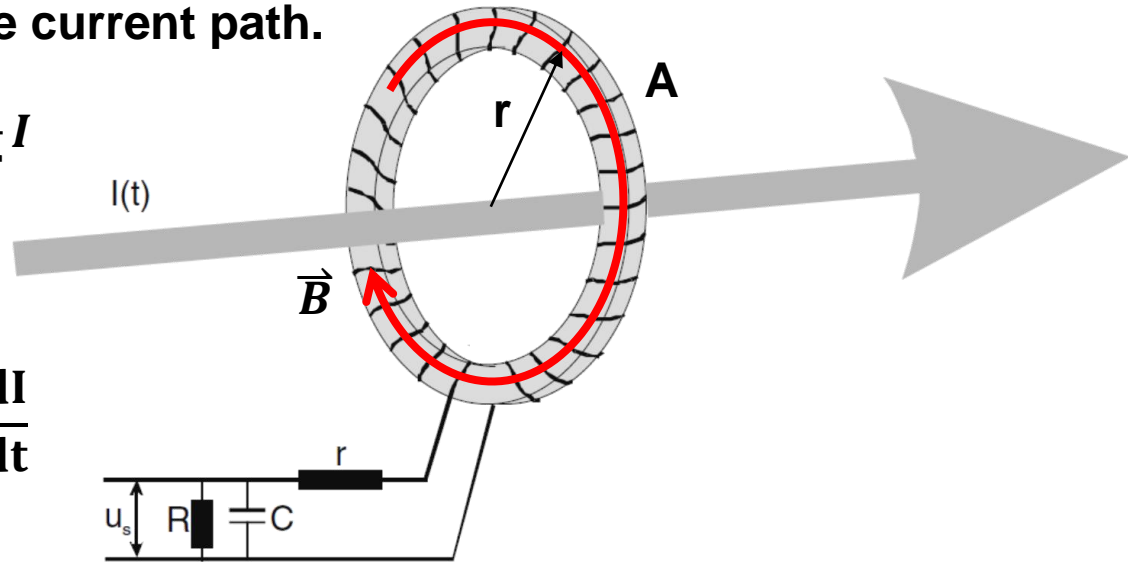


- In situ calibration is needed to obtain k . $|u(t)| = \frac{d\phi}{dt} = k \frac{di}{dt}$
- If in situ calibration is not possible, Rogowski coil instead of a simple current loop is used.
- Rogowski coil is a coil consisting of many windings lined up in a toroidal configuration encircling the current path.

$$\oint \vec{B} \cdot d\vec{l} = \mu_0 I \quad B = \frac{\mu_0 I}{2\pi r}$$

$$\phi_1 = BA = \frac{\mu_0 A}{2\pi r} I$$

$$|u| = \frac{d\phi}{dt} = N \frac{d\phi_1}{dt} = \frac{\mu_0 AN}{2\pi r} \frac{dI}{dt}$$

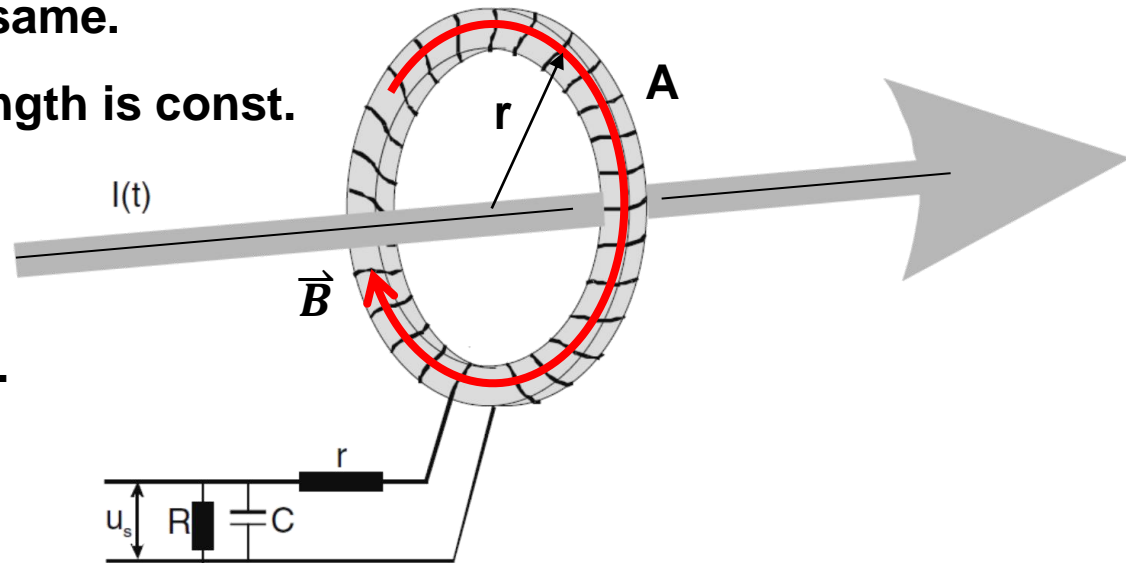


$$u_s(t) = \frac{1}{RC} \int u dt = \frac{1}{RC} \frac{\mu_0 AN}{2\pi r} \int \frac{dI}{dt} dt = \frac{1}{RC} \frac{\mu_0 AN}{2\pi r} I$$

Assumption for Rogowski coil



- Neglect the spatial dependence of the magnetic induction over the area A
- Cross section A are all the same.
- Number of turns per unit length is const.
- When #/ of turns increase,
L may be large
 $\Rightarrow L\omega \ll R$ may not be met.
 \Rightarrow use the opposite regime
where $L\omega \gg R$.
It becomes “self-integrated.”



Self-integrated current monitor where $L\omega \gg R$



$$R_o \gg R \quad L\omega \gg R_o + R$$

$$u - L \frac{dI}{dt} = u_s \quad u_s = IR_o$$

$$u - \frac{L}{R_o} \frac{du_s}{dt} = u_s \quad \frac{du_s}{dt} + \frac{R_o}{L} u_s = \frac{R_o}{L} u$$

$$e^{-\frac{R_o}{L}t} \frac{d}{dt} \left(u_s e^{\frac{R_o}{L}t} \right) = \frac{R_o}{L} u \quad \frac{d}{dt} \left(u_s e^{\frac{R_o}{L}t} \right) = \frac{R_o}{L} u e^{\frac{R_o}{L}t}$$

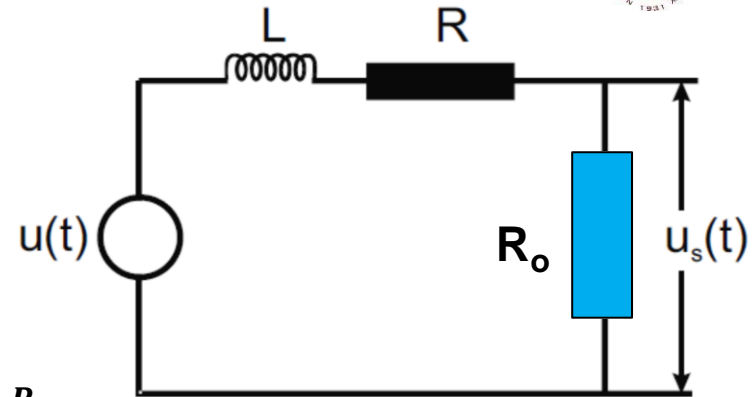
$$u_s e^{\frac{R_o}{L}t} - u_s(0) = \frac{R_o}{L} \int u e^{\frac{R_o}{L}t'} dt'$$

$$u_s = \frac{R_o}{L} e^{-\frac{R_o}{L}t} \int u e^{\frac{R_o}{L}t'} dt' \quad L\omega \gg R_o \quad t \frac{R_o}{L} \ll 1 \quad |u| = \frac{d\phi}{dt} = N \frac{d\phi_1}{dt} = \frac{\mu_o AN}{2\pi r} \frac{dI}{dt}$$

$$u_s = \frac{R_o}{L} \int u dt' = \frac{R_o}{L} \int \frac{\mu_o AN}{2\pi r} \frac{dI}{dt} dt' = \frac{R_o \mu_o AN}{L 2\pi r} I \quad \Leftarrow \text{self integrated!}$$

$u_s \propto R_o$

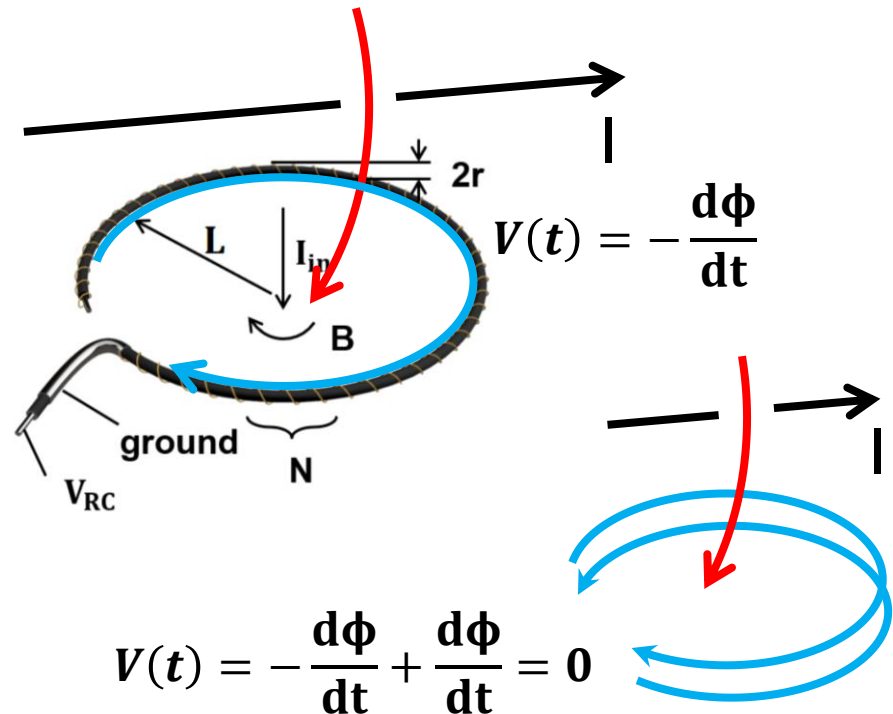
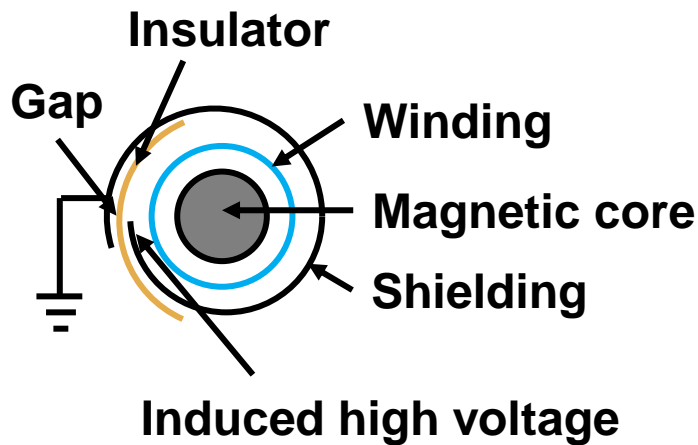
- Ferromagnetic material in the torus may be used to increase inductance.



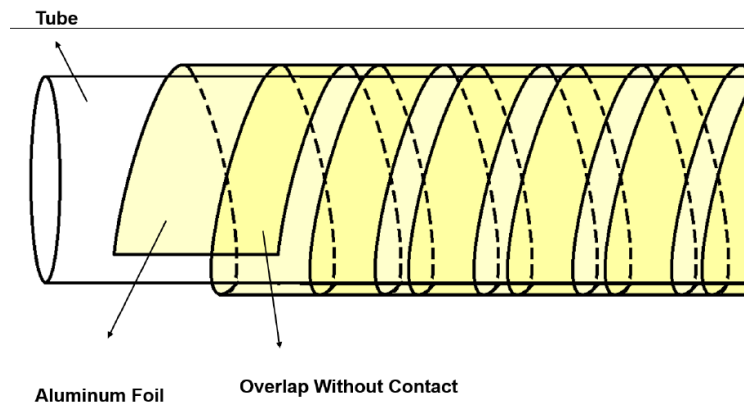
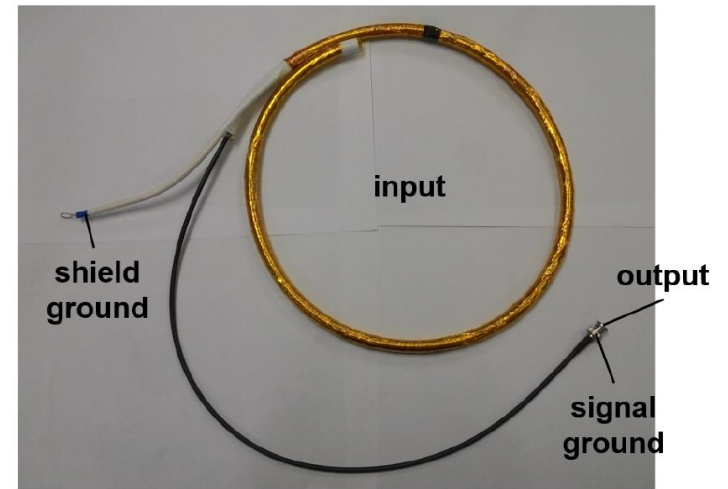
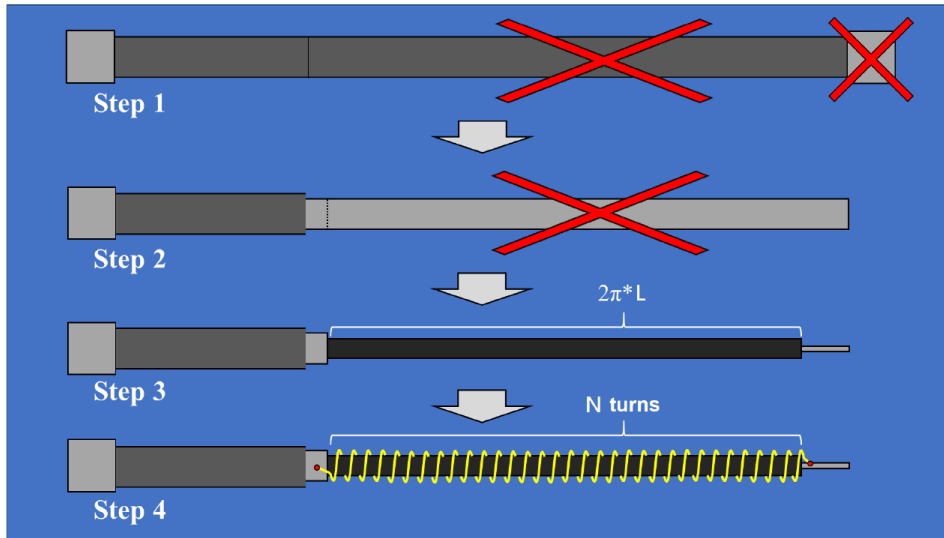
Additional note for Rogowski coil



- To reduce the capacitive coupling, wrap the Rogowski coil with a slotted metallic case. However, it needs to let the flux go into the winding. NO closed loop is allowed.
- A large flux penetrating the main opening of the torus may induce additional voltage. To compensate for this signal, feed one end of the wire back through the windings



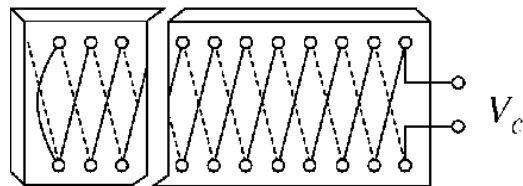
Fabrication of the Rogowski coil using a coaxial cable



Other ways of making compensated Rogowski coil

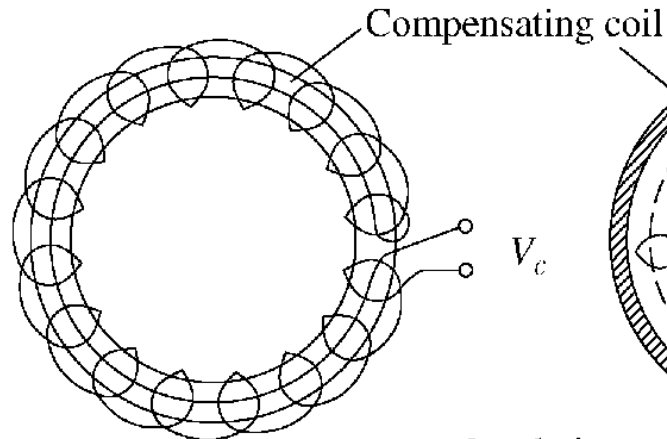


- Bifilar



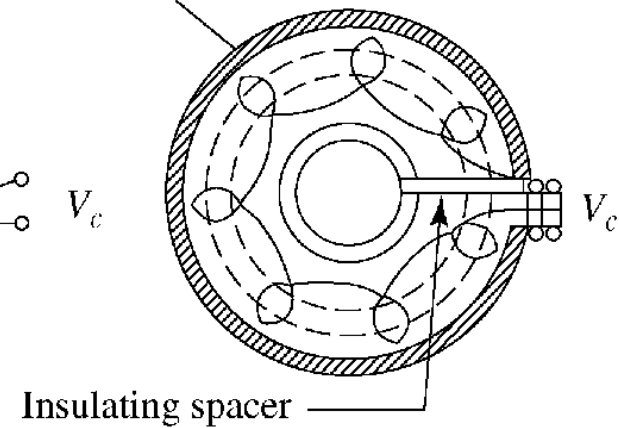
(a)

- Inner compensating coil



(b)

- Outer compensating coil



(c)

Current-viewing resistors (CVRs)



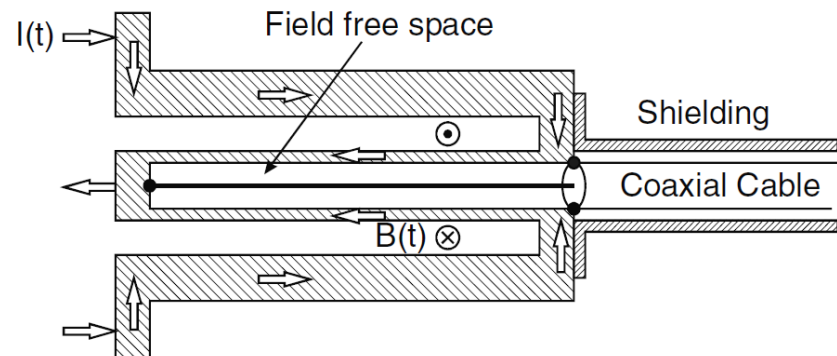
- It is also called “shunts.”
- Measurement of the voltage drop across a resistor of known value, incorporated into the circuit.

$$I = \frac{V}{R}$$

- The current path and the measuring circuit are coupled not only through the Ohmic resistor but also magnetically.

=> preferable to place the metering contact in a field-free space or reduce the coupling efficiency.

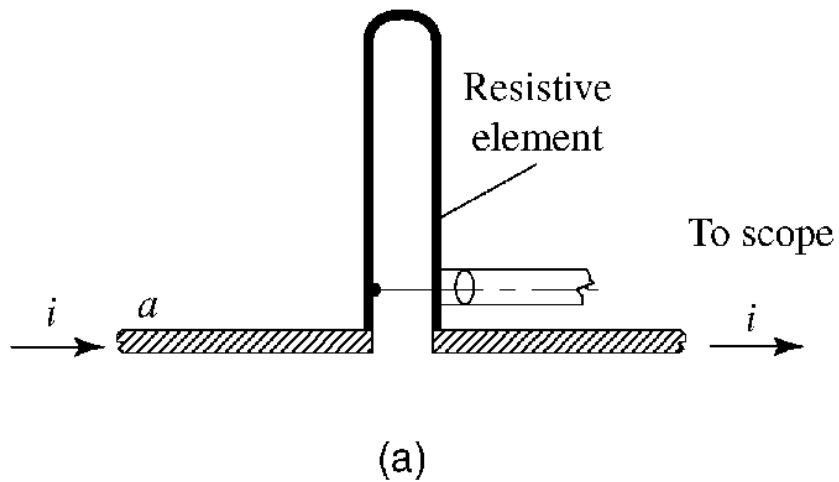
- Cylindrically symmetric shunt geometry provides an zero magnetic coupling.



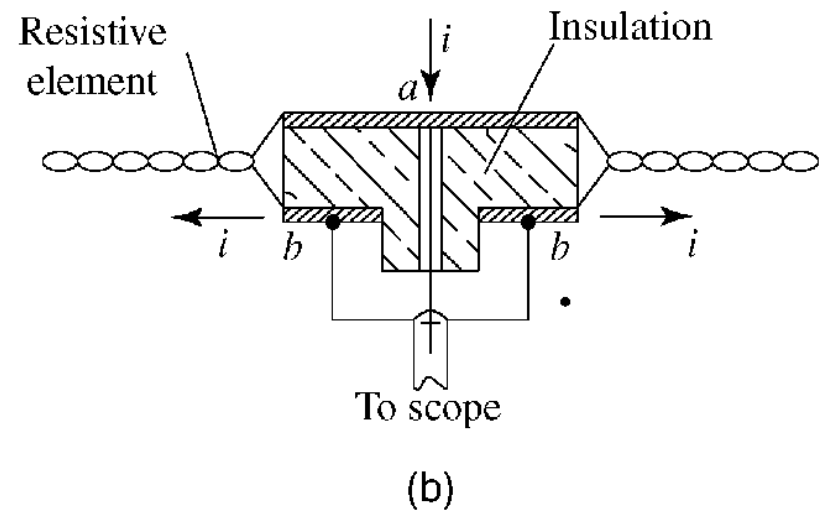
Shunts



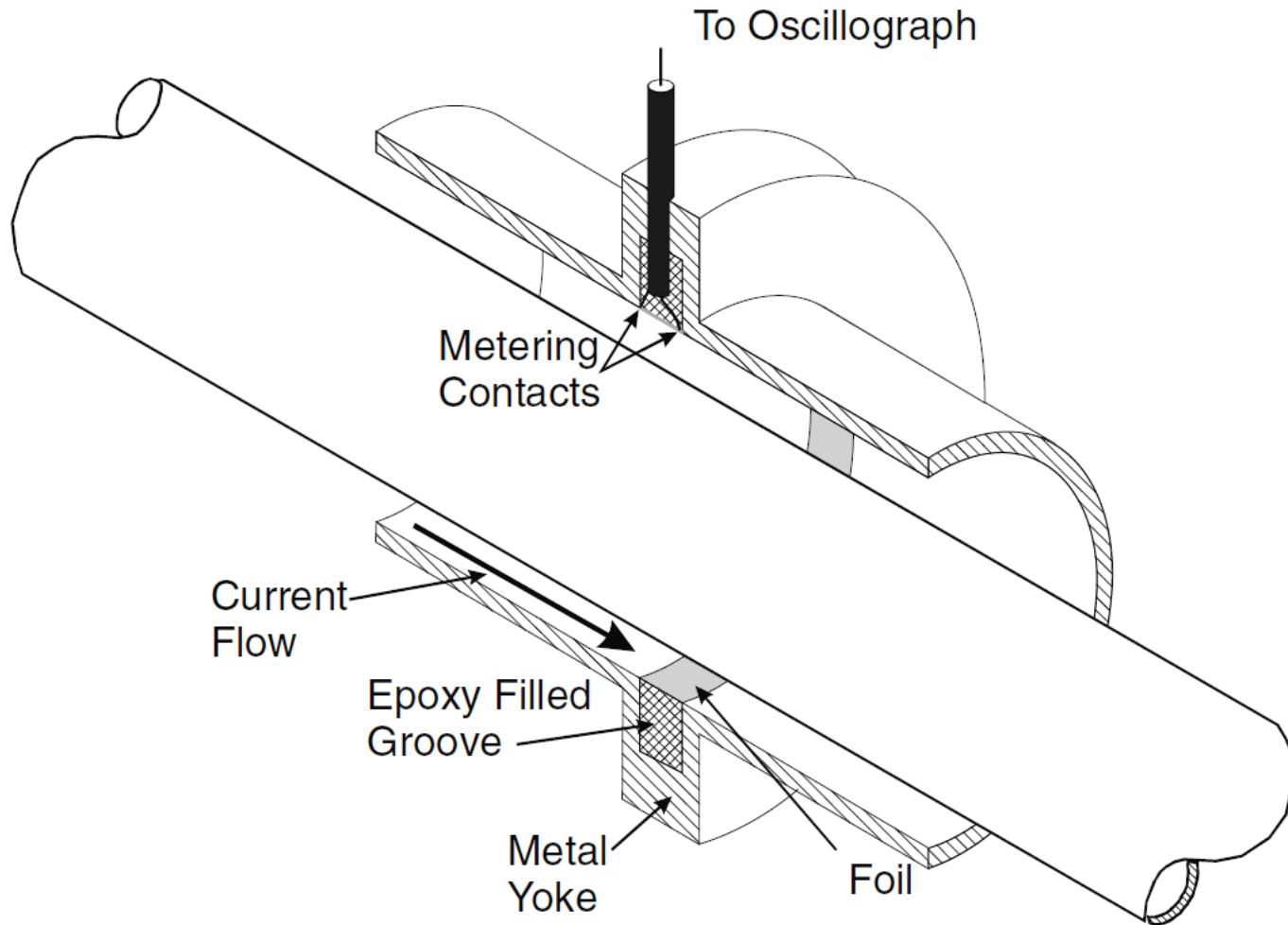
- **Folded strip shunt**



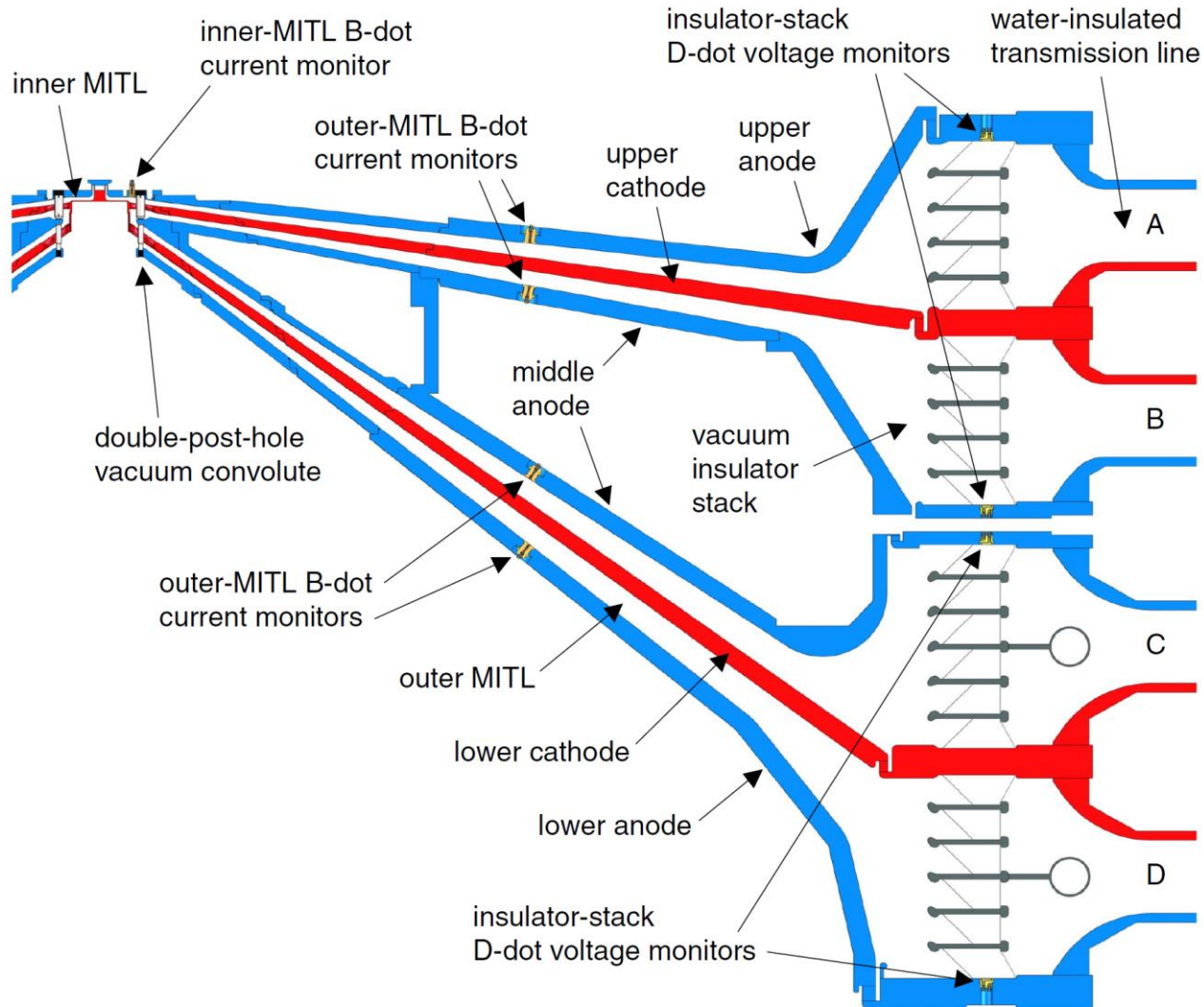
- **Parallel twisted shunt**



CVR integrated into the outer conductor of a coaxial transmission line



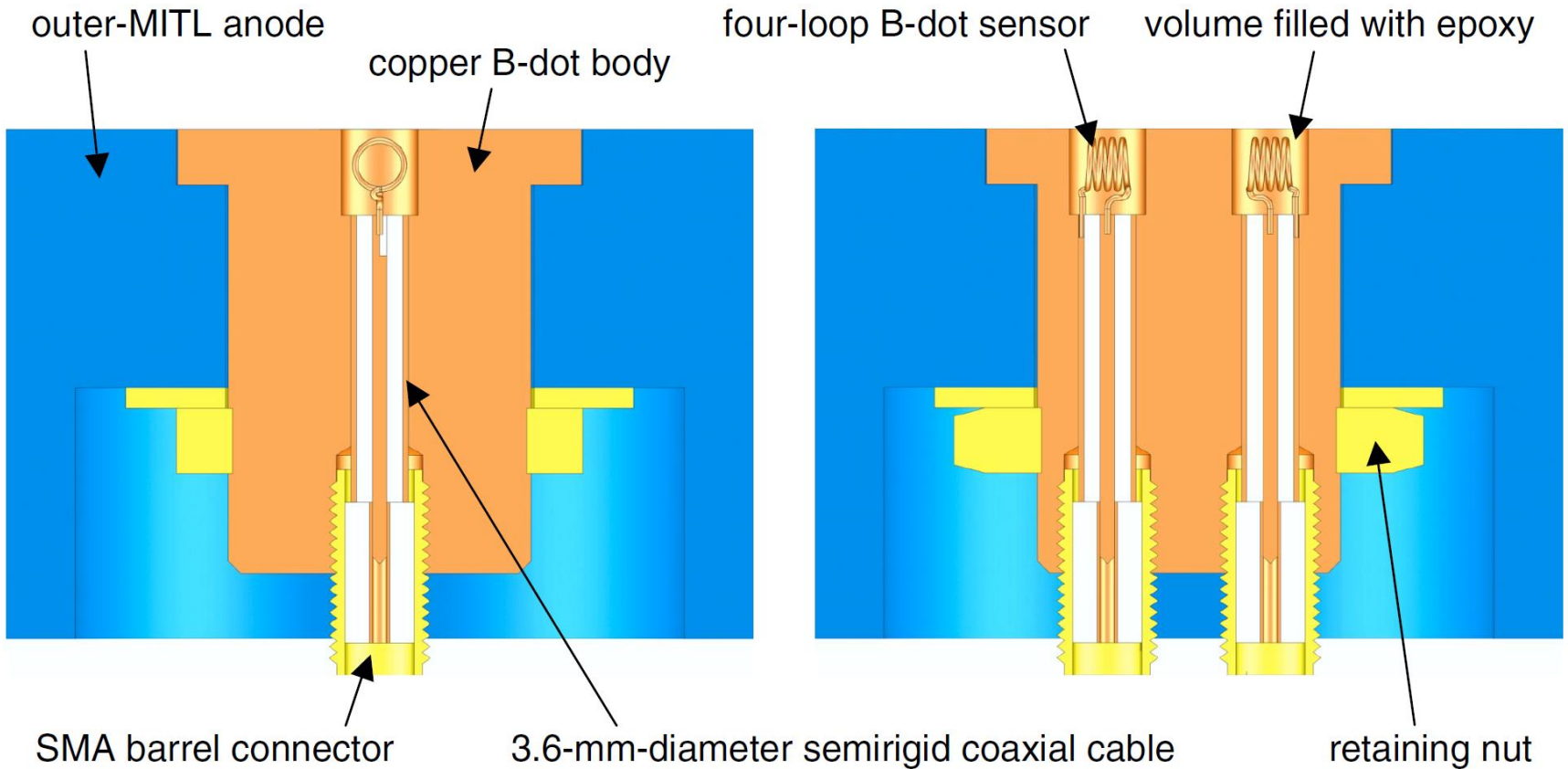
Example of current and voltage monitor using B-dot and D-dot monitors



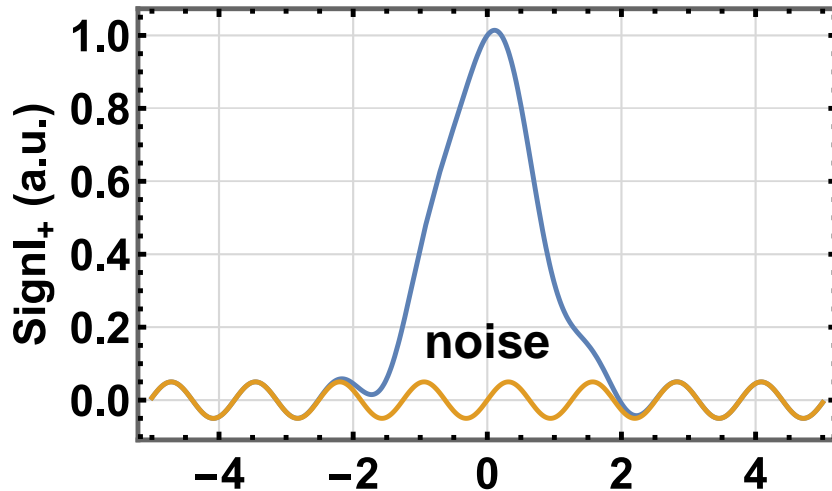
Differential current monitors



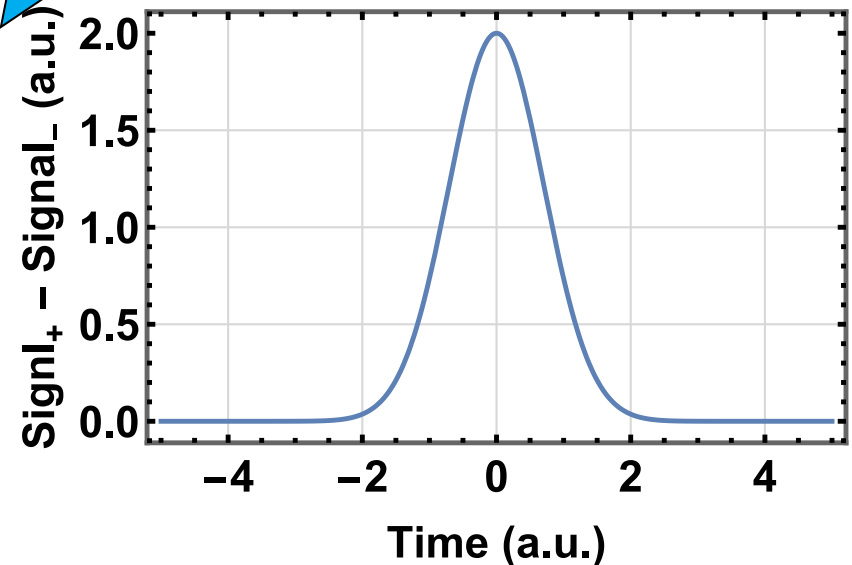
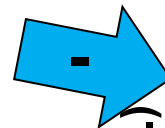
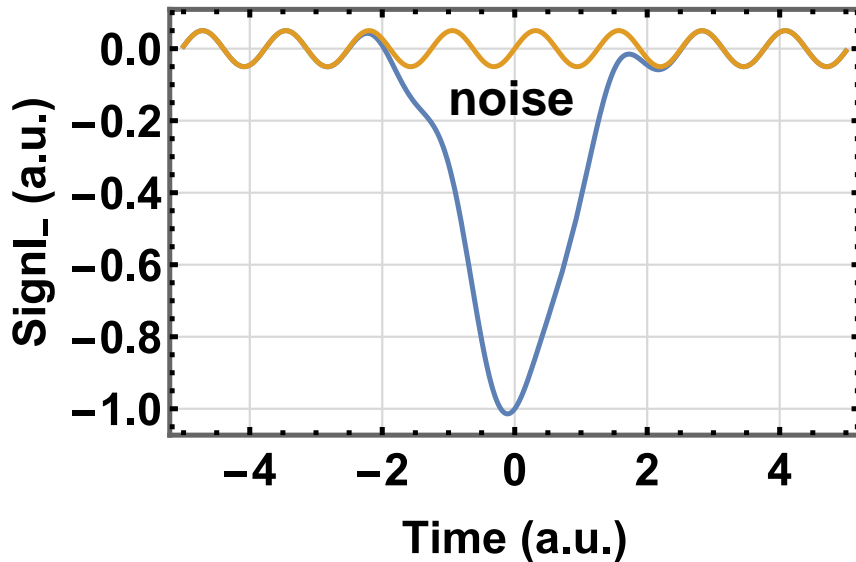
- **Outer MITL B-dot current monitors:**



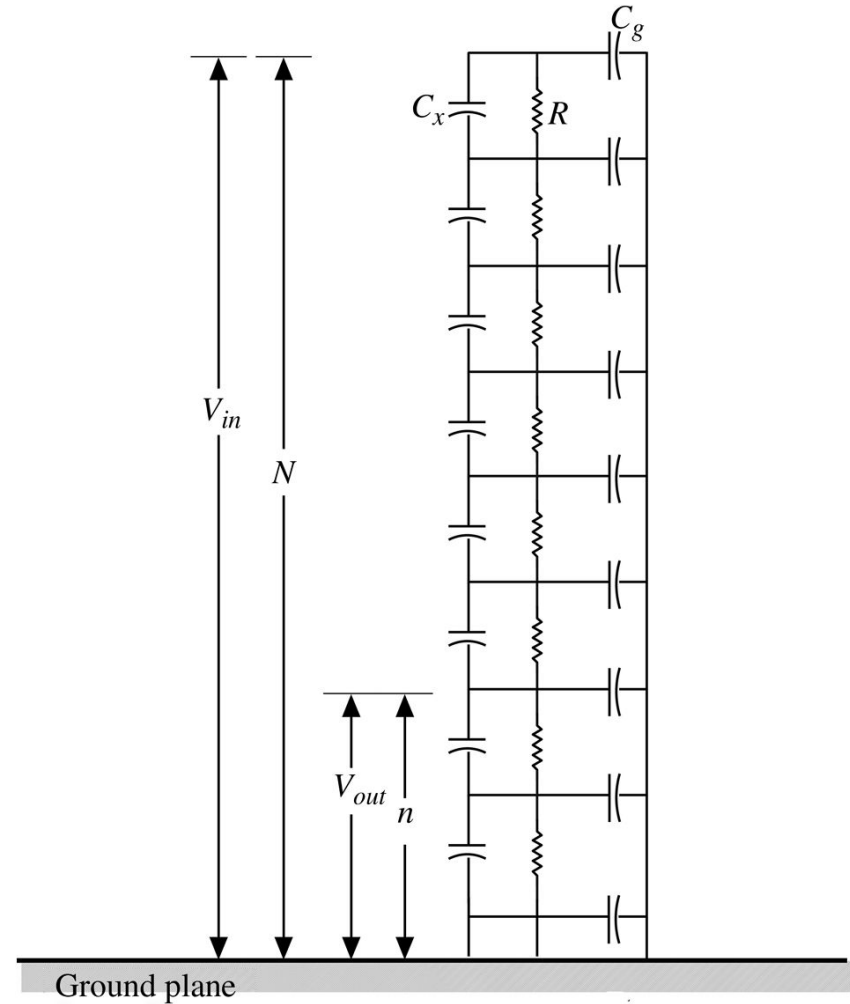
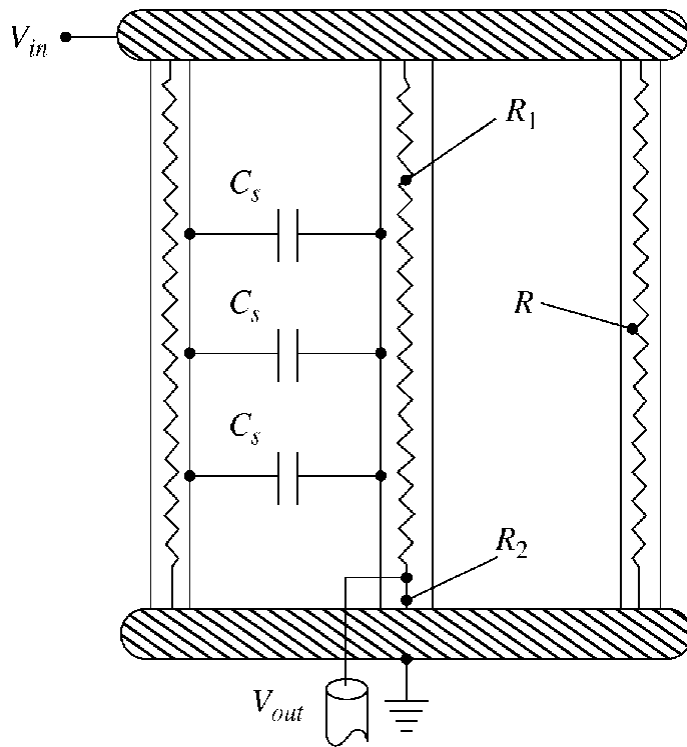
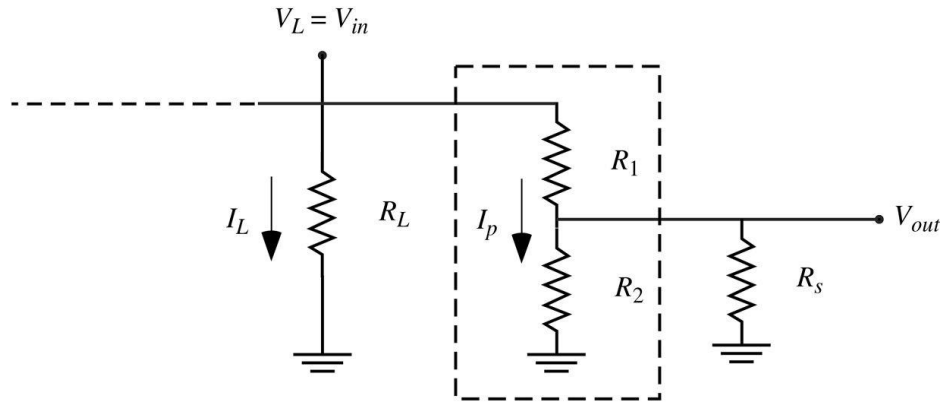
Differential current monitors



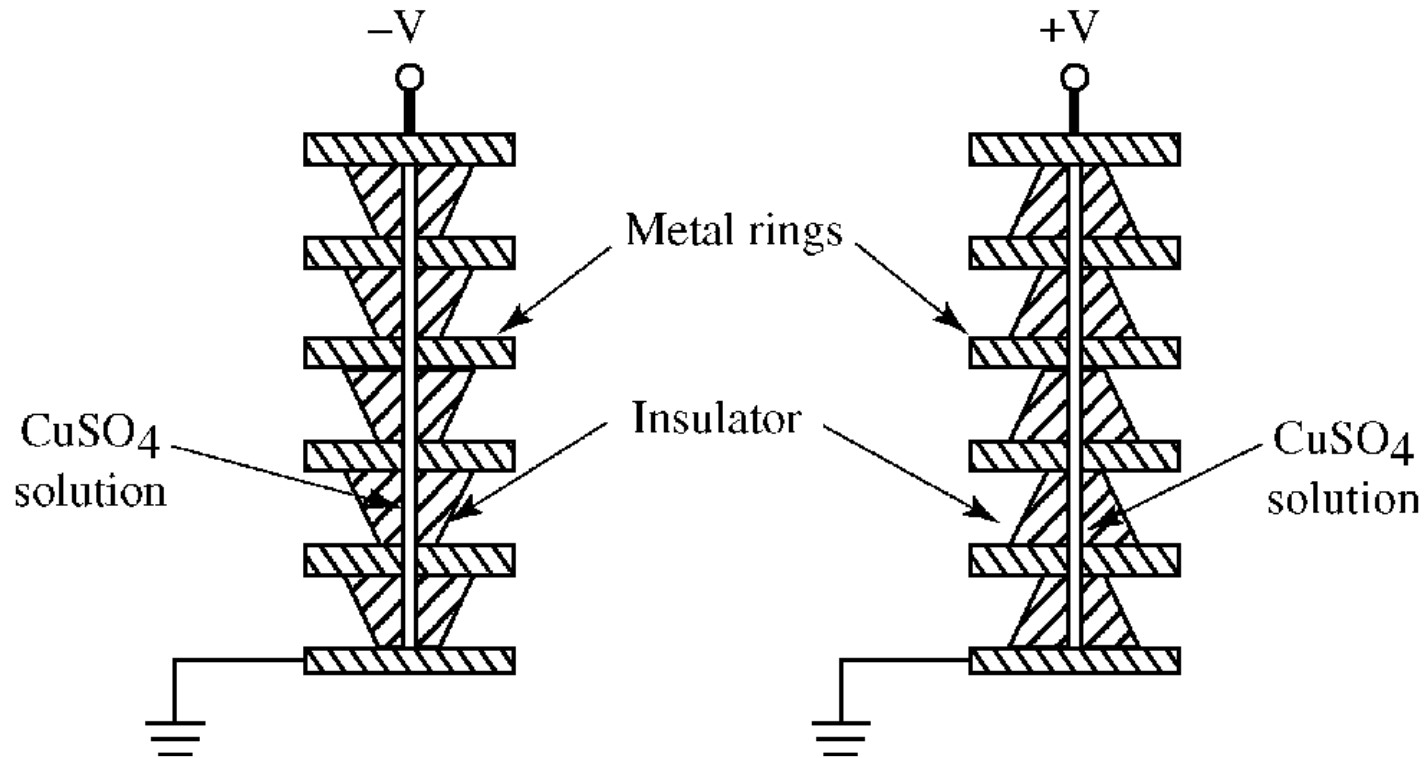
- The two B-dot sensors of each B-dot current monitor are designed to produce “opposite-polarity” signals for “common-mode-noise” rejection.



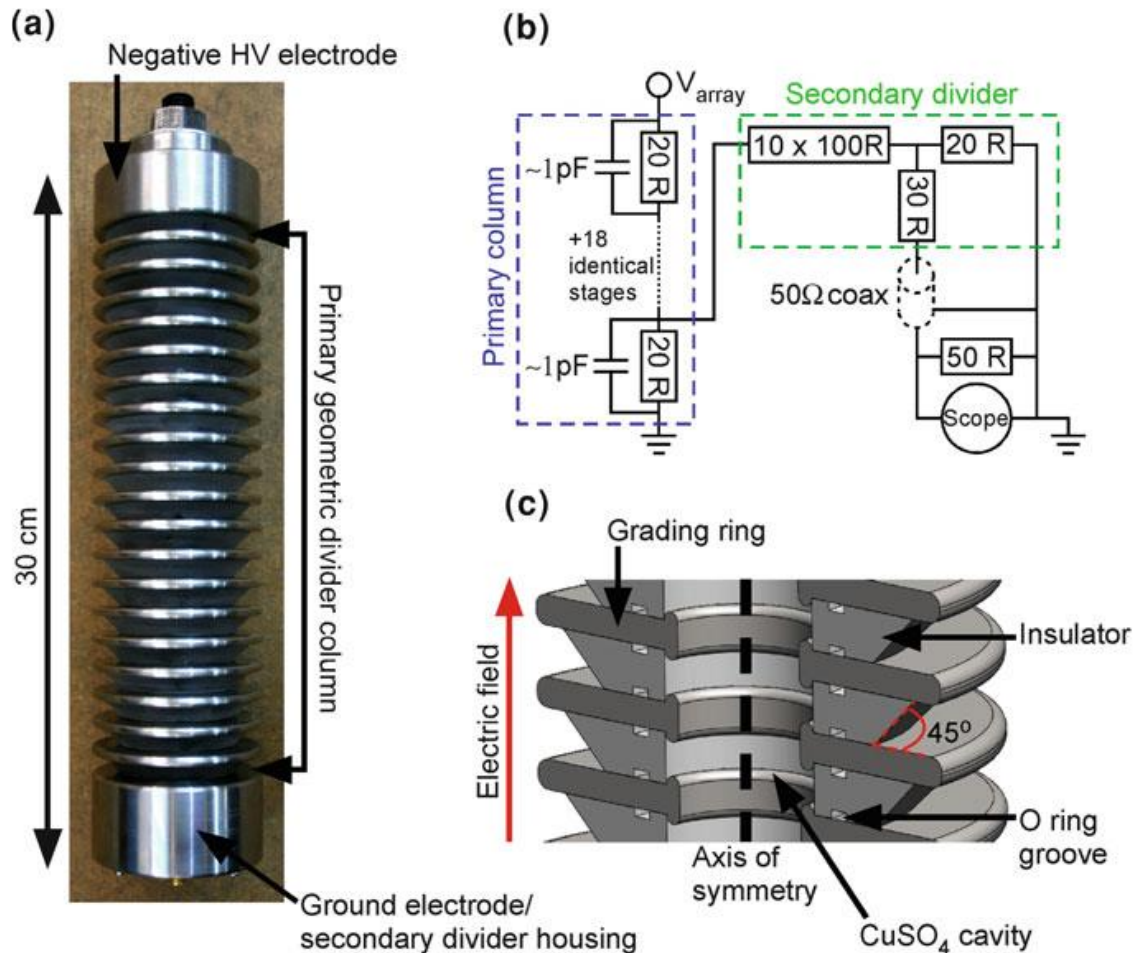
Voltage divider using resistors



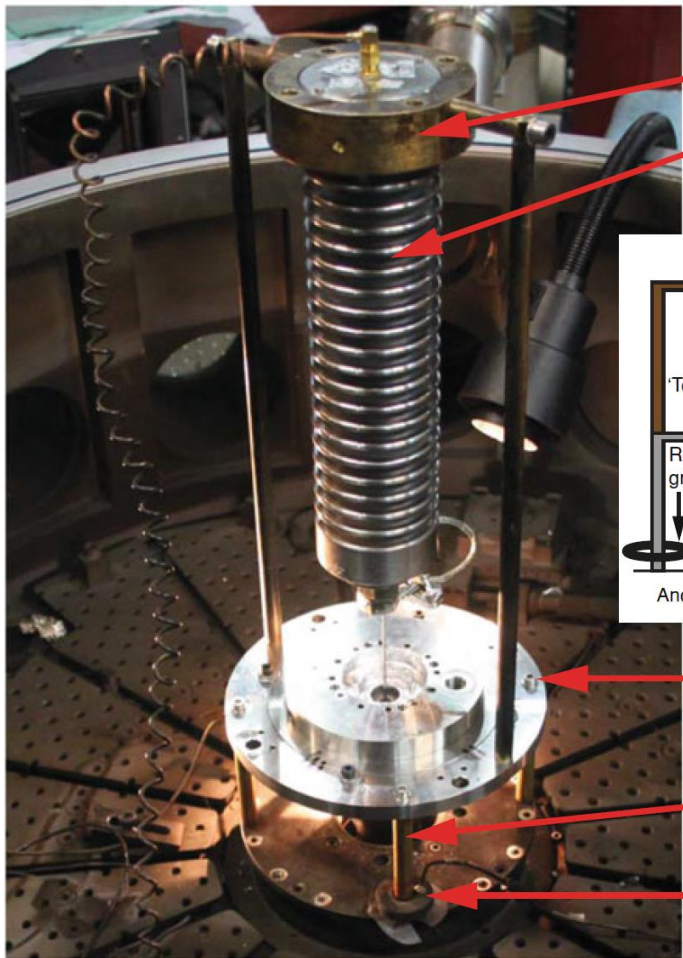
Voltage divider liquid resistors and grading electrodes



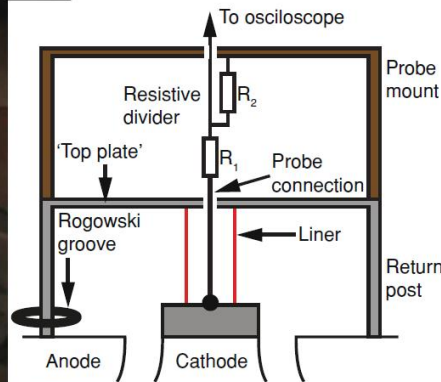
Voltage divider on Mega Ampere Generator for Plasma Implosion Experiments (MAGPIE) facility



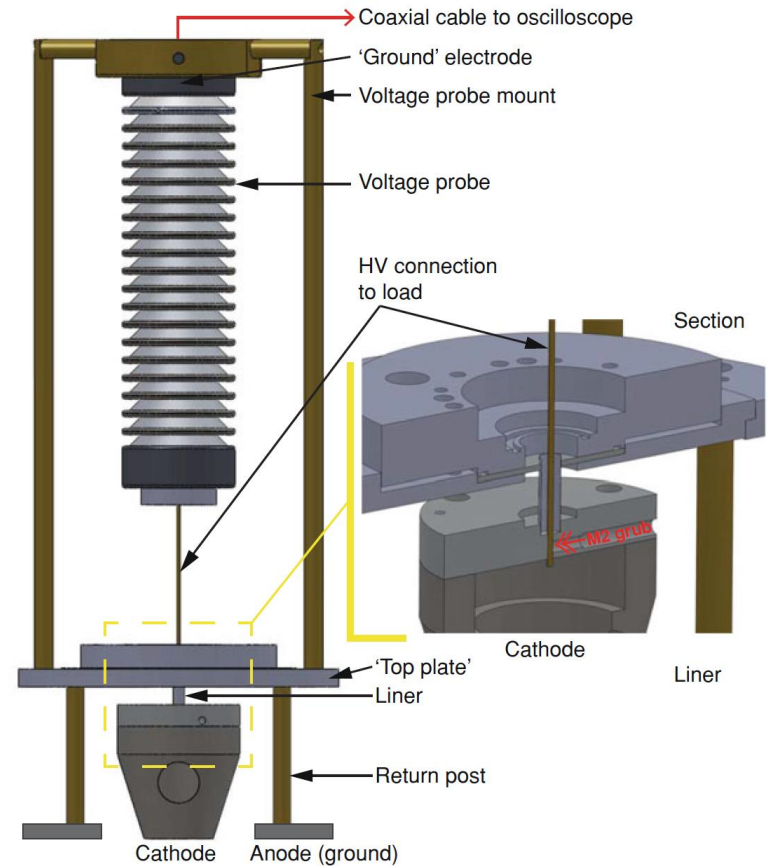
Voltage divider on Mega Ampere Generator for Plasma Implosion Experiments (MAGPIE) facility



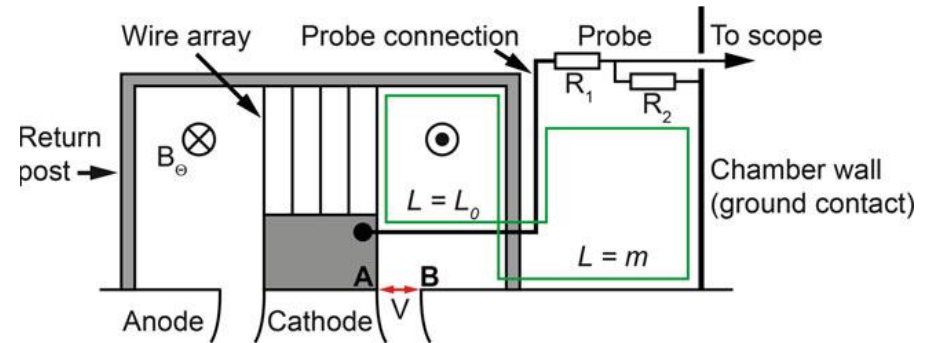
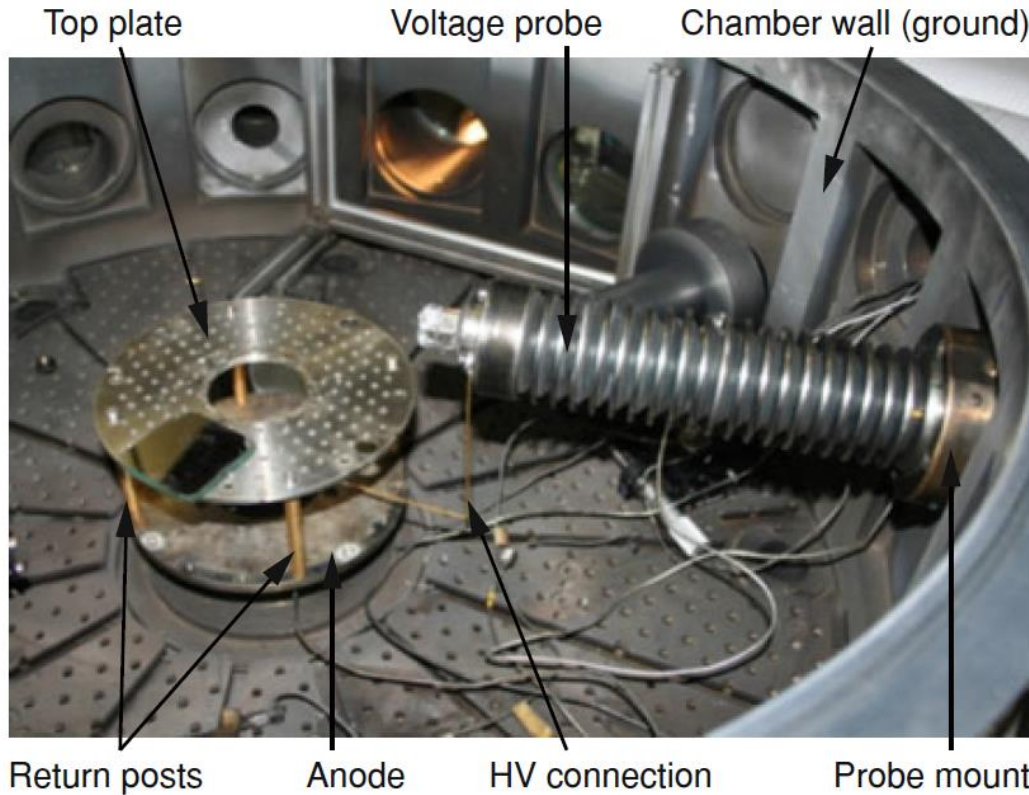
Probe mount
Voltage divider



'Top plate'
Return post
Rogowski groove

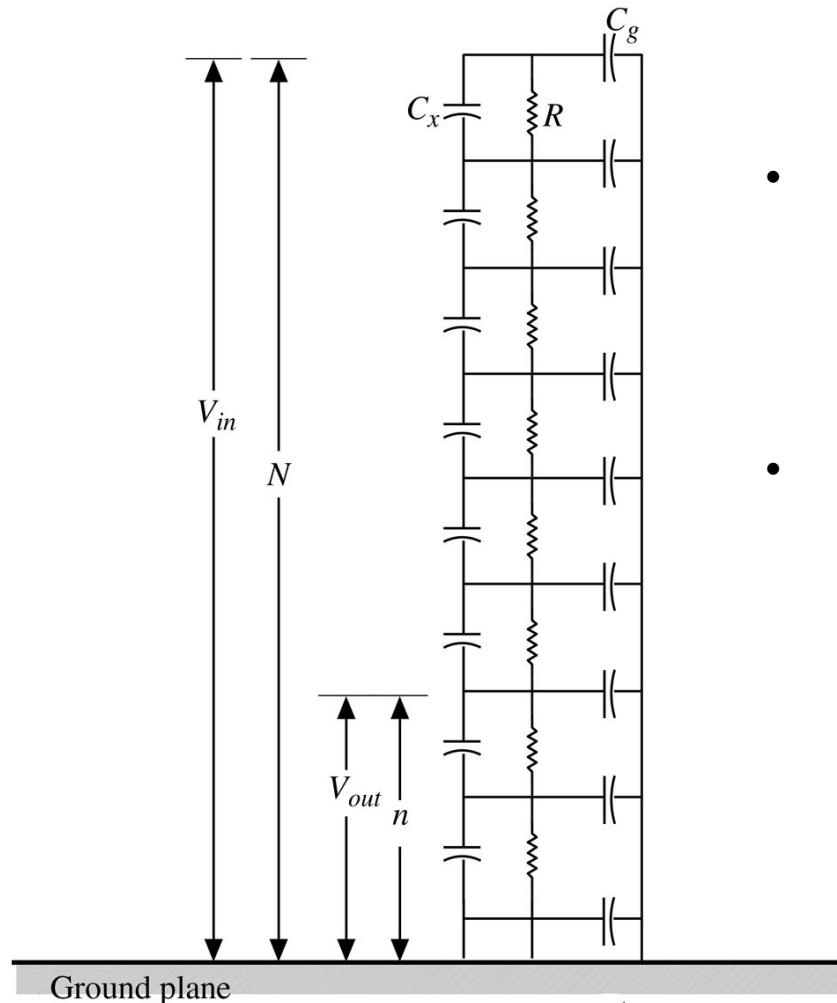


Voltage divider on Mega Ampere Generator for Plasma Implosion Experiments (MAGPIE) facility



Guy C. Burdiak, Cylindrical Liner Z-pinches as Drivers for Converging Strong Shock Experiments

Voltage divider using both resistors and capacitors



- **Low frequency:**

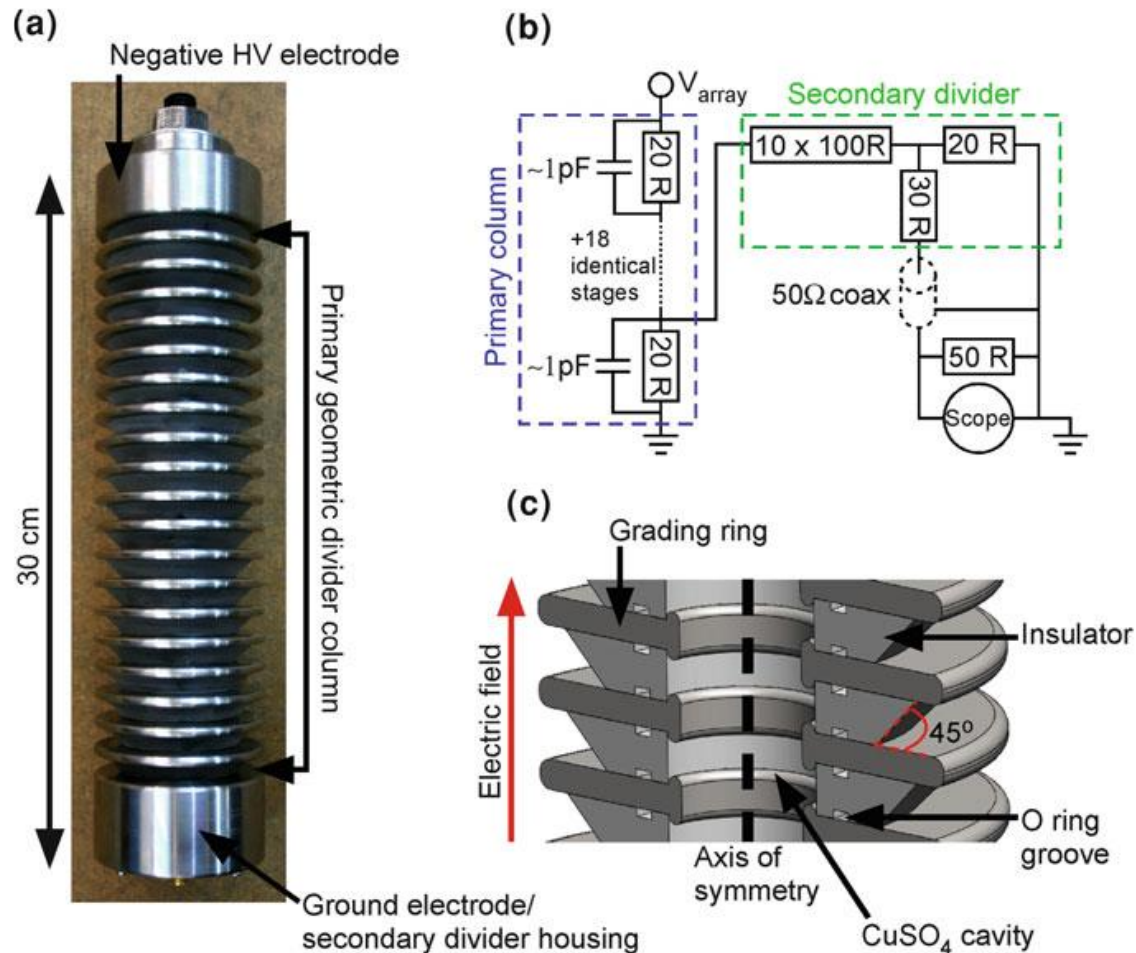
$$V_{out} = \frac{R_o}{\Sigma R_o} V_{in} = \frac{R_o}{NR_o} V_{in} = \frac{1}{N} V_{in}$$

- **High frequency:**

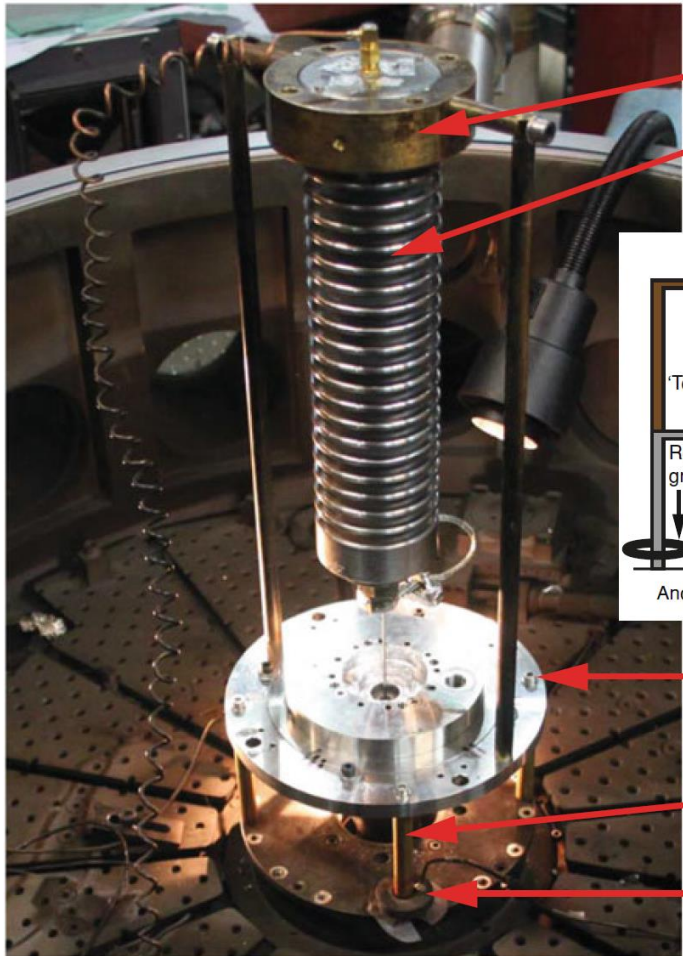
$$\begin{aligned} V_{out} &= \frac{\frac{C_o}{N-1}}{\frac{C_o}{N-1} + C_o} V_{in} = \frac{\frac{1}{N-1}}{\frac{1}{N-1} + 1} V_{in} \\ &= \frac{1}{1 + (N-1)} V_{in} = \frac{1}{N} V_{in} \end{aligned}$$

$$\text{or } V_{out} = \frac{1}{\Sigma \frac{1}{j\omega C_o}} V_{in} = \frac{1}{N} V_{in}$$

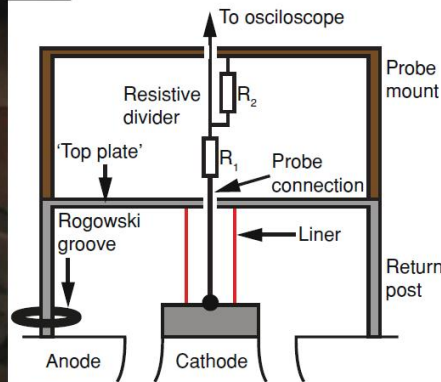
Voltage divider on Mega Ampere Generator for Plasma Implosion Experiments (MAGPIE) facility



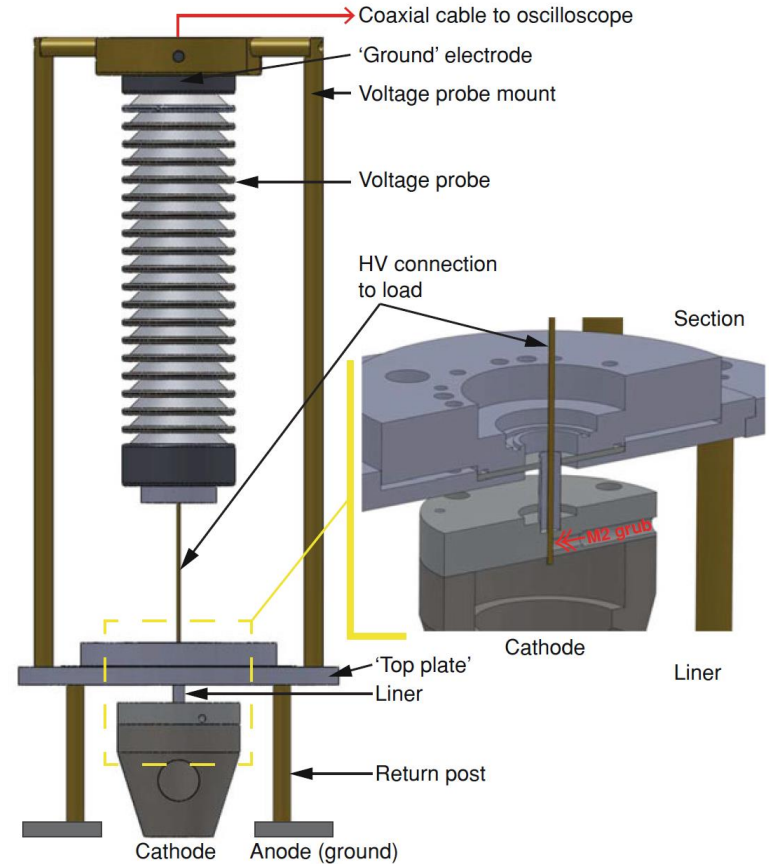
Voltage divider on Mega Ampere Generator for Plasma Implosion Experiments (MAGPIE) facility



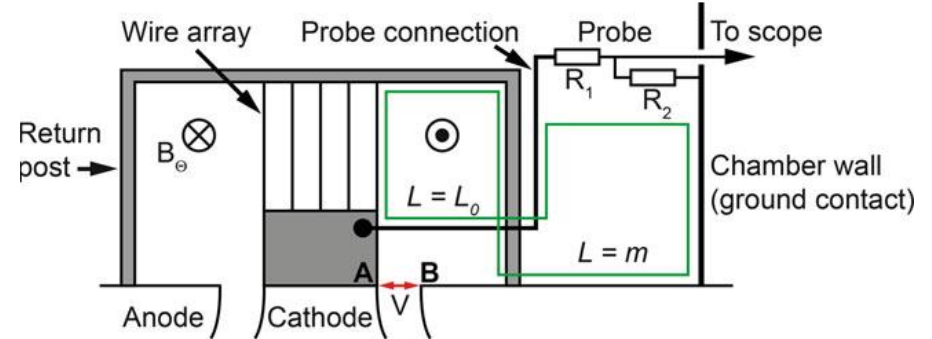
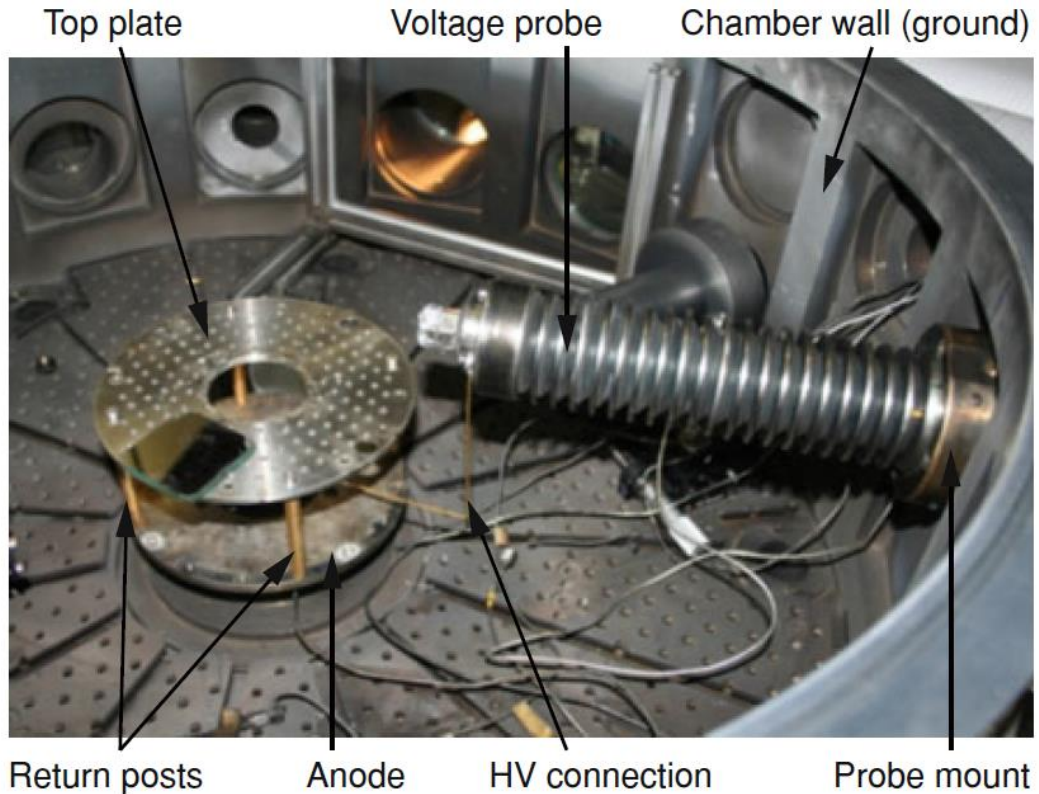
Probe mount
Voltage divider



'Top plate'
Return post
Rogowski groove

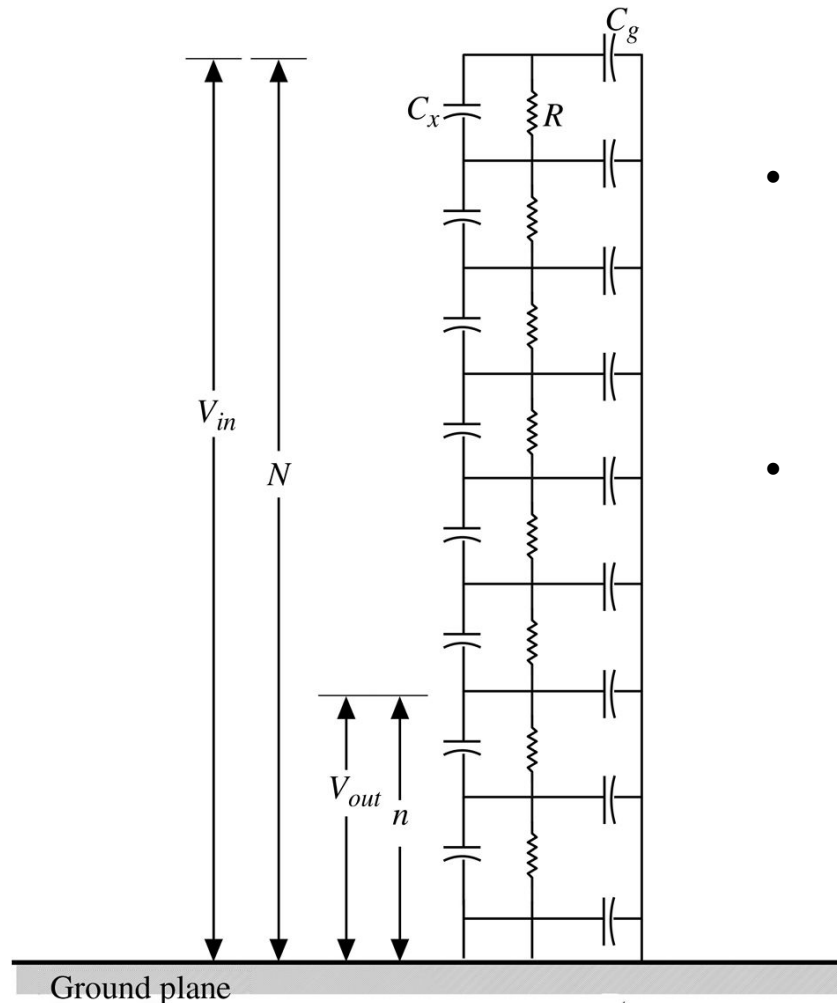


Voltage divider on Mega Ampere Generator for Plasma Implosion Experiments (MAGPIE) facility



Guy C. Burdiak, Cylindrical Liner Z-pinches as Drivers for Converging Strong Shock Experiments

Voltage divider using both resistors and capacitors



- **Low frequency:**

$$V_{out} = \frac{R_o}{\Sigma R_o} V_{in} = \frac{R_o}{NR_o} V_{in} = \frac{1}{N} V_{in}$$

- **High frequency:**

$$\begin{aligned} V_{out} &= \frac{\frac{C_o}{N-1}}{\frac{C_o}{N-1} + C_o} V_{in} = \frac{\frac{1}{N-1}}{\frac{1}{N-1} + 1} V_{in} \\ &= \frac{1}{1 + (N-1)} V_{in} = \frac{1}{N} V_{in} \end{aligned}$$

$$\text{or } V_{out} = \frac{\frac{1}{j\omega C_o}}{\Sigma \frac{1}{j\omega C_o}} V_{in} = \frac{1}{N} V_{in}$$

Outlines



- Power and voltage adding
 - Marx generator
 - LC generator
 - Line pulse transformers
 - Induction voltage adder (IVA)
 - Linear induction accelerator (LIA)
 - Linear transformer driver (LTD)
- Diagnostics
 - Voltage measurement
 - Current measurement
- **Applications of pulsed-power system**

Karlsruhe Light Ion Facility (KALIF)

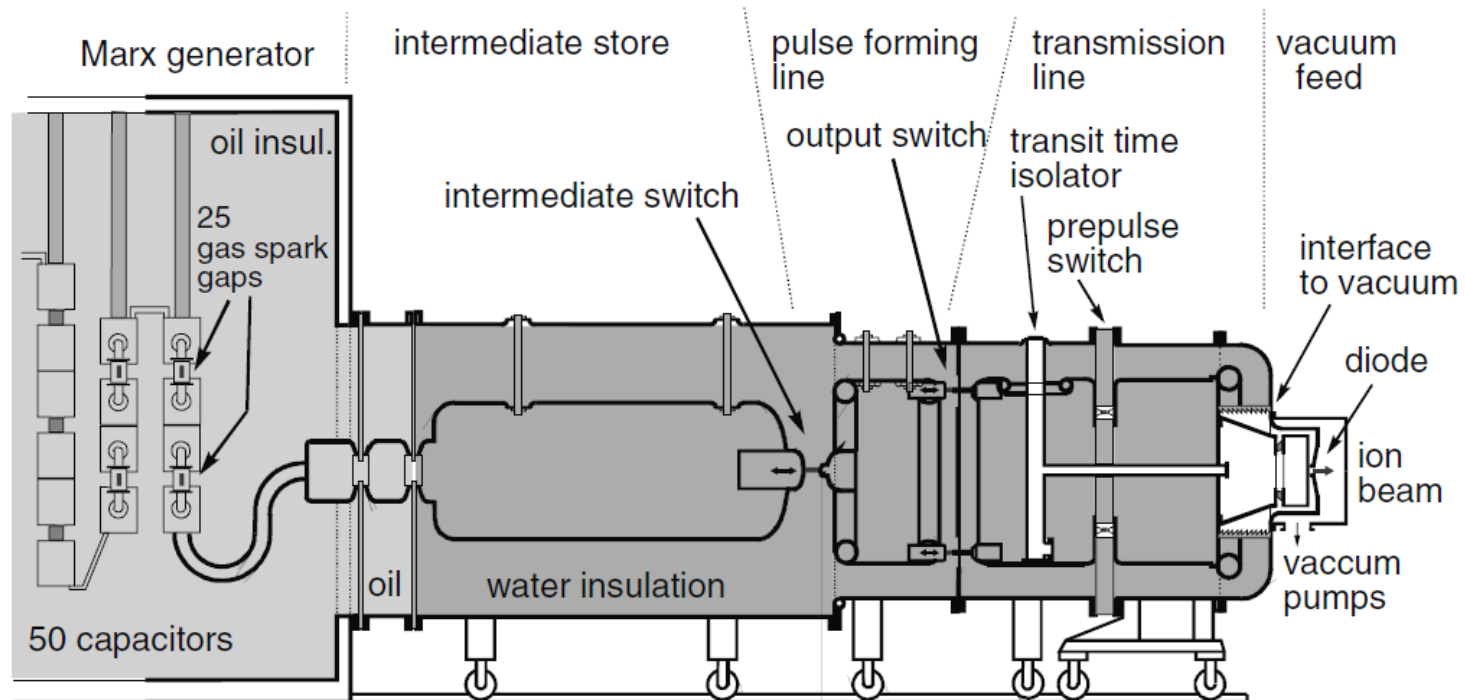
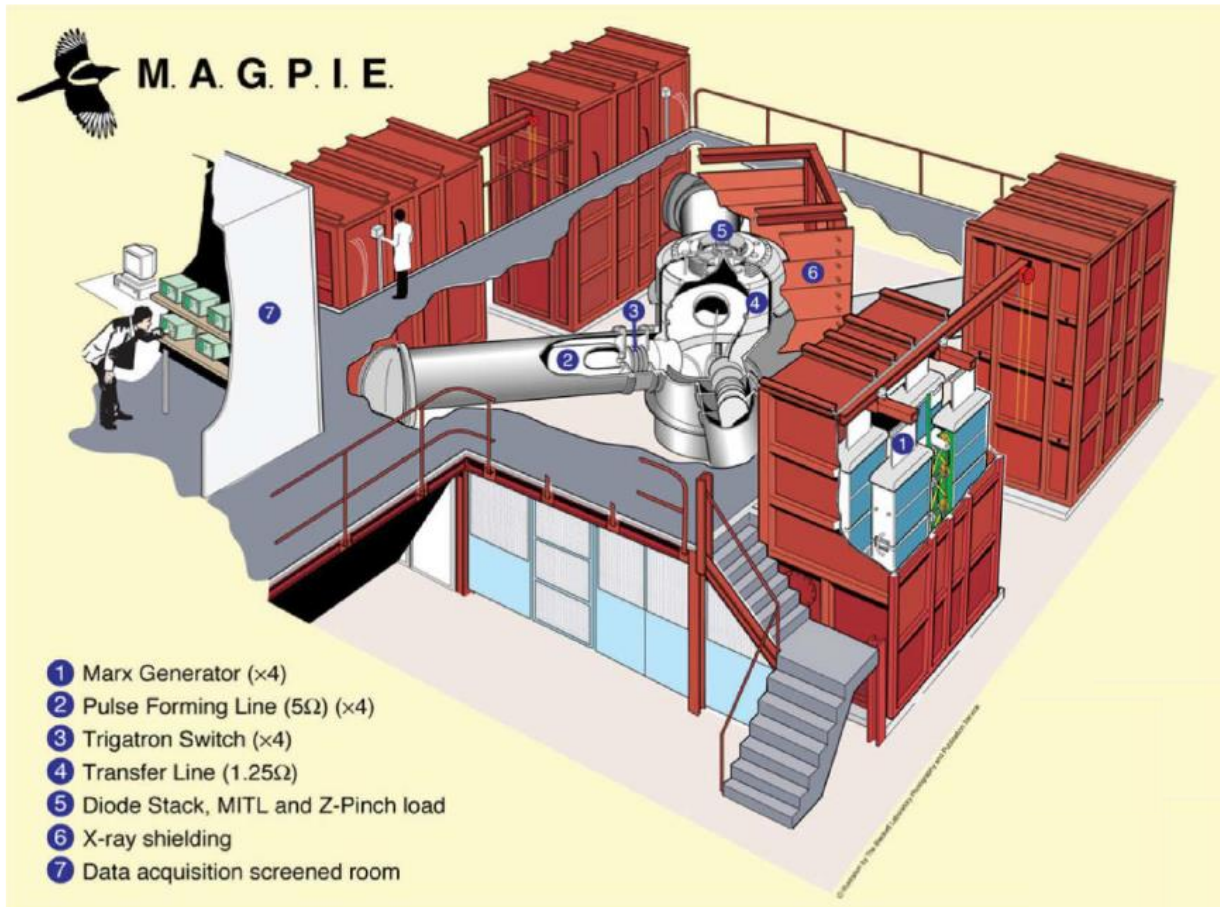


Fig. 8.1. Schematic illustration of the 1.5 TW pulse generator KALIF. The data for the pulse at the vacuum interface are: power = 1.5 TW, voltage = 1.7 MV, pulse duration = 50 ns, pulse energy = 75 kJ, electrical efficiency = 30%

Magpie at Imperial college

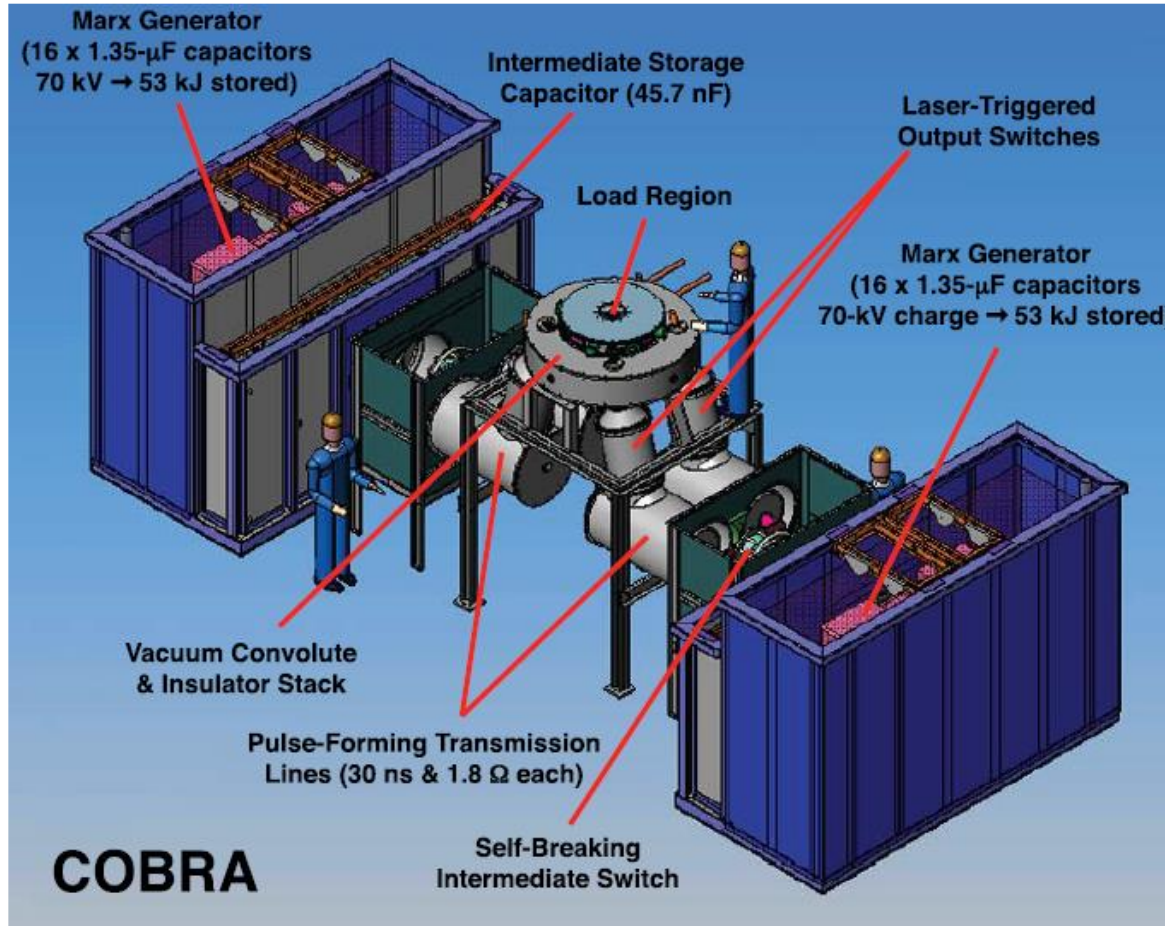


$E = 86 \text{ kJ}$

$I = 1 \text{ MA}$

$T_{\text{rise}} = 250 \text{ ns}$

Cobra at Cornell University

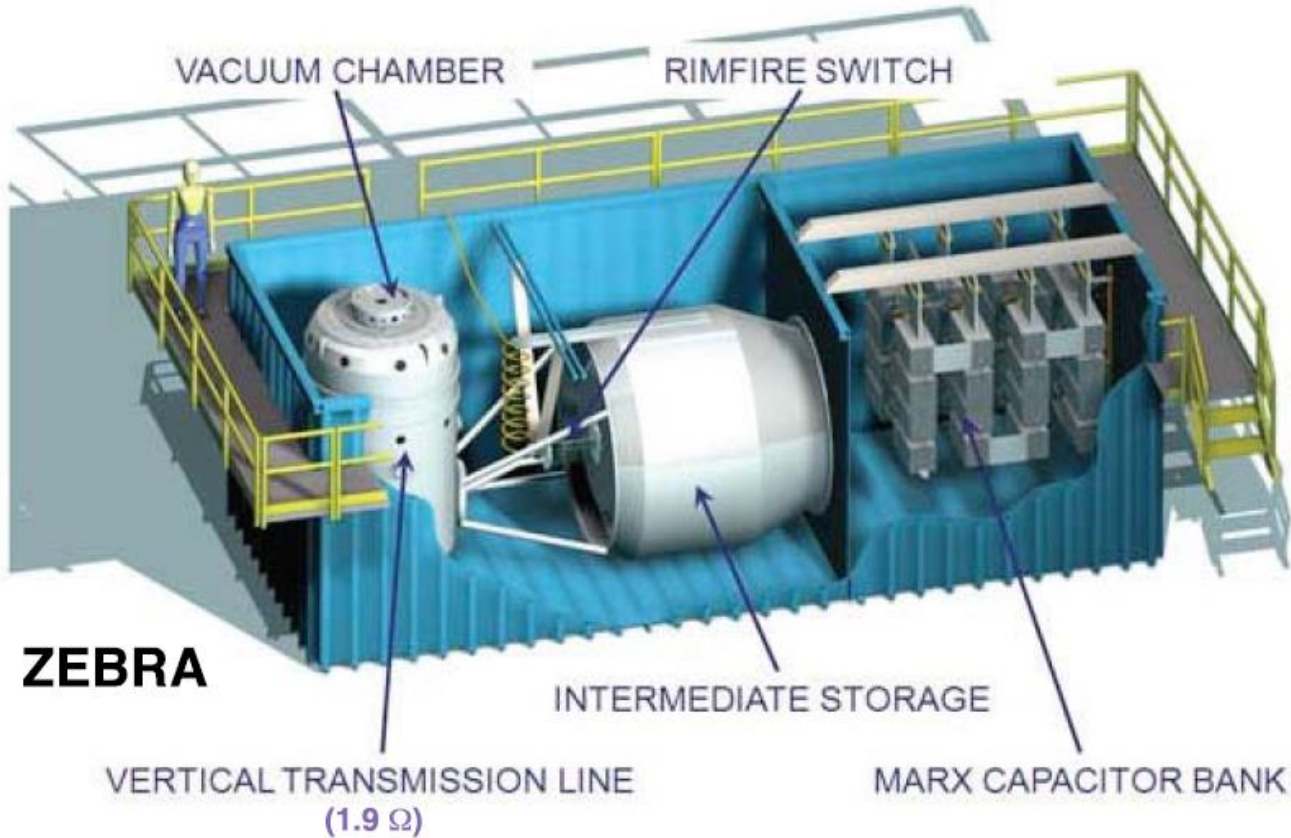


$$E = 105 \text{ kJ}$$

$$I = 1 \text{ MA}$$

$$T_{\text{rise}} = 100 \text{ ns}$$

Zebra at University of Nevada, Reno

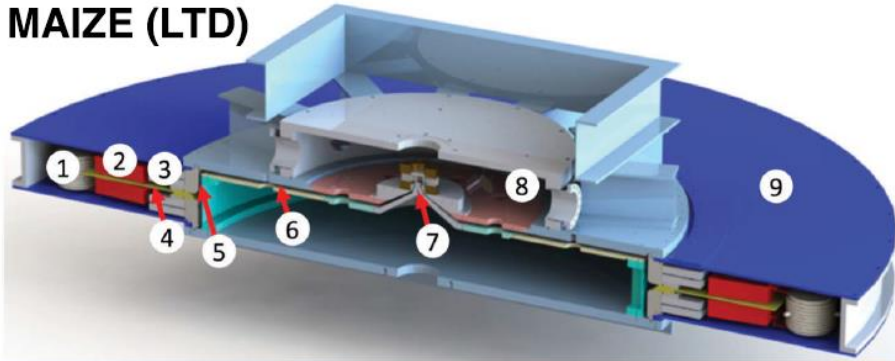


$E = 200 \text{ kJ}$
 $I = 1 \text{ MA}$
 $T_{\text{rise}} = 100 \text{ ns}$

Maize LTD at University of Michigan



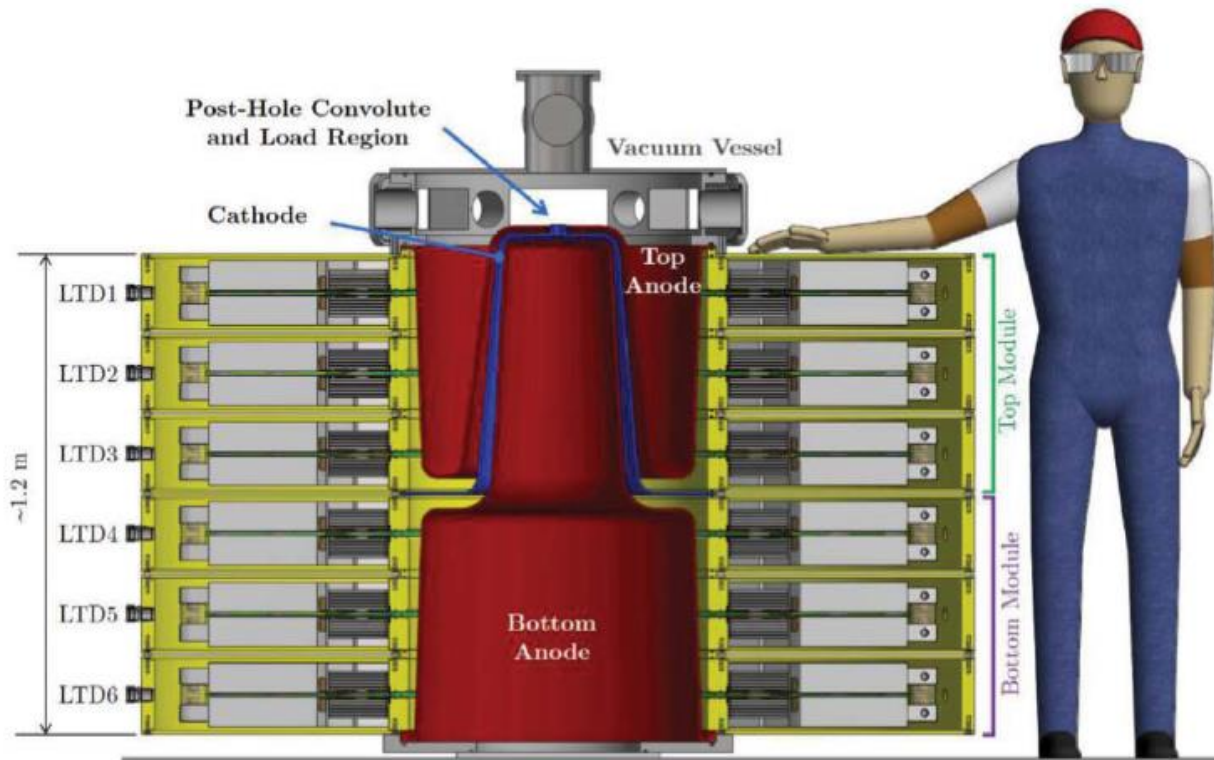
MAIZE (LTD)



$E = 16 \text{ kJ}$
 $I = 1 \text{ MA}$
 $T_{\text{rise}} = 100 \text{ ns}$



Hades at University of Rochester



$E = 75 \text{ kJ}$

$I = 1 \text{ MA}$

$T_{\text{rise}} = 125 \text{ ns}$

Particle Beam Fusion Accelerator (PBFA 2) and the Z-Machine

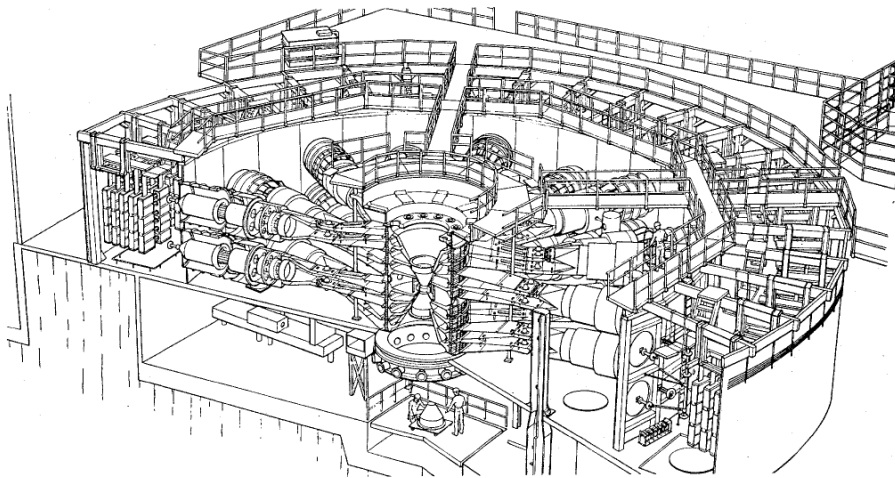


Fig. 8.2. Perspective drawing of the multimodular generator PBFA 2

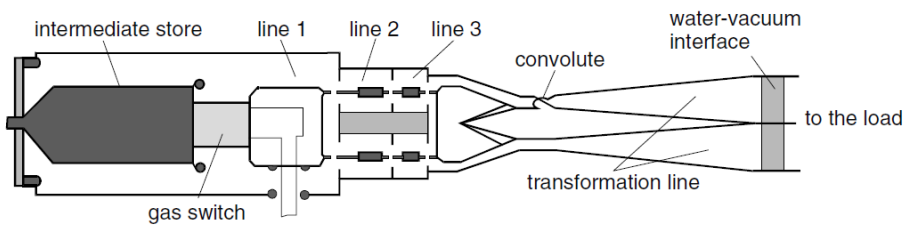


Fig. 8.3. Pulse-forming network of a single module of the PBFA 2 device

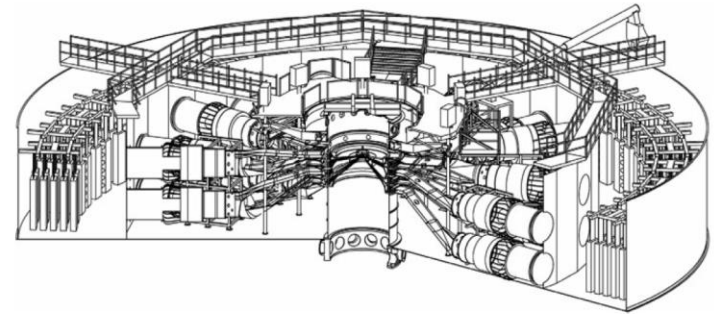


Fig. 8.4. Schematic illustration of the Z-Machine for driving Z-pinch, located at Sandia National Laboratory

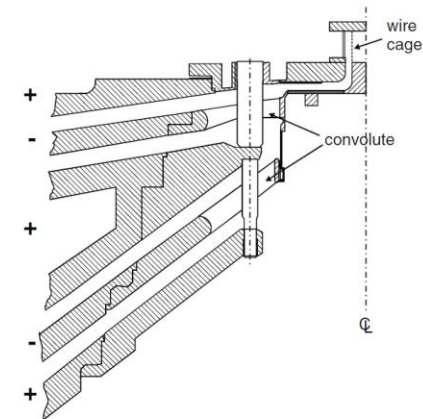
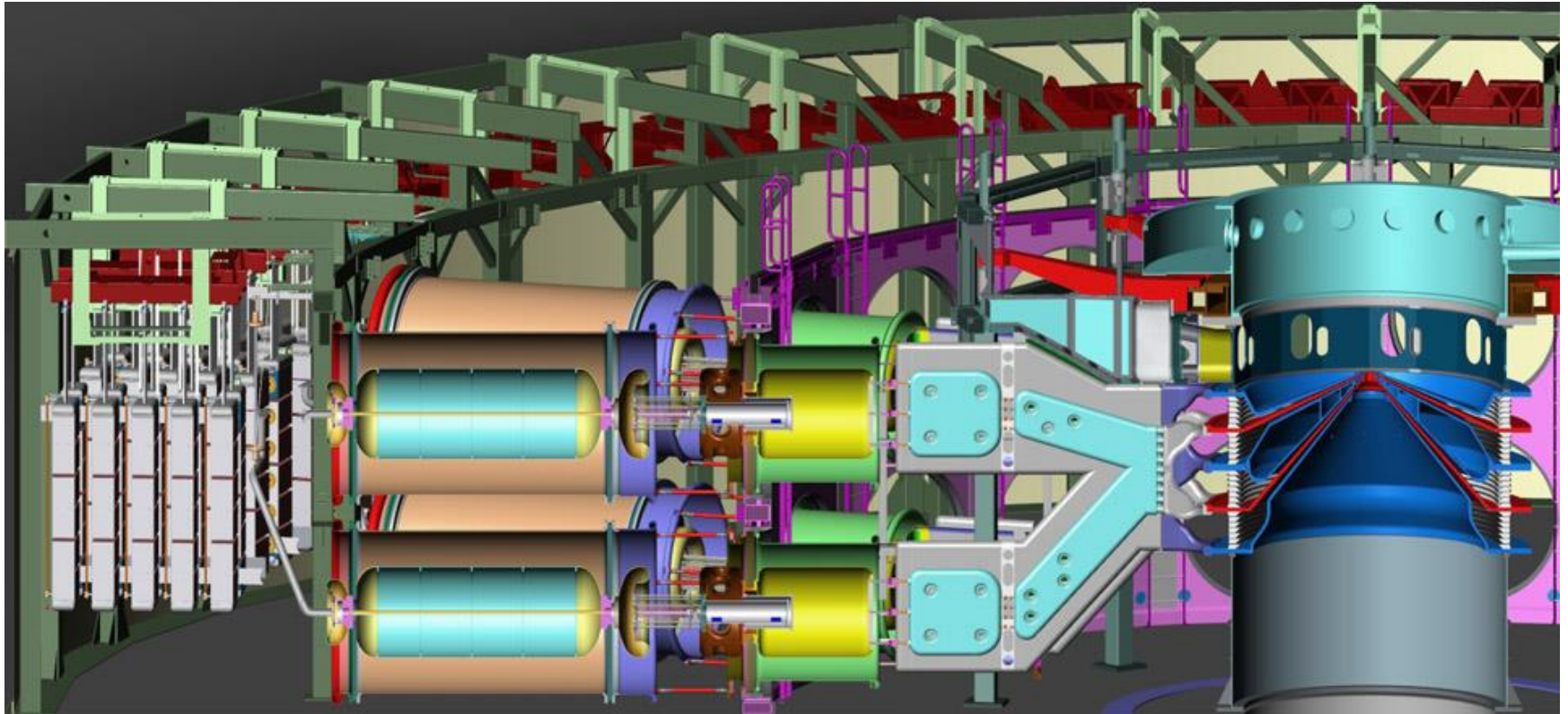


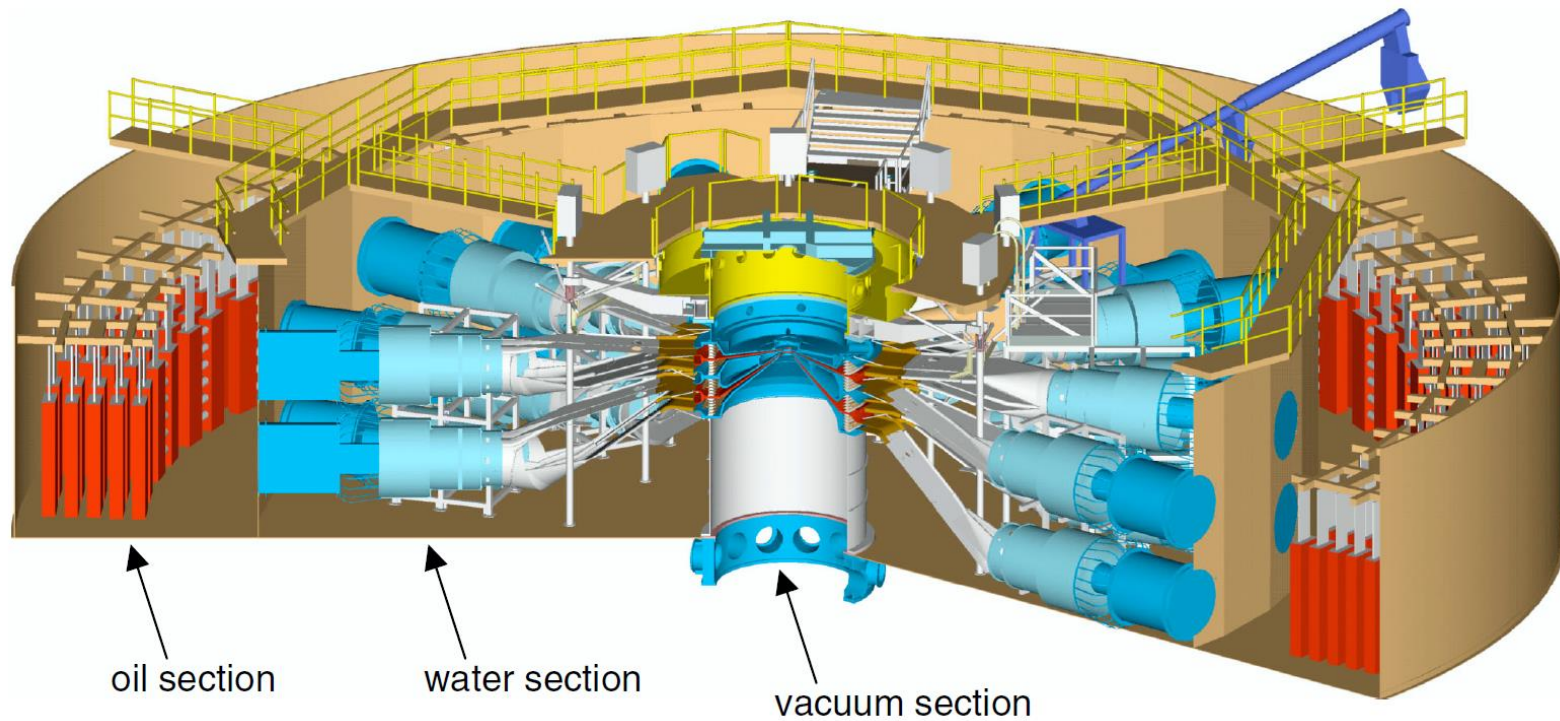
Fig. 8.5. Post-hole convolute in the Z-Machine

Sandia's Z machine is the world's most powerful and efficient laboratory radiation source

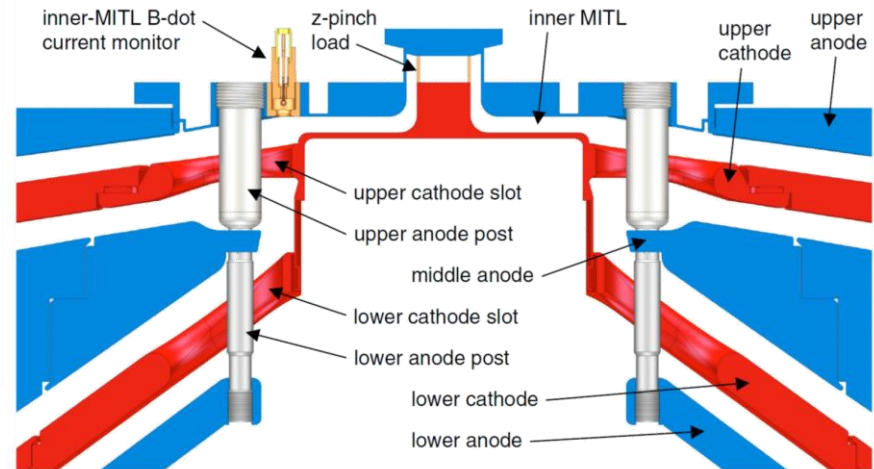
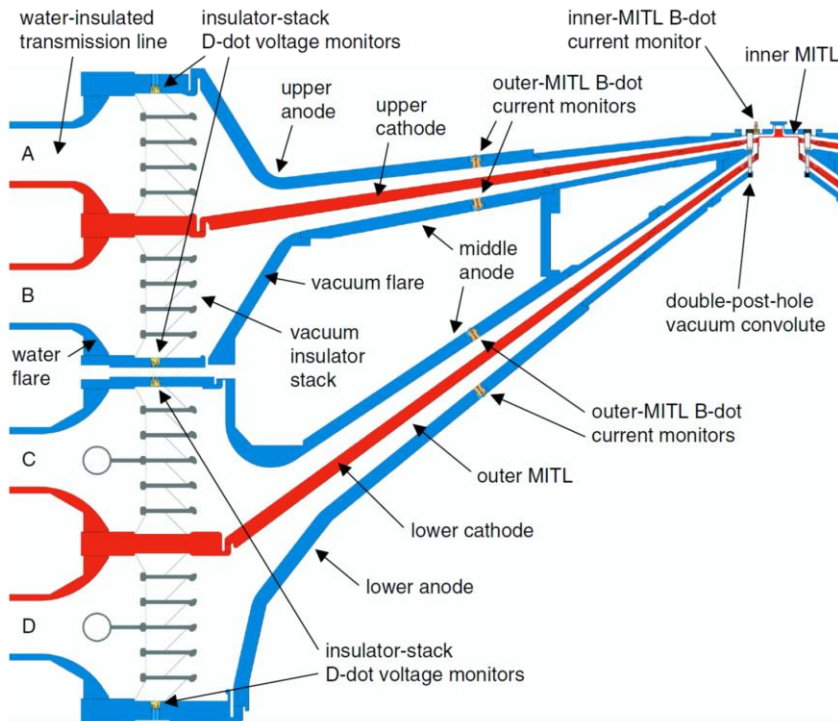


- **Stored energy: 20 MJ**
- **Marx charge voltage: 85 kV**
- **Peak electrical power: 85 TW**
- **Peak current: 26 MA**
- **Rise time: 100 ns**
- **Peak X-ray emissions: 350 TW**
- **Peak X-ray output: 2.7 MJ**

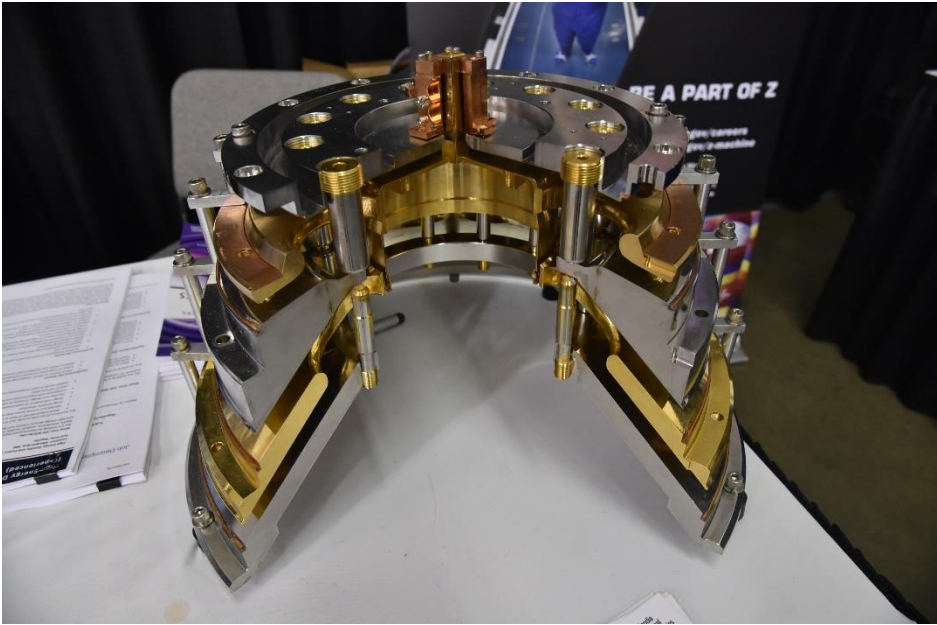
Z pulsed-power accelerator: 20 MA, 3MV, 55TW



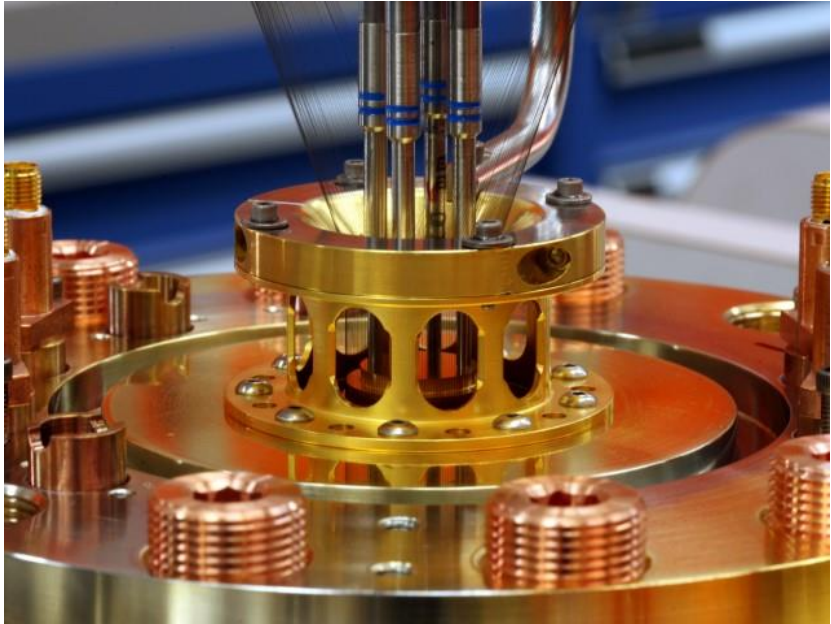
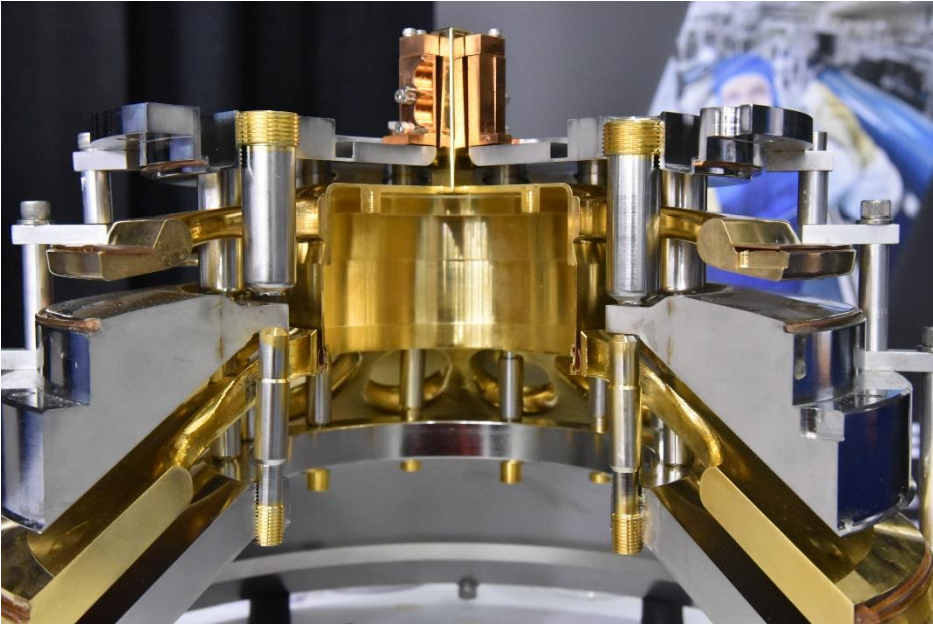
Self-magnetically insulated vacuum transmission lines (MITLs)



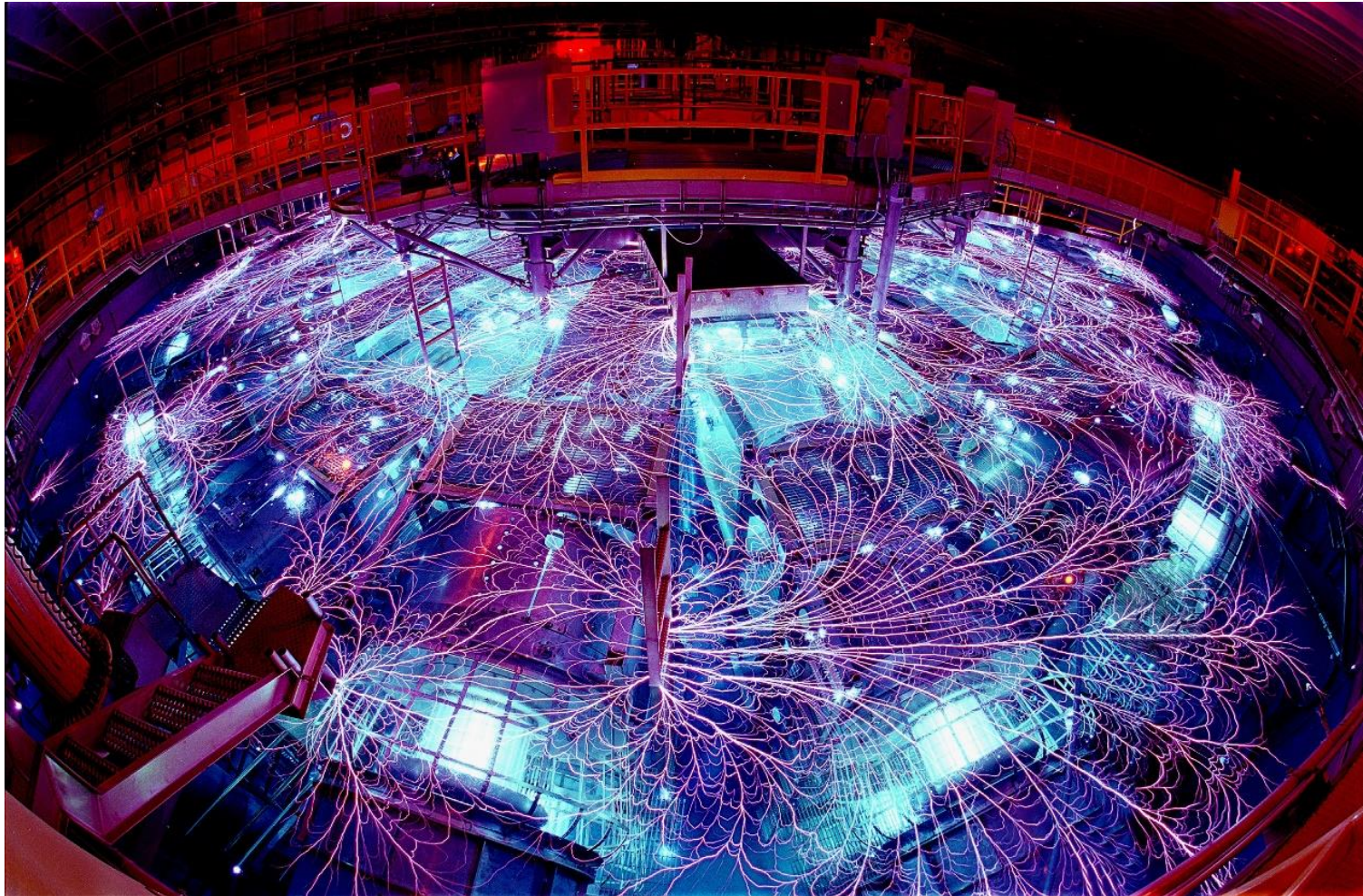
Z machine



Z machine



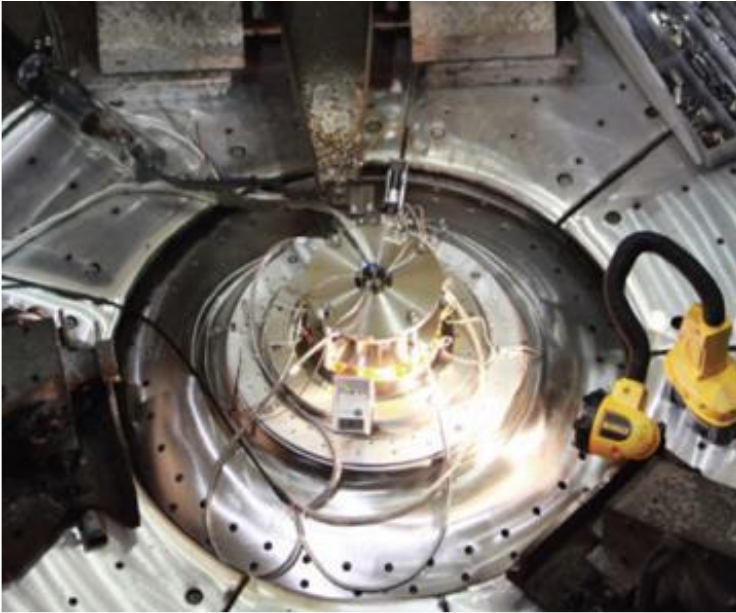
Z machine discharge



Before and after shots



- Before shots

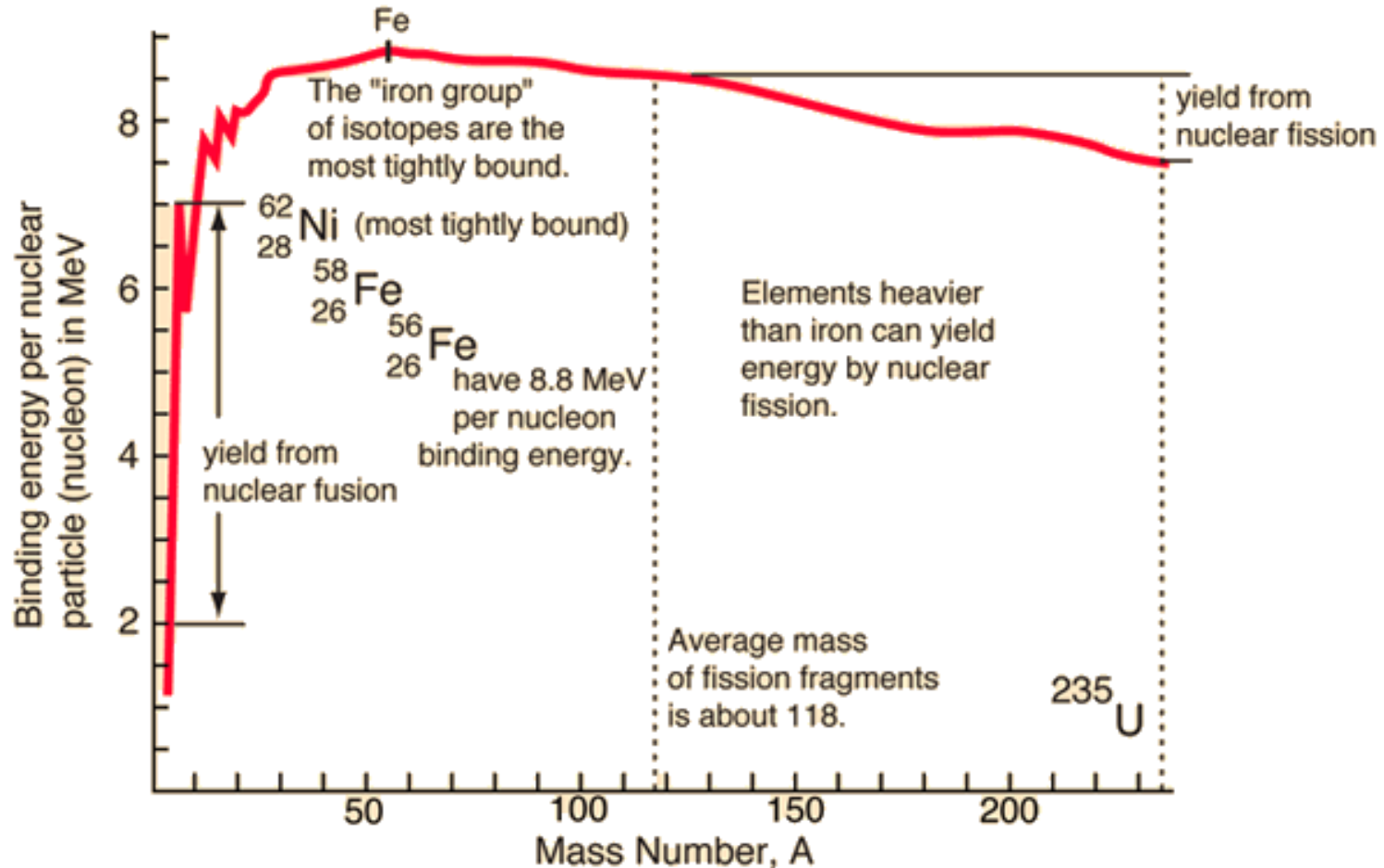


- After shots



SAND2017-0900PE_The sandia z machine - an overview of the world's most powerful pulsed power facility.pdf

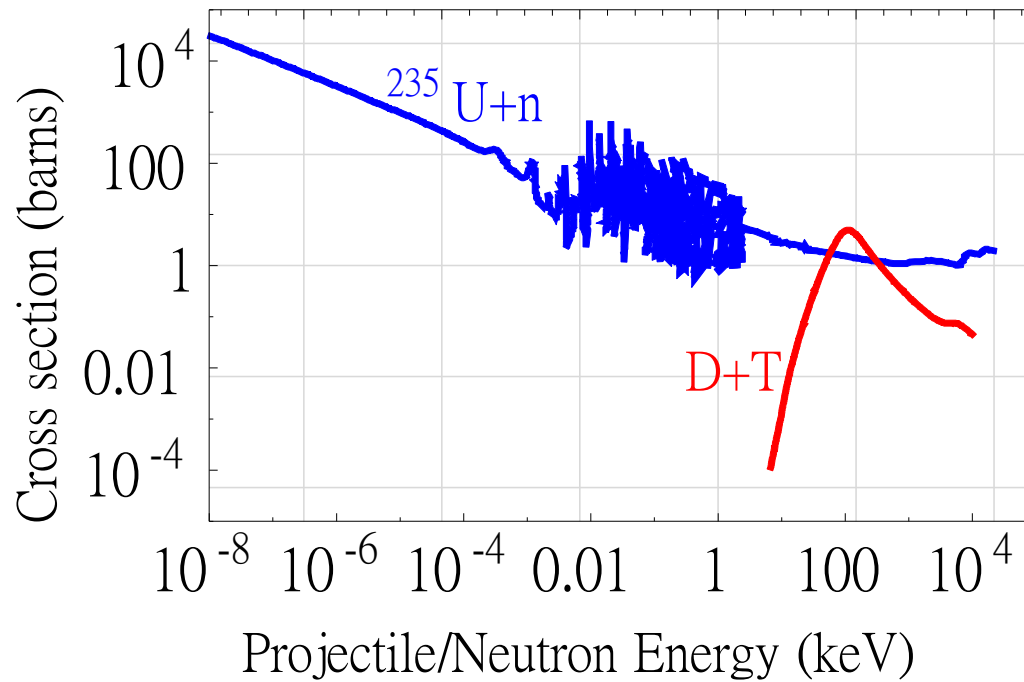
The “iron group” of isotopes are the most tightly bound



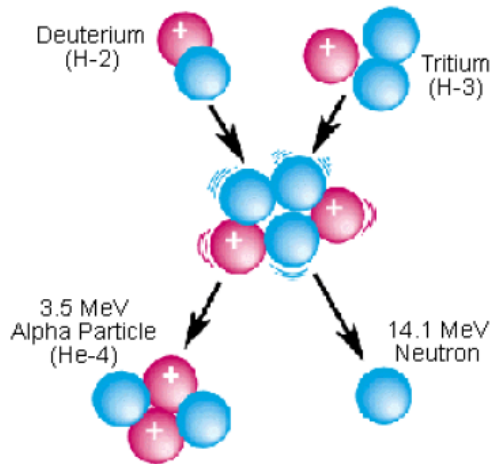
Fusion is much harder than fission



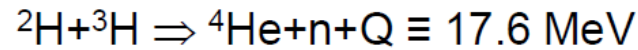
- **Fission:** $n + {}_{92}^{235}\text{U} \rightarrow {}_{92}^{236}\text{U} \rightarrow {}_{56}^{144}\text{Ba} + {}_{36}^{89}\text{Kr} + 3n + 177\text{ MeV}$
- **Fusion:** $D + T \rightarrow \text{He}^4 (3.5\text{ MeV}) + n (14.1\text{ MeV})$



The fusion process

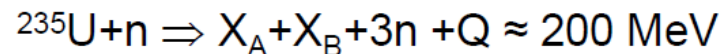
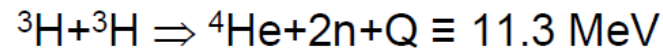
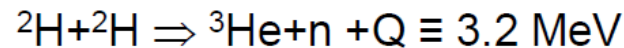
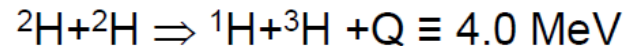


Deuterium-Tritium Fusion Reaction



Energy release $Q=17.6 \text{ MeV}$

In comparison

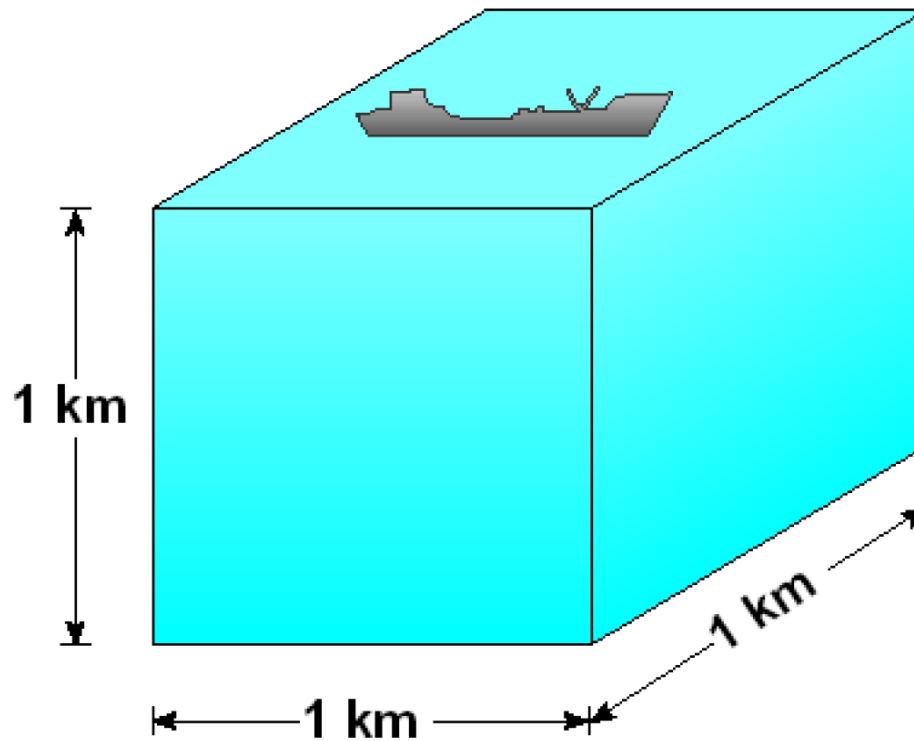


Fusionable Material, deuterium ^2H (D) and tritium ^3H (t):

Deuterium: natural occurrence (heavy water) (0.015%).

Tritium: natural occurrence in atmosphere through cosmic ray bombardment; radioactive with $T_{1/2}=12.3 \text{ y}$.

Enormous fusion fuel can be produced from sea water



= Total energy
of world oil
reserve

“Advantages” of hydrogen bomb



$$\text{Fusion of } ^2\text{H} + ^3\text{H}: \quad \frac{Q}{A} = \frac{17.6 \text{ MeV}}{(3 + 2) \text{ amu}} = 3.5 \frac{\text{MeV}}{\text{amu}}$$

$$\text{Fission of } ^{235}\text{U}: \quad \frac{Q}{A} = \frac{200 \text{ MeV}}{236 \text{ amu}} = 0.85 \frac{\text{MeV}}{\text{amu}}$$

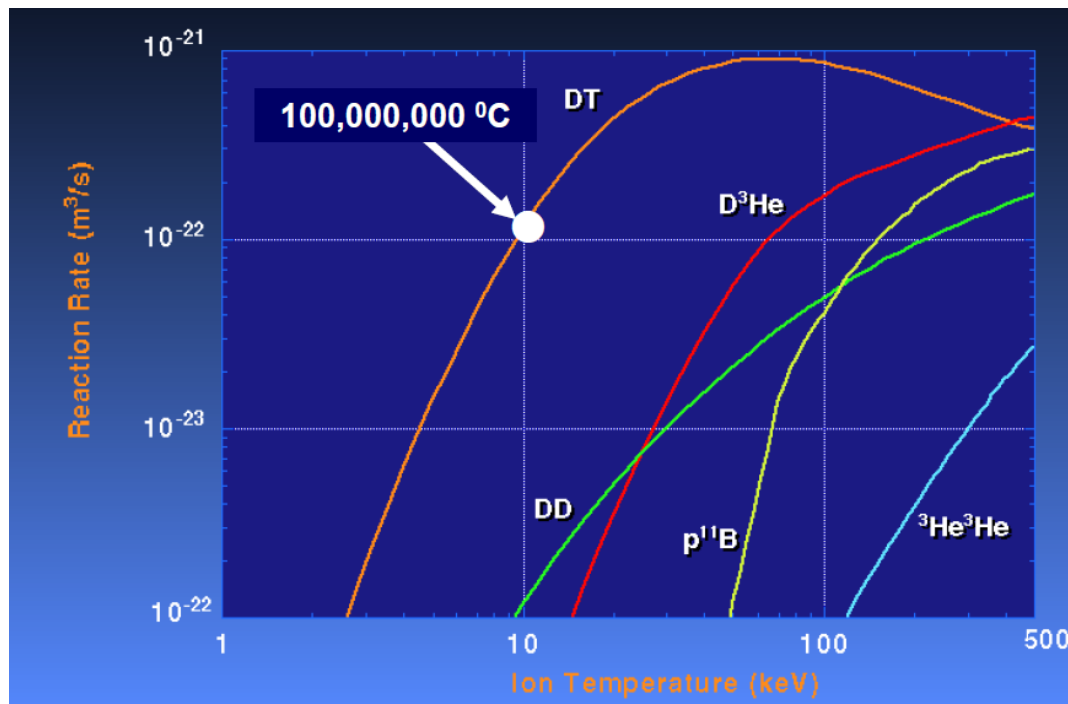
Fusion is 4 times more powerful than fission
and generates 24 times more neutrons!

Fusion doesn't come easily



averaged reaction rate : $\langle \sigma v \rangle = \int \int d\vec{v}_1 d\vec{v}_2 \sigma_{1,2}(v) v f_1(v_1)$

$$f_j(v_j) = \left(\frac{m_j}{2\pi k_B T} \right)^{3/2} \exp \left(-\frac{m_j v_j^2}{2k_B T} \right)$$

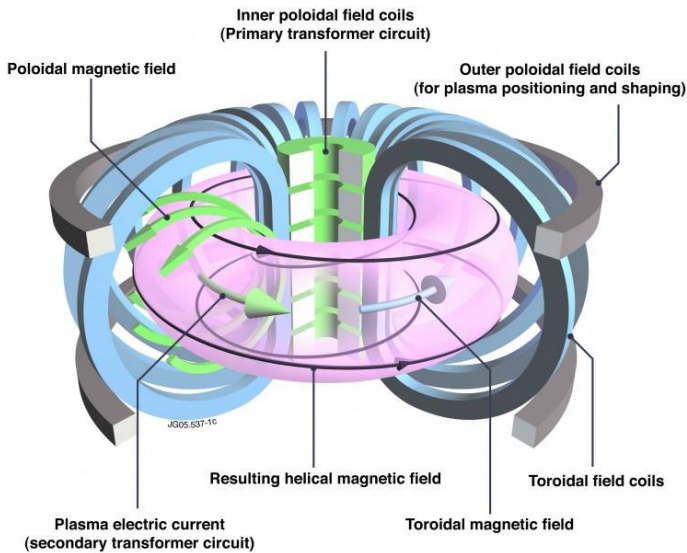


- Use α particles to heat the plasma $D + T \rightarrow He^4 (3.5 \text{ MeV}) + n (14.1 \text{ MeV})$

Magnetic confinement fusion (MCF) vs Inertial confinement fusion (ICF)

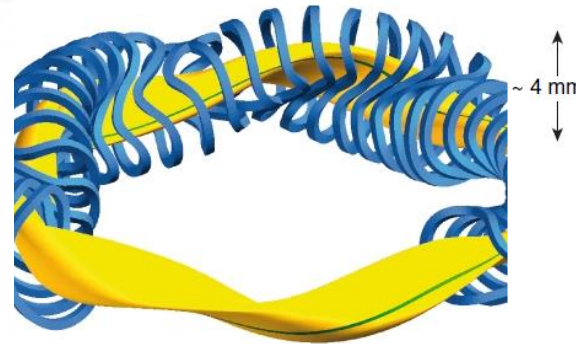


Tokamak

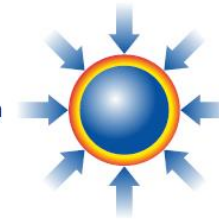


$P \sim \text{atm}$, $\tau \sim \text{sec}$, $T \sim 10 \text{ keV}$

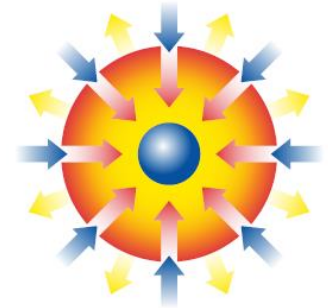
Stellarator



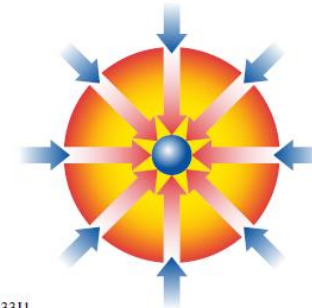
Laser light shines on the target



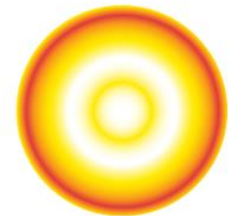
The target is compressed



The target is ignited



The target burns



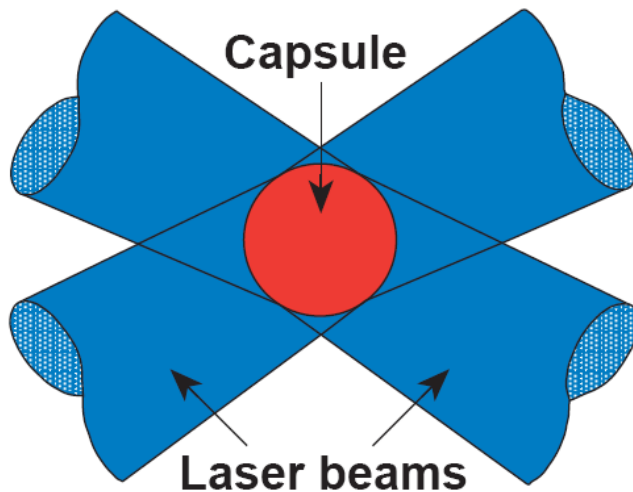
U733J1

$P \sim \text{Gigabar}$, $\tau \sim \text{nsec}$, $T \sim 10 \text{ keV}$

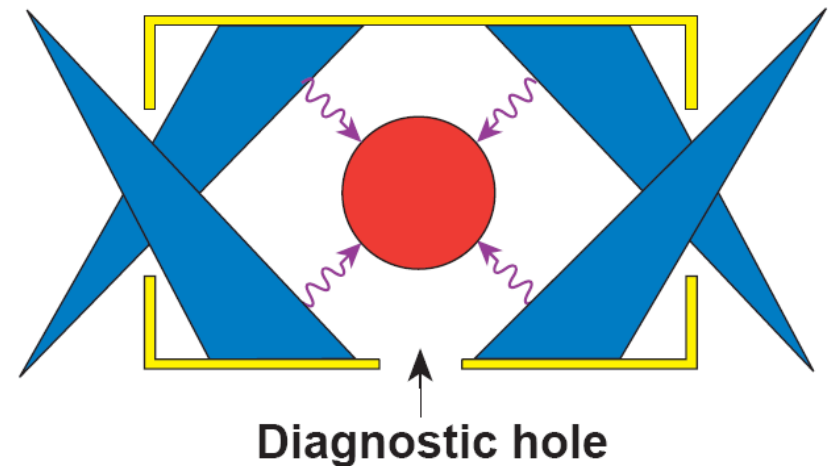
Inertial confinement fusion



Direct-drive target



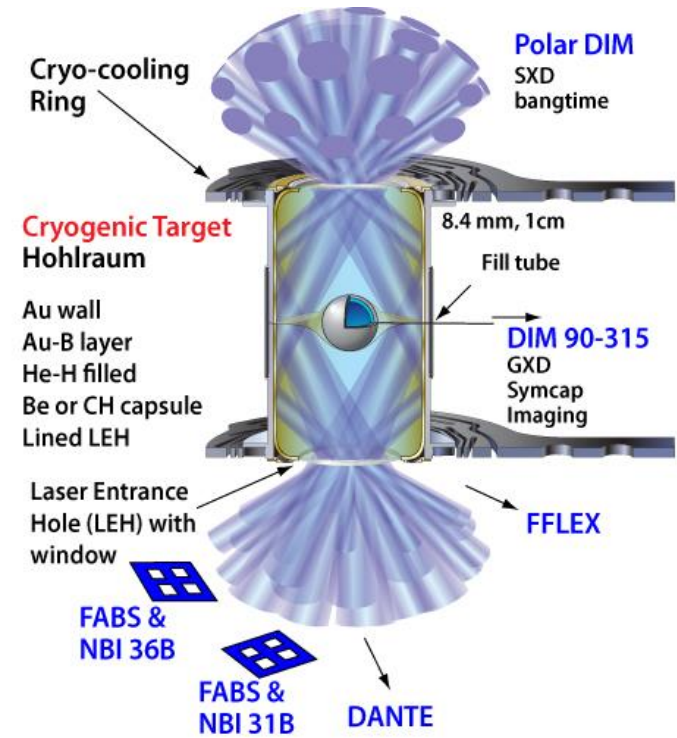
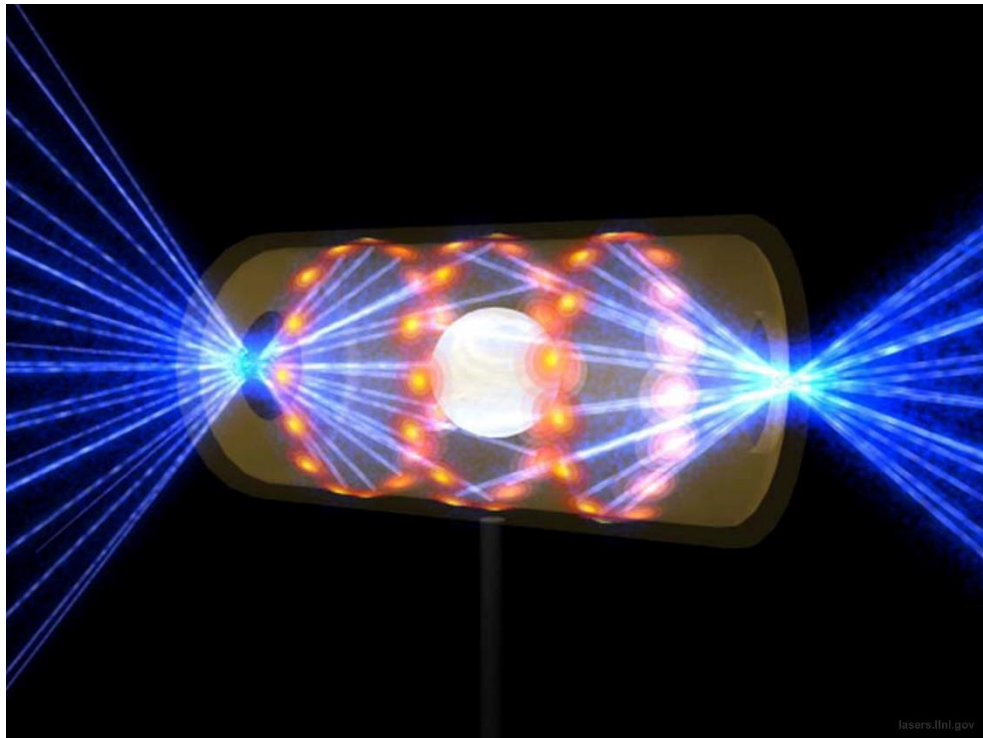
Indirect-drive target



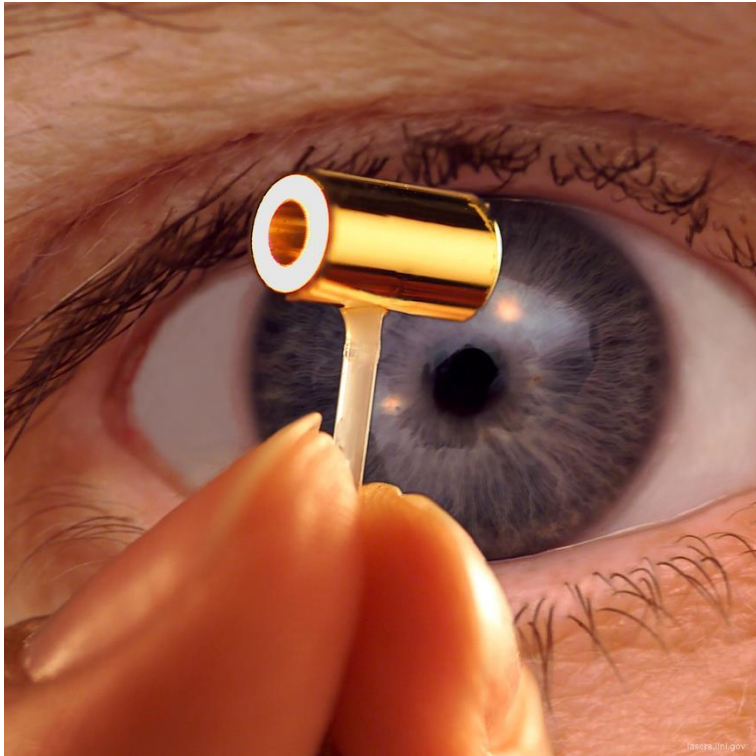
Hohlraum using
a cylindrical high-Z case

Reference:
Riccardo Betti,
University of Rochester,
HEDSA HEDP summer school,
San Diego, CA, August 16-21, 2015

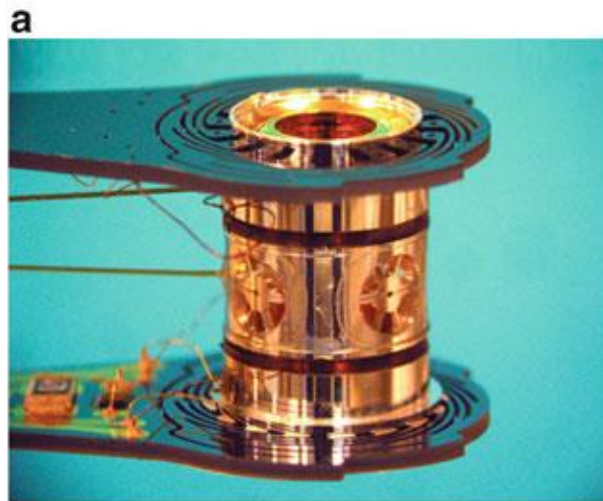
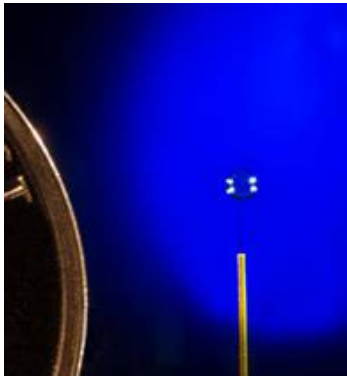
Hohlraum at National Ignition Facility (NIF)



NIF target

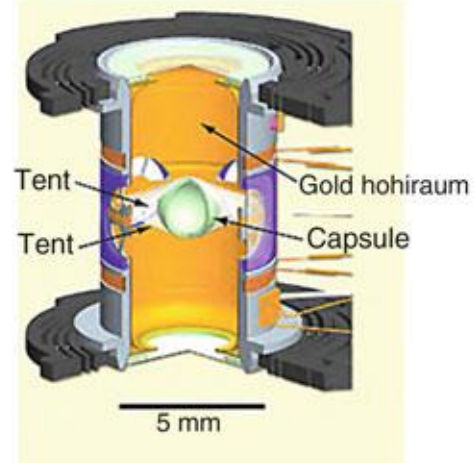
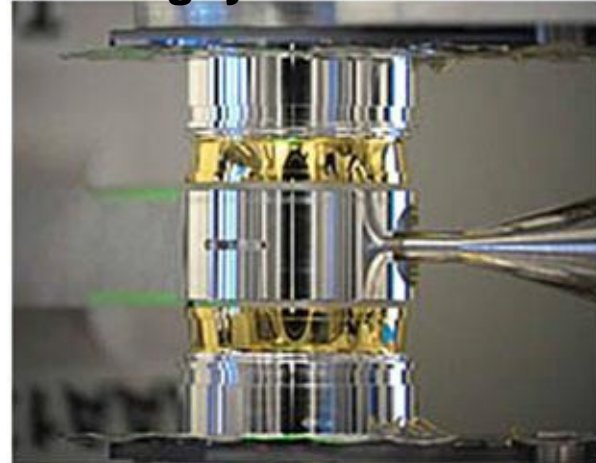
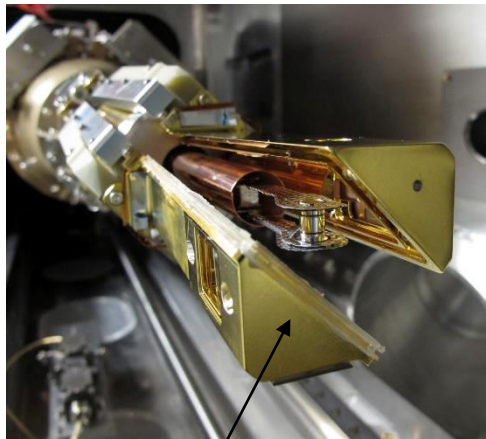


Targets used in ICF



c Rugby hohlraum

d Tent holder



Cryogenic shroud

<https://www.lle.rochester.edu>

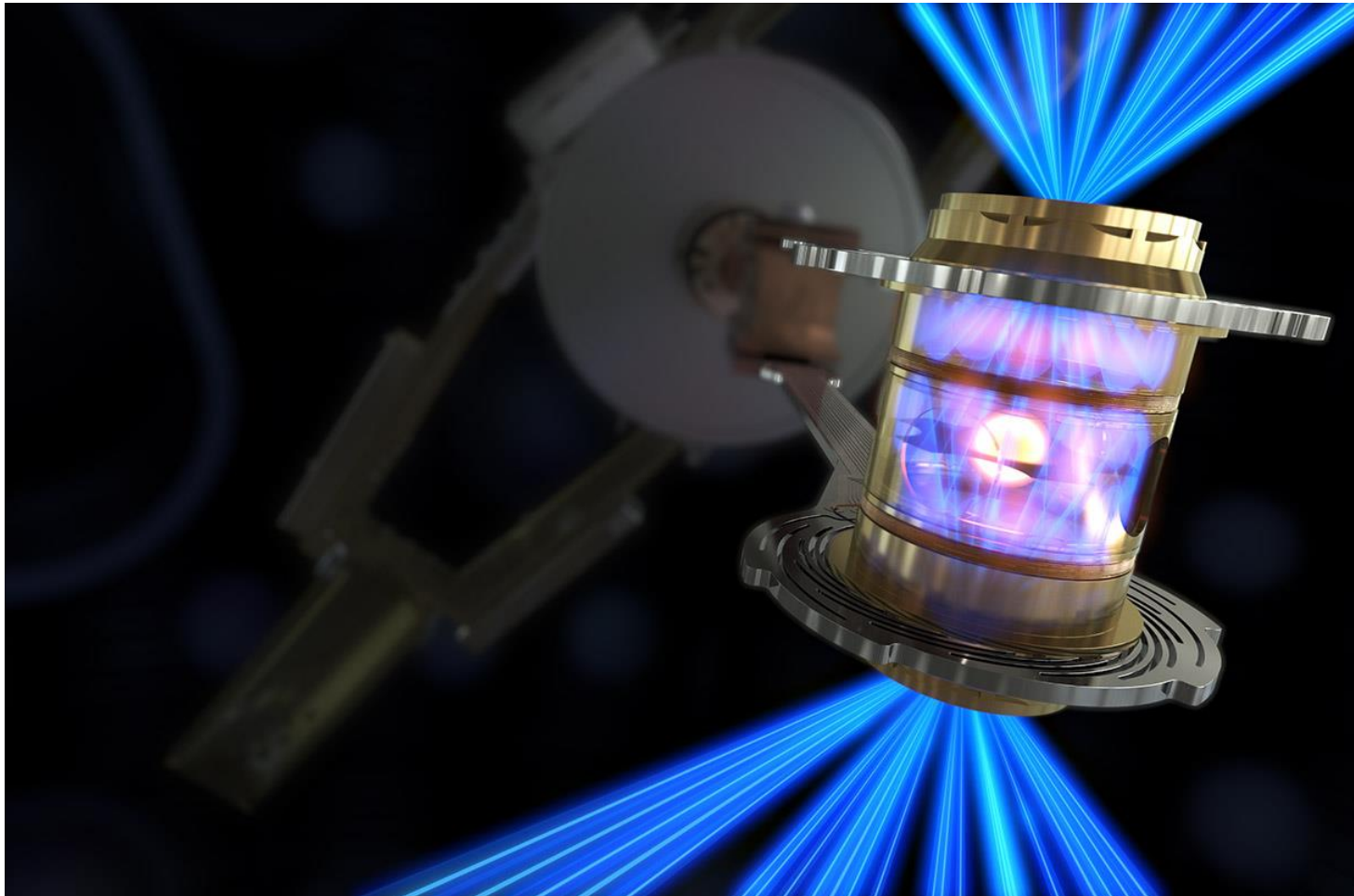
https://upload.wikimedia.org/wikipedia/commons/7/7b/Nif-shot_target-arm-before_big.jpg

<https://www.lle.rochester.edu/index.php/2014/11/10/next-generation-cryo-target/>

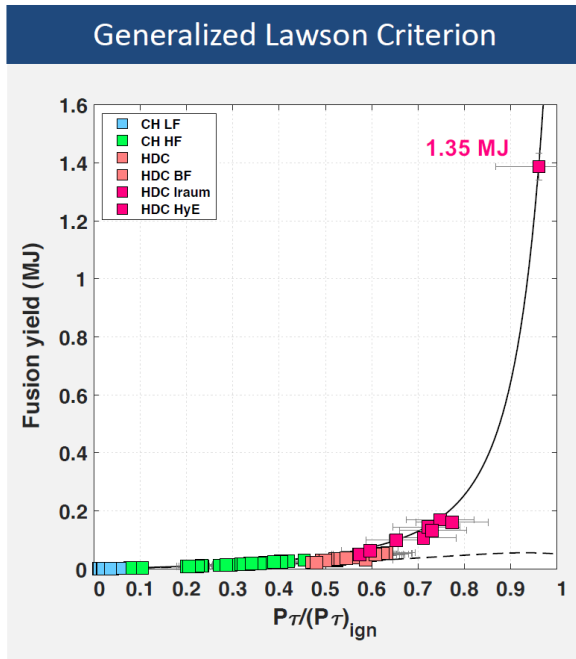
NIF achieved ignition ($Q=1.5$) on Dec. 5, 2022



- Input Laser energy: 2.05 MJ
- Output energy: 3.15 MJ



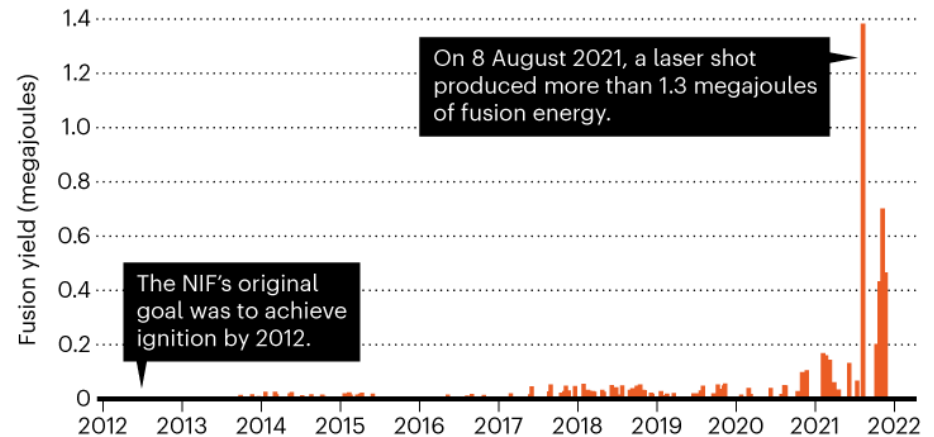
National Ignition Facility (NIF) achieved a yield of more than 1.3 MJ from ~1.9 MJ of laser energy in 2021 (Q~0.7)



- National Ignition Facility (NIF) achieved a yield of more than 1.3 MJ (Q~0.7). This advancement puts researchers at the threshold of fusion ignition.

THE ROAD TO IGNITION

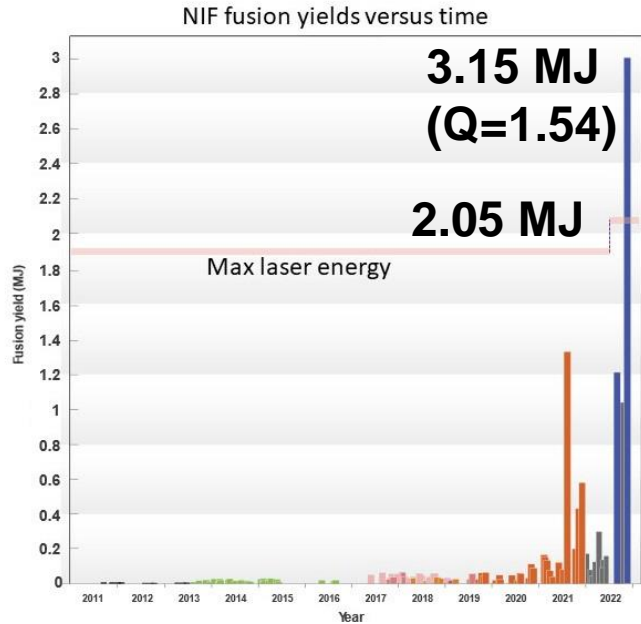
The National Ignition Facility (NIF) struggled for years before achieving a high-yield fusion reaction (considered ignition, by some measures) in 2021. Repeat experiments, however, produced less than half the energy of that result.



©nature

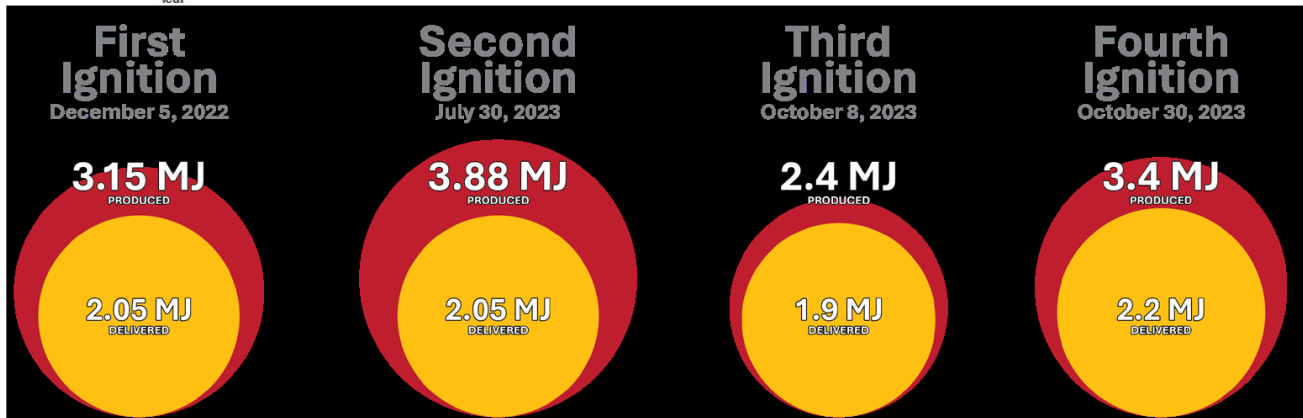
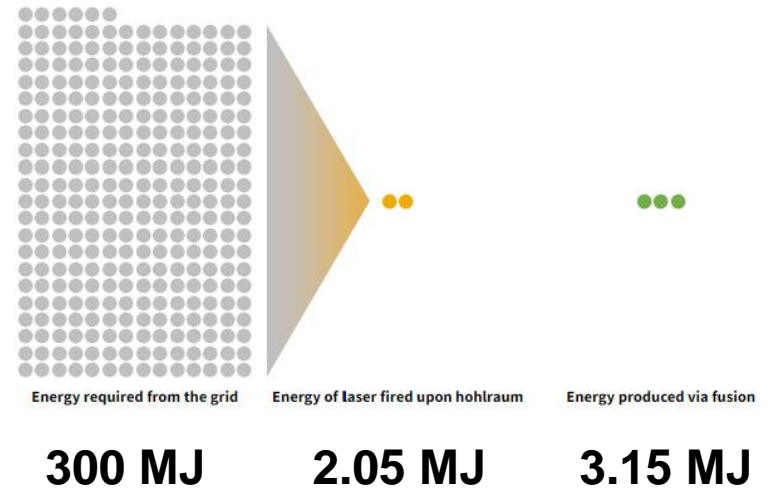
- Laser-fusion facility heads back to the drawing board.

“Ignition” (target yield larger than one) was achieved in NIF on 2022/12/5



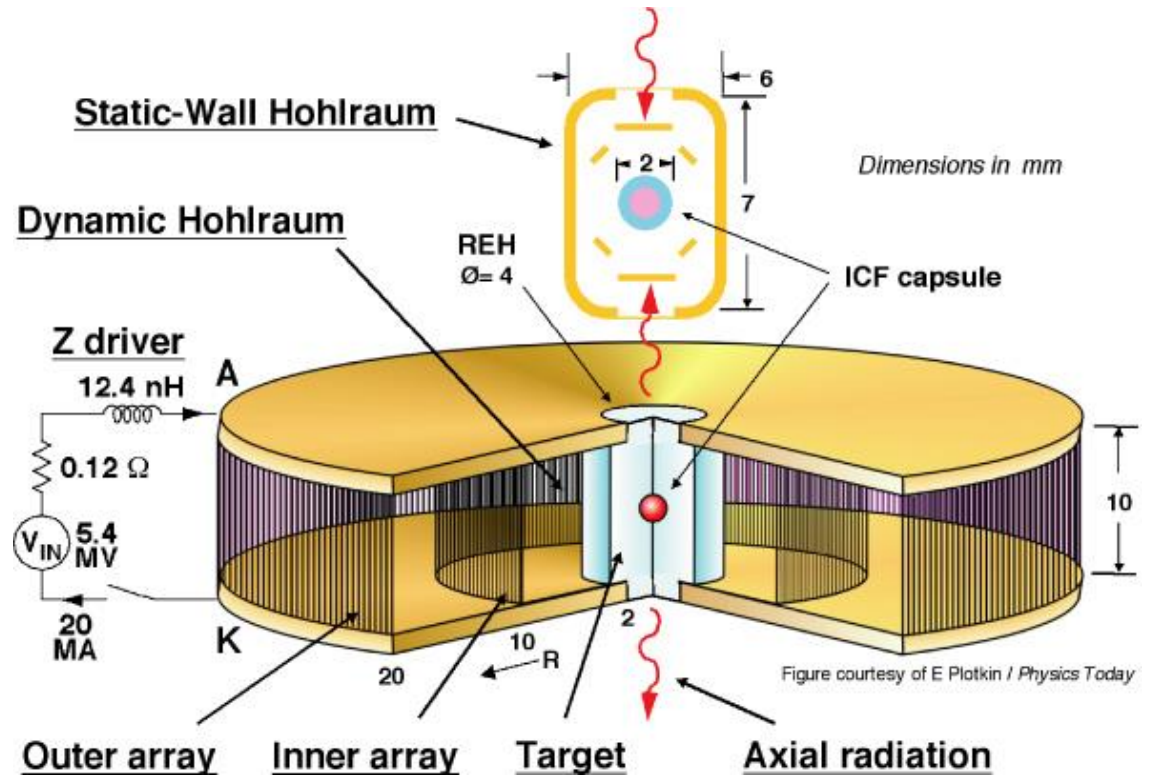
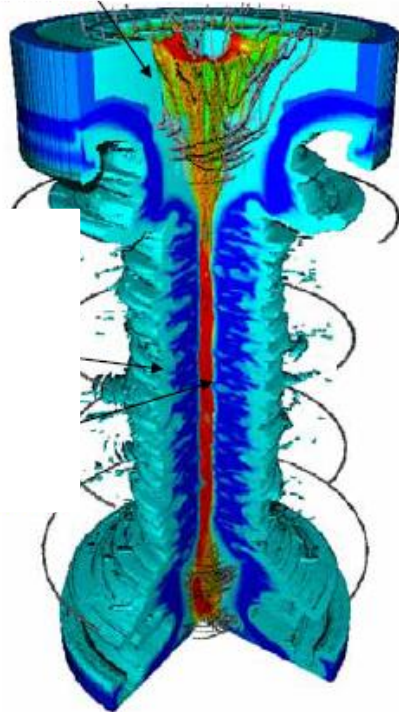
NIF's ignition achievement in perspective

Energy in megajoules ● = 1

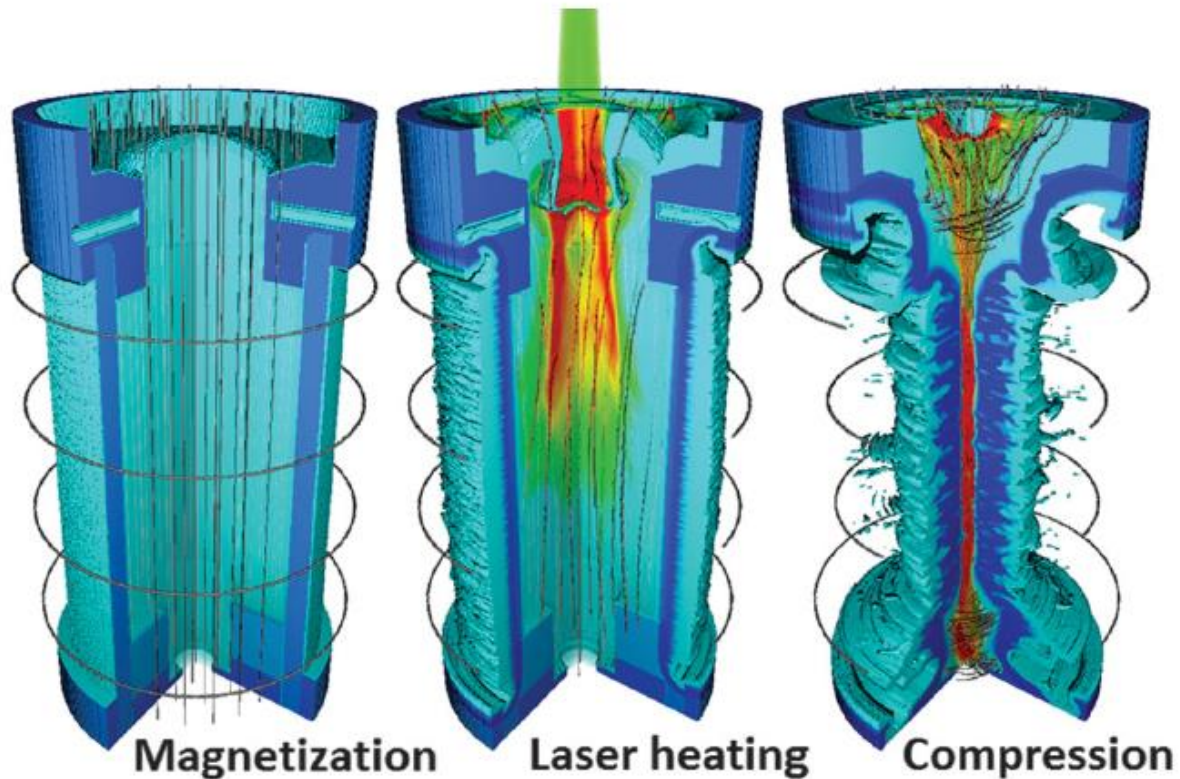


<https://physicstoday.scitation.org/doi/10.1063/PT.6.2.20221213a/full/>
The age of ignition: anniversary edition, LLNL-BR-857901

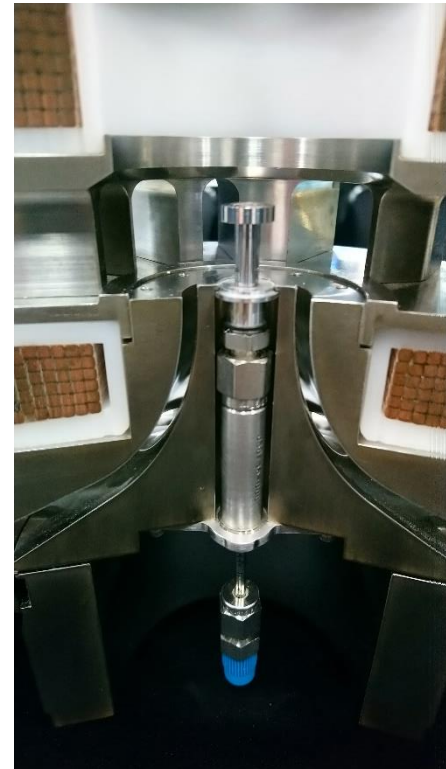
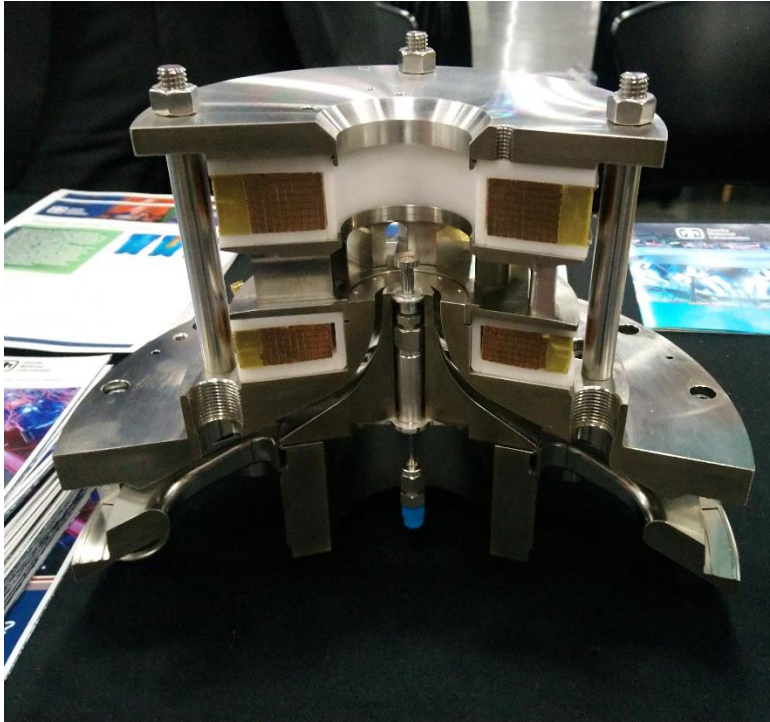
ICF via z pinch or z-pinch driven dynamic-hohlraums



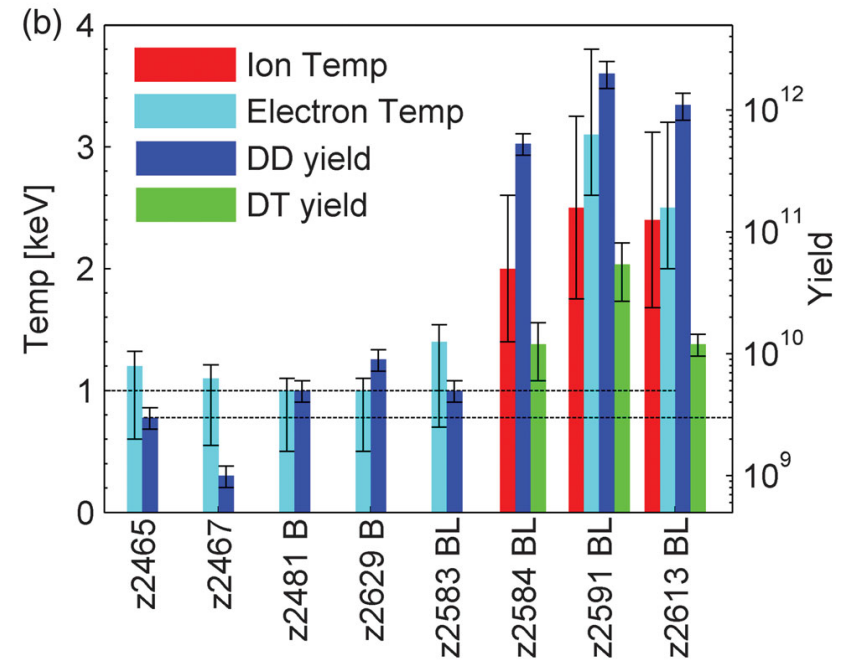
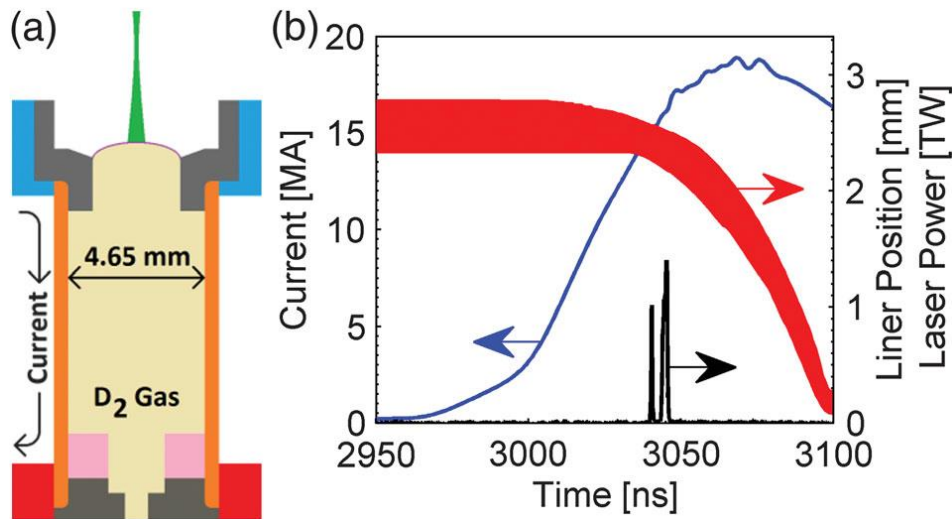
magnetized liner inertial fusion (MagLIF)



MagLIF target



Neutron yield increased by 100x with preheat and external magnetic field.

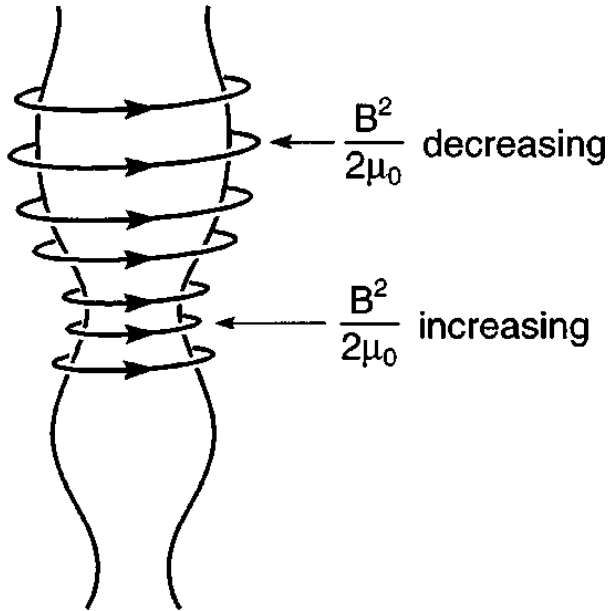


Sheared flow stabilizes MHD instabilities

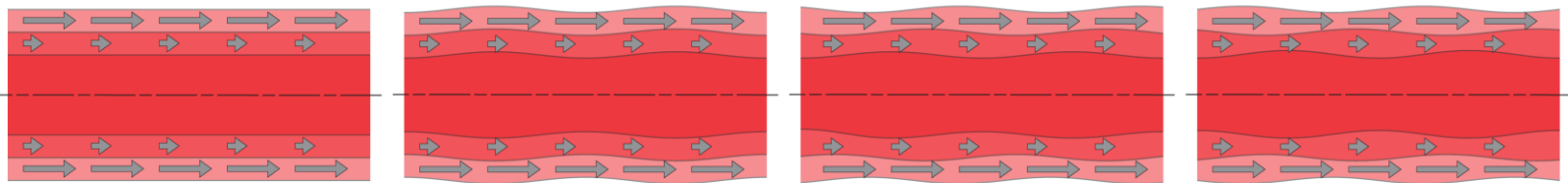
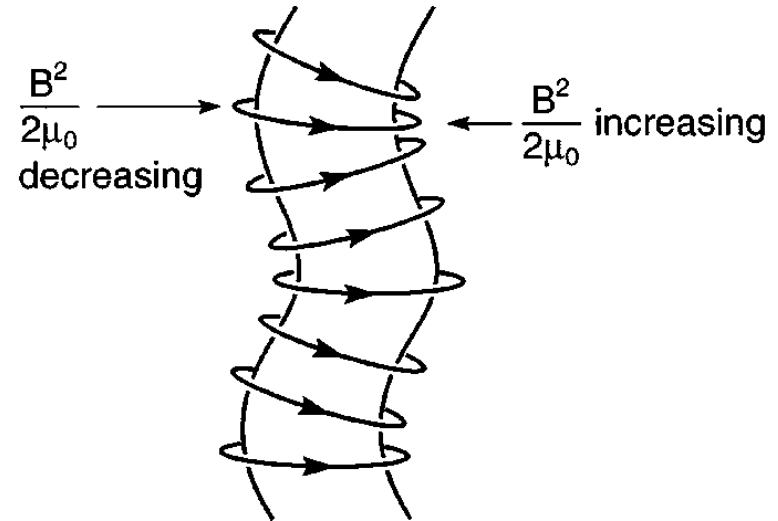


$m = 0$ (sausage)

Perturbation $\propto e^{(im\theta + ikz + \gamma t)}$



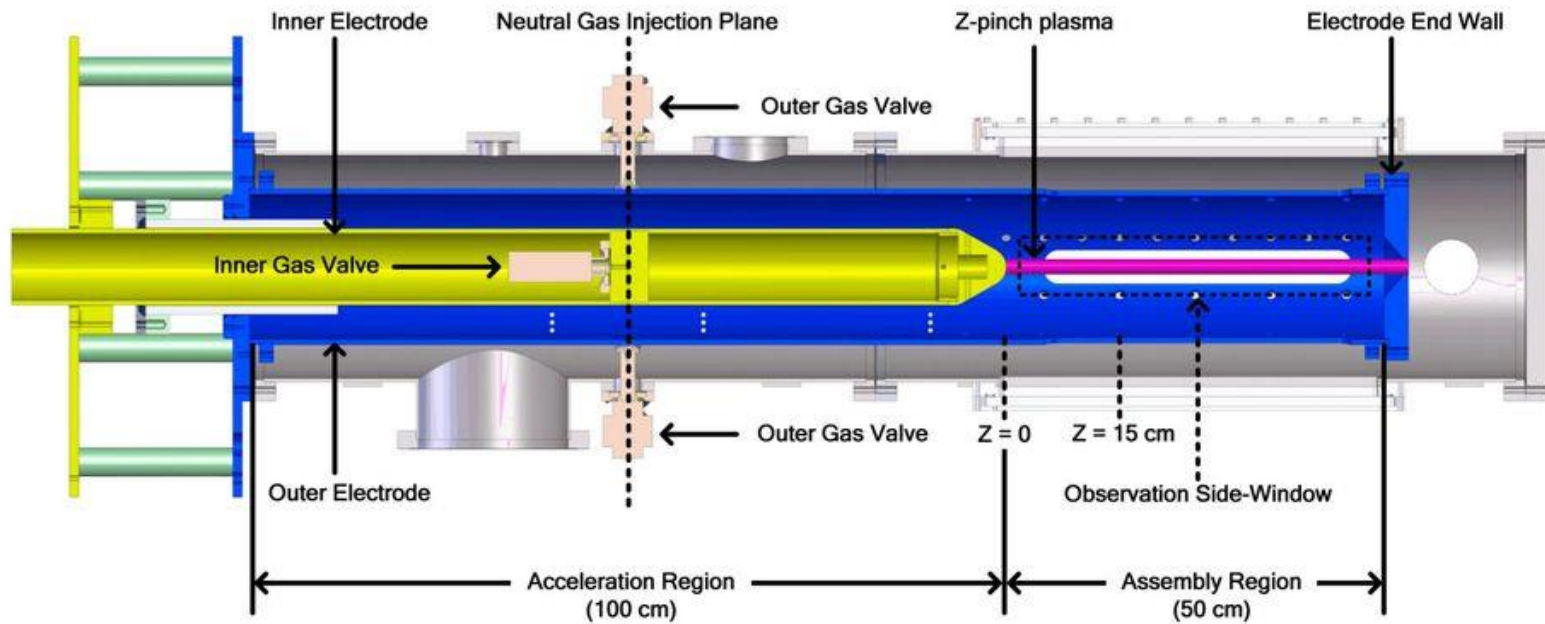
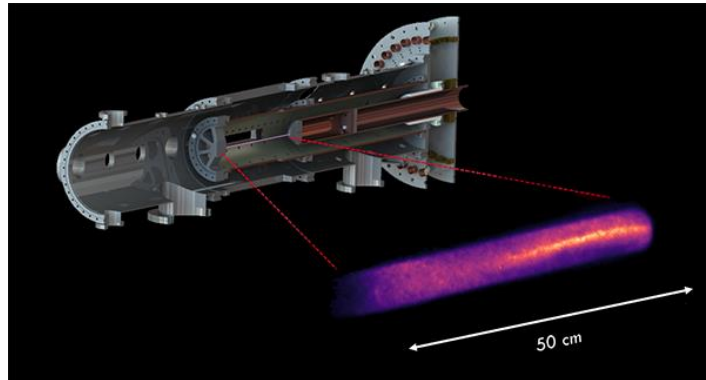
$m = 1$ (kink)



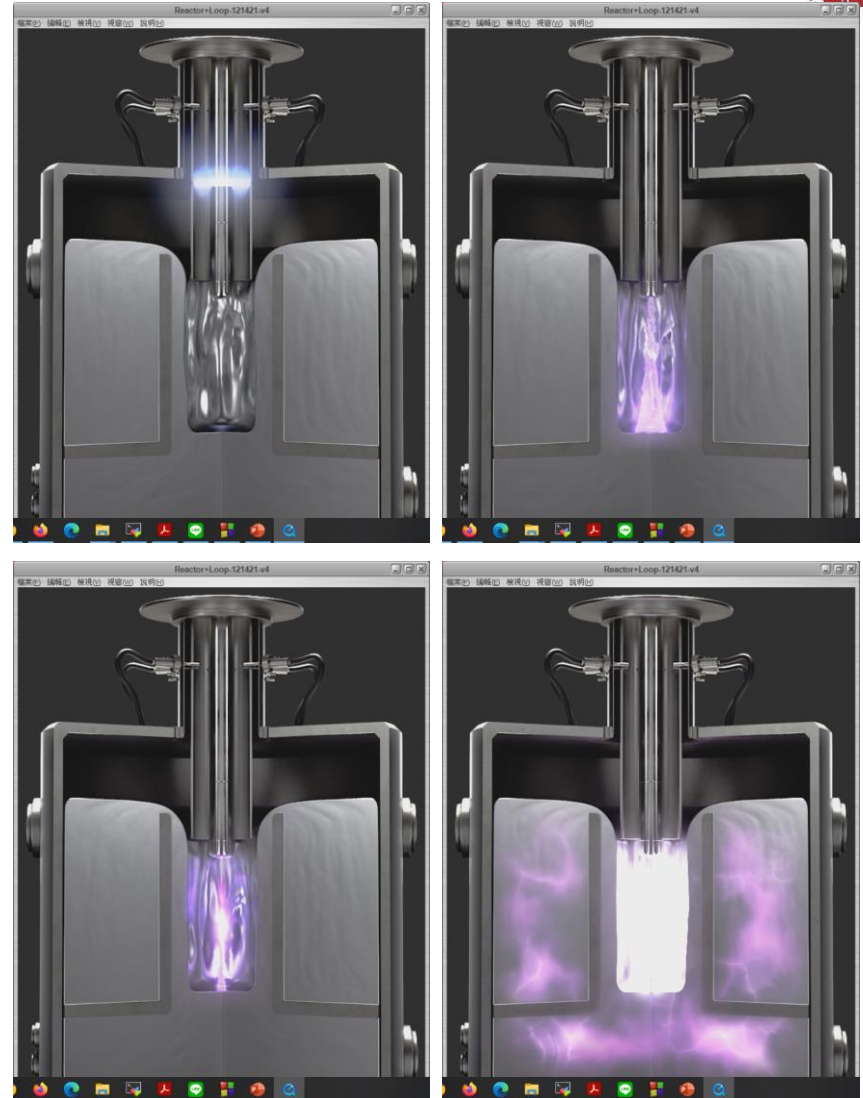
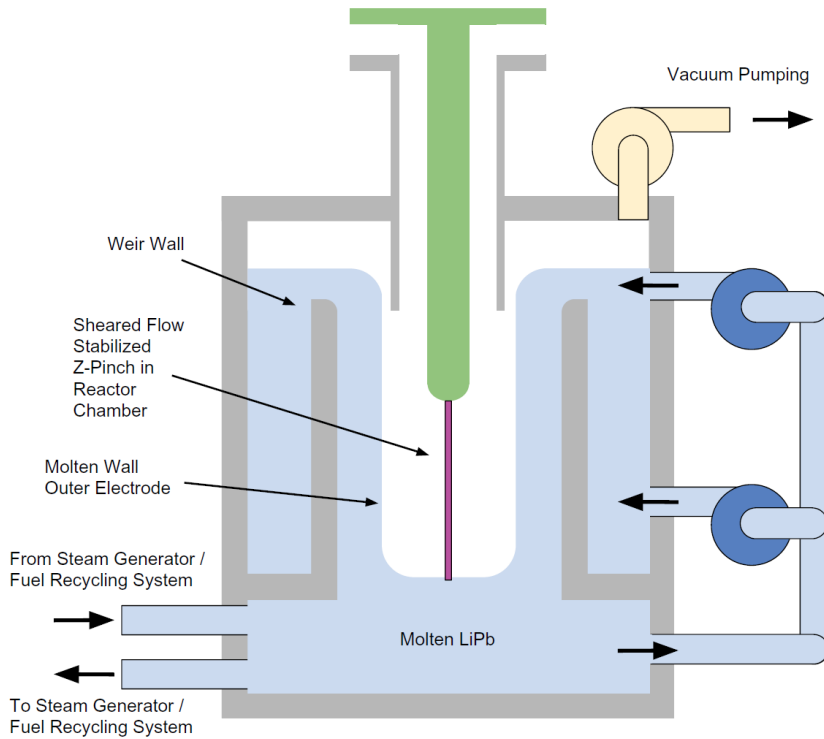
$$\frac{dV_z}{dr} \neq 0$$

M. G. Haines, etc., Phys. Plasmas 7, 1672 (2000)
 U. Shumlak, etc., Physical Rev. Lett. 75, 3285 (1995)
 U. Shumlak, etc., ALPHA Annual Review Meeting 2017

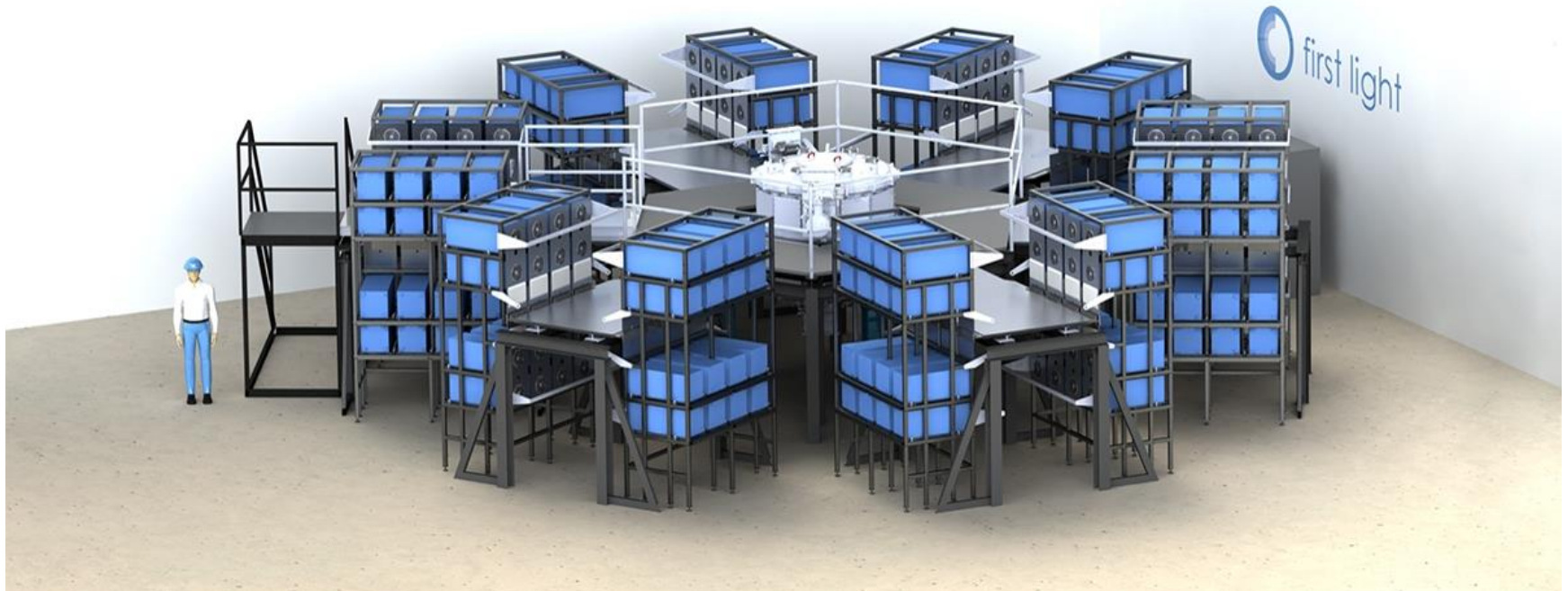
A z-pinch plasma can be stabilized by sheared flows



Fusion reactor concept by ZAP energy



First light fusion, UK



- **2.5 MJ @ 200 kV**
- **14 MA with $t_{\text{rise}} \sim 2 \text{ us}$**

First light fusion, UK

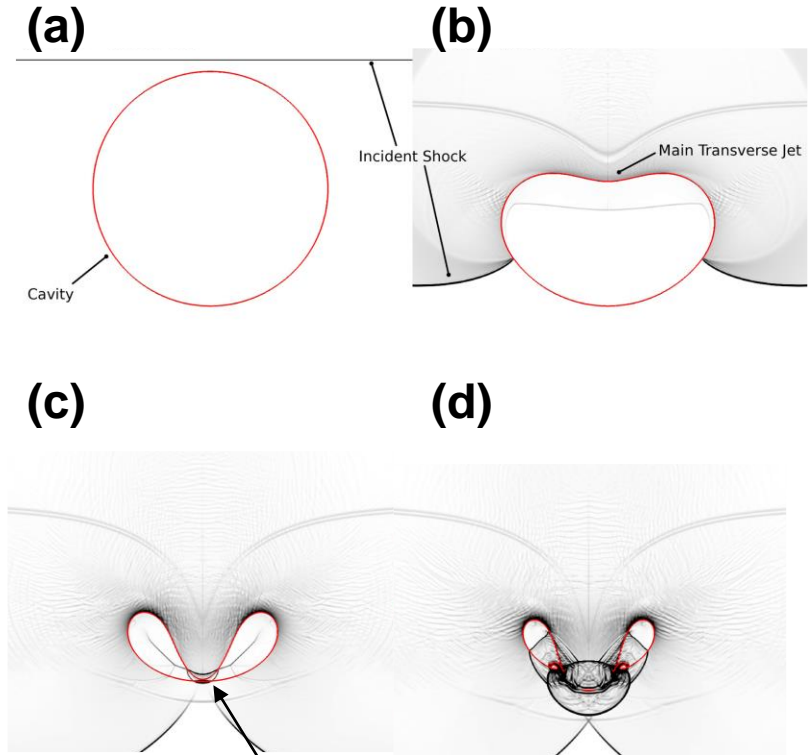
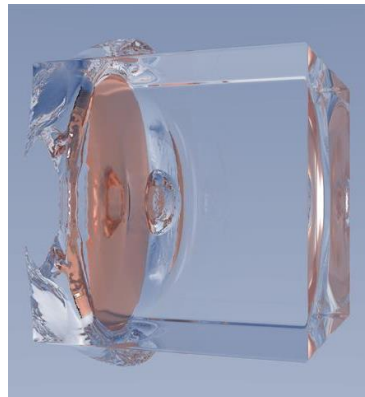
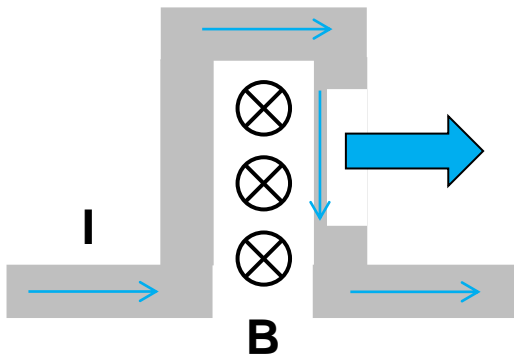


https://www.all-electronics.de/wp-content/uploads/2019/08/1_Pic_192-capacitors-around-vacuum-chamber_lowres-1024x768.jpg

Projectile Fusion is being established at First Light Fusion Ltd, UK



- **Stored energy: 2.5 MJ @ 200 kV**
($C_{\text{tot}}=125 \mu\text{F}$)
- $I_{\text{peak}}=14 \text{ MA w/ } T_{\text{rise}} \sim 2 \mu\text{s.}$

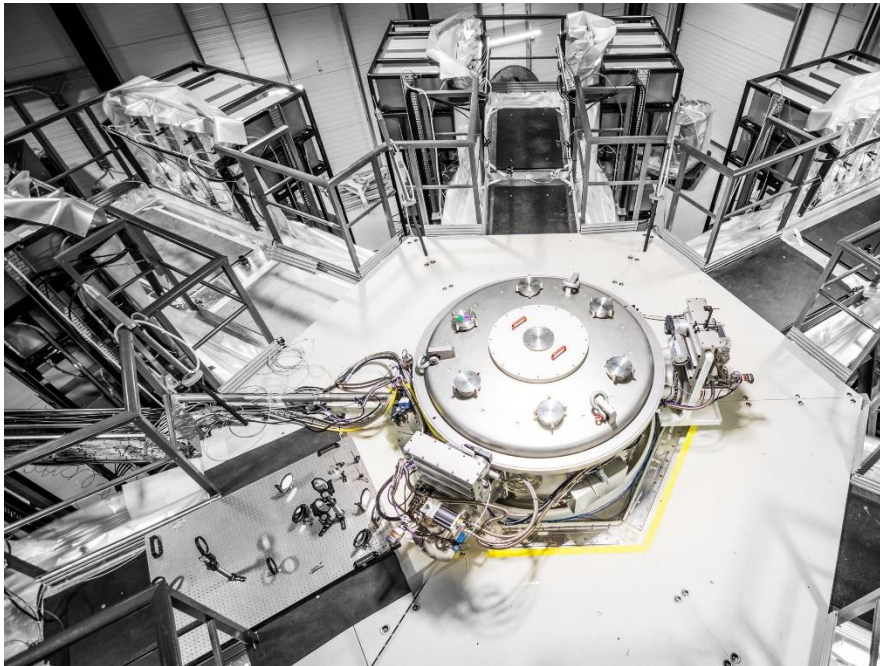


- **High pressure is generated by the colliding shock.**

<https://firstlightfusion.com/>

B. Tully and N. Hawker, Phys. Rev. **E93**, 053105 (2016)

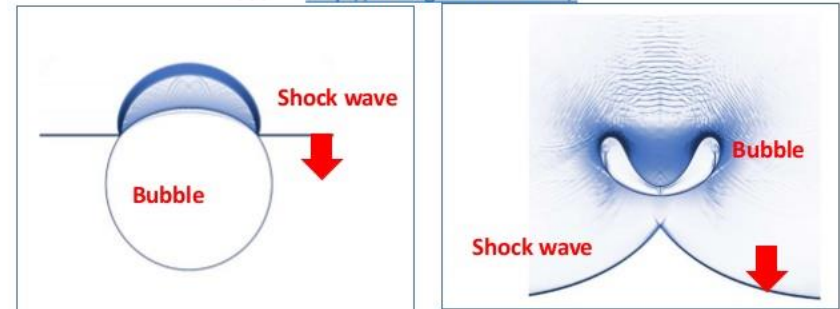
First light fusion, UK – achieving ignition using shock wave



First Light Fusion

First Light Fusion is a spin-off from Oxford University department of mechanical engineering and claims to be able to harness instabilities by using asymmetrical implosion.

See <http://firstlightfusion.com/>



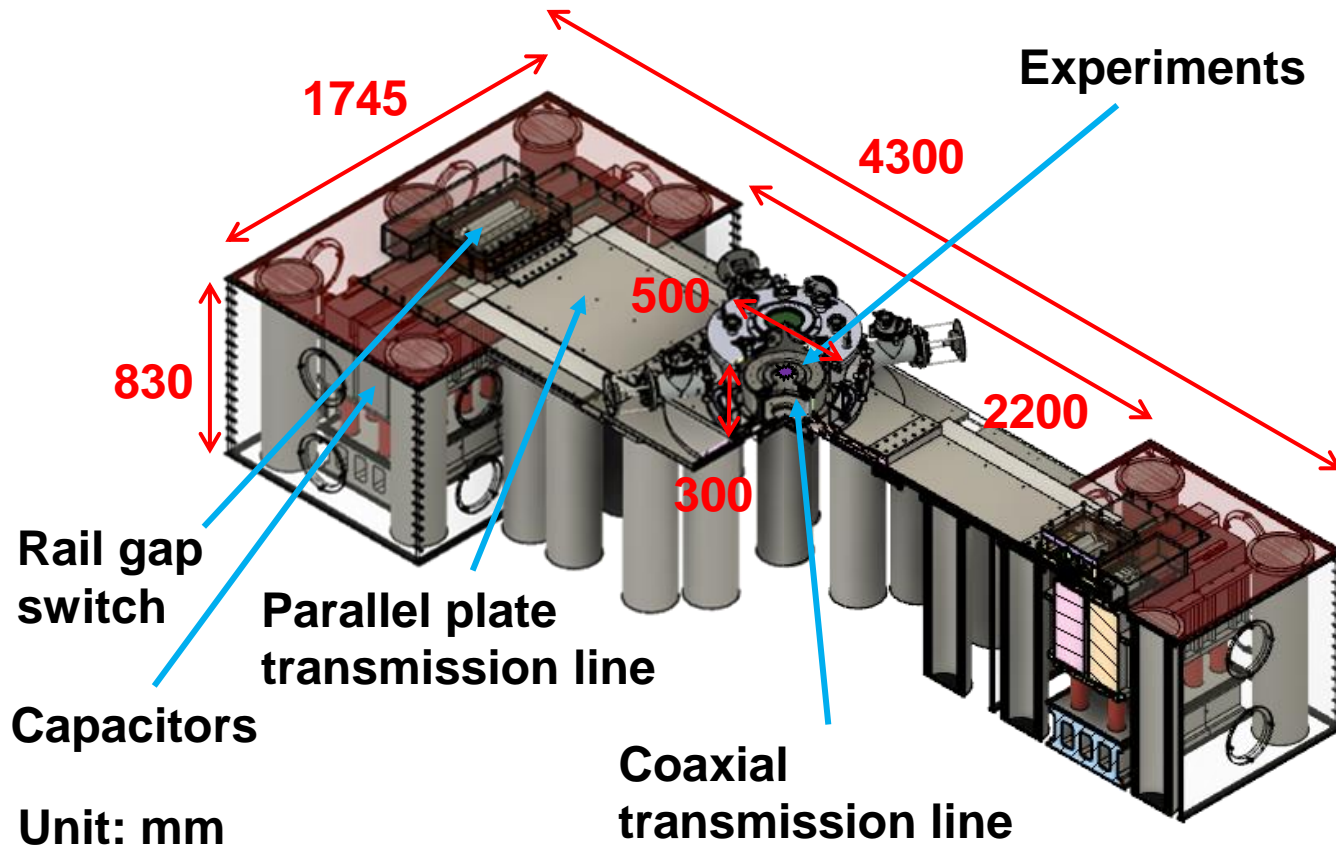
A gas gun is used to eject the projectile



<https://www.youtube.com/watch?v=JN7lyxC11n0>

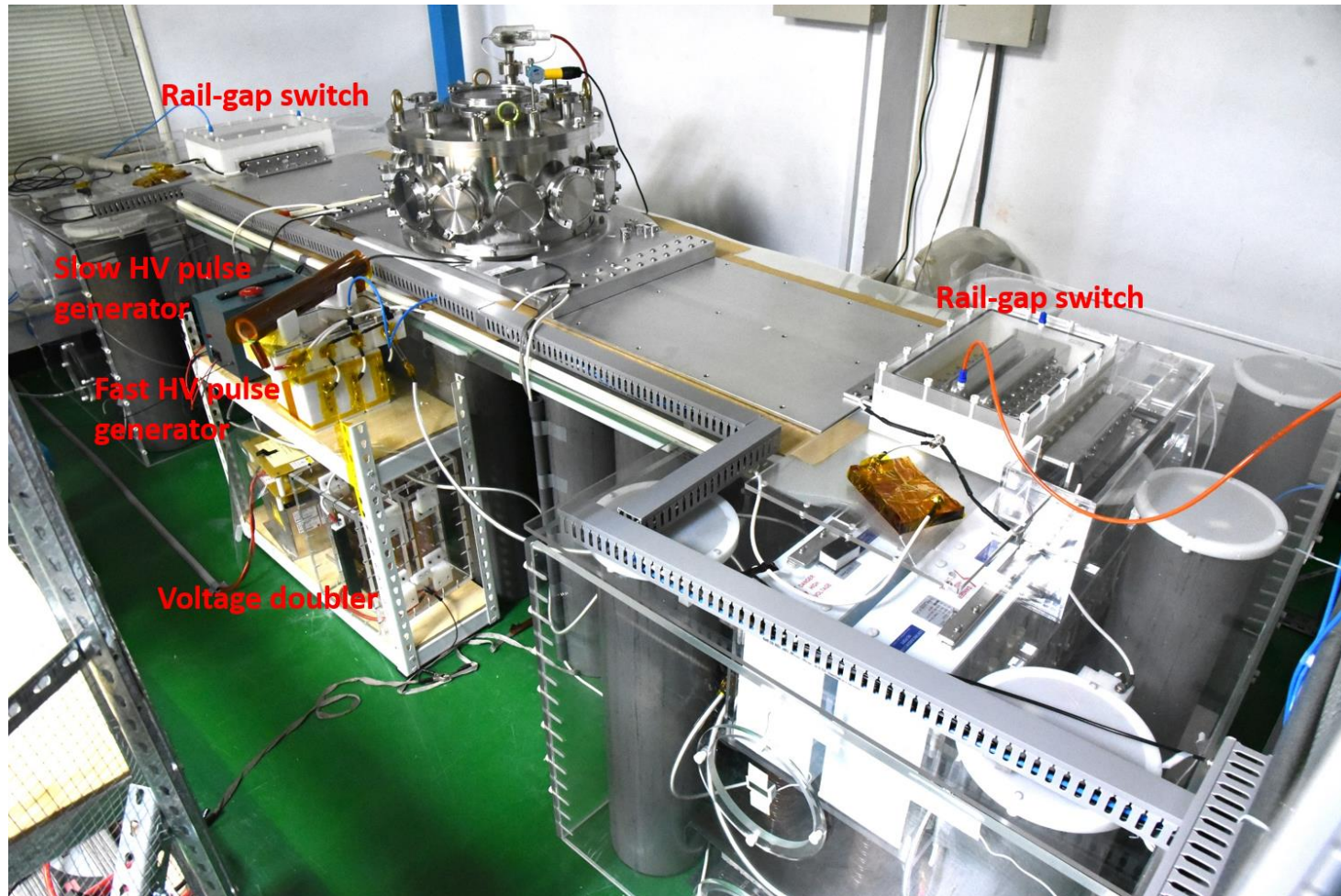
<https://www.youtube.com/watch?v=aW4eufac-f8>

The pulsed-power system was built by only students

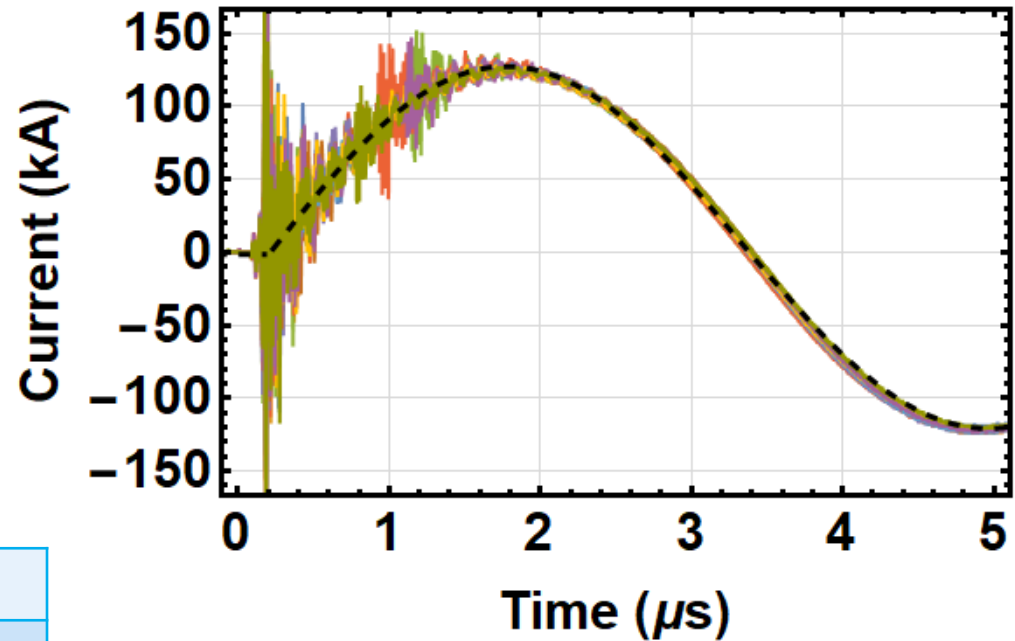
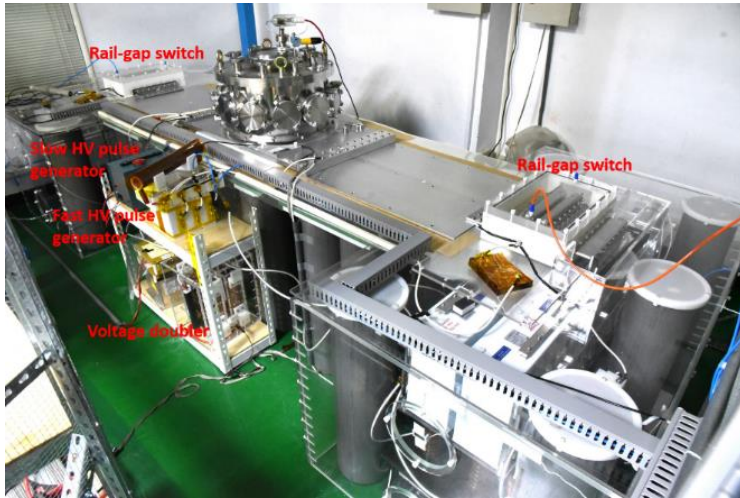


- A 1 kJ pulsed-power system at ISAPS, NCKU started being operated since September, 2019.

The 1-kJ pulsed-power system

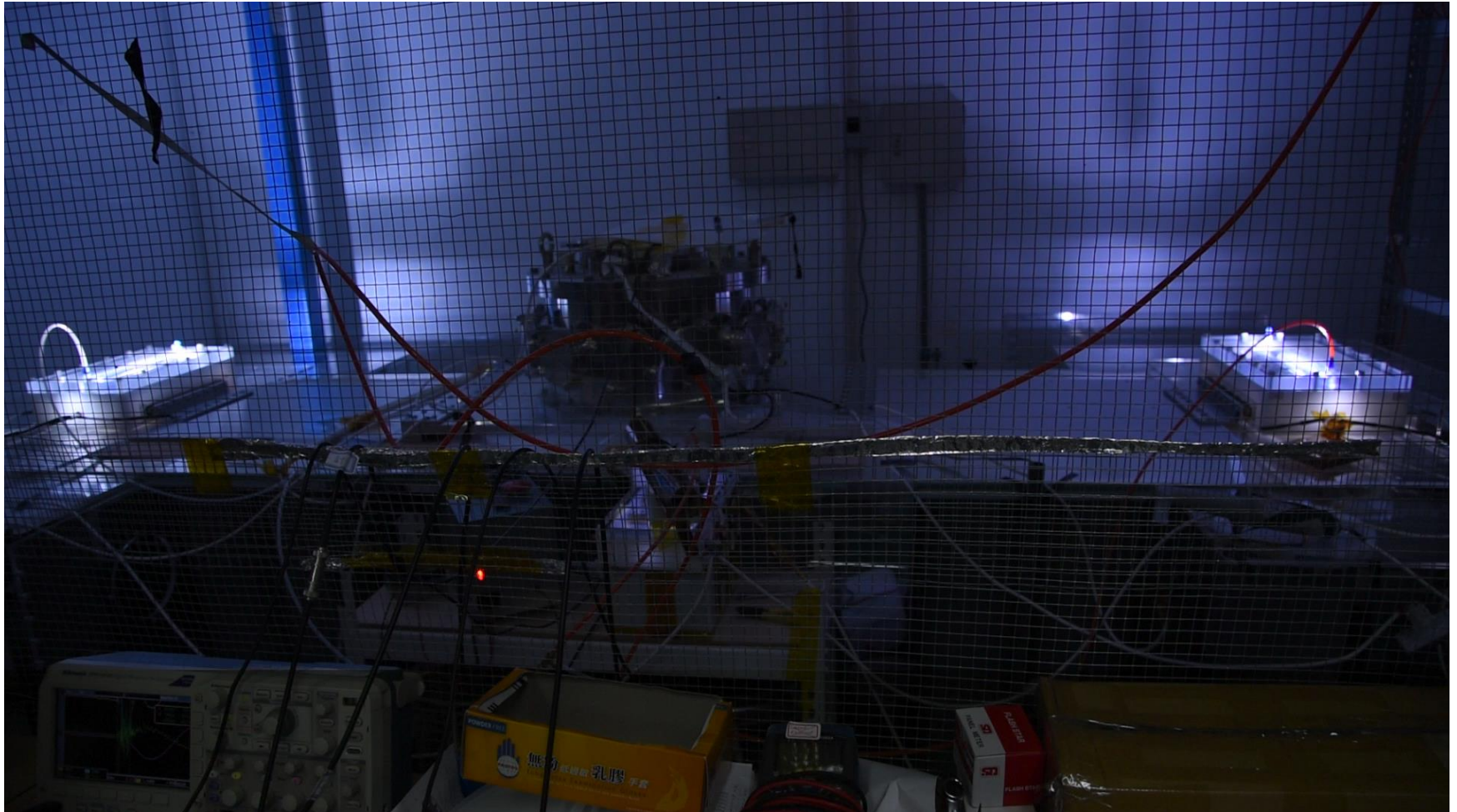


A peak current of ~ 135 kA with a rise time of ~ 1.6 μ s is provided by the pulsed-power system

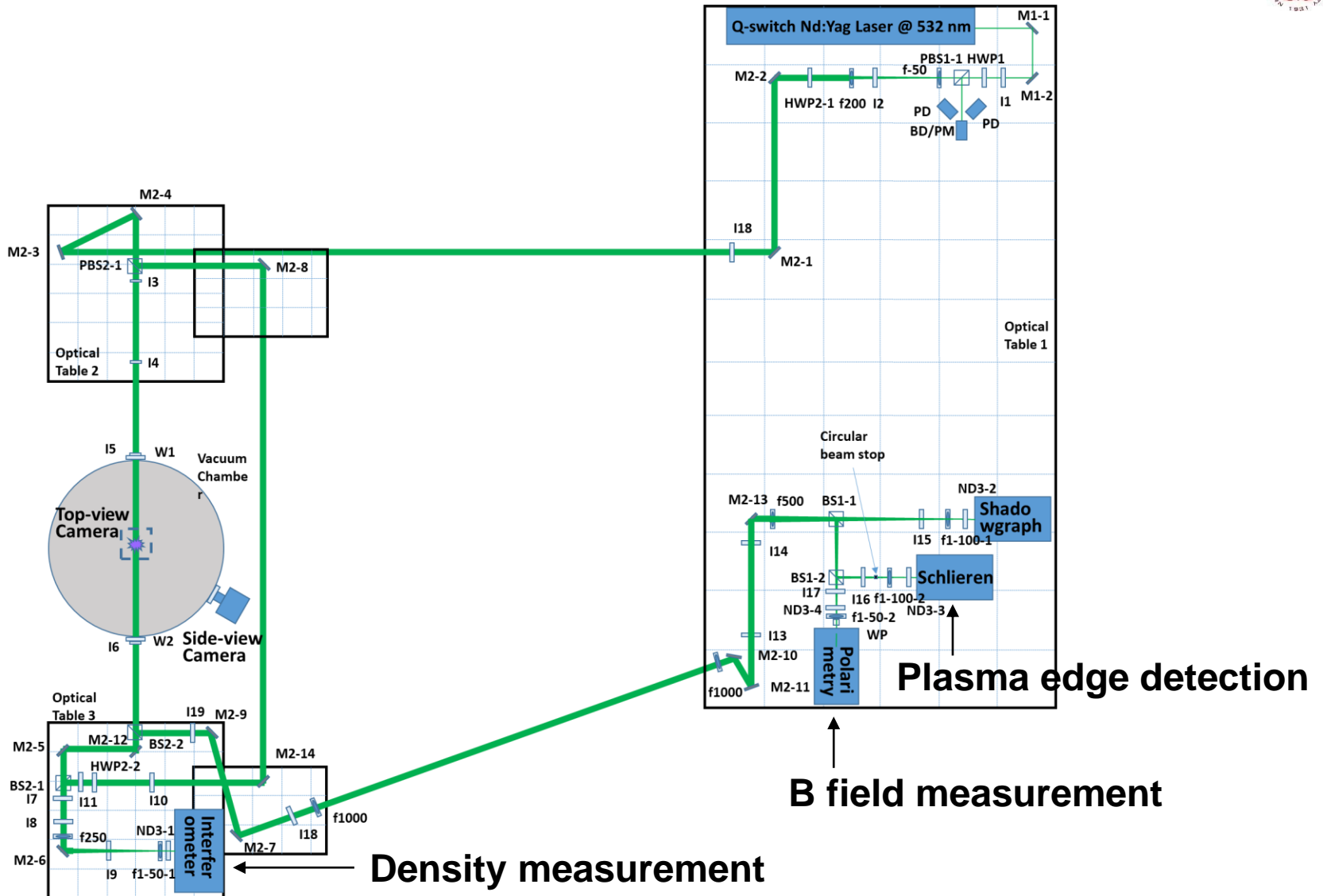


Capacitance (μ F)	5
V_{charge} (kV)	20
Energy (kJ)	1
Inductance (nH)	204 ± 4
Rise time (quarter period, ns)	1592 ± 3
I_{peak} (kA)	135 ± 1

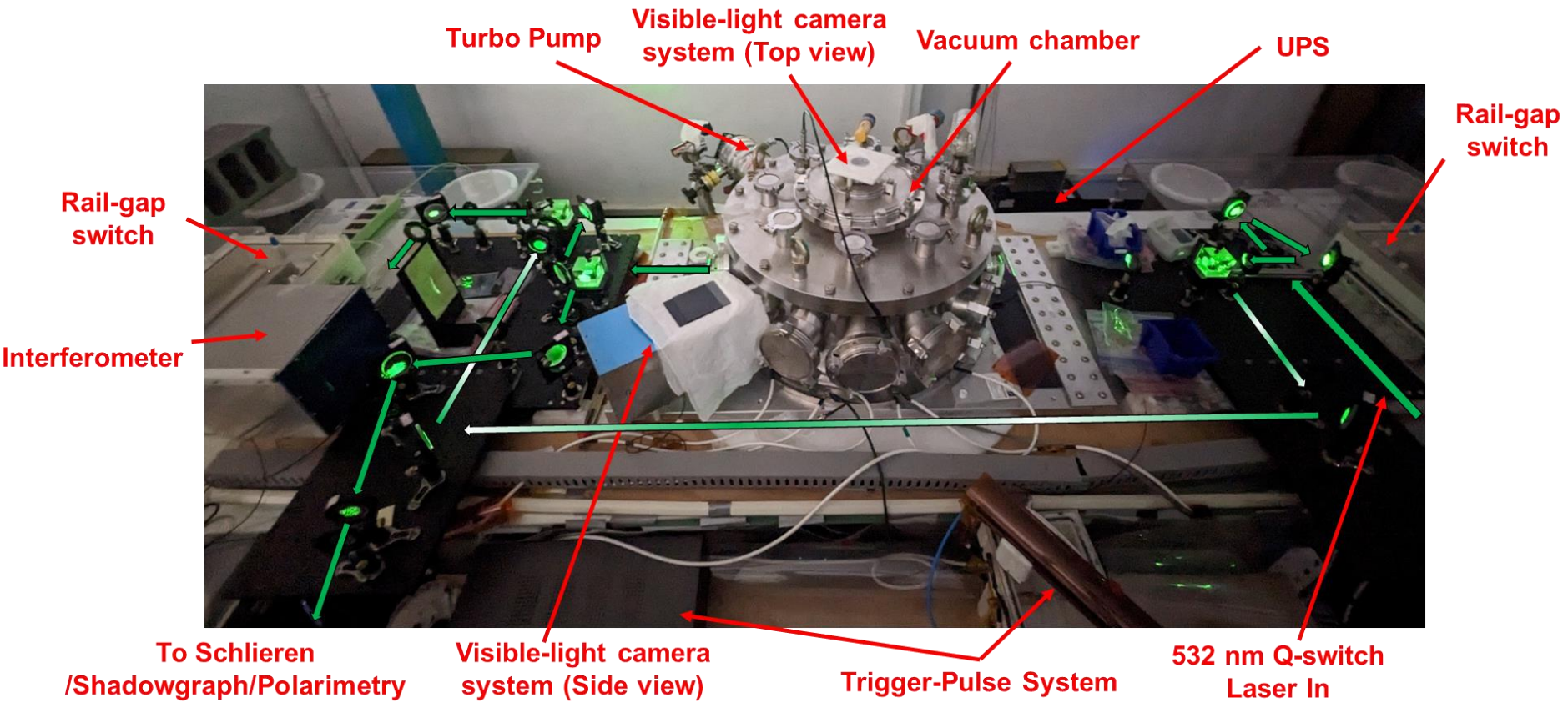
First shot with two synchronized rail-gap switches



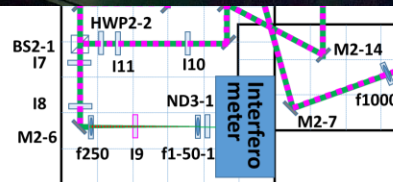
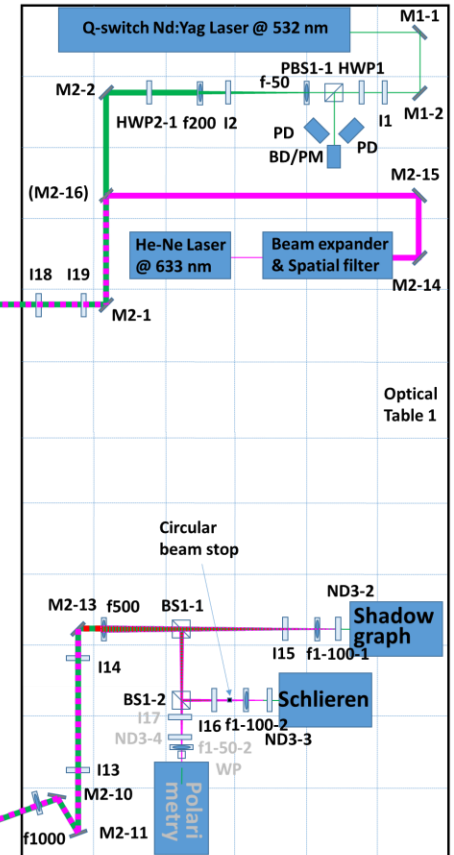
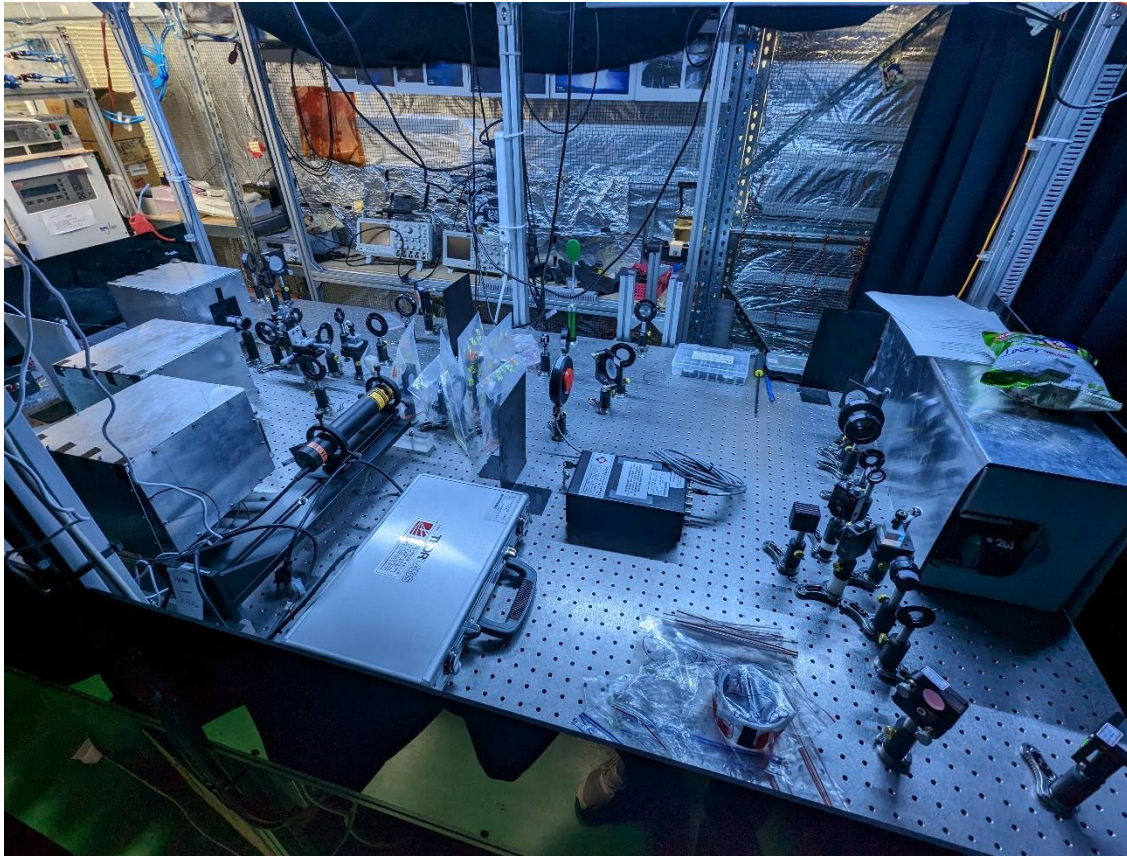
Time-resolved imaging system with temporal resolution in the order of nanoseconds was implemented



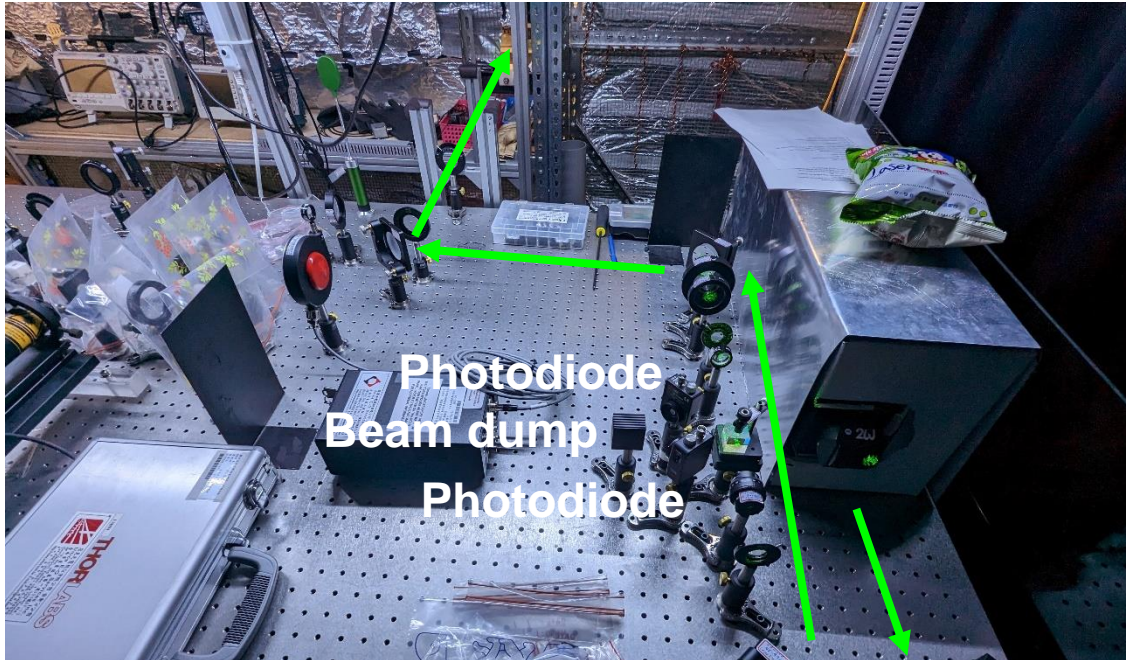
Varies diagnostics were integrated to the system



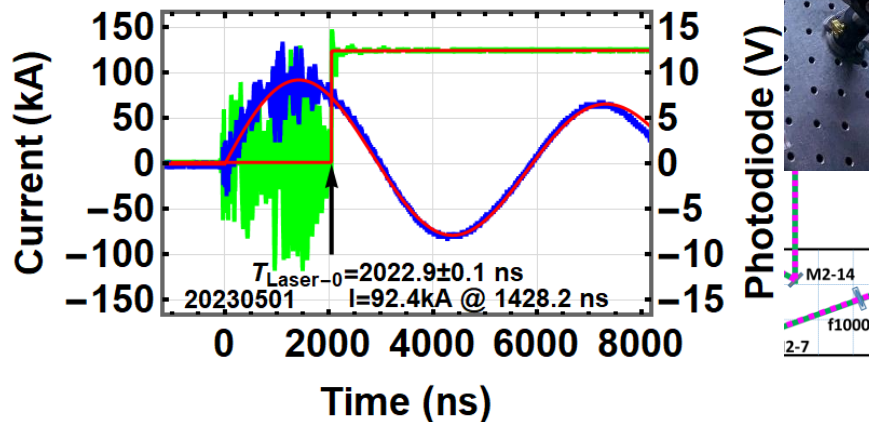
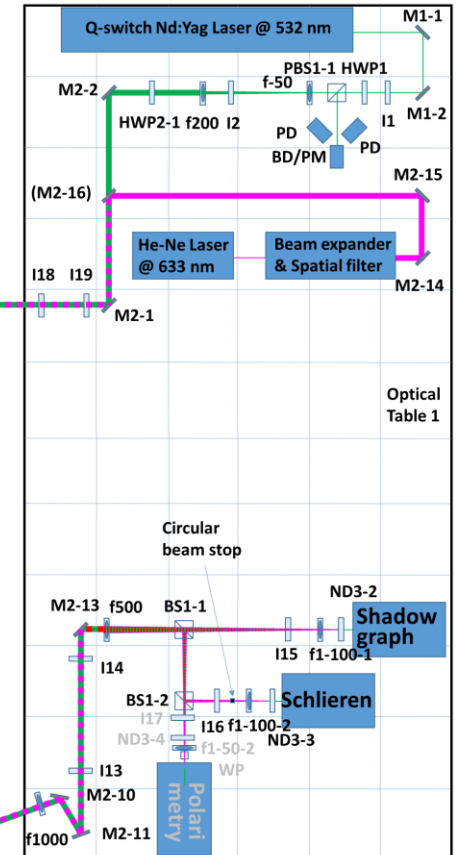
Beam path



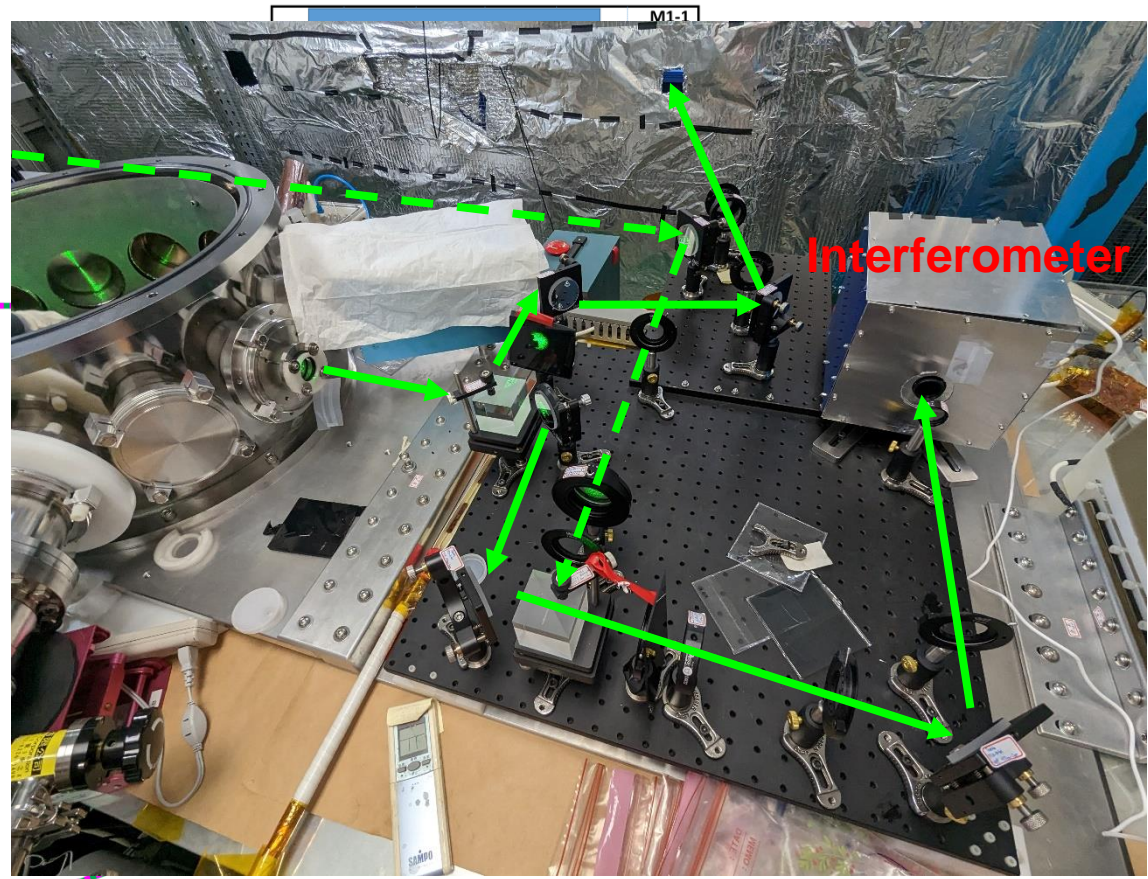
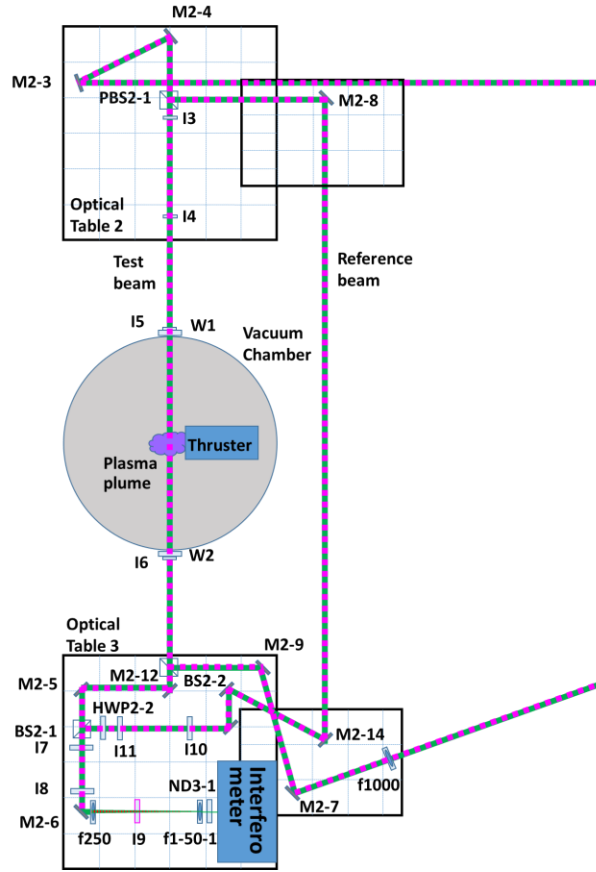
Beam path



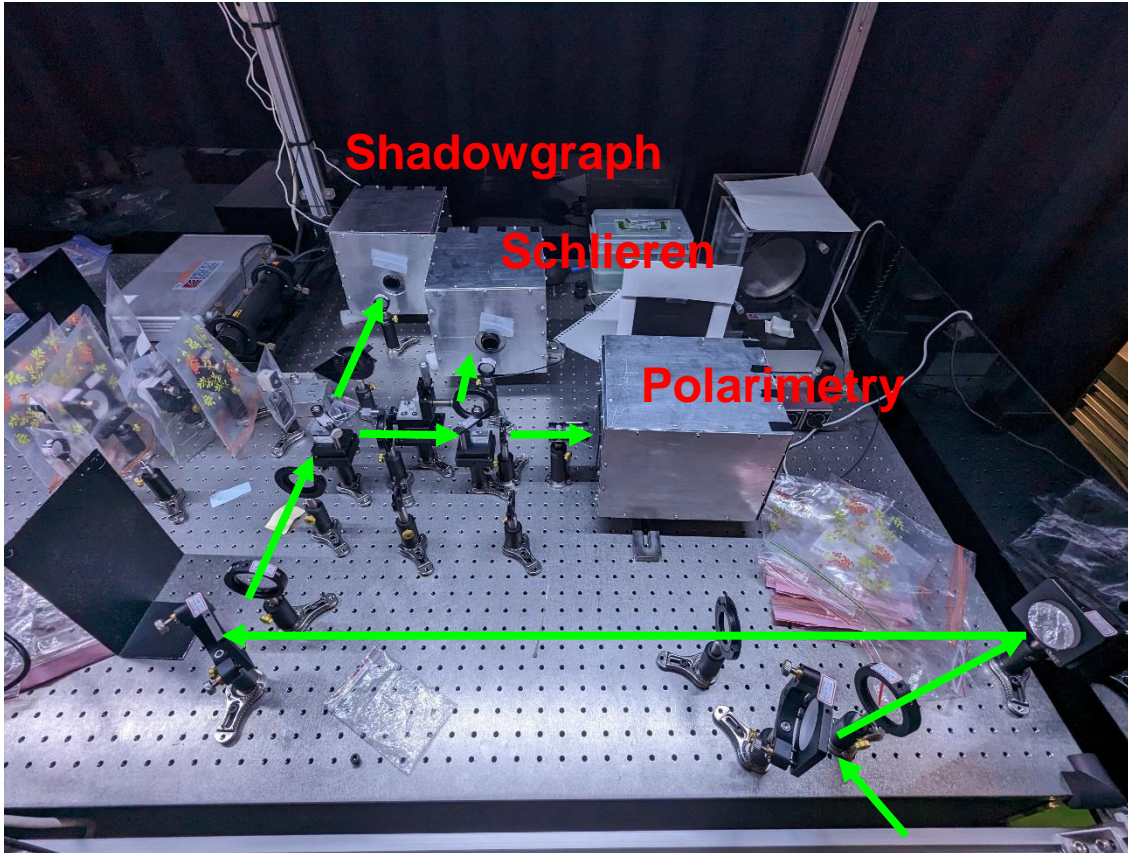
Photodiode
Beam dump
Photodiode



Beam path



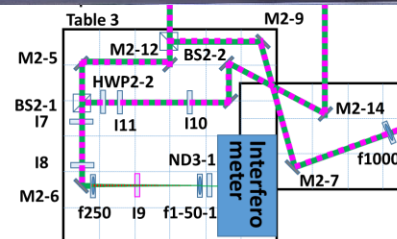
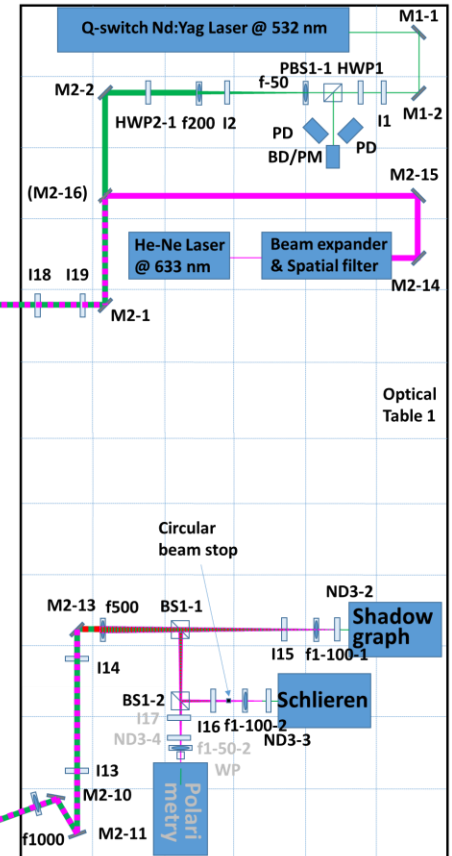
Beam path



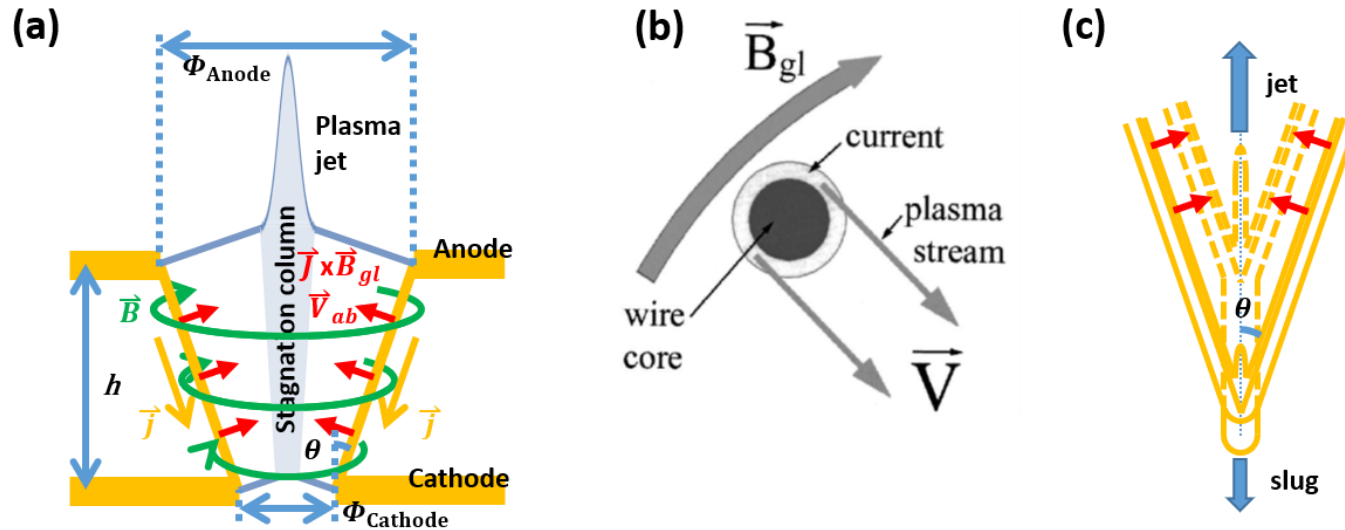
Shadowgraph

Schlieren

Polarimetry



Laboratory astrophysics: plasma jet can be generated by a conical-wire array driven by the PGS machine



- Herbig-Haro (HH) 111 is a plasma jet driven by a compact molecular core in the L1617 cloud complex where a young star locates*. The plasma jet in HH 111 is well collimated with the velocity of 220–330 km/s**.

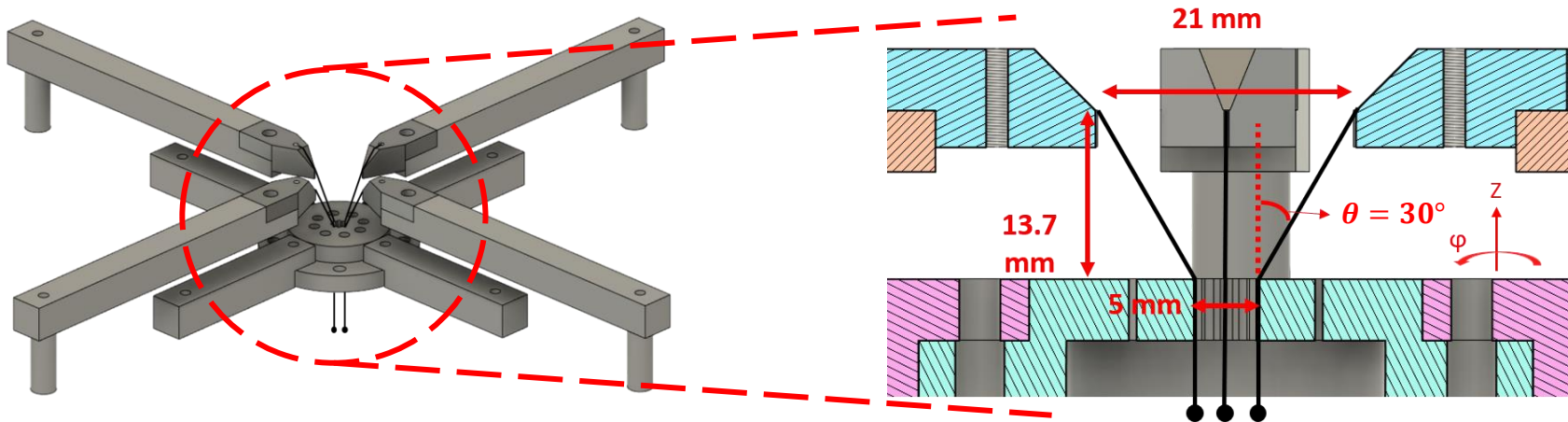


*Bo Reipurth and Steve Heathcote. 50 Years of Herbig-Haro Research, pages 3–18. Springer Netherlands, Dordrecht, 1997.

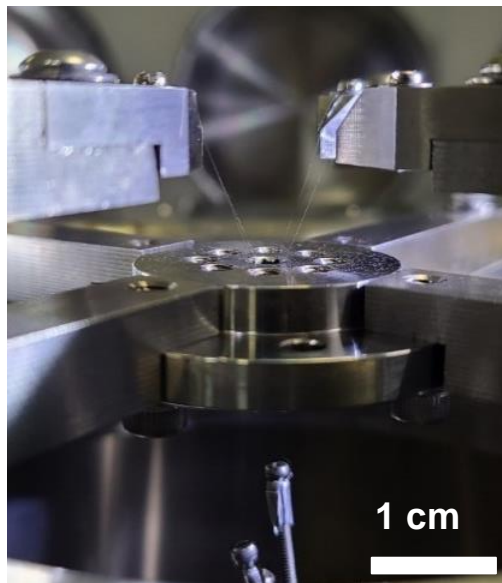
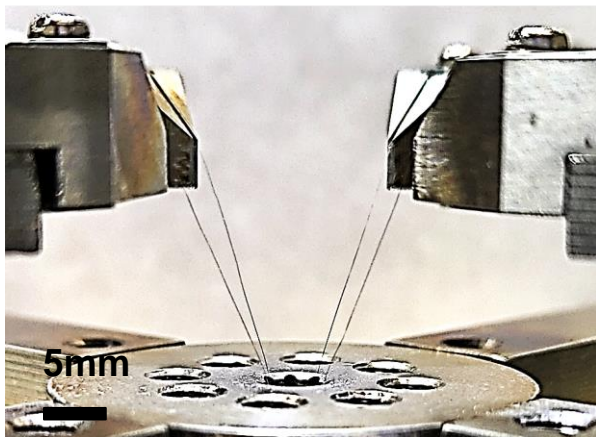
**Patrick Hartigan, Jon A. Morse, Bo Reipurth, Steve Heathcote, and John Bally. The Astrophysical Journal, 559(2):L157–L161, oct 2001.

*** Bo Reipurth and John Bally. Annual Review of Astronomy and Astrophysics, 39(1):403–455, sep 2001.

Our conical-wire array consists of 4 tungsten wires with an inclination angle of 30° with respect to the axis



- Conical-wire array

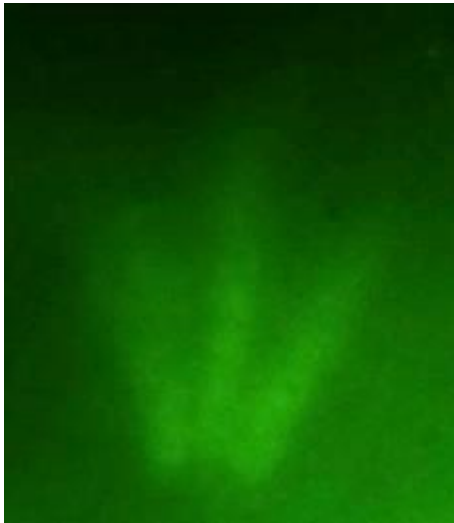


- Material : Tungsten.
- Number of wires : 4.
- Diameter : $20 \mu\text{m}$.

Self-emission of the plasma jet in the UV to soft x-ray regions was captured by the pinhole camera



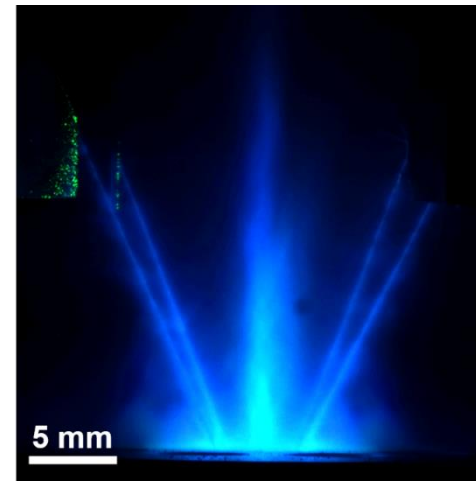
- Image in UV/soft x ray



(Brightness is increased by 40 %.)

- Pinhole diameter: 0.5 mm, i.e., spatial resolution: 1 mm.

- Image in visible light

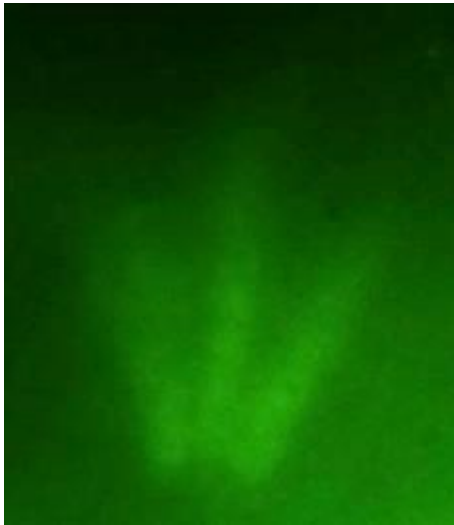


(Enhanced by scaling the intensity range linearly from 0 – 64 to 0 – 255.)

The MCP was burned due to the higher DC voltage supply



- Image in UV/soft x ray

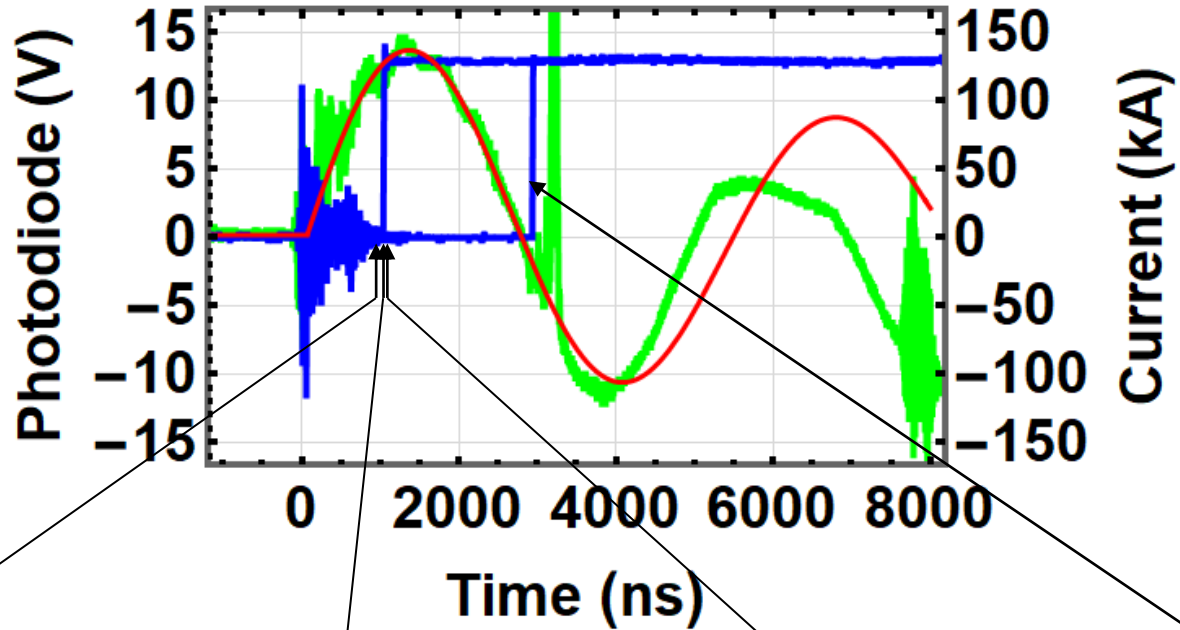


(Brightness is increased by 40 %.)

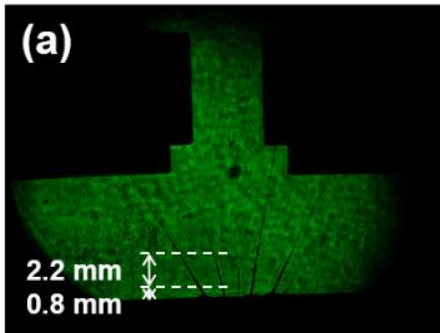


- Pinhole diameter:
0.5 mm, i.e., spatial
resolution: 1 mm.

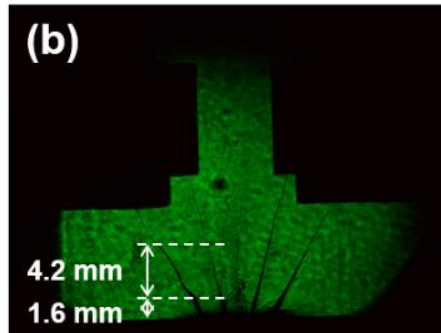
Plasma jet propagation was observed using laser diagnostics



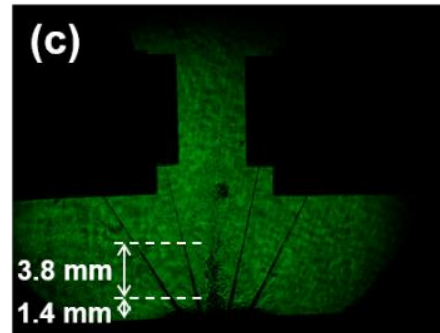
- Shadowgraph images:



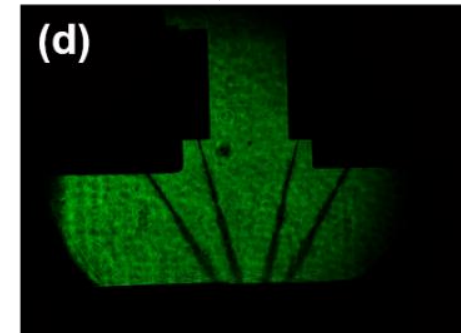
930 ± 20 ns



975 ± 2 ns



985 ± 3 ns

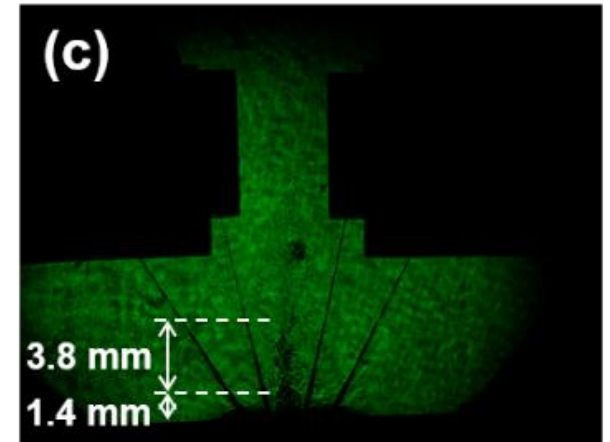
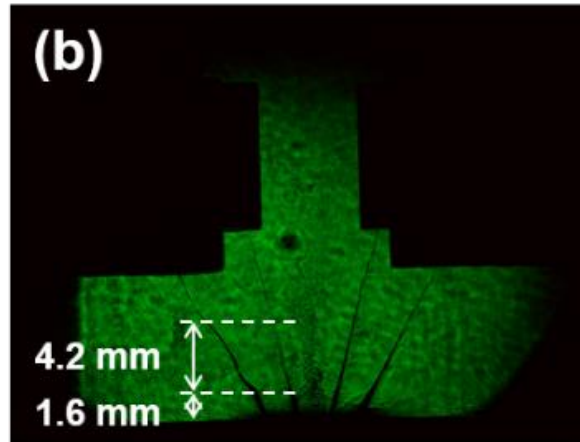
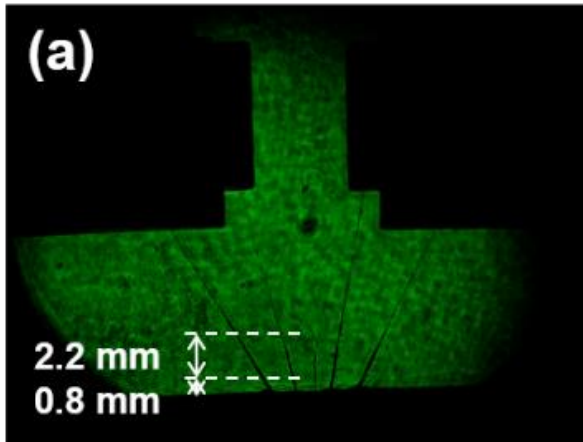


2945 ± 2 ns

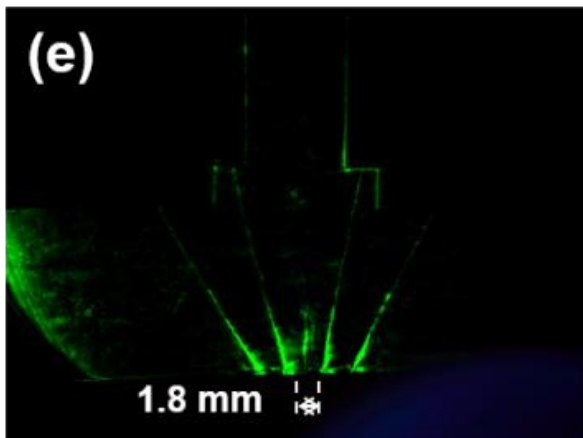
Length of the plasma jet at different time was obtained by the Schlieren images at different times



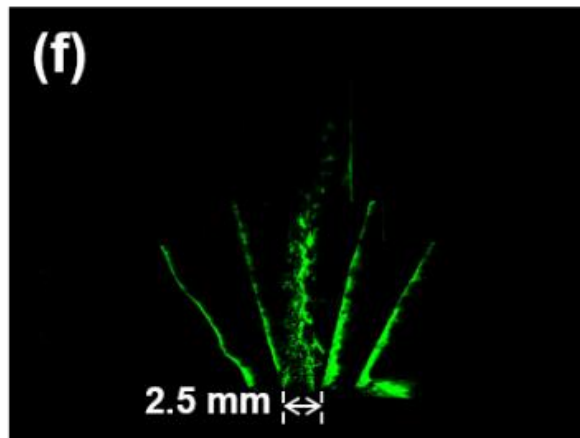
- Shadowgraph images:



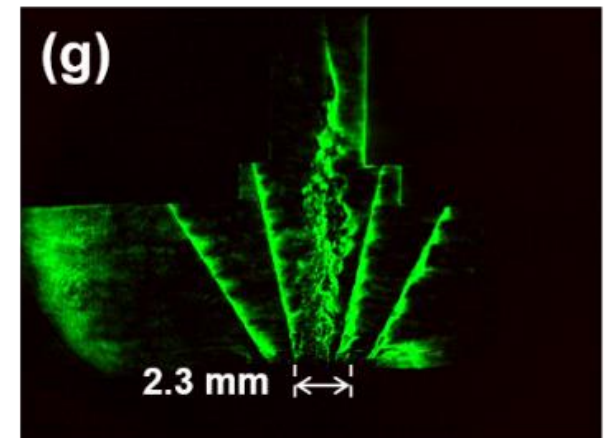
- Schlieren images:



930 ± 20 ns

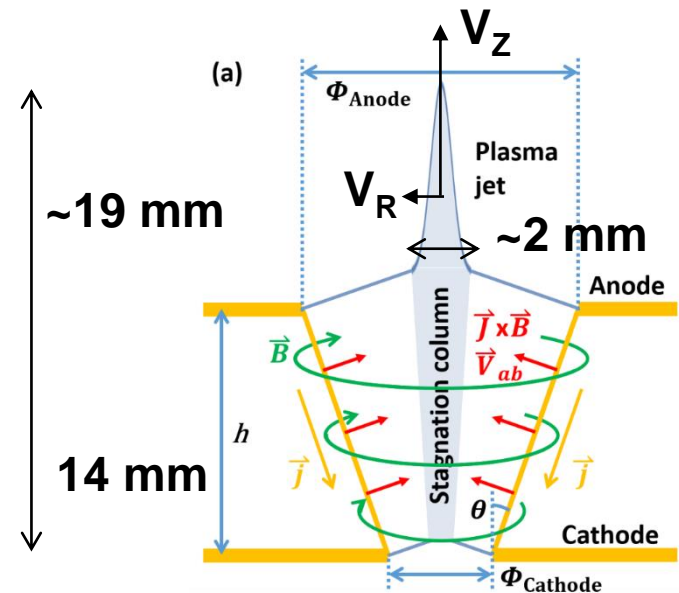
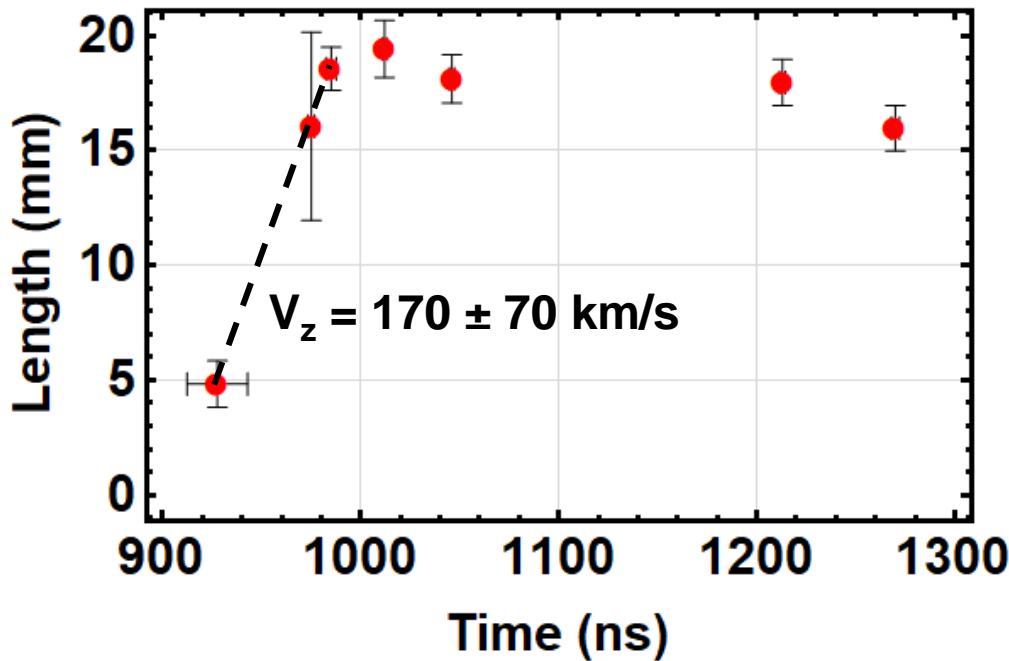


975 ± 2 ns



985 ± 3 ns

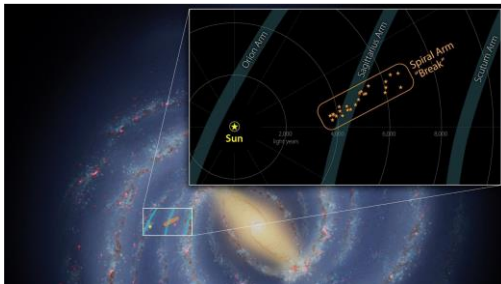
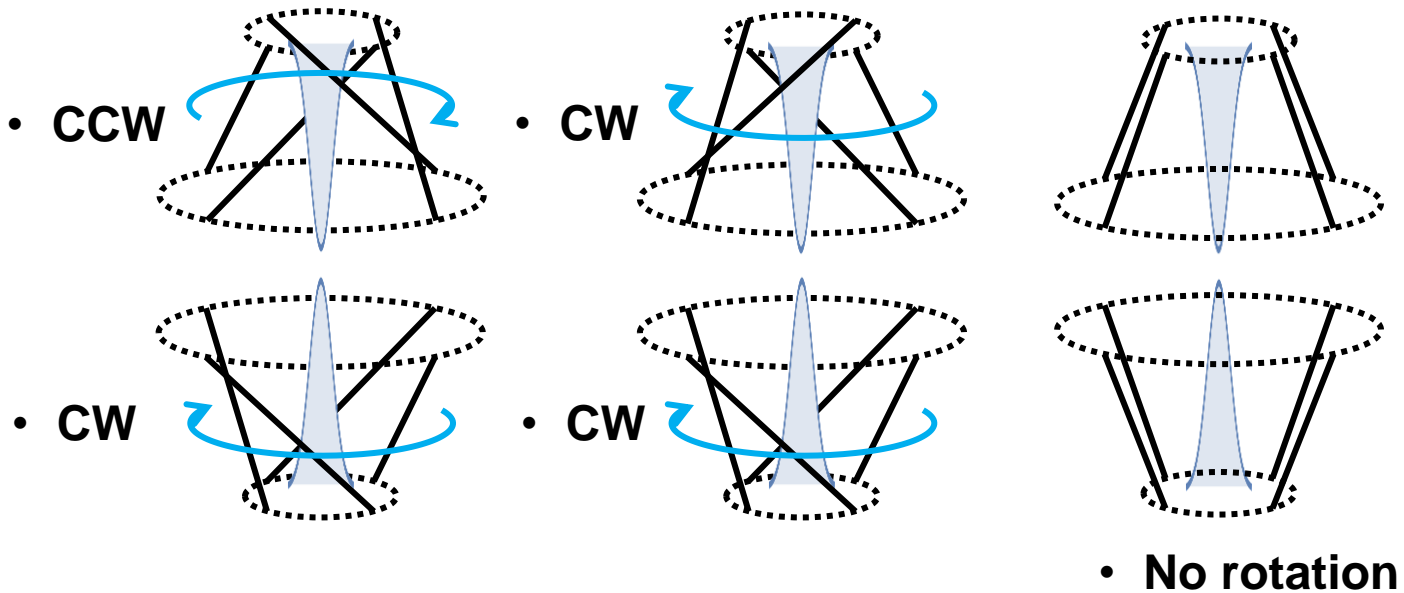
The measured plasma jet speed is 170 ± 70 km/s with the corresponding Mach number greater than 5



$$M = \frac{V_z}{V_R} \geq \frac{Z}{r} \approx \frac{(19 - 14) \text{ mm}}{\frac{2 \text{ mm}}{2}} = 5$$

$$V_{ab} = V_j \frac{\sin \theta}{1 + \cos \theta} = 50 \pm 20 \text{ km/s}$$

Can a rotating plasma disk be formed? To be continue...

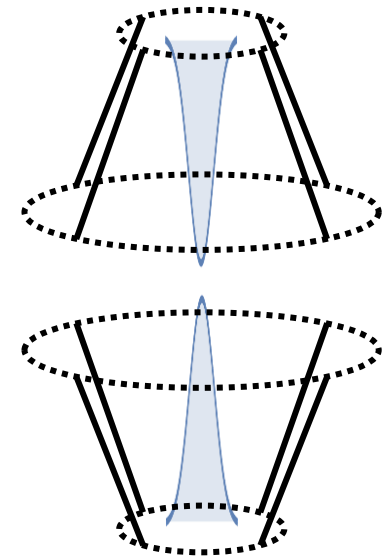
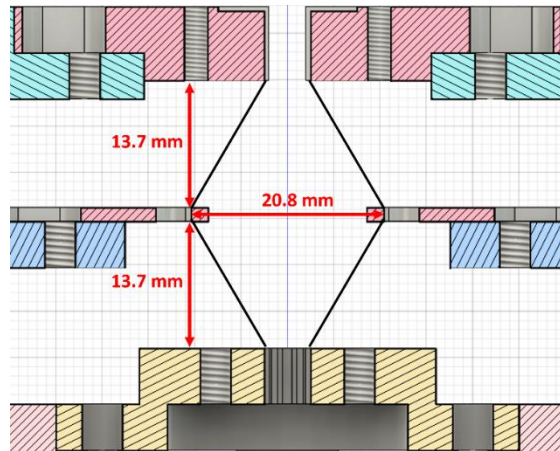
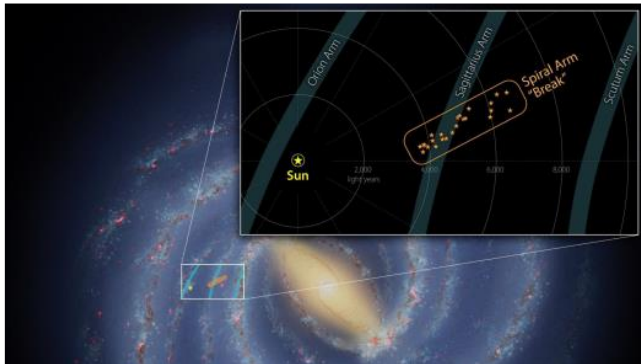


- **Astronomers Find a ‘Break’ in One of the Milky Way’s Spiral Arms.**

Plasma disk can be formed when two head-on plasma jets collide with each other



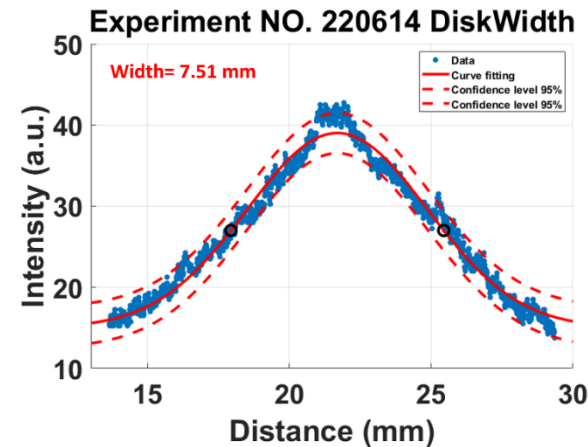
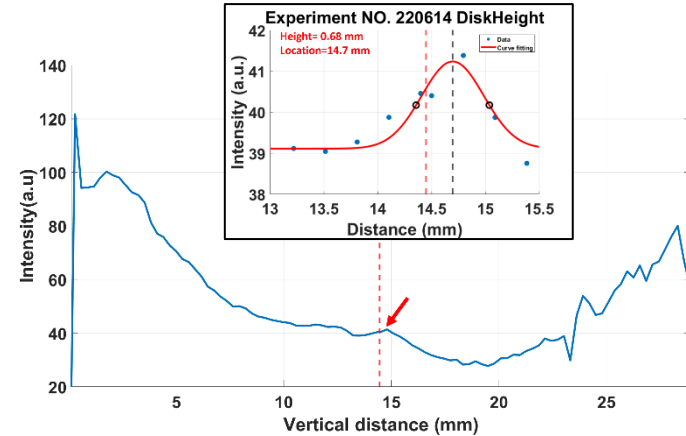
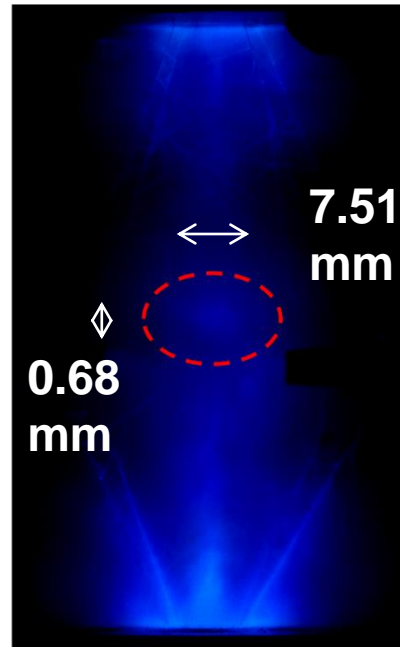
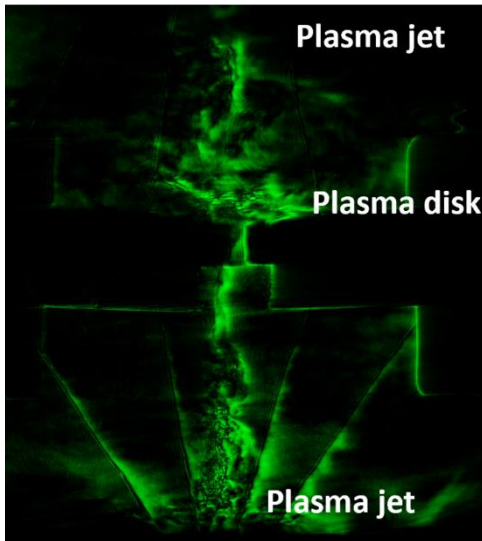
- Astronomers Find a 'Break' in One of the Milky Way's Spiral Arms.



A plasma disk with a height of ~ 0.68 mm and a width of ~ 7.51 mm was generated ~ 0.15 mm above the middle plane



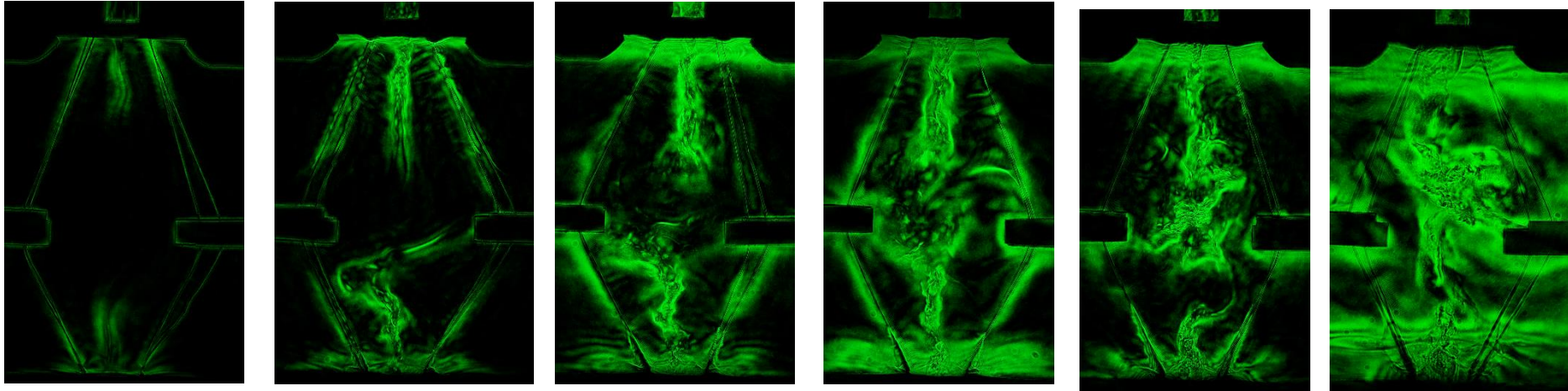
- Schlieren image:
- Time-integrated image:



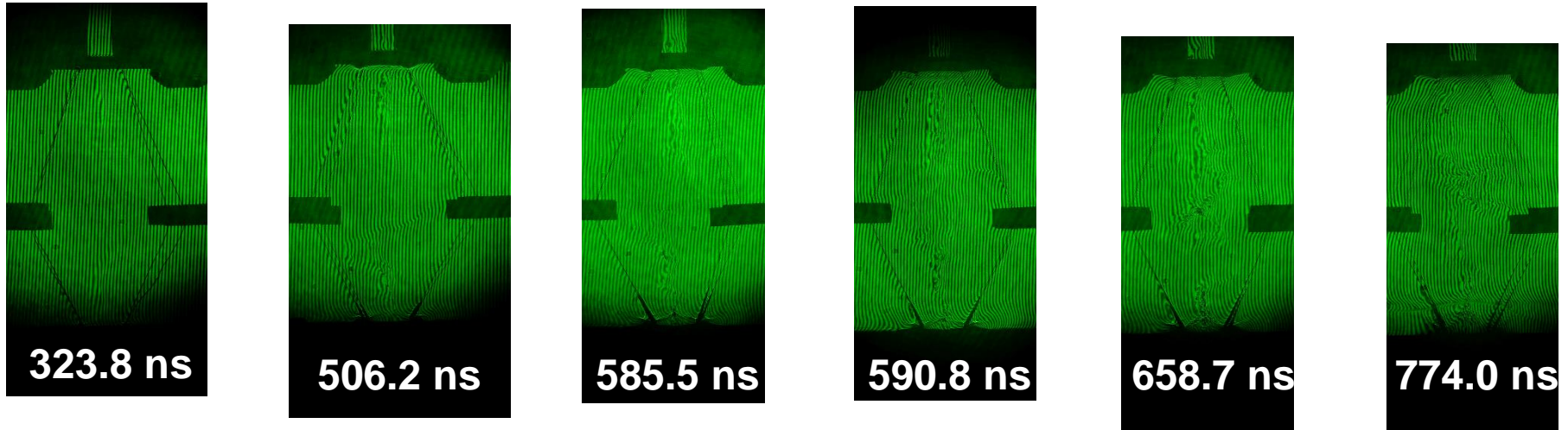
Plasma disk can be formed when two head-on plasma jets collide with each other



Schlieren



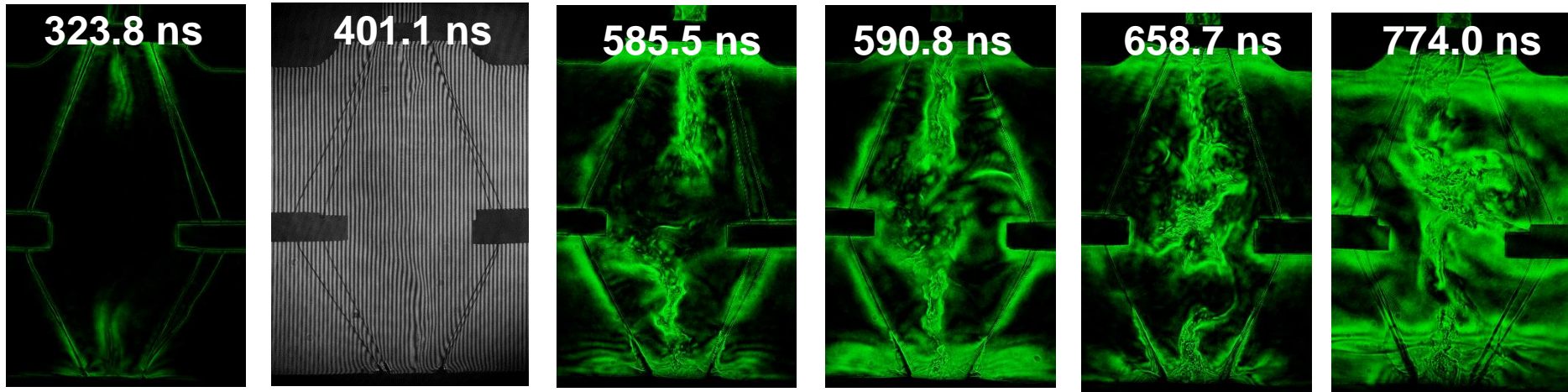
Interferometer



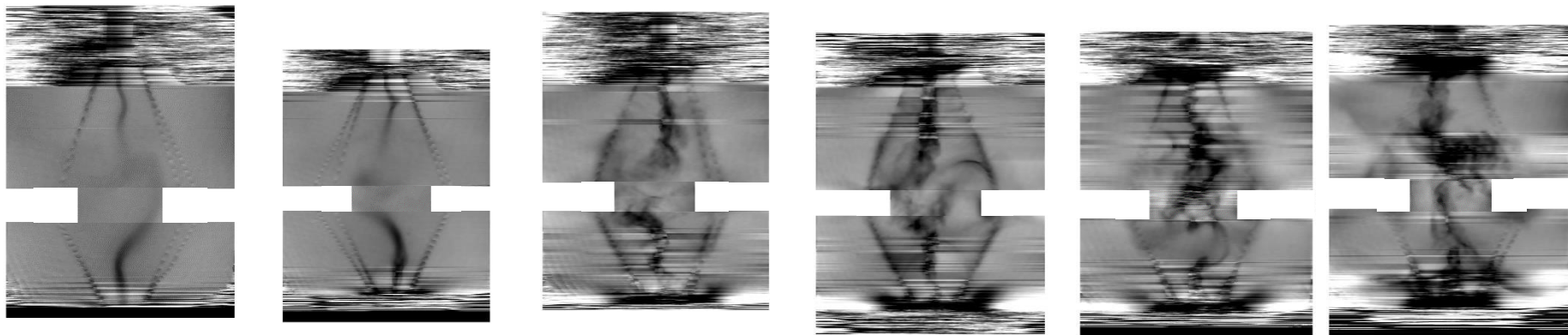
The plasma disk with a number density of $\sim 10^{18} \text{ cm}^{-3}$ was generated



Schlieren



Interferometer



$$-2\pi \sim 2\pi \Rightarrow 0 \sim 4.2 \times 10^{17} \text{ cm}^{-2}$$

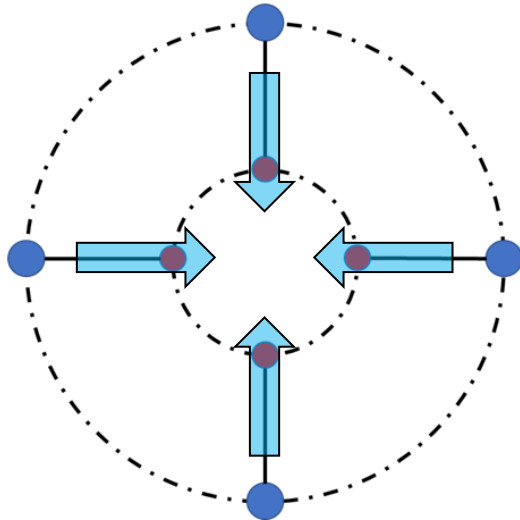
$$\Rightarrow 8.4 \times 10^{17} \text{ cm}^{-3} \text{ for } L = 5\text{mm}$$



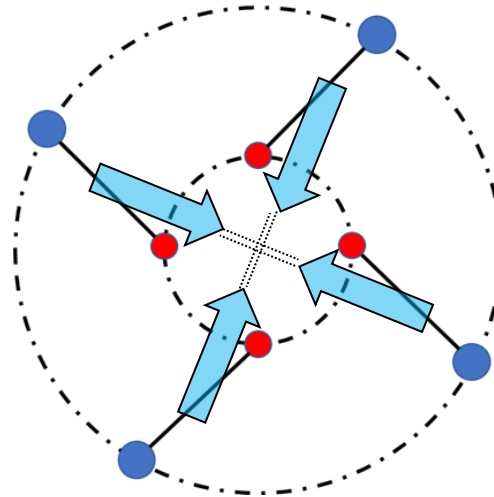
What if we twist the conical-wire array?



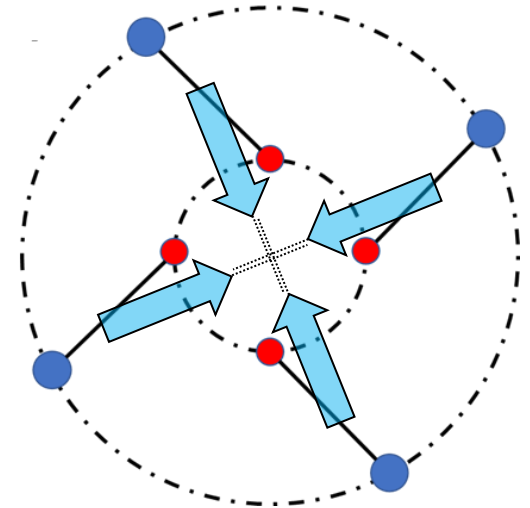
- **Non-rotation**



- **Clockwise 45°**



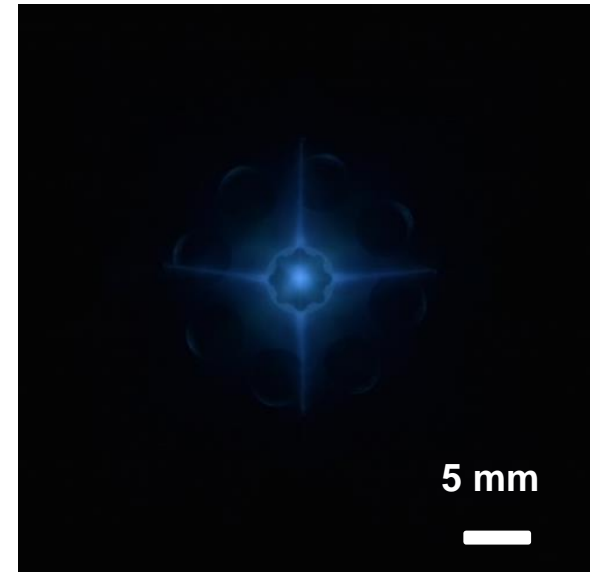
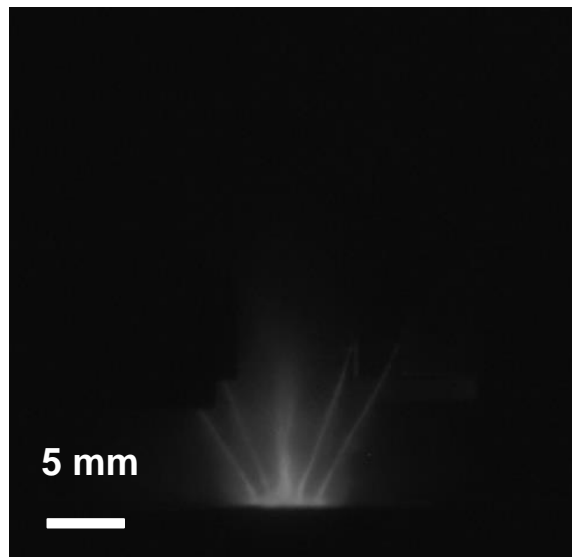
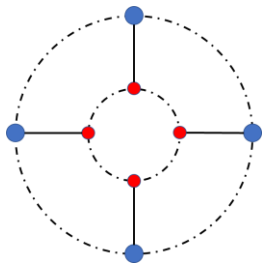
- **CCW 45°**



The plasma jet is a bright spot from the top view



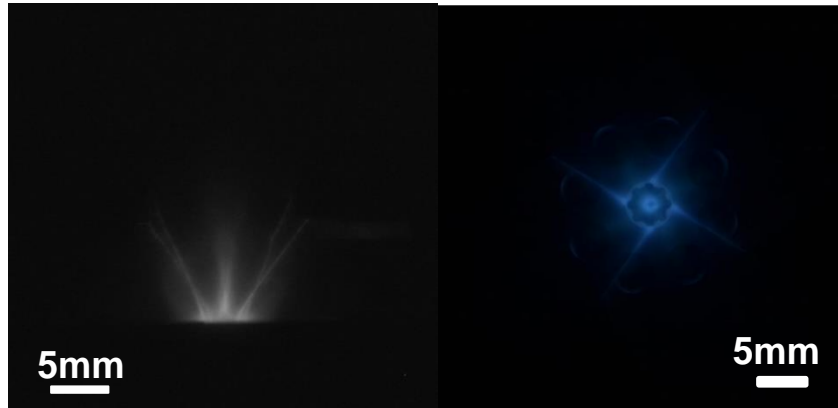
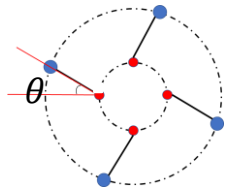
- **Non-rotation**



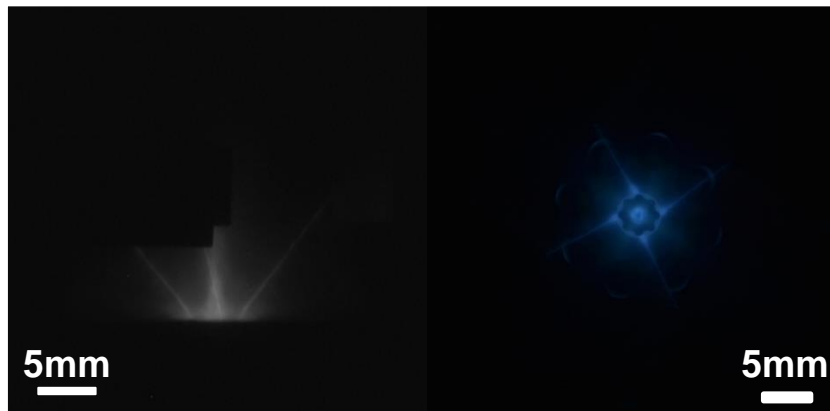
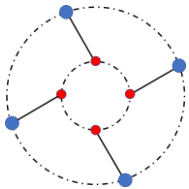
Hollow plasma jets were generated when the conical-wire arrays were twisted



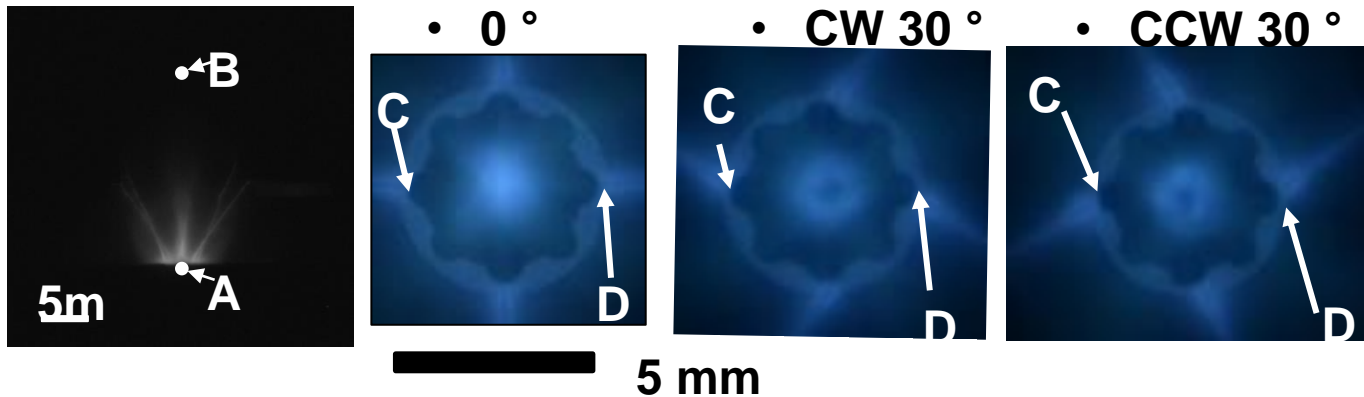
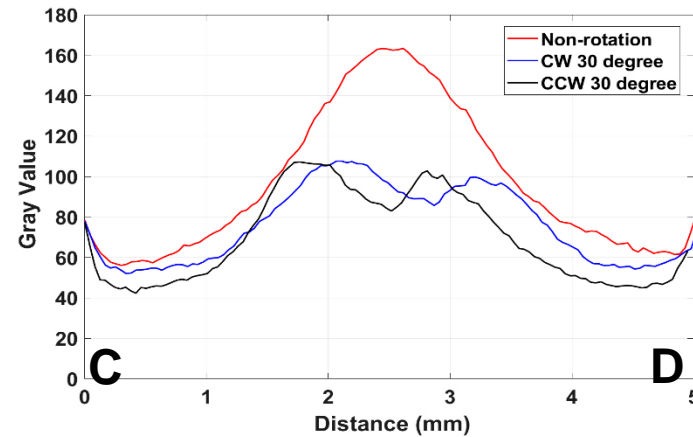
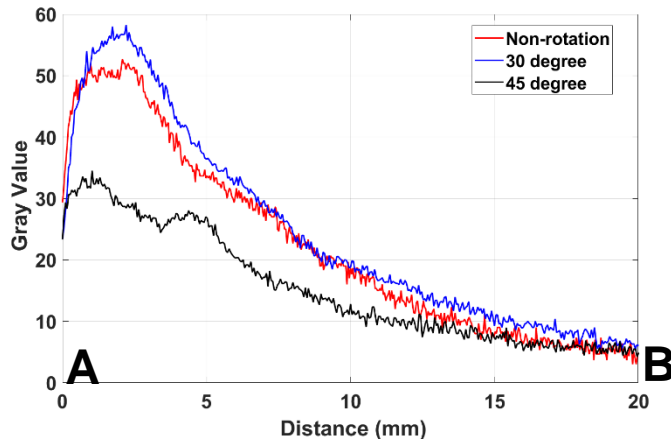
- **Clockwise 30 °**



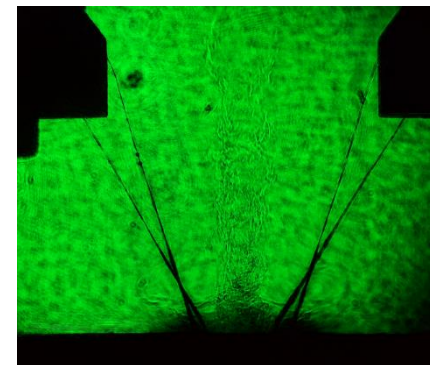
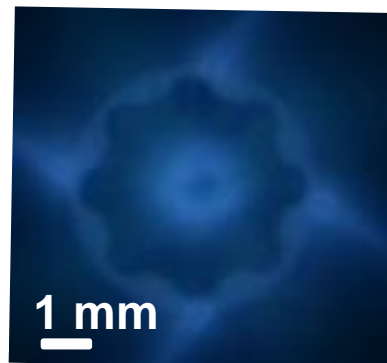
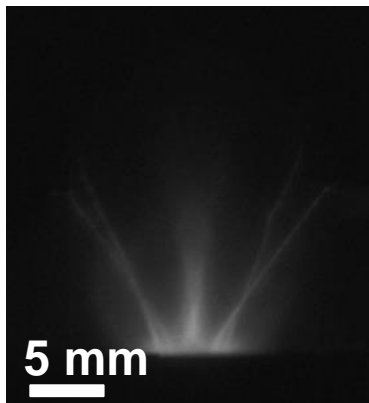
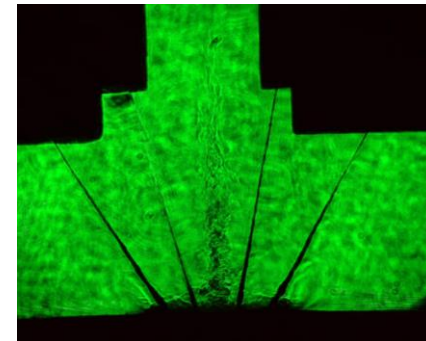
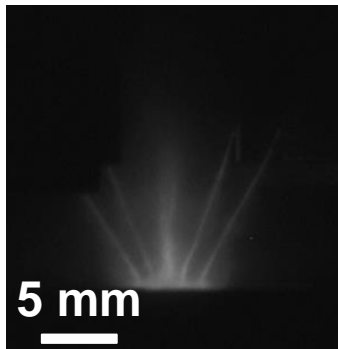
- **Counter clockwise 30 °**



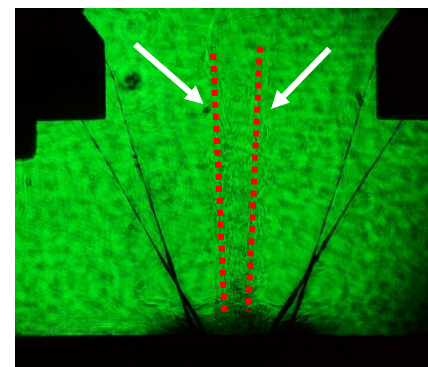
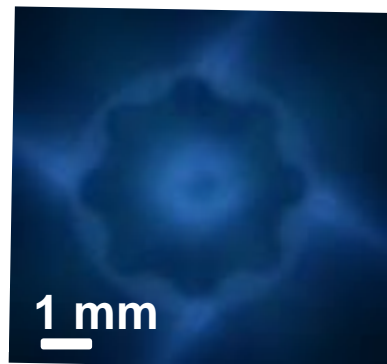
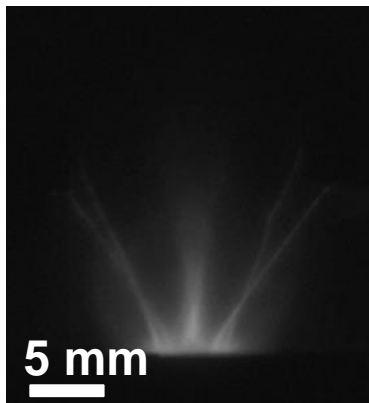
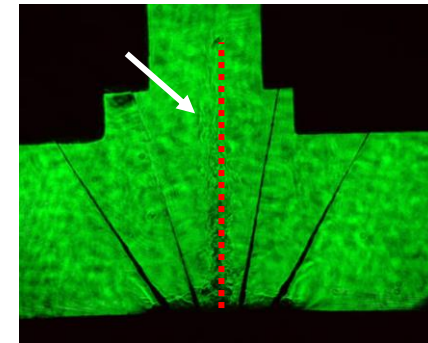
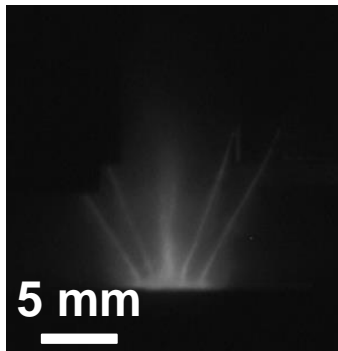
The hollow region at the center was due to angular momentum conservation of the in-coming plasma flow



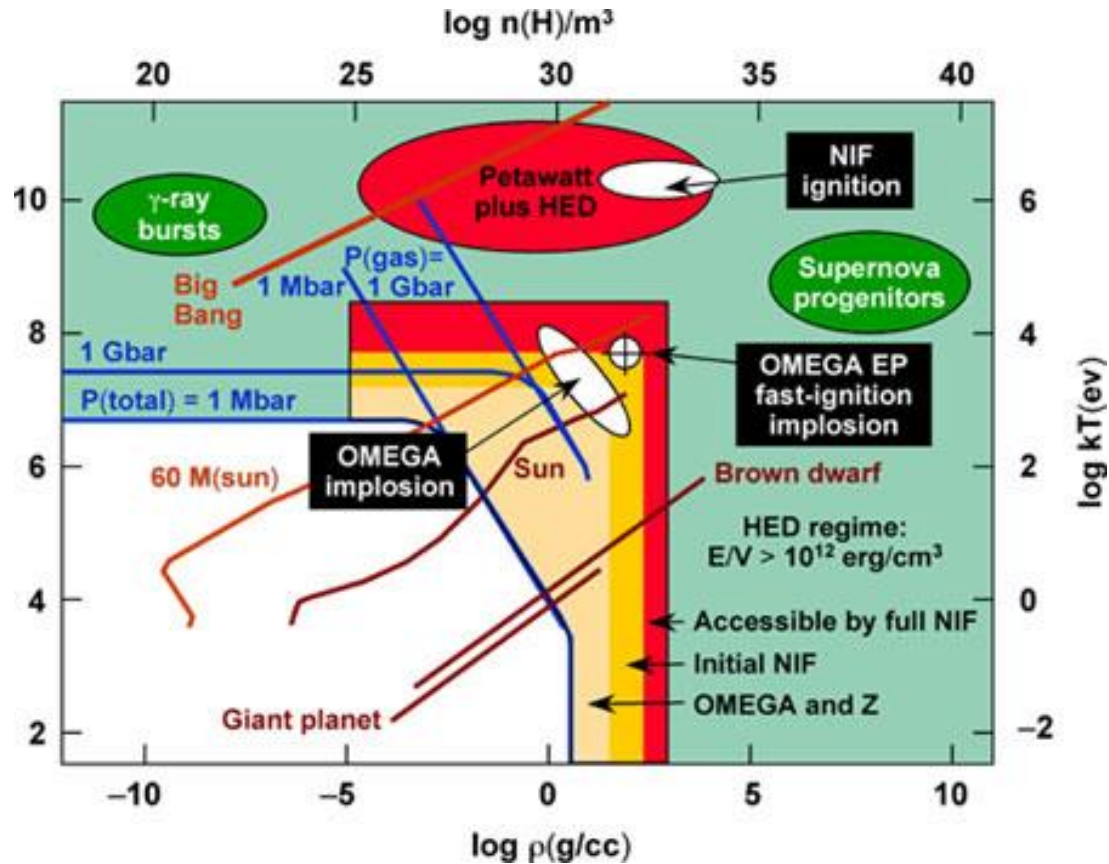
A “tornado” is generated by the twisted conical-wire array



A “tornado” is generated by the twisted conical-wire array



High energy density plasma (HEDP) is the regime where the pressure is greater than 0.1 T Pa (1 Mbar)



- The energy density of HEDP regime is higher than 1 kJ of energy per 10 mm^3 .

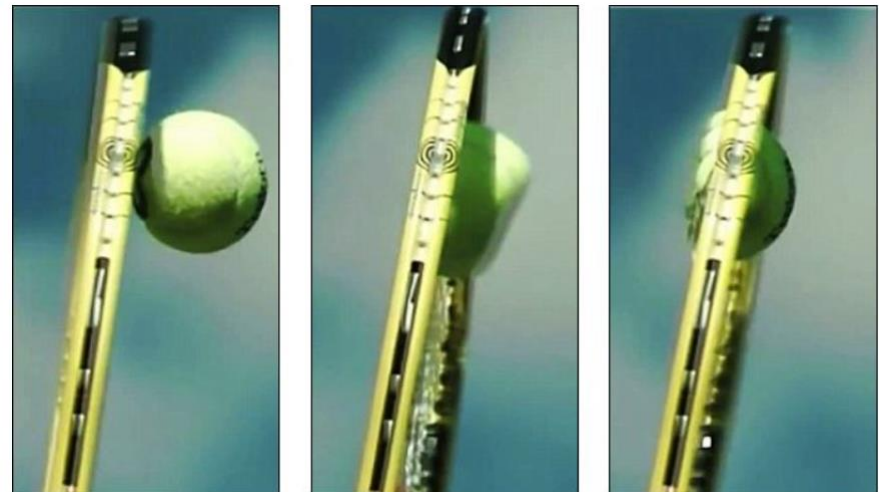
Softer material can be compressed to higher density



- **Compression of a baseball**



- **Compression of a tennis ball**



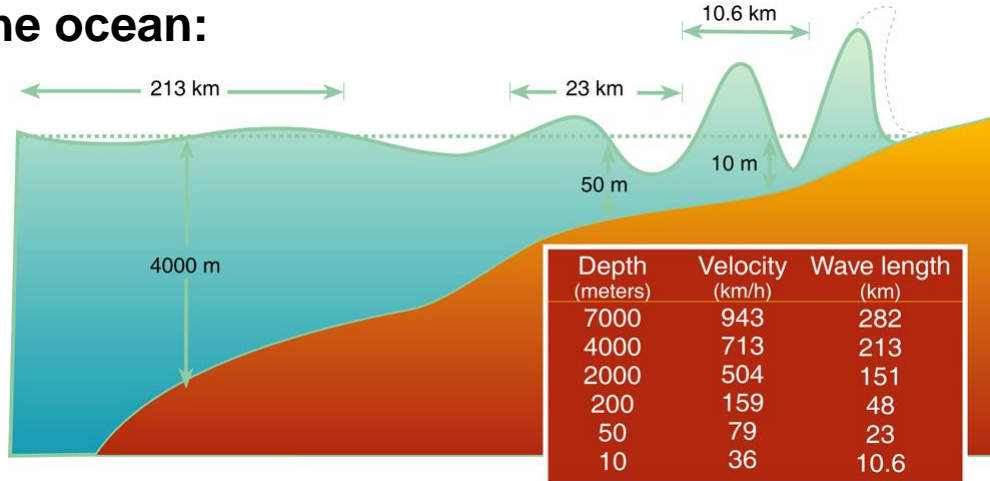
<https://www.youtube.com/watch?v=uxlldMoAwbY>

<https://newsghana.com.gh/wimbledon-slow-motion-video-of-how-a-tennis-ball-turns-to-goo-after-serve/>

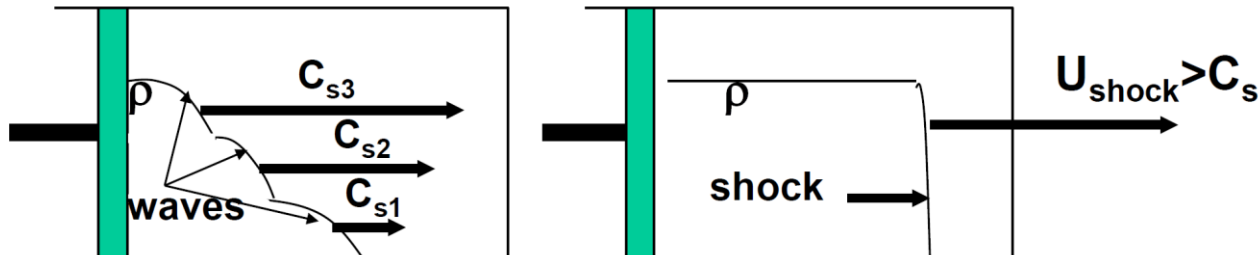
A shock is formed due to the increasing sound speed of a compressed gas/plasma



- Wave in the ocean:



- Acoustic/compression wave driven by a piston:



$$c_s \sim \sqrt{\gamma \frac{p}{\rho}} \sim \sqrt{\frac{\alpha \rho^{5/3}}{\rho}} \sim \sqrt{\alpha} \rho^{1/3}$$

A wave with small amplitude (perturbation) travels with the sound speed



$$\frac{\partial \rho}{\partial t} + \nabla \cdot (\rho \vec{u}) = 0$$

$$\rho \left(\frac{\partial \vec{u}}{\partial t} + \vec{u} \cdot \nabla \vec{u} \right) = -\nabla p + \rho \vec{f}$$

$$\frac{\partial}{\partial t} \left(\frac{\rho u^2}{2} + \rho \varepsilon \right) + \nabla \cdot \vec{u} \left[\left(\frac{\rho u^2}{2} + \rho \varepsilon \right) + p \right] = \rho \vec{f} \cdot \vec{u} - \nabla \cdot \vec{q}$$

$$\rho = \rho_0 + \Delta \rho$$

$$p = p_0 + \Delta p$$

$$\vec{u} = \vec{u}_0 + \Delta \vec{u} \equiv (u_0 + \Delta u) \hat{x} \equiv \Delta u \hat{x}$$

$$\frac{\partial \Delta \rho}{\partial t} = -\rho_0 \frac{\partial \Delta u}{\partial x}$$

$$\rho_0 \frac{\partial \Delta u}{\partial t} = -\frac{\partial p}{\partial x} = -\left(\frac{\partial p}{\partial \rho} \right)_s \frac{\partial \Delta \rho}{\partial x} \equiv -c_s^2 \frac{\partial \Delta \rho}{\partial x}$$

$$\frac{\partial^2 \Delta \rho}{\partial t^2} = c_s^2 \frac{\partial^2 \Delta \rho}{\partial x^2}$$

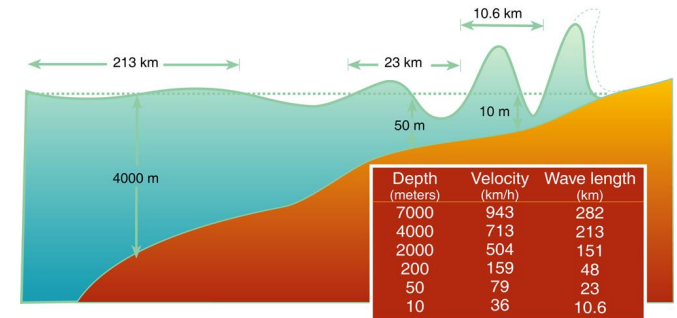
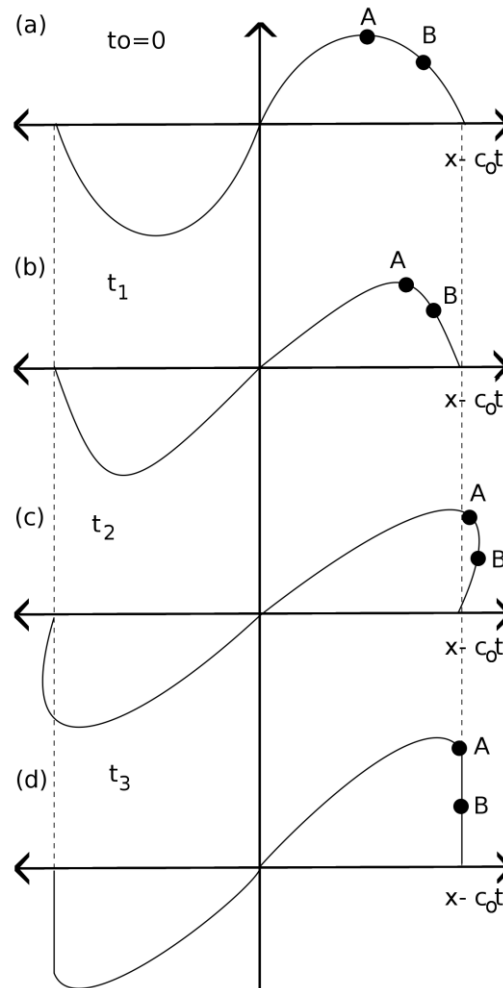
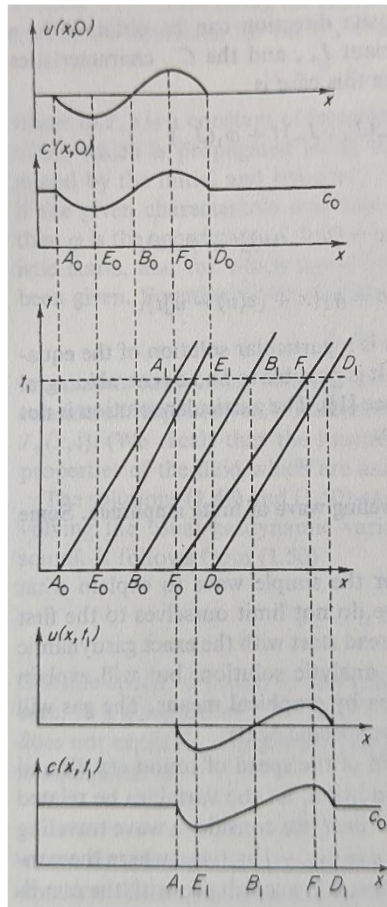
$$\Delta \rho = \Delta \rho(x \pm c_s t)$$

$$\Delta p = \Delta p(x \pm c_s t)$$

$$\Delta u = \Delta u(x \pm c_s t)$$

$$c_s \sim \sqrt{\gamma \frac{p}{\rho}} \sim \sqrt{\frac{\alpha \rho^{5/3}}{\rho}} \sim \sqrt{\alpha} \rho^{1/3}$$

A wave is distorted when the sound speed is not a constant

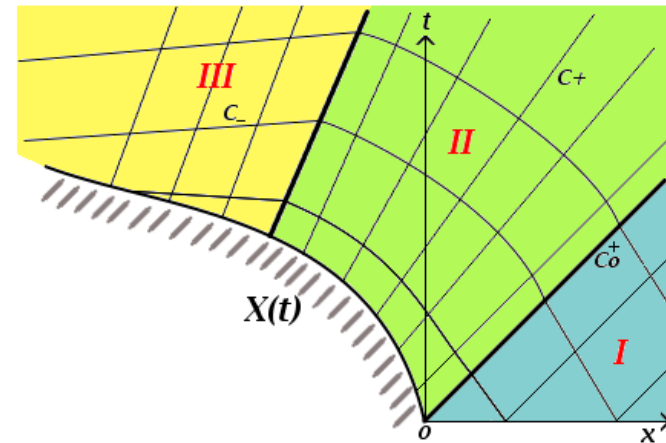
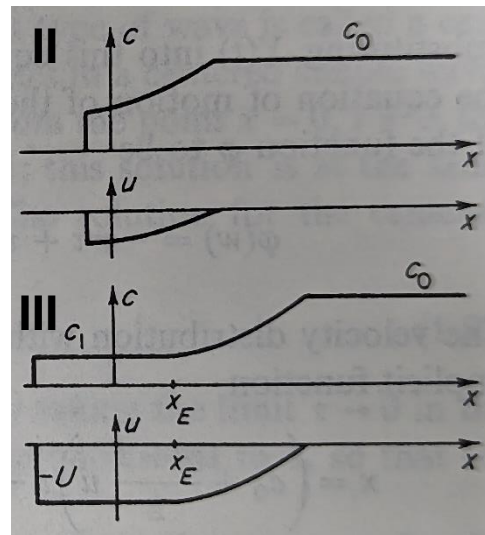
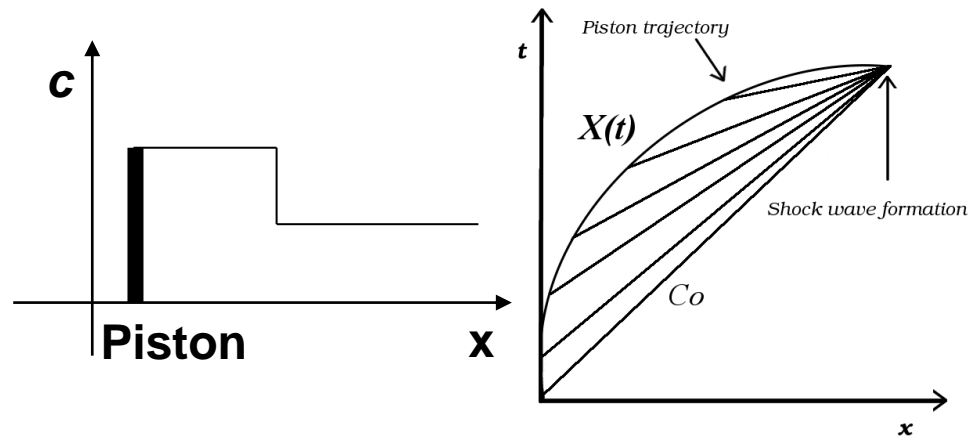
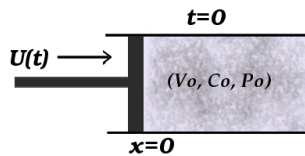


• A shock wave is formed when a discontinuity is formed.

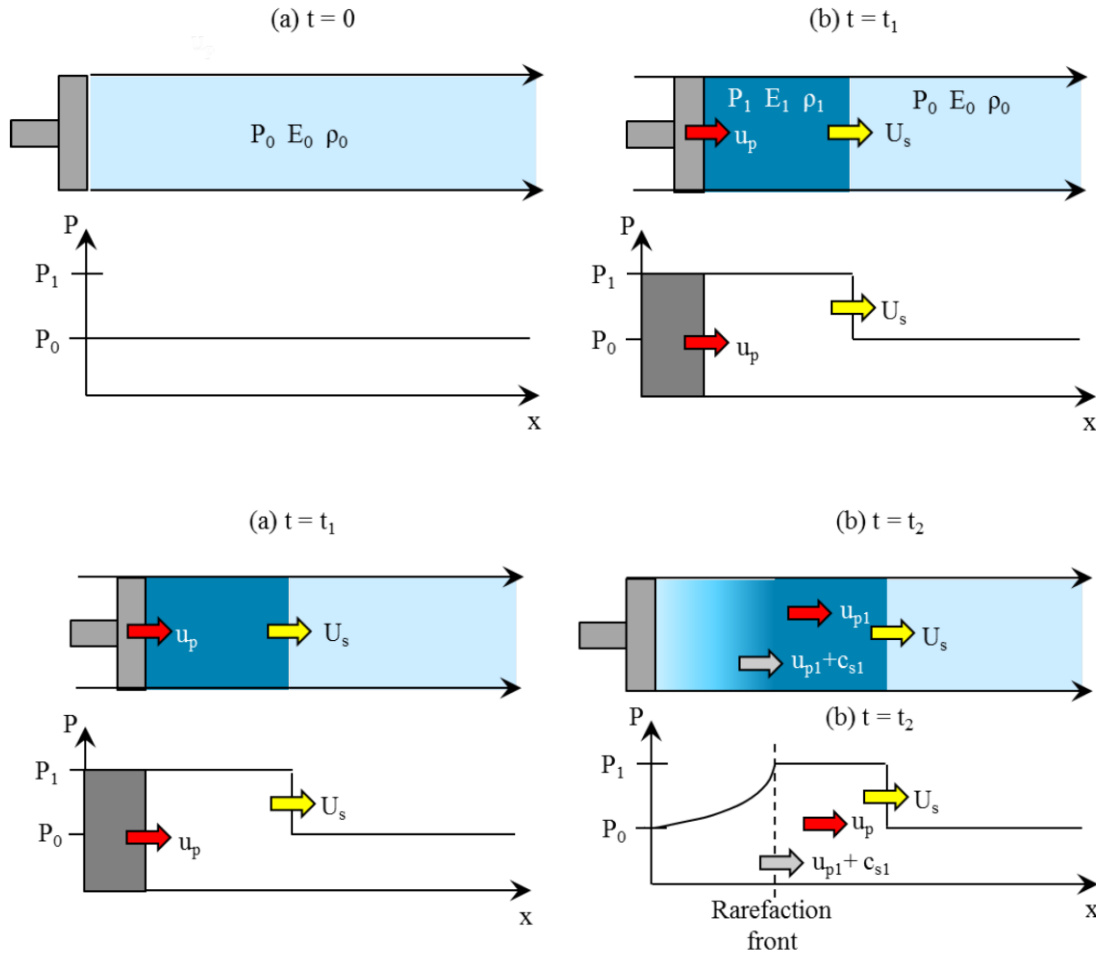
$$c_s \sim \sqrt{\alpha \rho}^{1/3}$$

Y. B. Zel'dovich & Y. P. Raizer, Physics of shock waves and high-temperature hydrodynamic phenomena
 Maria Alejandra Barrios Garcia, PhD Thesis, U of Rochester, 2010
<http://neamtic.ioc-unesco.org/tsunami-info/the-cause-of-tsunamis>

A shock is formed when characteristics merge while a rarefaction wave is formed when characteristics spread out

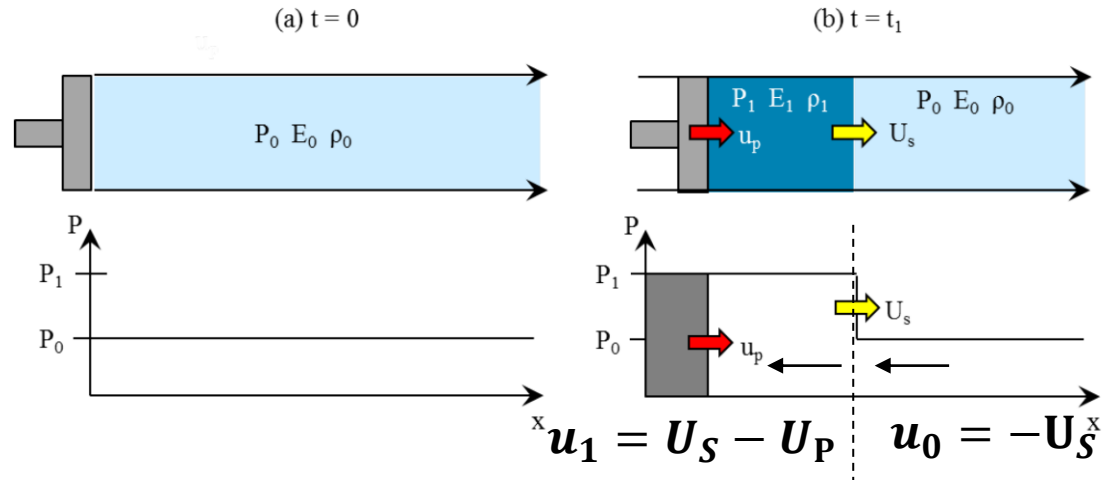


A shock or a rarefaction wave may be formed depending on the driving force from the piston



- Show simulations.

Mass, momentum, and energy is conserved across the shock front



$$\frac{\partial \rho}{\partial t} + \nabla \cdot (\rho \vec{u}) = 0$$

$$\rho \left(\frac{\partial \vec{u}}{\partial t} + \vec{u} \cdot \nabla \vec{u} \right) = -\nabla p + \rho \vec{f}$$

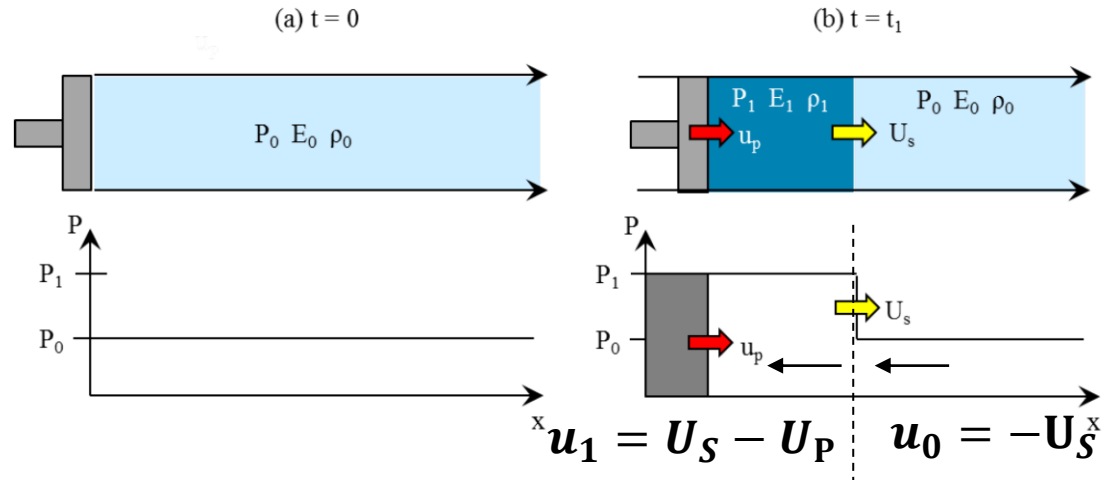
$$\frac{\partial}{\partial t} \left(\frac{\rho u^2}{2} + \rho \epsilon \right) + \nabla \cdot \vec{u} \left[\left(\frac{\rho u^2}{2} + \rho \epsilon \right) + p \right] = \rho \vec{f} \cdot \vec{u} - \nabla \cdot \vec{q}$$

$$\rho_1 u_1 = \rho_0 u_0$$

$$p_1 + \rho_1 u_1^2 = p_0 + \rho_0 u_0^2$$

$$\epsilon_1 + \frac{p_1}{\rho_1} + \frac{u_1^2}{2} = \epsilon_0 + \frac{p_0}{\rho_0} + \frac{u_0^2}{2}$$

The Hugoniot equations relate the pre- and post-shock conditions via the particle velocity (U_p) and shock velocity (U_s)



$$\rho_1 u_1 = \rho_0 u_0$$

$$p_1 + \rho_1 u_1^2 = p_0 + \rho_0 u_0^2$$

$$\epsilon_1 + \frac{p_1}{\rho_1} + \frac{u_1^2}{2} = \epsilon_0 + \frac{p_0}{\rho_0} + \frac{u_0^2}{2}$$

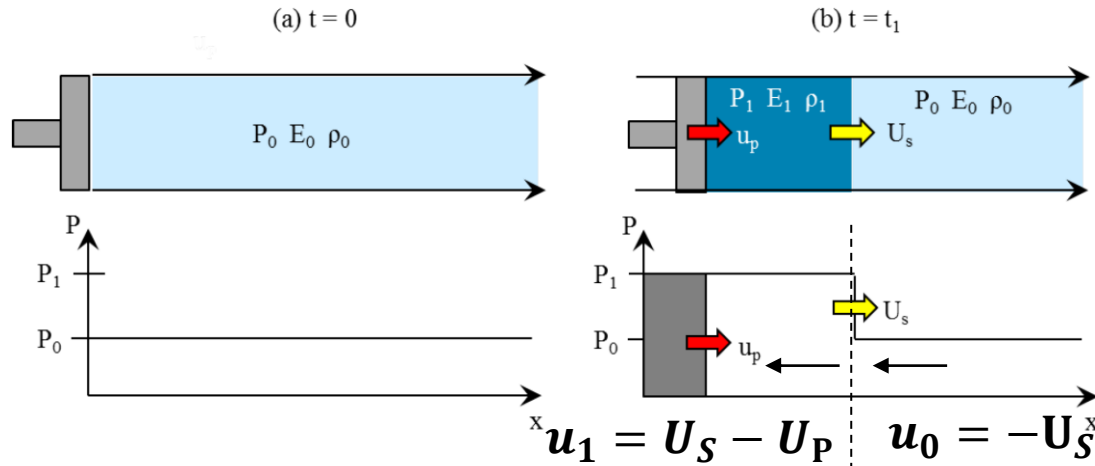
$$\rho_0 U_s = \rho_1 (U_s - U_p)$$

$$p_1 - p_0 = \rho_0 U_s U_p$$

$$u_0 \left[\frac{\rho_0 u_0^2}{2} + \rho_0 \epsilon_0 + p_0 \right] = u_1 \left[\frac{\rho_1 u_1^2}{2} + \rho_1 \epsilon_1 + p_1 \right]$$

$$p_0 u_0 - p_1 u_1 = \rho_1 u_1 \left(\epsilon_1 + \frac{u_1^2}{2} \right) - \rho_0 u_0 \left(\epsilon_0 + \frac{u_0^2}{2} \right) = \rho_0 u_0 \left[\left(\epsilon_1 + \frac{u_1^2}{2} \right) - \left(\epsilon_0 + \frac{u_0^2}{2} \right) \right]$$

The Hugoniot equations relate the pre- and post-shock conditions via the particle velocity (U_p) and shock velocity (U_s) – cont.



$$\rho_0 U_s = \rho_1 (U_s - U_p)$$

$$p_1 - p_0 = \rho_0 U_s U_p$$

$$u_0 \left[\frac{\rho_0 u_0^2}{2} + \rho_0 \epsilon_0 + p_0 \right] = u_1 \left[\frac{\rho_1 u_1^2}{2} + \rho_1 \epsilon_1 + p_1 \right]$$

$$p_0 u_0 - p_1 u_1 = \rho_1 u_1 \left(\epsilon_1 + \frac{u_1^2}{2} \right) - \rho_0 u_0 \left(\epsilon_0 + \frac{u_0^2}{2} \right) = \rho_0 u_0 \left[\left(\epsilon_1 + \frac{u_1^2}{2} \right) - \left(\epsilon_0 + \frac{u_0^2}{2} \right) \right]$$

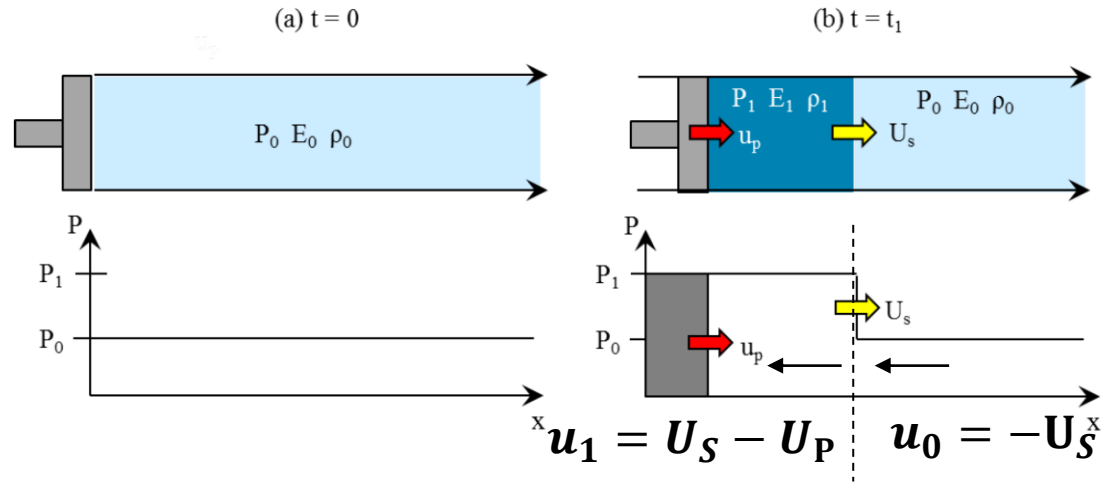
Let $V_{1,2} \equiv \frac{1}{\rho_{1,2}}$

$$u_0^2 = V_0^2 \frac{p_1 - p_0}{V_0 - V_1}$$

$$u_1^2 = V_1^2 \frac{p_1 - p_0}{V_0 - V_1}$$

$$\epsilon_1 - \epsilon_0 = \frac{1}{2} (p_0 + p_1) (V_0 - V_1)$$

The density is only compressed by a limited amount even in a strong shock



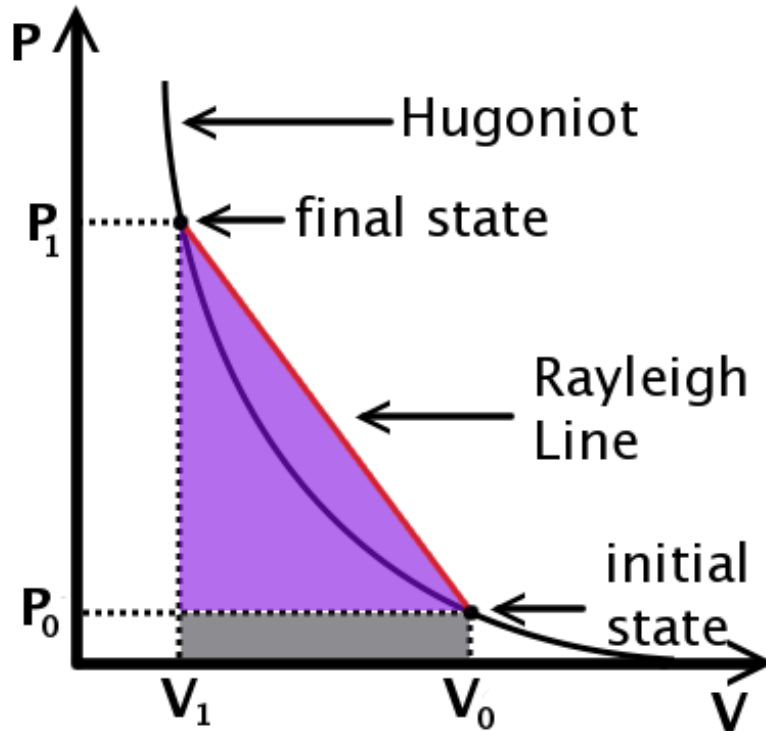
$$V_{0,1} \equiv \frac{1}{\rho_{0,1}} \quad u_0^2 = V_0^2 \frac{p_1 - p_0}{V_0 - V_1} \quad u_1^2 = V_1^2 \frac{p_1 - p_0}{V_0 - V_1} \quad \epsilon_1 - \epsilon_0 = \frac{1}{2}(p_0 + p_1)(V_0 - V_1)$$

$$\frac{\rho_1}{\rho_0} = \frac{V_0}{V_1} = \frac{p_1(\gamma + 1) + p_0(\gamma - 1)}{p_1(\gamma - 1) + p_0(\gamma + 1)} \sim \frac{\gamma + 1}{\gamma - 1} \left(\text{for } \frac{p_1}{p_0} \gg 1 \right) \sim 4 \left(\text{for } \gamma = \frac{5}{3} \right)$$

$$u_0^2 = \frac{V_0}{2} [(\gamma - 1)p_0 + (\gamma + 1)p_1] = \frac{p_0}{\rho_0} \frac{(\gamma + 1)p_1/p_0 + (\gamma - 1)}{2}$$

$$u_1^2 = \frac{V_0}{2} \frac{[(\gamma + 1)p_0 + (\gamma - 1)p_1]^2}{(\gamma - 1)p_0 + (\gamma + 1)p_1}$$

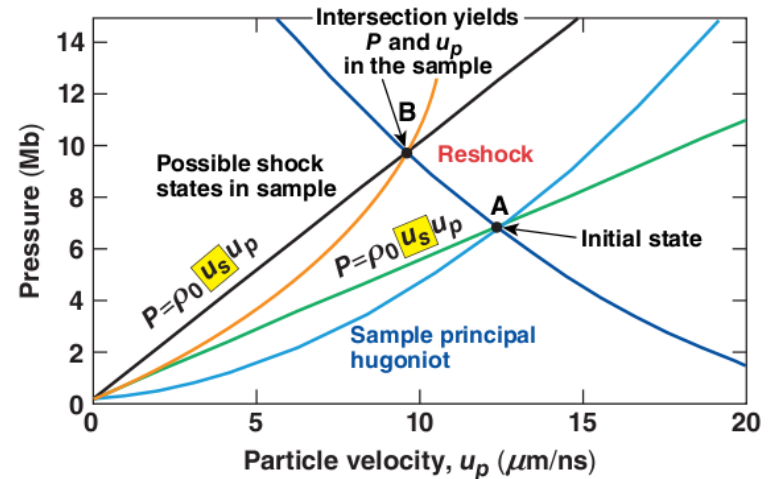
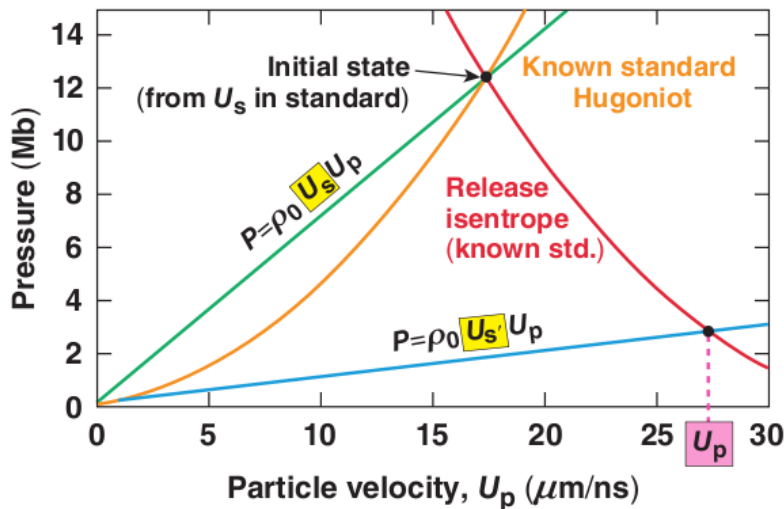
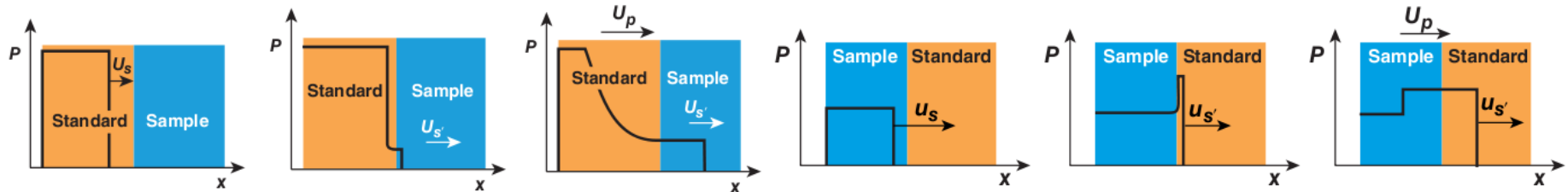
The Hugoniot curve is a curve on the p, V diagram passing through the initial state p_0, V_0



$$\frac{V_0}{V_1} = \frac{p_1(\gamma + 1) + p_0(\gamma - 1)}{p_1(\gamma - 1) + p_0(\gamma + 1)}$$

$$V_{0,1} \equiv \frac{1}{\rho_{0,1}}$$

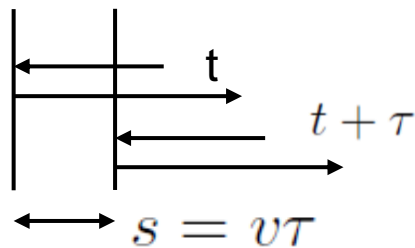
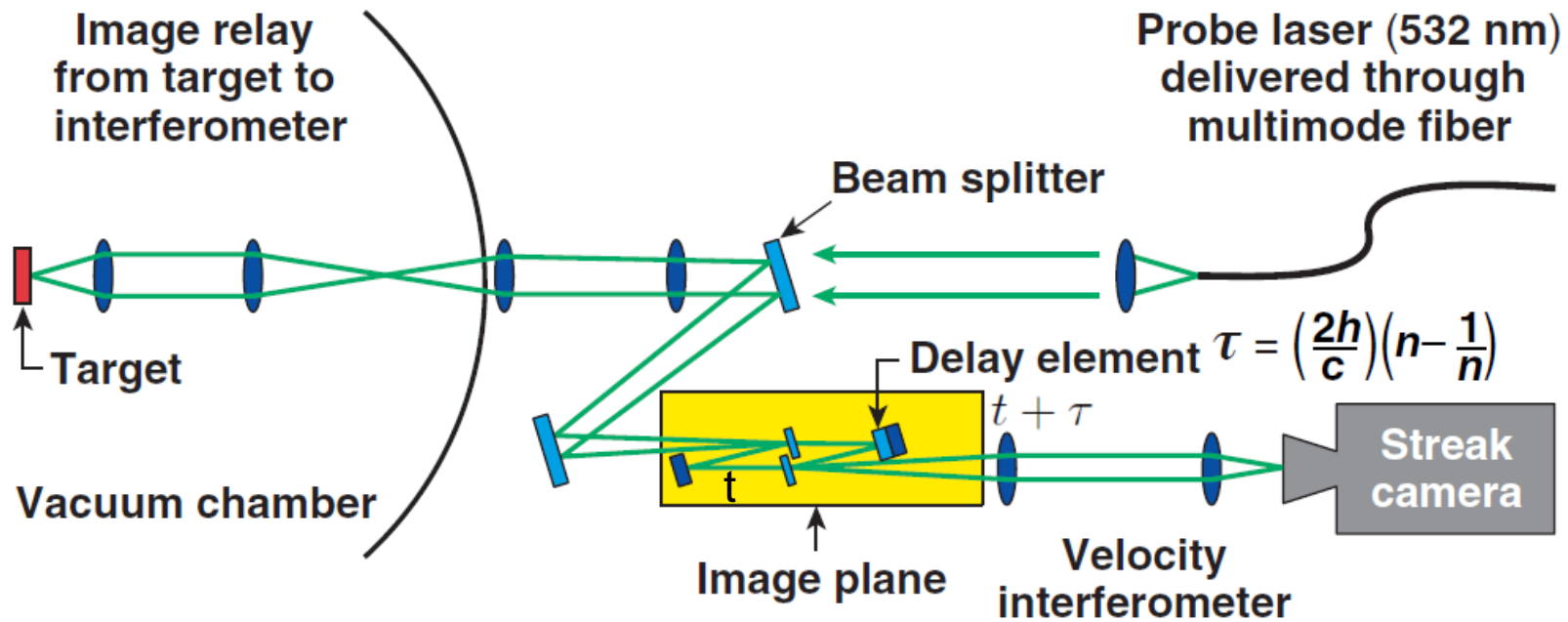
Pressure can be referred by measuring the shock speed with a sample with known Hugoniot curve



$$p_1 - p_0 = \rho_0 U_s U_p$$

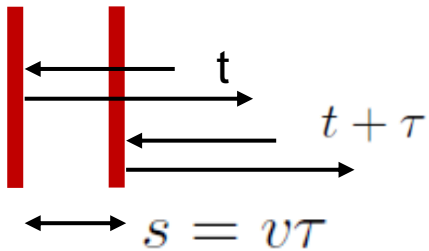
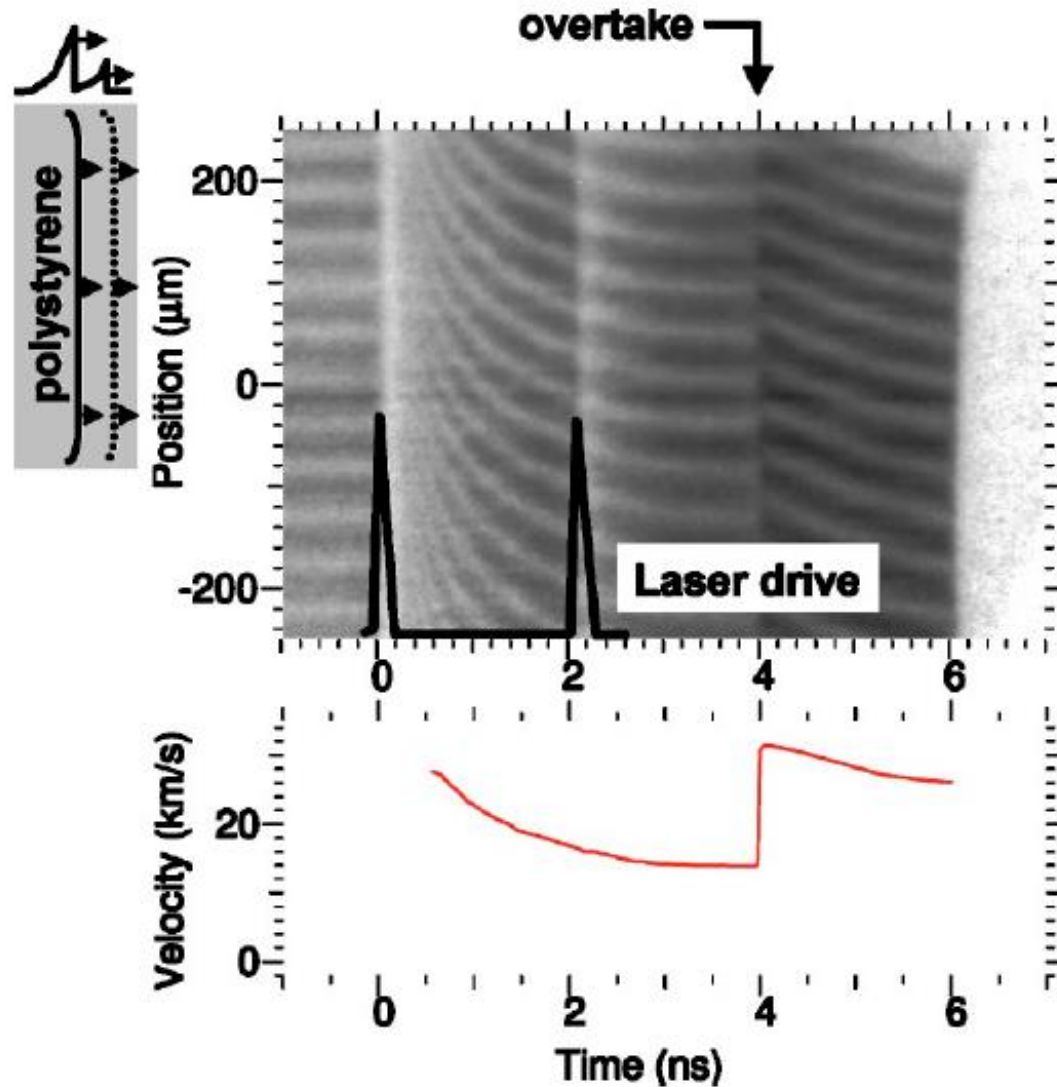
Isentrope: adiabatic flow with no change in entropy

Shock velocities are measured using time-resolved Velocity Interferometer System for Any Reflector (VISAR)

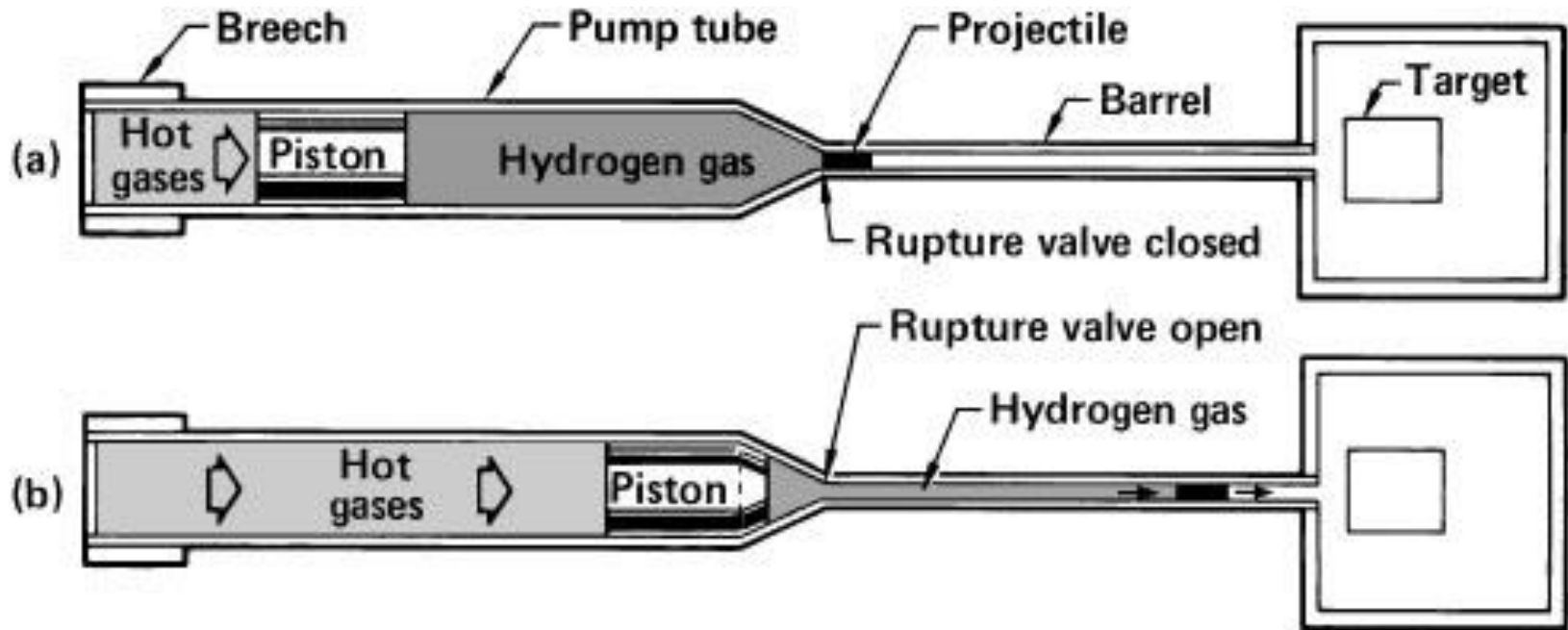


$$\Delta\phi = \frac{v\tau}{\lambda} \propto v$$

Shock velocities are measured using time-resolved Velocity Interferometer System for Any Reflector (VISAR)



A piston can be driven by a gas gun



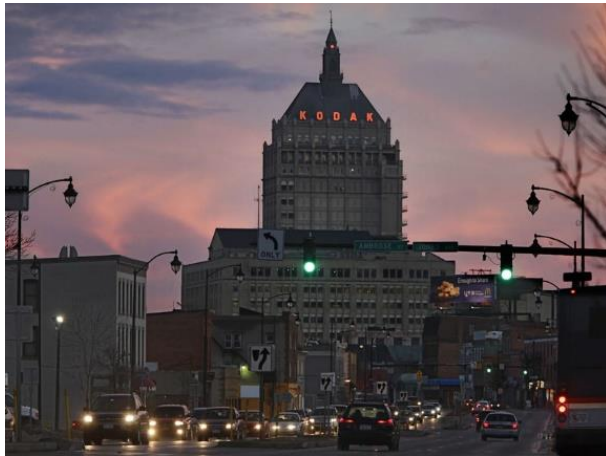
Rochester is known as “The World's Image Center”



There are many famous optical companies at Rochester



Kodak



Eastman school of music



BAUSCH + LOMB

Laboratory for Laser Energetics, University of Rochester is a pioneer in laser fusion

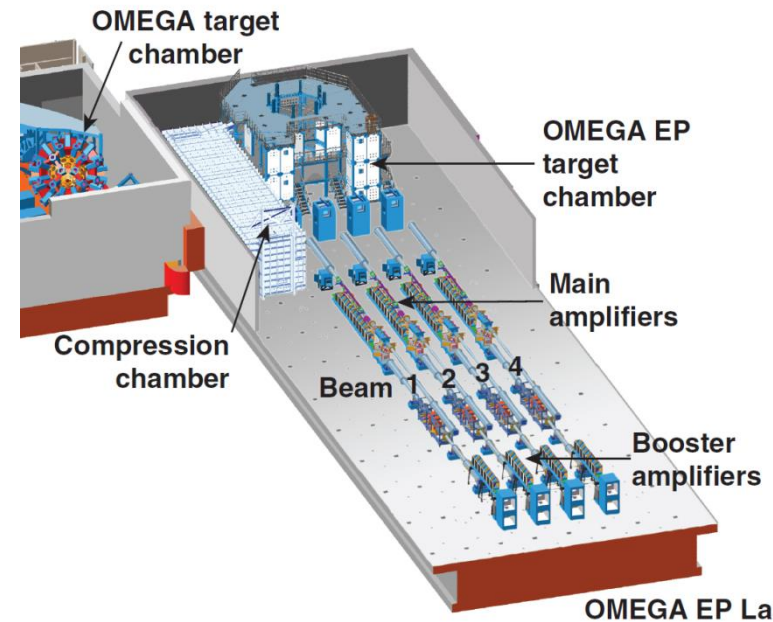
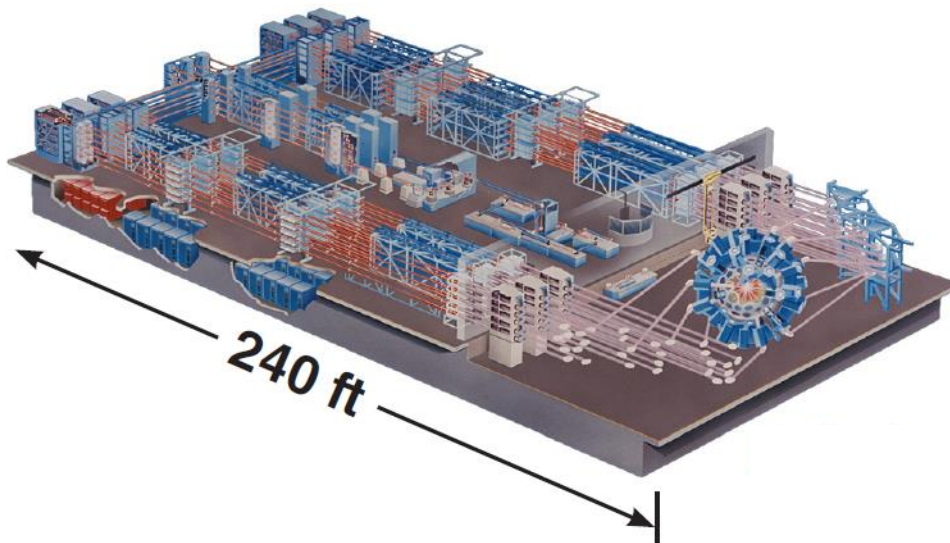


- **OMEGA Laser System**

- 60 beams
- >30 kJ UV on target
- 1%~2% irradiation nonuniformity
- Flexible pulse shaping

- **OMEGA EP Laser System**

- 4 beams; 6.5 kJ UV (10ns)
- Two beams can be high-energy petawatt
 - 2.6 kJ IR in 10 ps
 - Can propagate to the OMEGA or OMEGA EP target chamber



The OMEGA Facility is carrying out ICF experiments using a full suite of target diagnostics

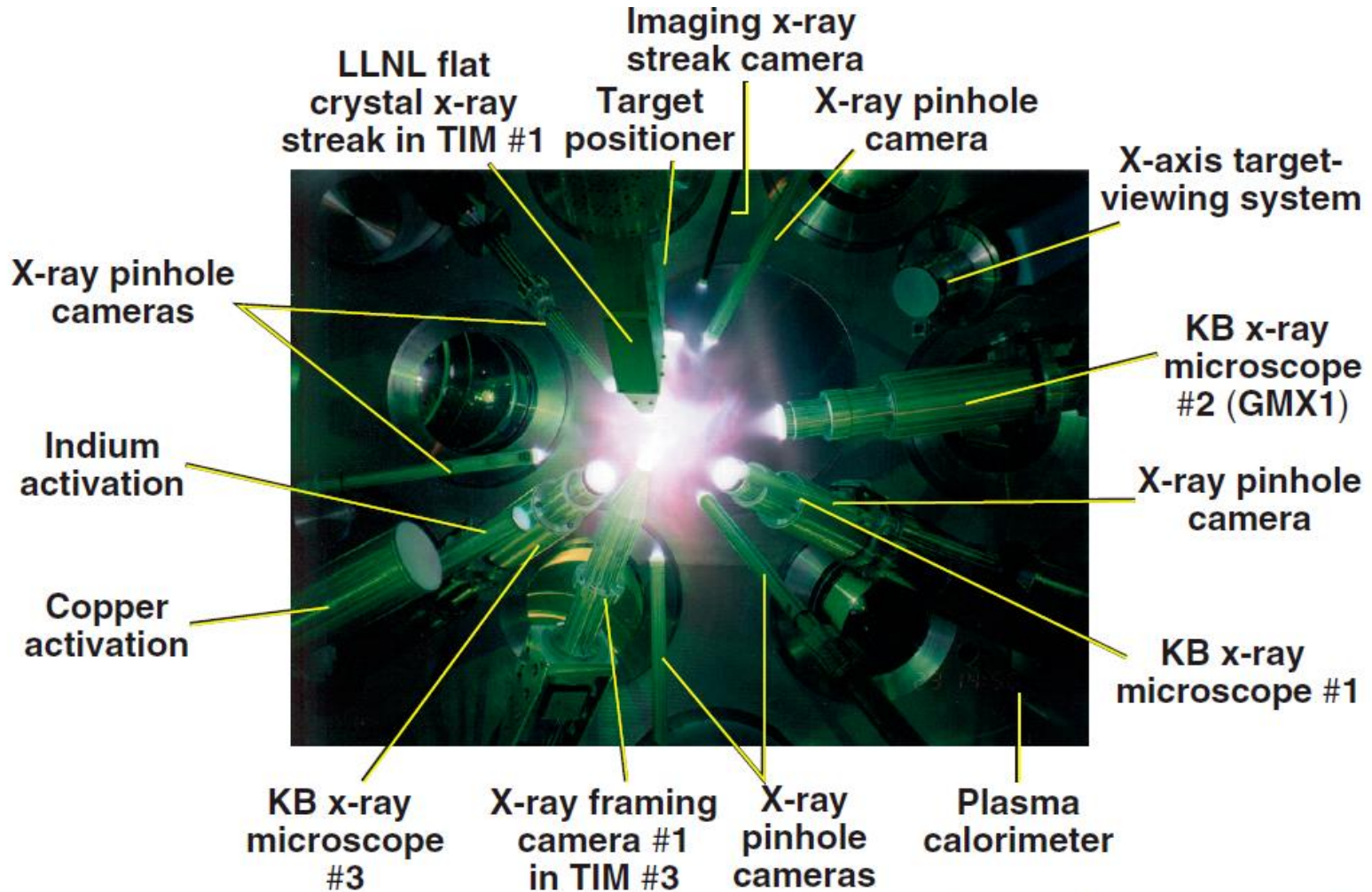
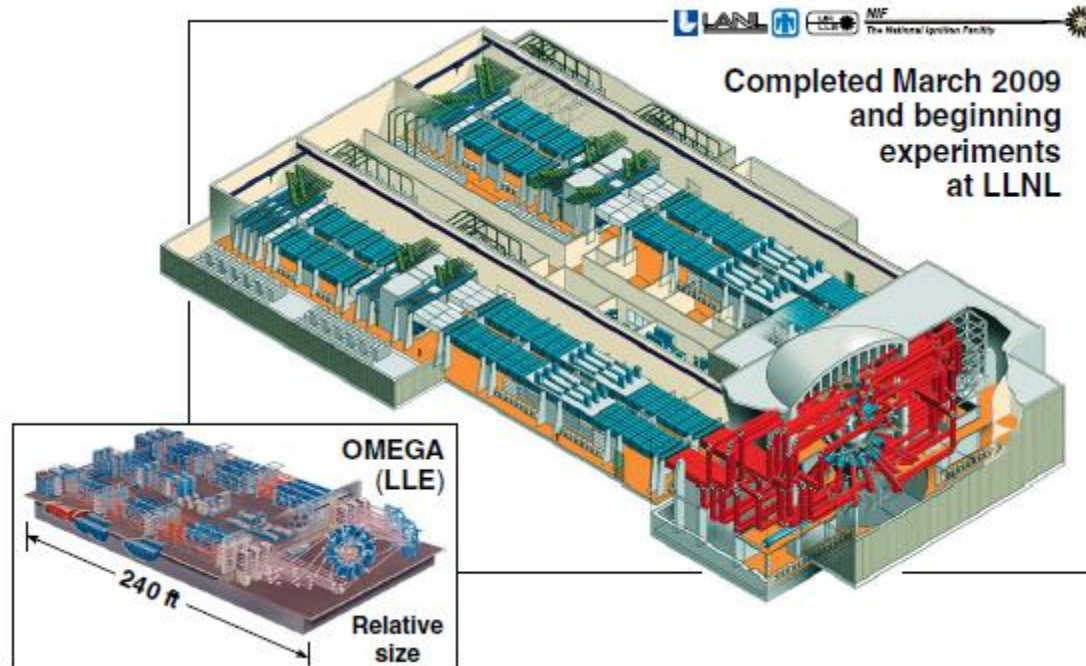


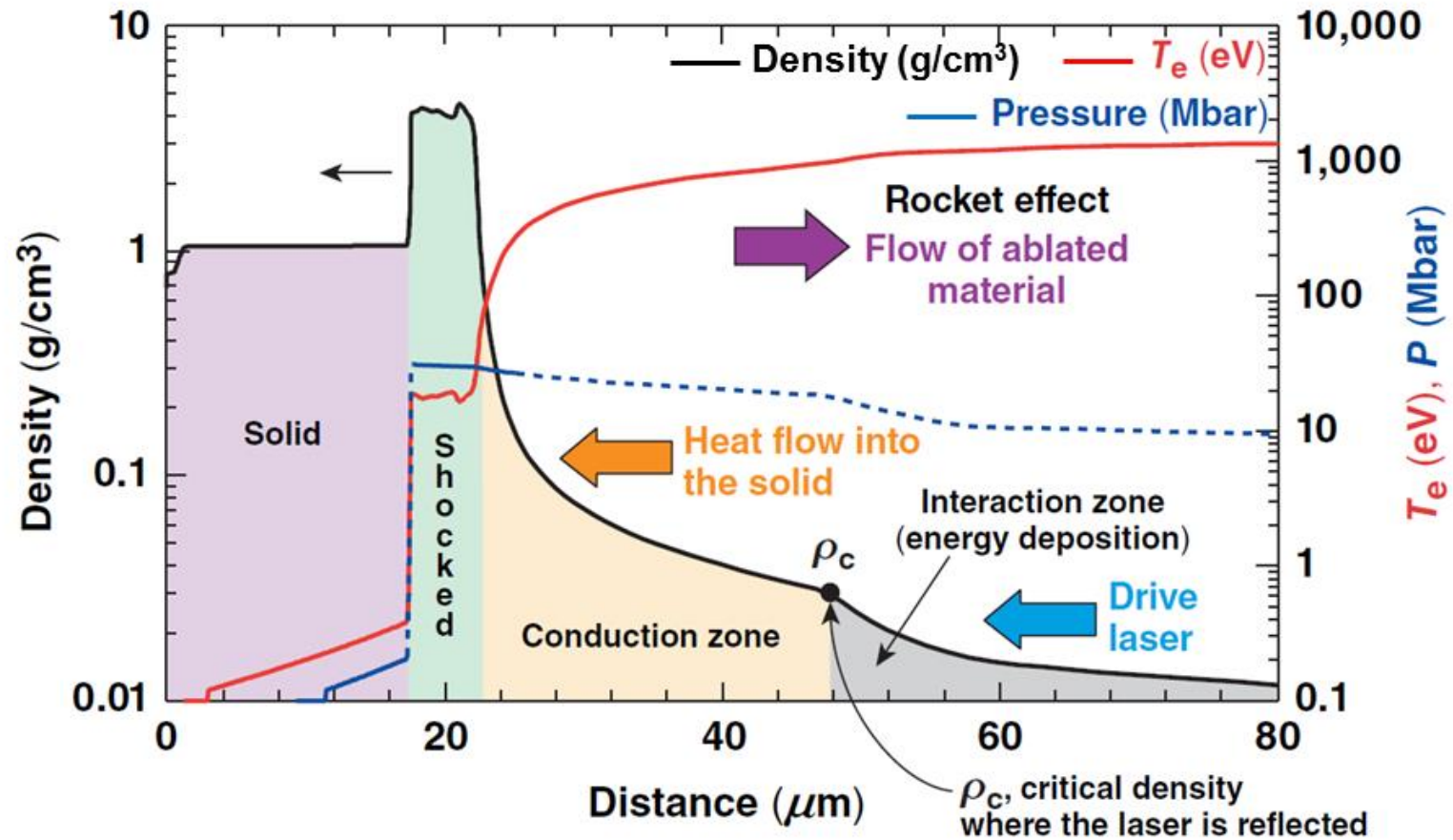
Photo taken from port H11B

The 1.8-MJ National Ignition Facility (NIF) will demonstrate ICF ignition and modest energy gain



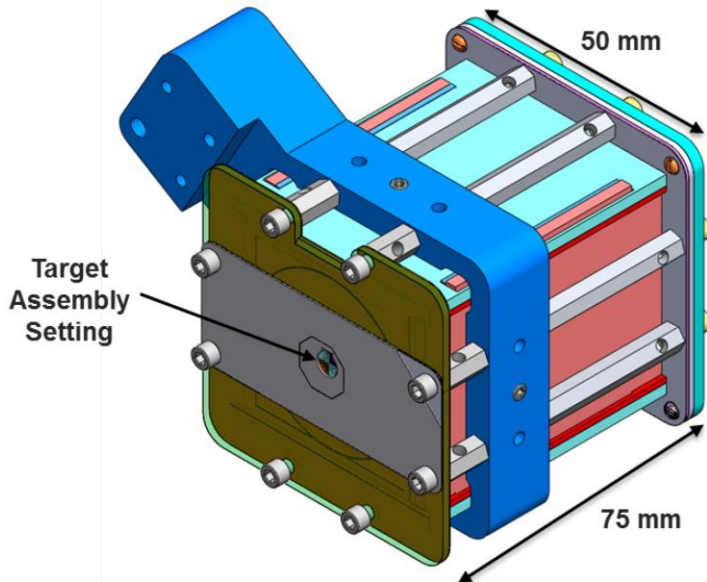
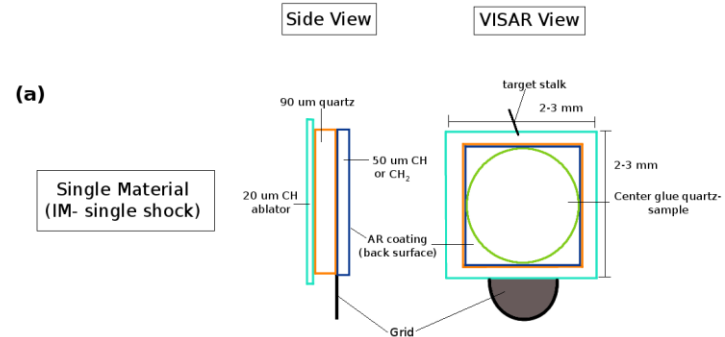
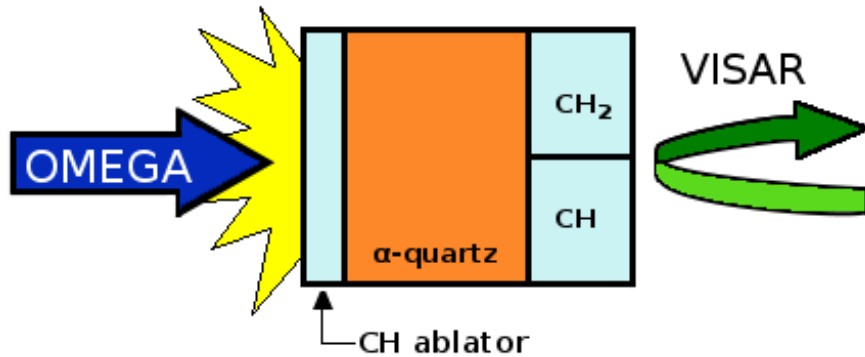
OMEGA experiments are integral to an ignition demonstration on the NIF.

A strong shock can be generated using a high power laser

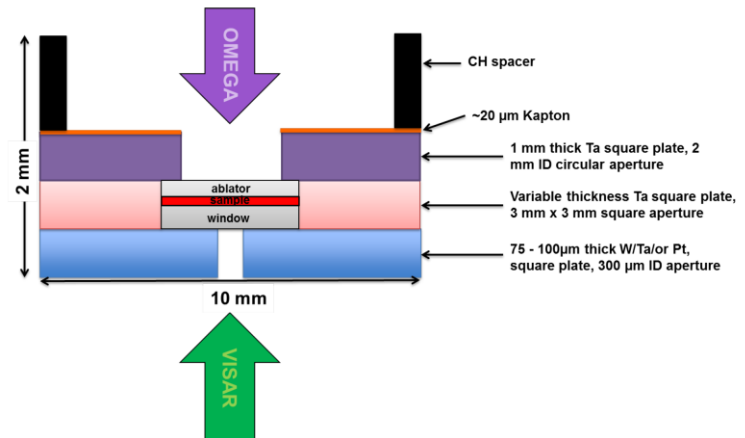


E11006d

The powder x-ray diffraction image plate (PXRDIP) package for studying the shock phenomena

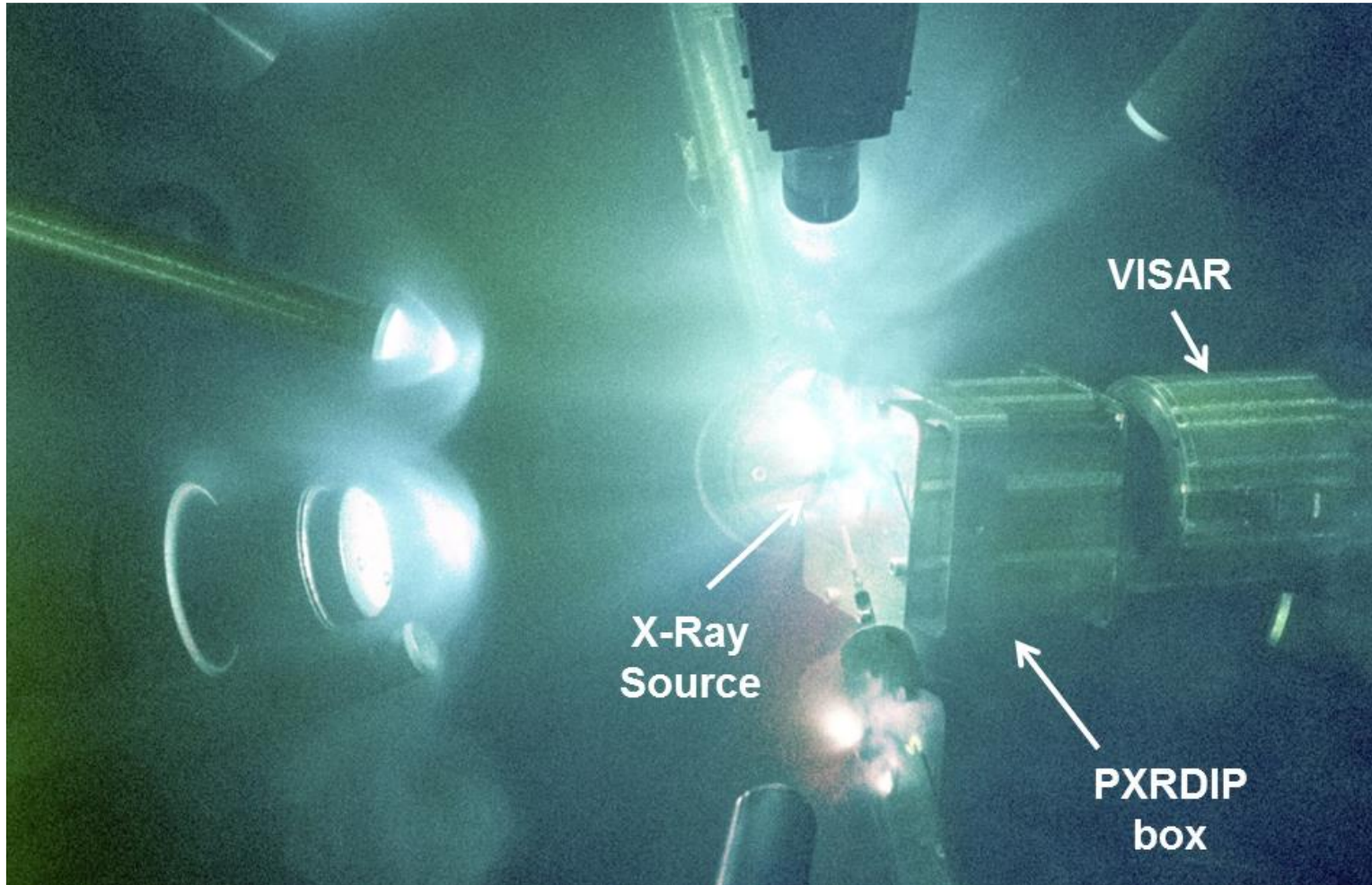


16 Omega beams

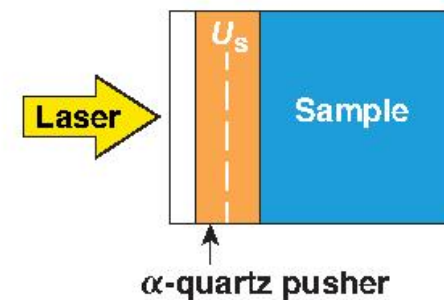
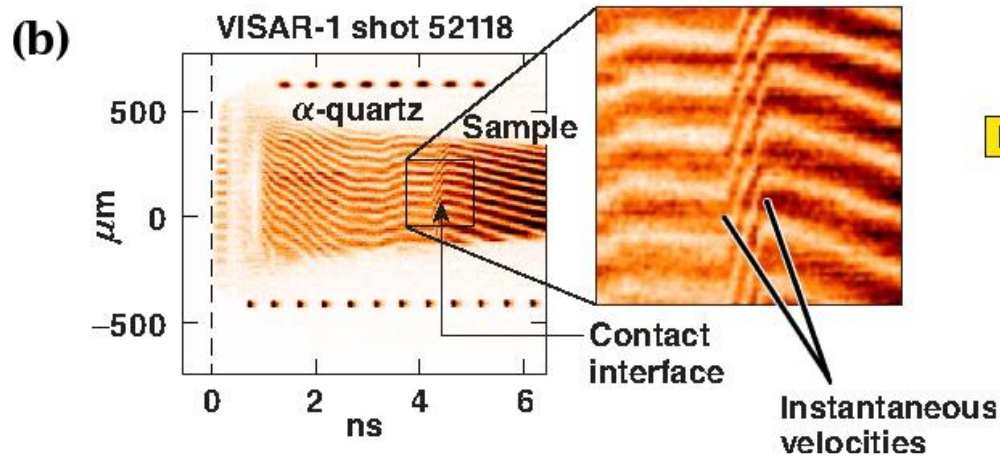
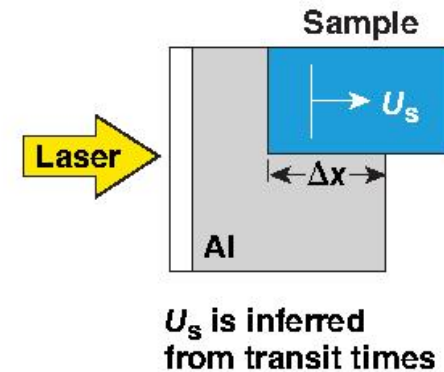
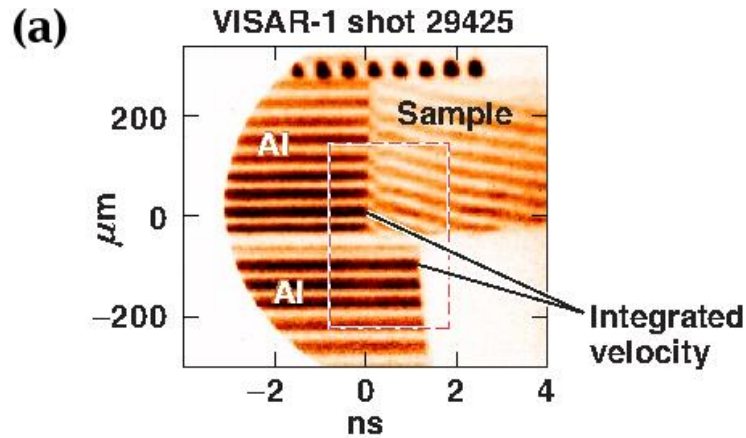


Maria Alejandra Barrios Garcia, PhD Thesis, U of Rochester, 2010
 Danae Nicole Polsin, PhD Thesis, U of Rochester, 2018
 J. R. Rygg, etc., Rev. Sci. Instrum. 83, 113904 (2012)

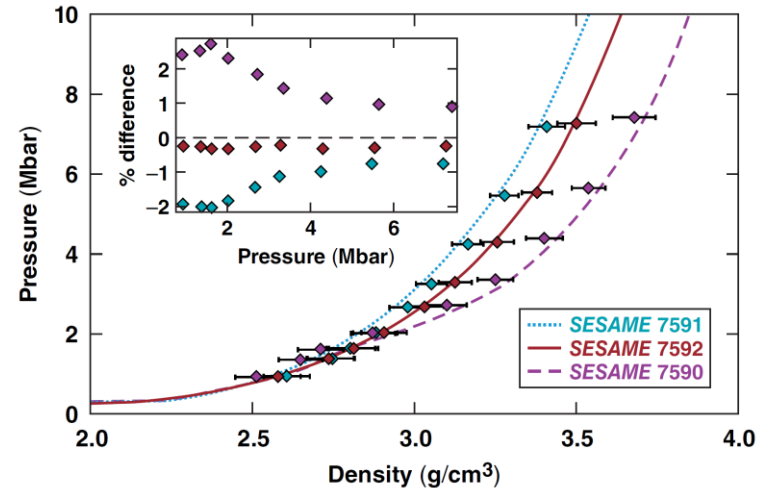
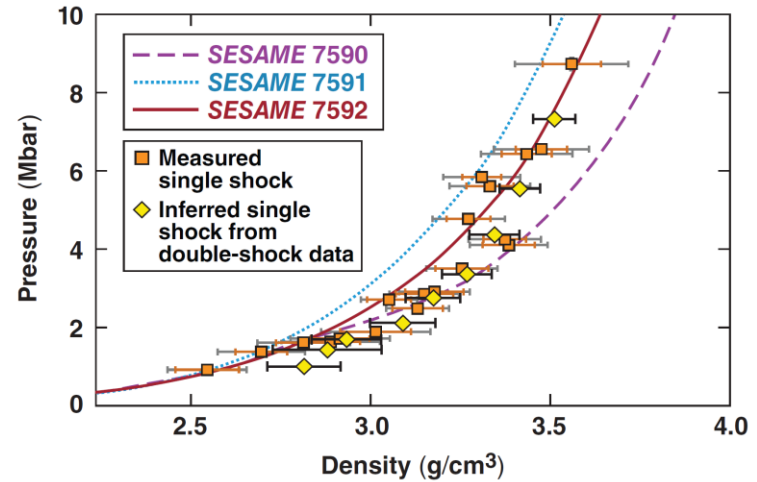
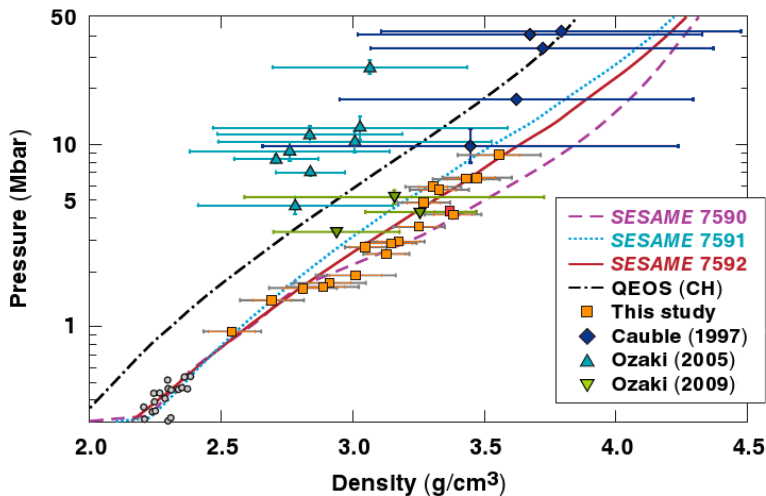
The PXRDIP box in the chamber



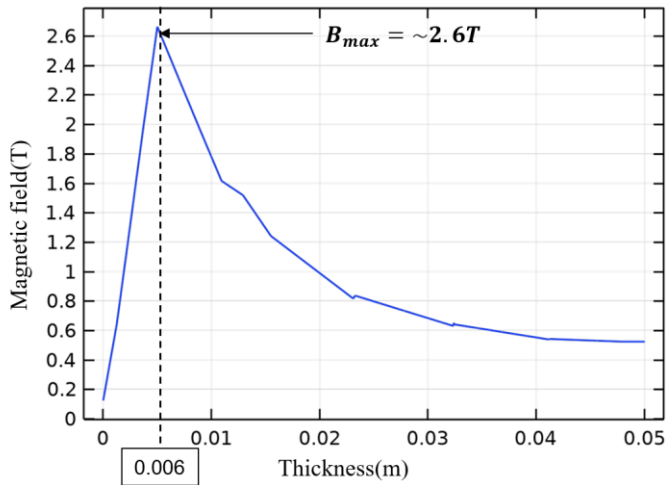
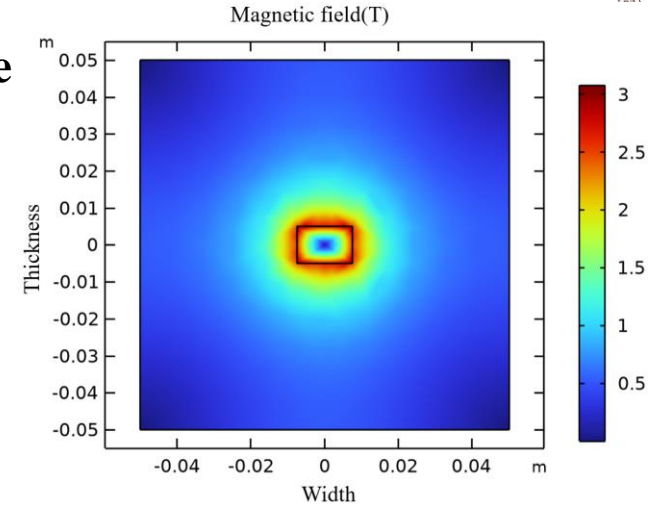
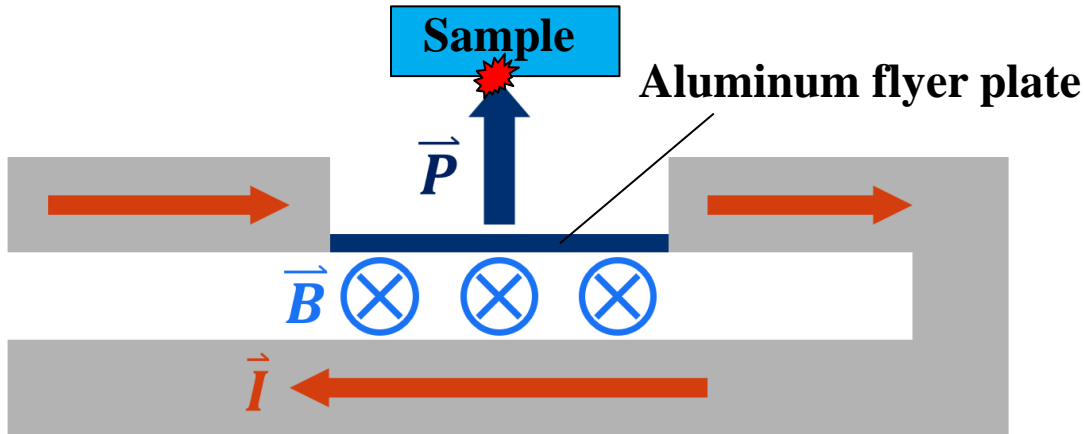
Interference pattern shifts when a shock breakout



The pressure studied using high-power laser is in the range of 1 TPa (10 Mbar)

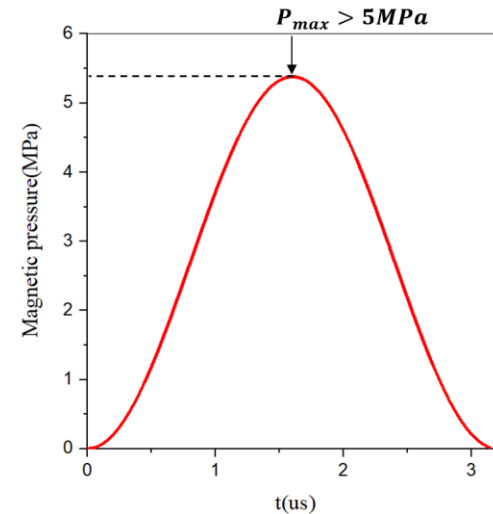


A flyer plate can be used to as the “piston” to generate the shock in a sample

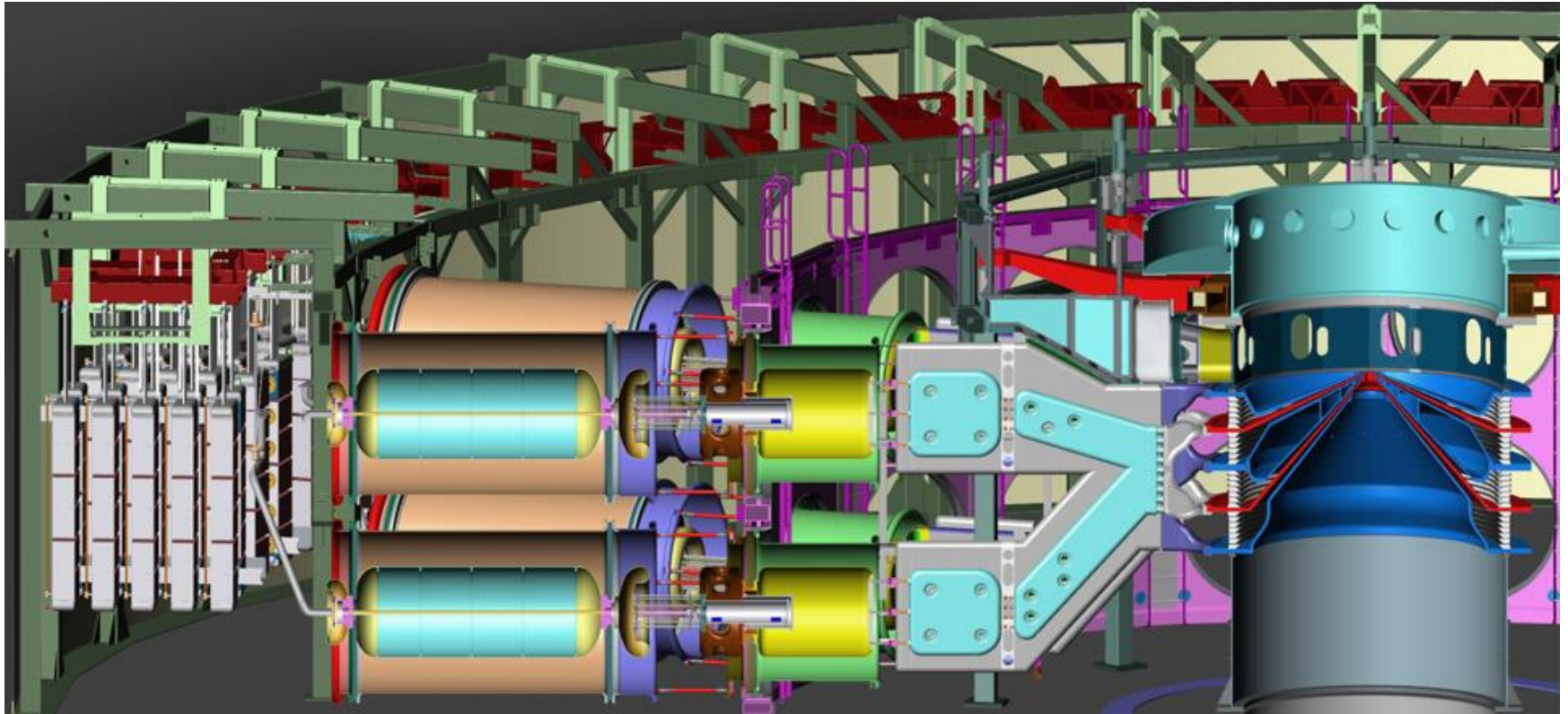


$$B = \frac{\mu_0 I}{w}$$

$$P = \frac{B^2}{2\mu_0} = \frac{\mu_0 I^2}{2w^2}$$

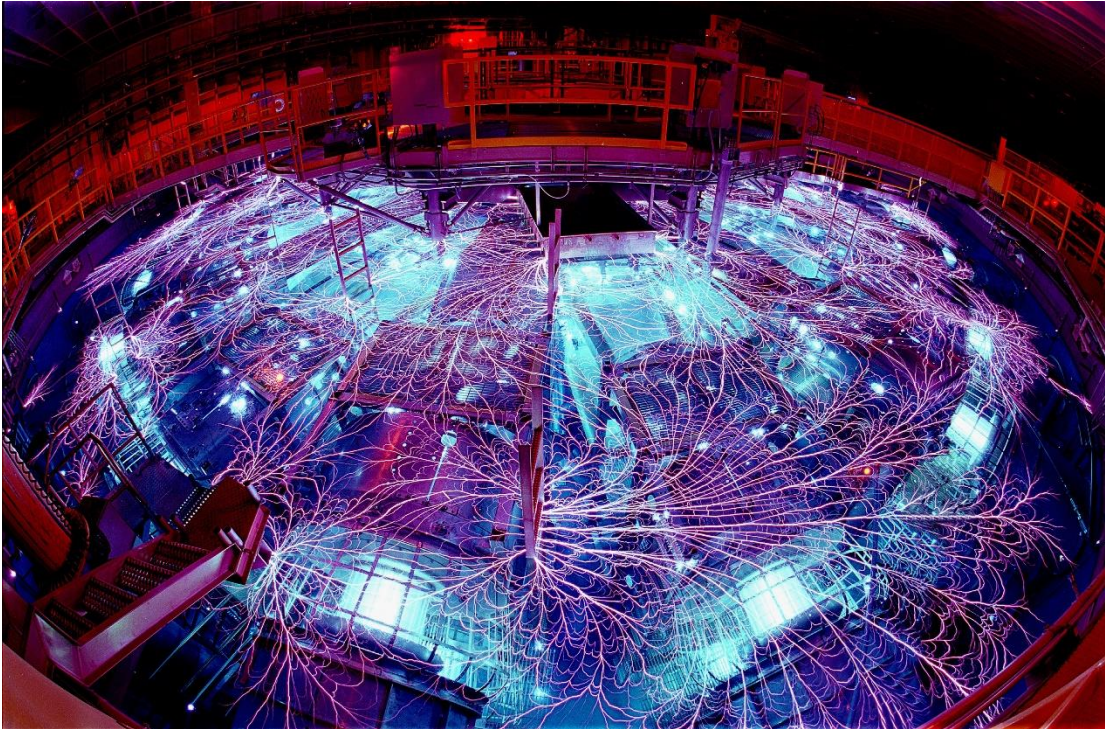


Sandia's Z machine is the world's most powerful and efficient laboratory radiation source

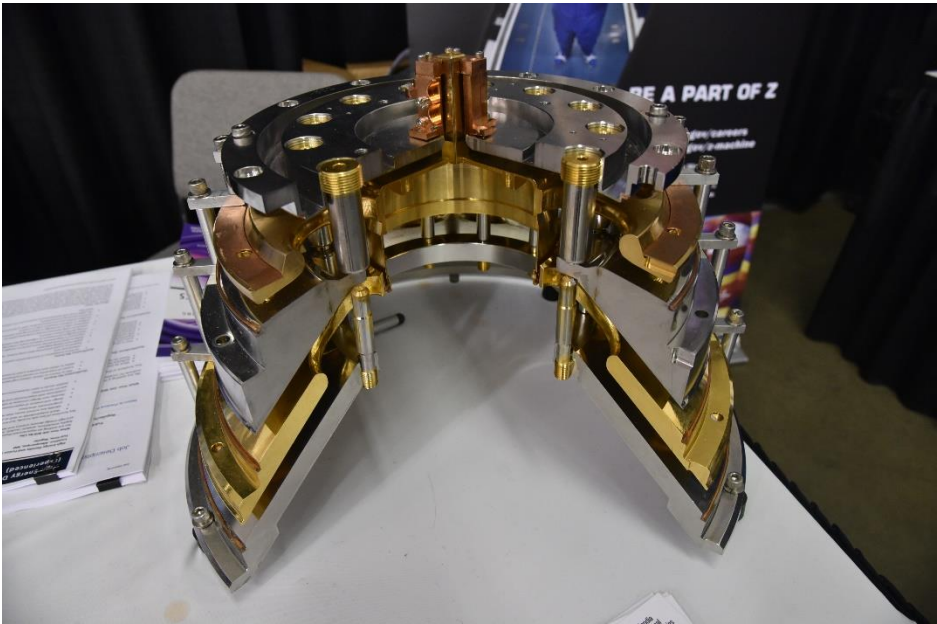


- **Stored energy: 20 MJ**
- **Marx charge voltage: 85 kV**
- **Peak electrical power: 85 TW**
- **Peak current: 26 MA**
- **Rise time: 100 ns**
- **Peak X-ray emissions: 350 TW**
- **Peak X-ray output: 2.7 MJ**

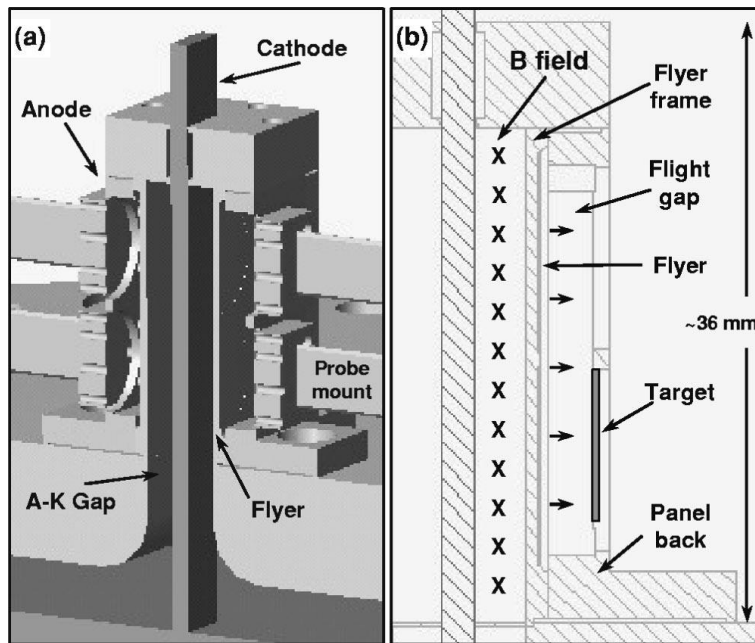
Z machine discharge



Z machine



The flyer plate used in the Z machine

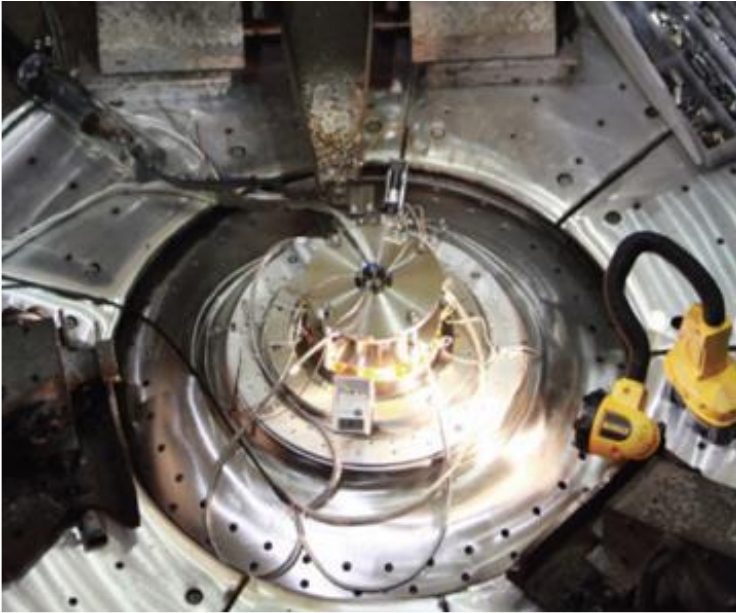


M. D. Knudson, etc., J. Applied Physics 94, 4420 (2003)
<https://newsreleases.sandia.gov/releases/2005/nuclear-power/z-saturn.html>
Pulsed Power Driven Experiments in the Institute of Shock Physics, by Simon Bland

Before and after shots



- Before shots

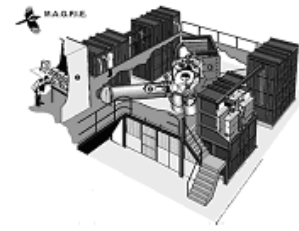


- After shots



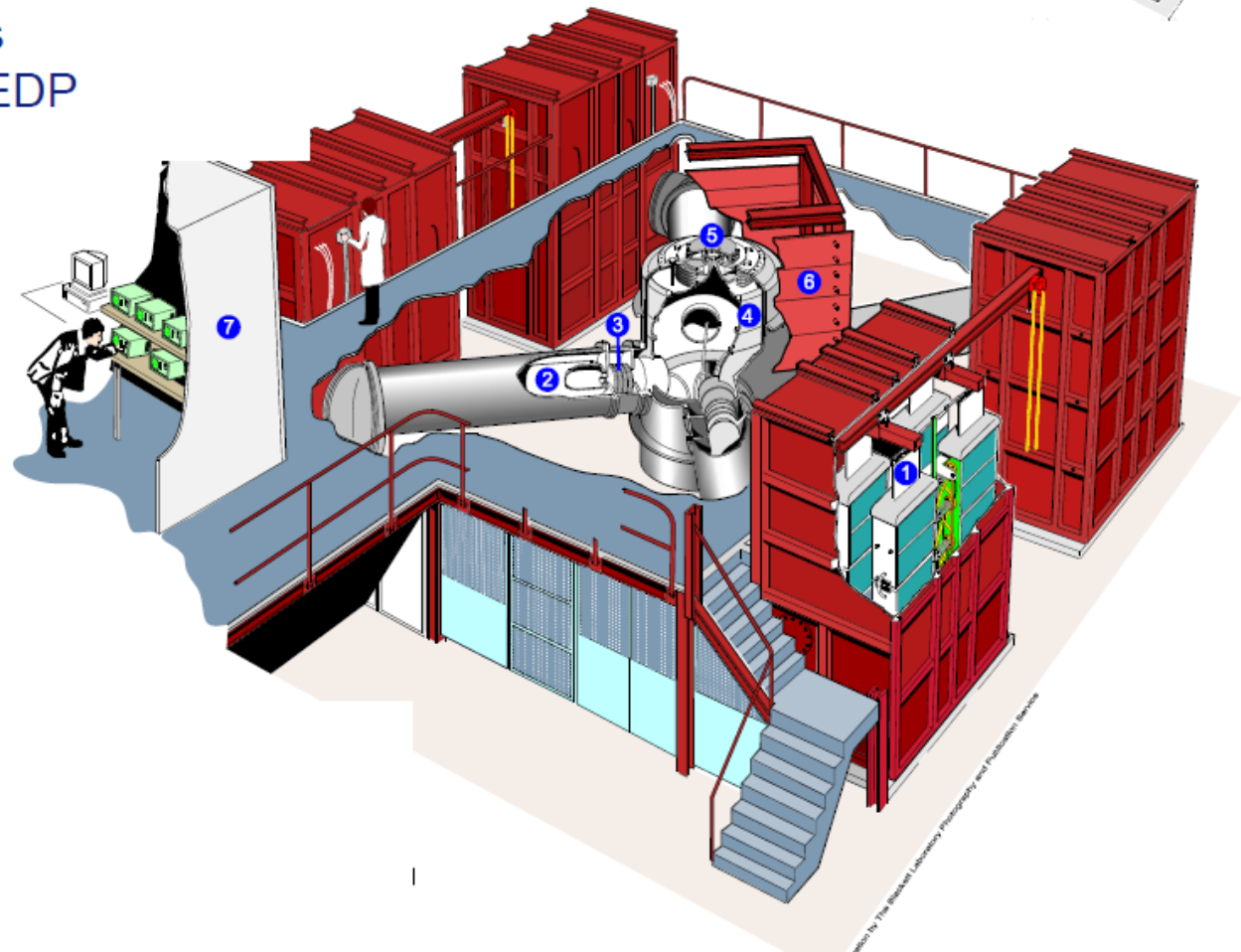
SAND2017-0900PE_The sandia z machine - an overview of the world's most powerful pulsed power facility.pdf

Imperial College MAGPIE facility



At Imperial the 1.5MA 240 ns
MAGPIE generator drives HEDP
experiments on a daily basis

**Mega
Ampere
Generator for
Plasma
Implosion
Experiments**



Get experience in magnetically driven isentropic compression experiments
Can also look at shocks in plasmas - e.g. astro relevant radiative shock waves
And using plasma explore new methods of applying high pressures to targets



Prelude to experiments: new power feed and vacuum chamber

Original vacuum chamber was only ~30cm diameter x 15cm tall
Anode and cathode move by 6mm during vacuum
Water ingress meant vacuum time was 3hrs

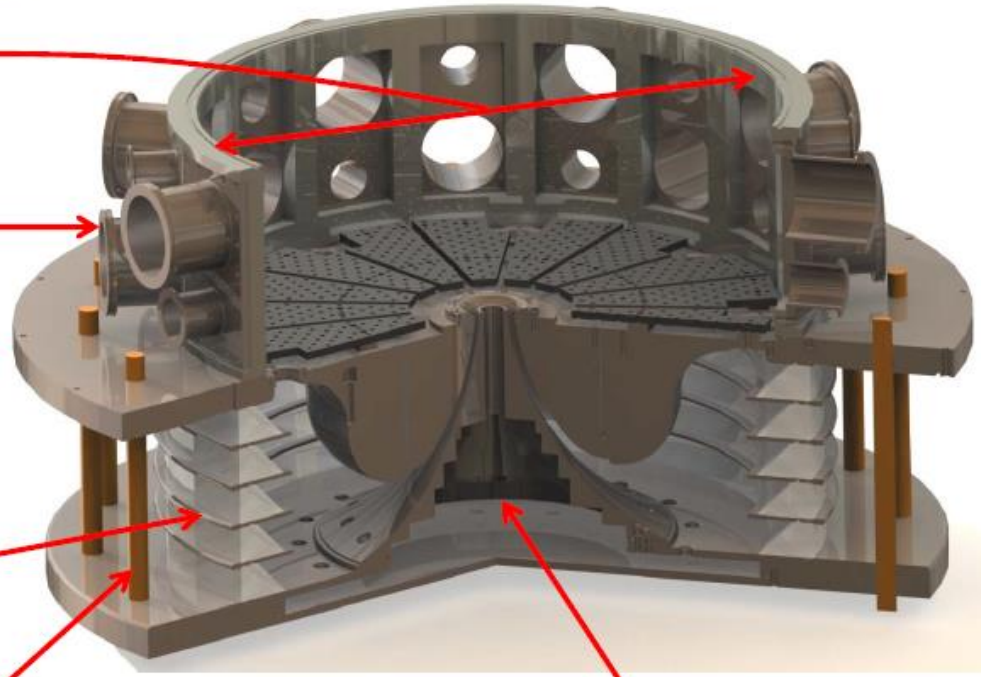
~70cm internal diameter

Chamber surrounded by 16 port plates with ISO100 and ISO 63

Reinforced steel plates to reduce flex

Rexolite diode rings increase strength reduce water absorption

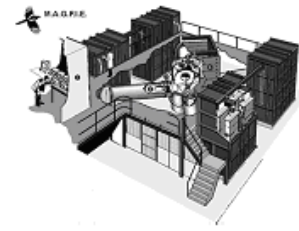
New Torlon bolts don't stretch



Vacuum section below MITL removes force on cathode

Anode and cathode now move ~25um

Vacuum time <1hr



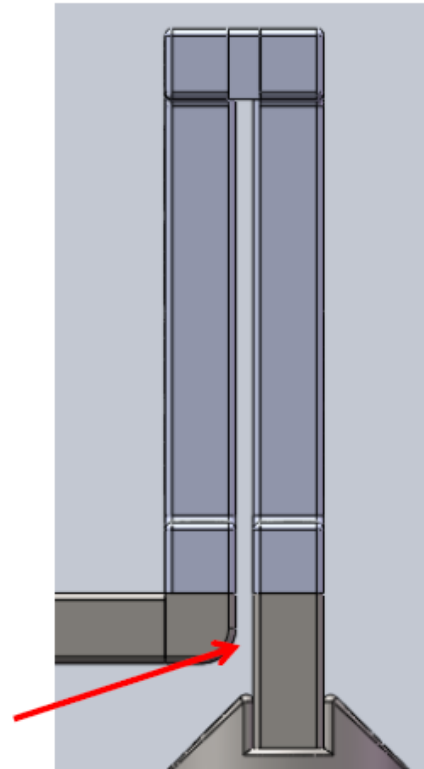
Design and manufacturing issues:

- Will the gap breakdown?
- How uniform is the drive?

EM simulations difficult due to large scale of electrodes c.f. gap in stripline...

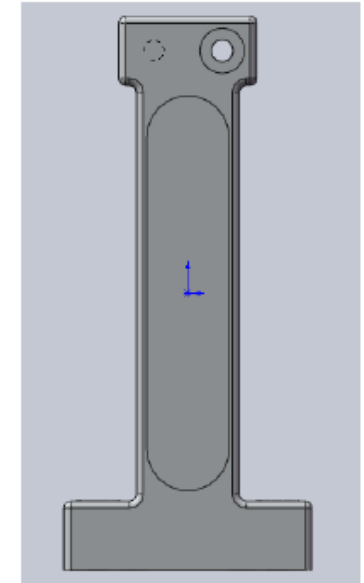
=> electrodes designed from simple assumptions and results will serve as test for code

1 – 2 mm gap in stripline
voltages ~200kV



Side view of stripline

80mm



Front view of one electrode with target area outlined

- Need to use a soft material and needs to be easily machined - Copper
- Target thicknesses 1-7mm - shocks expected after ~5mm thickness
- How to support over large areas, polish etc

Initial experiments: Feb 2010



Typically for shock experiments:

flatness $\sim 5\mu\text{m}$, roughness $< \mu\text{m}$ via. diamond machining

Overkill for initial experiments (and very expensive)

Tour de Force by Imperial College Instrumentation workshop

2 part 'glued electrode' electrode - target area and support

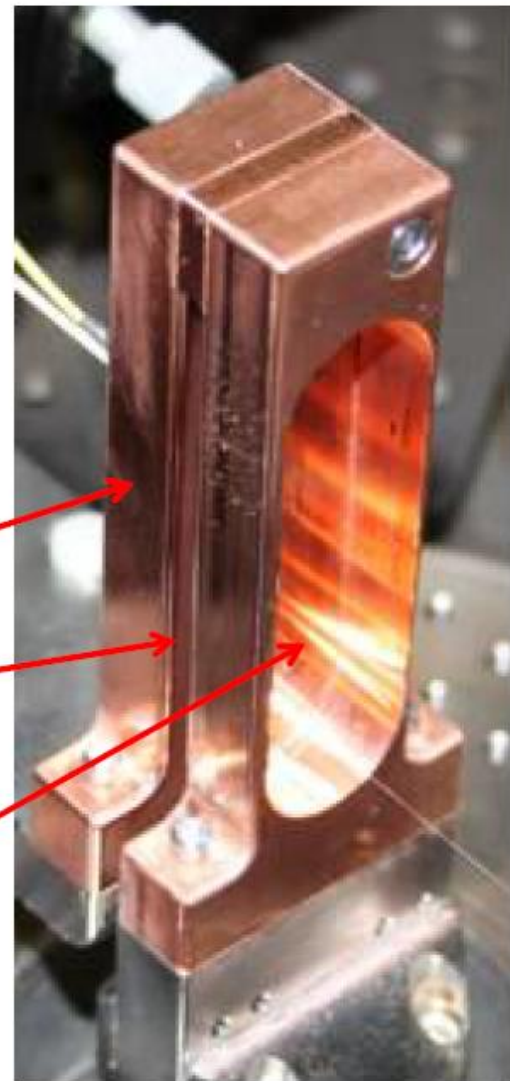
4 axis CNC mill allows fast production of blanks

Precision ground then hand polished – mirror finish $\sim 5\mu\text{m}$

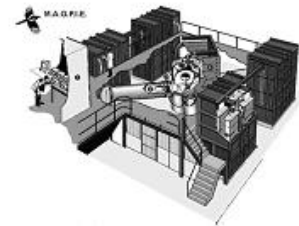
Return electrode

Gap (2mm)

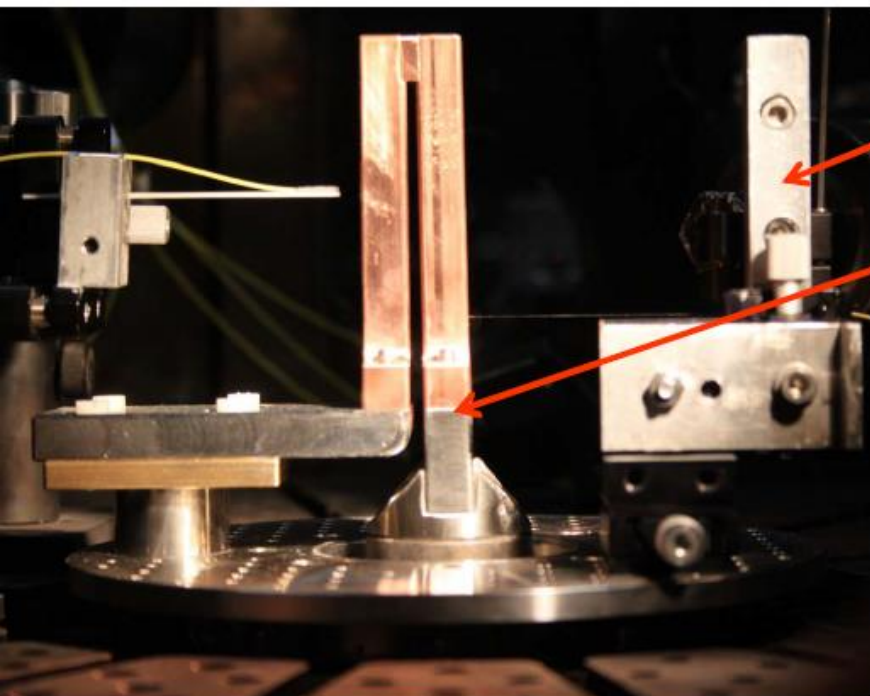
Target area
(60x17mm)



Close up of 20mm wide copper strip line in MAGPIE



Initial experiments: Feb 2010

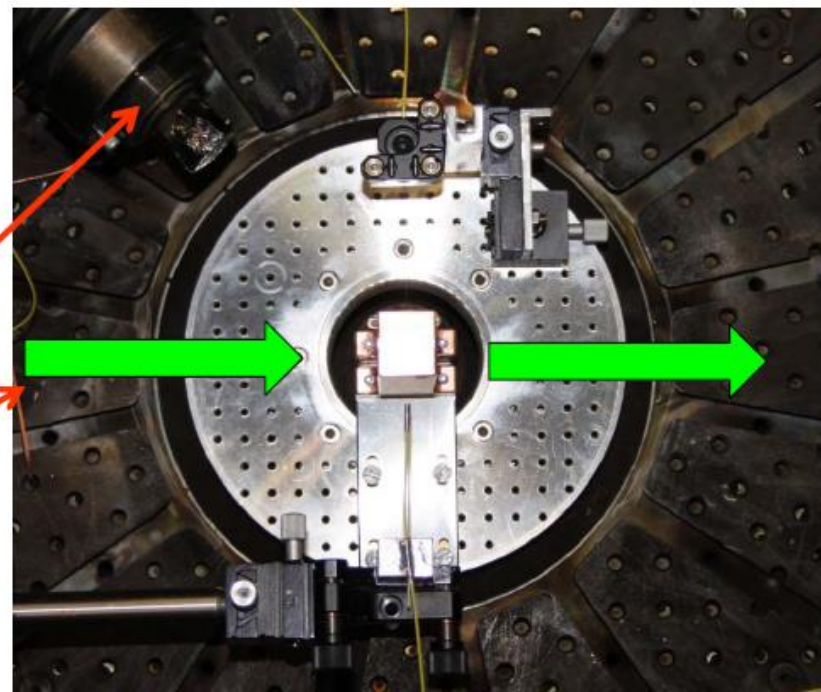


Side view of strip line

Holder for Het-V probes

Stripline mounted on break away system
to prevent damage to MAGPIE

Top down view



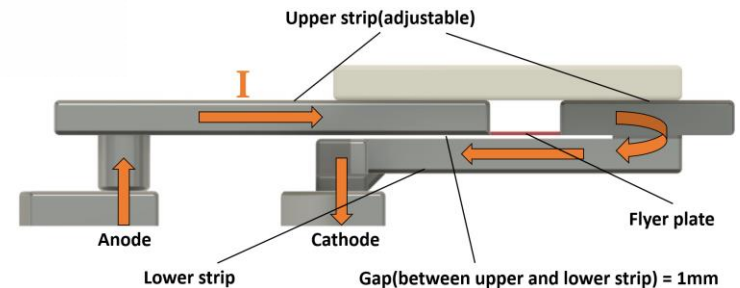
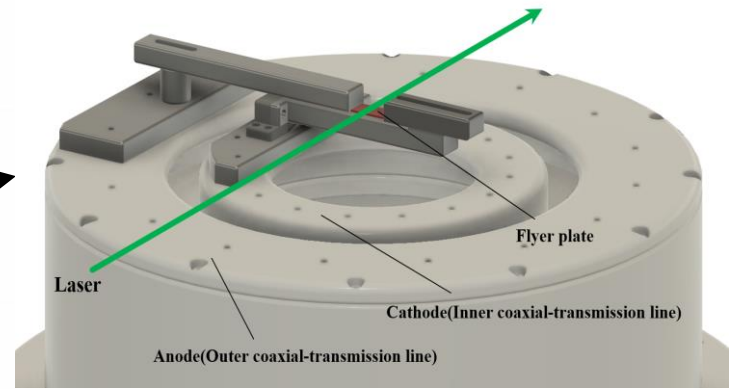
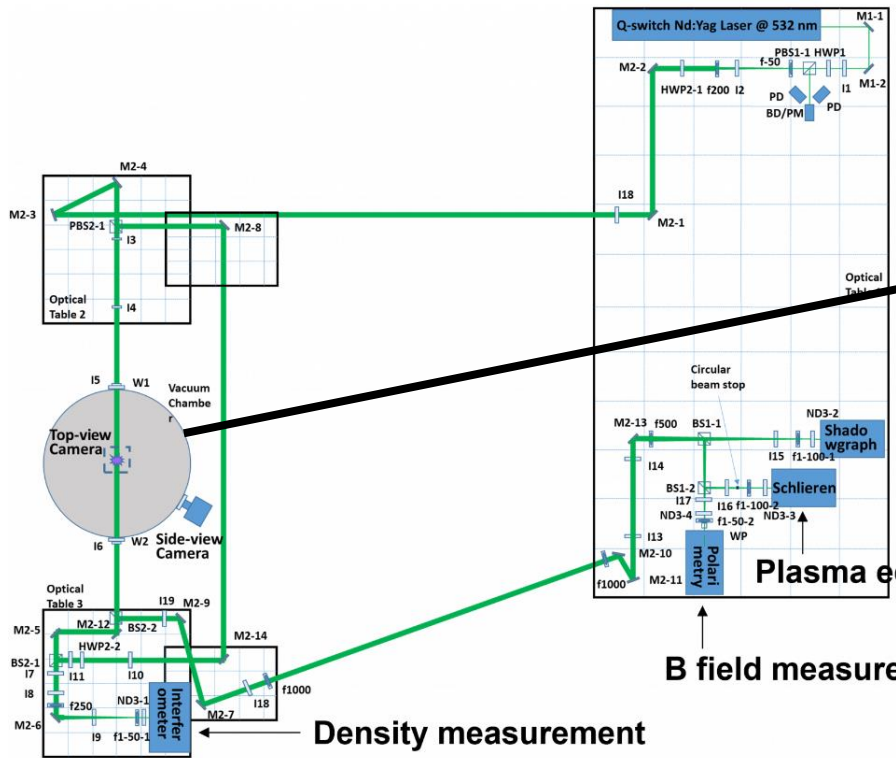
Resistive voltage probe

Path of probing laser

Pulsed Power Driven Experiments in the
Institute of Shock Physics, by Simon Bland

1/2 inch armoured plate top and bottom
to 'catch' stripline (not shown)

The design of our flyer-plate launcher



Density measurement

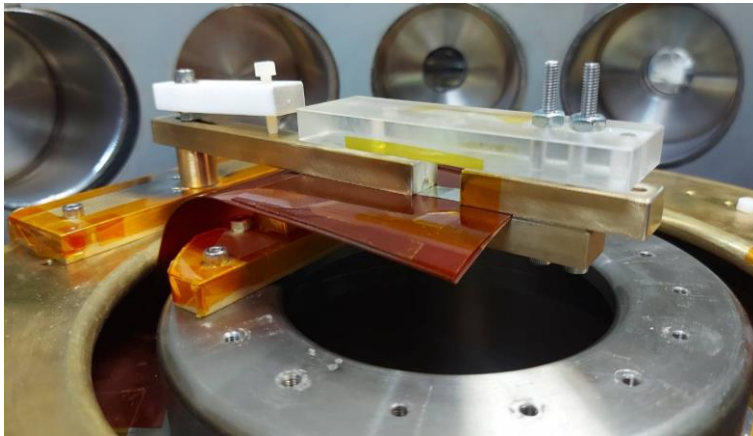
B field measurement

Plasma edge detection

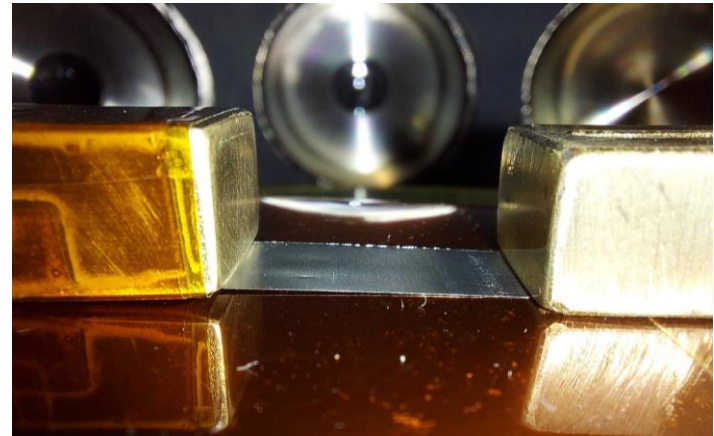
Photos of our flyer-plate launcher



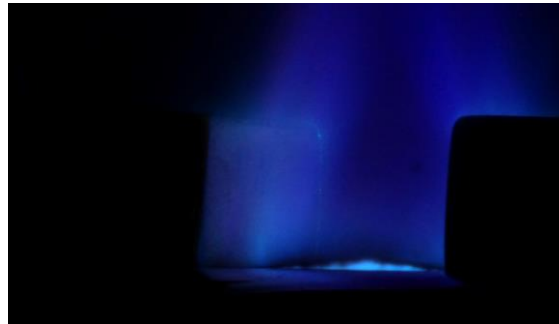
- **Assembly with target**



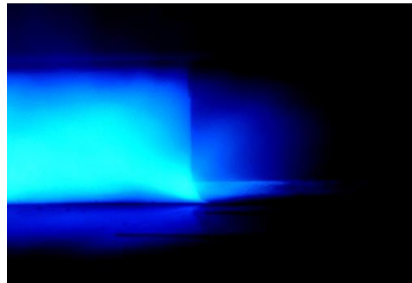
- **Assembly w/o target**



- **Self emission w/o a target**



- **Self emission w/ a target**



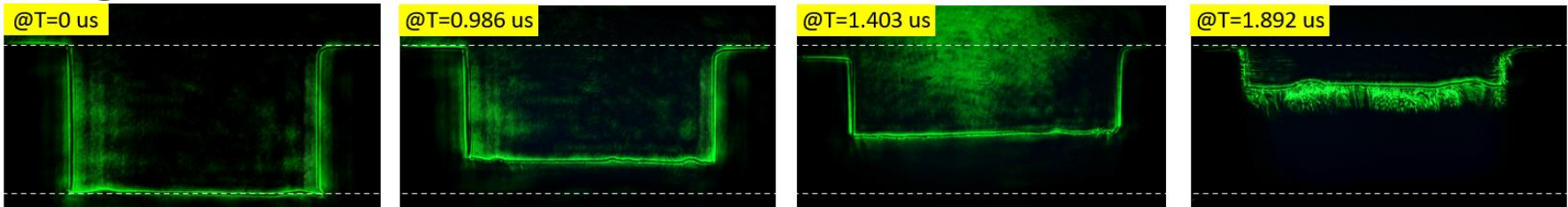
- **After shot**



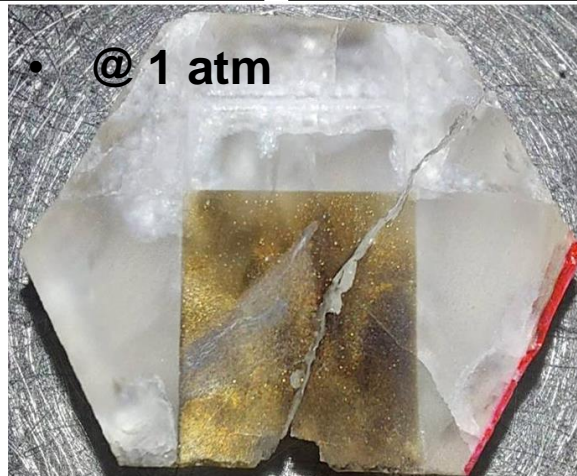
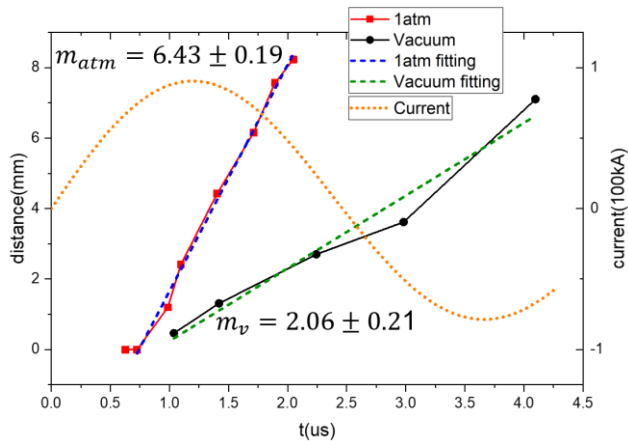
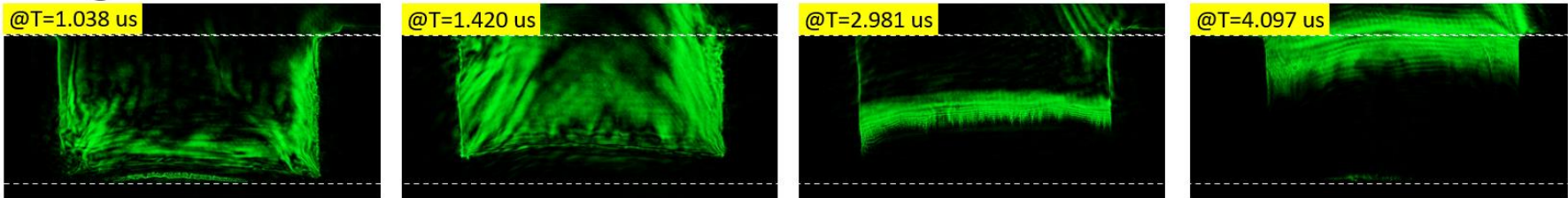
Velocities of the flyer plate were different when experiments were conducted in 1 atm and in vacuum



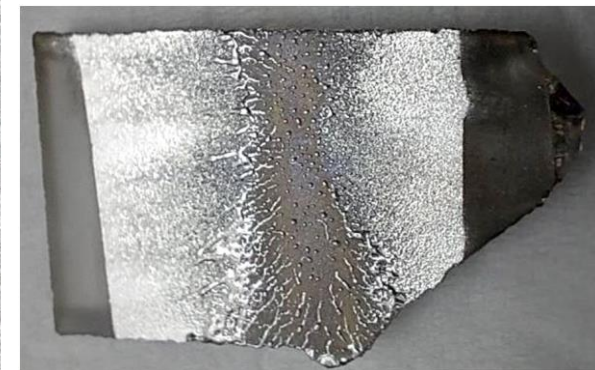
- @ ~1 atm



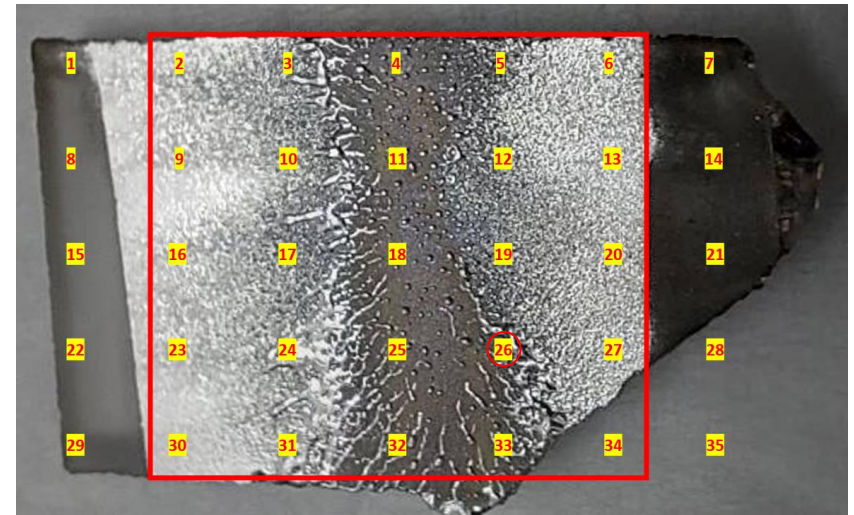
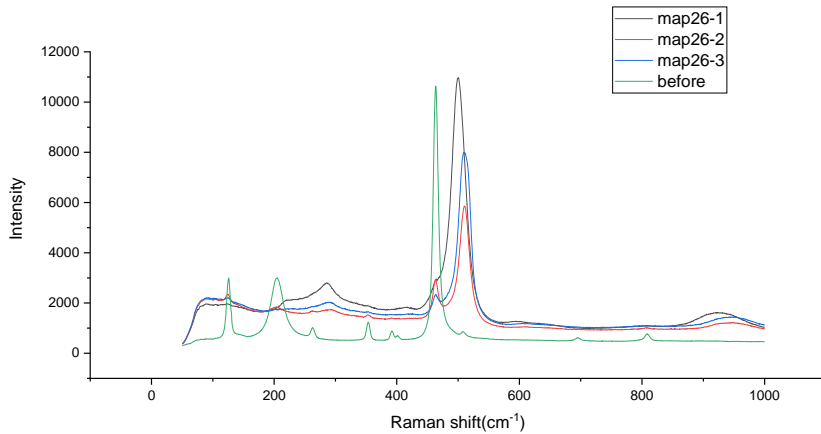
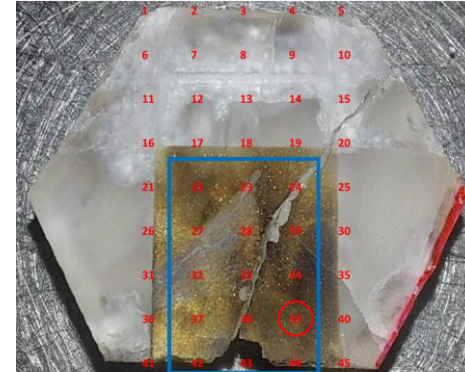
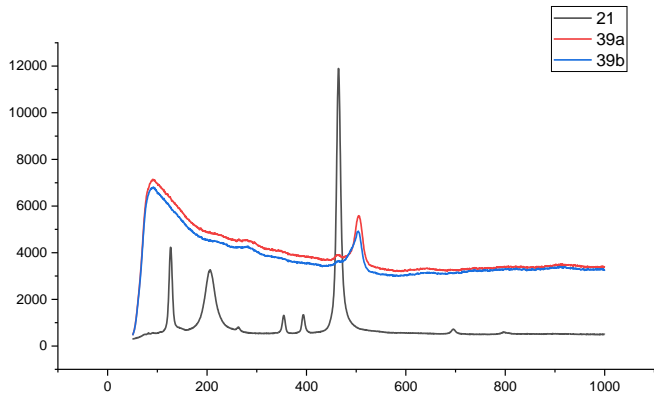
- @ $\sim 10^{-5}$ torr



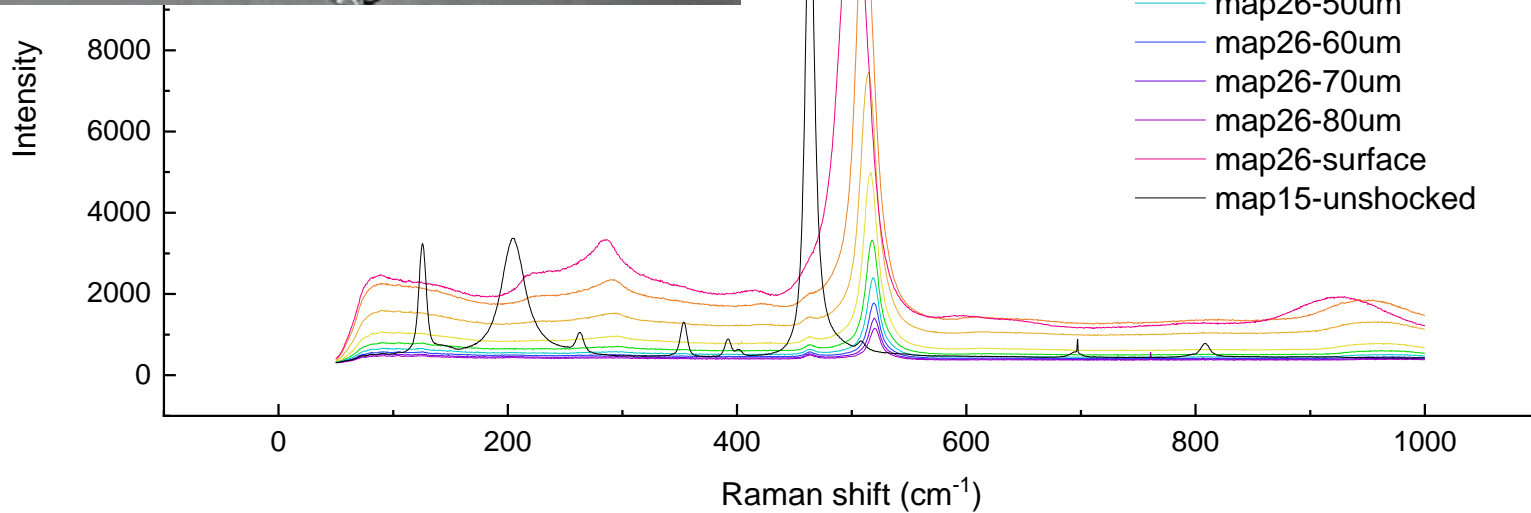
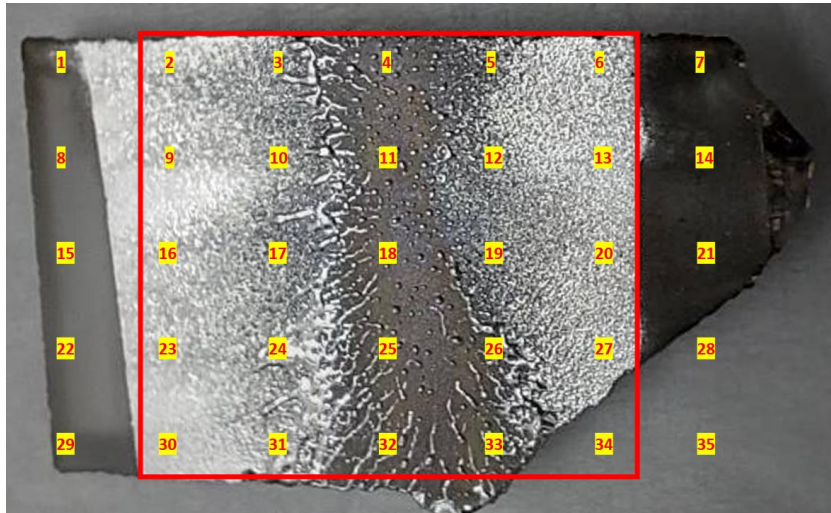
- @ $\sim 10^{-5}$ torr



Raman shift of the SiO₂ sample behaved differently after being shocked



Raman shift of 520 cm^{-1} was observed suggesting that Coesite was formed



The raman shift indicated that a pressure more than 2 Gpa was generated

